Identification, Characterization and Targeting of Cancer Initiating Cells in Pediatric Sarcomas

---

Dissertation

zur

Erlangung der naturwissenschaftlichen Doktorwürde

(Dr. sc. nat.)

vorgelegt der

Mathematisch-naturwissenschaftlichen Fakultät

der

Universität Zürich

von

Sampoorna Satheesha

aus

Indien

Promotionskomitee

Prof. Dr. Beat W. Schäfer (Leitung der Dissertation und Vorsitz)

Prof. Dr. Michael O. Hengartner

Prof. Dr. Lukas Sommer

Zürich, 2014

The experimental work presented in this thesis was performed at the Department of Oncology and Children's Research Center, University Children's Hospital Zurich. The supervision of this thesis was conducted by Prof. Dr. Beat W. Schäfer (Department of Oncology, University Children's Hospital Zurich), Prof. Dr. Michael O. Hengartner (Rector, University of Zurich) and Prof. Dr. Lukas Sommer (Department of Anatomy, University of Zurich).

Zurich, 2014

Sampoorna Satheesha

Future physicians may laugh at our mixing of primitive cocktails of poisons to kill the most elemental and magisterial disease known to our species. But much of this battle will remain the same: the relentlessness, the inventiveness, the resilience, the queasy pivoting between defeatism and hope, the hypnotic drive for universal solutions, the disappointment of defeat, the arrogance and hubris.

- Siddhartha Mukherjee
"The Emperor of All Maladies: A Biography of Cancer"

Generalizations in biology are almost invariably of a probabilistic nature. As one wit formulated it, there is only one universal law in biology: 'All biological laws have exceptions.'

- Ernst Mayr
"The Growth of Biological Thought"

Peace of mind isn't at all superficial to technical work. It's the whole thing.

- Robert M. Pirsig
"Zen and the Art of Motorcycle Maintenance"

To
My parents

Table of contents

1. Summary

Sarcomas comprise of a diverse set of neoplasms that present with features of mesenchymal and neural crest lineages and can occur in various anatomical sites. Although quite rare in adults, they represent the third most common cancer type in the pediatric population. Current clinical management involves a multimodal approach that consists of high-dose conventional chemotherapy, surgery and/or radiotherapy. Significant improvement in survival outcomes was initially noted upon implementation of these modalities but the clinical benefits have now reached a plateau. The outcome for patients with recurrent or metastatic disease is still very poor. Additionally systemic treatment with conventional cytotoxic drugs and radiotherapy cause severe acute and chronic morbidity and could lead to secondary neoplasms later in life. Therefore there is an urgent need for rationally selected therapeutic avenues and improved treatment protocols.

It is becoming increasingly apparent that intra-tumoral heterogeneity is a key determinant of clinical outcome. Based on the source of heterogeneity two major models of tumor progression have been proposed: clonal evolution model and the cancer stem cell (CSC) model. The former is based on cancer being purely a disease of the genome, wherein stochastic genetic events give rise to a genetically heterogeneous tumor with diverse subclones that follow Darwinian laws of natural selection to aid in tumor progression and recalcitrance and importantly are equipotent in their tumorigenic capacity in xenotransplantation assays. In this case the cancer-initiating cell (CIC) population would be characterized by a genetic lesion alone. The 'cancer stem cell' model on the other hand views cancer as a developmental disease and therefore as a hierarchically organized mass following the principles of organogenesis. It seeks to incorporate the phenotypic and functional heterogeneity within tumors and postulates that tumorigenic behaviour is compartmentalized to a rare de-differentiated CIC population. Using high-throughput next-generation sequencing recent studies are beginning to show that the two models of tumor development may not be mutually exclusive.

The studies presented in this thesis investigate the cellular organization of the most common pediatric sarcoma, Rhabdomyosarcoma (RMS), in order to offer improved clinical management. RMS presents as two major histological subtypes – Embryonal (ERMS) and Alveolar (ARMS). ERMS account for 70% of diagnosed RMS cases and have a relatively more complex genome. ARMS on the other hand have fewer mutations and in about 80% of the cases present with a chromosomal translocation that leads to the expression of a potent oncogenic fusion transcription factor PAX3/7-FOXO1. In brief, using *in vitro* sphere formation assay and *in vivo*

xenotransplantation we show that human ERMS cancer cell lines possess subpopulation of primitive CICs. Furthermore we present evidence that ERMS CICs are maintained by hedgehog signaling and importantly the hedgehog-active ERMS CICs could have prognostic value. Therefore ERMS tumors seem to be hierarchically organized wherein a subpopulation of cells have enhanced self-renewal and tumor initiation capacity. On the contrary, our investigations in ARMS show that the majority of the tumor population possesses CIC properties which are ultimately defined by the activity of the fusion protein PAX3-FOXO1.

Although many studies have reported functional heterogeneity within different pediatric sarcoma entities there has been no significant breakthrough in terms of targeting sarcoma CICs. Our studies offer targeting hedgehog signaling as means to inhibit ERMS CICs and further highlight that novel rationally selected treatment strategies in ERMS need to take into account not only the mutational background but also the hierarchical organization of the tumor. Furthermore the two histological subtypes, which are currently treated with similar protocols in the clinics, seem to follow different organizational principles and hence would need tumor type specific treatment strategy. Therefore our attempts to identify and characterize RMS CICs not only led to significant advances in experimental RMS disease modeling but also have important clinical implications. Overall our studies underscore the importance of assessing intra-tumoral heterogeneity in pediatric sarcomas to identify key targeting nodes for a lasting cure.

2. Zusammenfassung

Sarkomas sind eine heterogene Gruppe von Krebskrankheiten welche Eigenschaften mesenchymaler und neuralleisten Abstammung aufweisen. Sie können an verschiedenen anatomischen Stellen auftreten. Obwohl sie im Erwachsenenalter eher selten sind, repräsentieren sie die dritthäufigste Tumorgruppe in Kindern. Die klinische Behandlung erfolgt in einem multimodalen Ansatz mittels Hochdosis Chemotherapie, Operation und/oder Bestrahlung. Nachdem dadurch die Überlebensrate ursprünglich signifikant verbessert werden konnte, haben wir nun ein Plateau in der Behandlung erreicht. Die Überlebensrate für Patienten mit Metastasen oder Rückfällen ist deshalb immer noch sehr gering. Zusätzlich sind die Behandlungen mit zytotoxischen Medikamenten und Radiotherapie akut toxisch und können sekundäre Tumore im späteren Leben auslösen. Deshalb besteht ein dringender Bedarf an neuen, sinnvoll ausgewählten therapeutischen Strategien, um bestehende Behandlungsprotokolle zu verbessern.

Es wird immer deutlicher, dass intra-tumorale Heterogenität ein wichtiger Faktor für den klinischen Erfolg darstellt. Darauf basierend wurden zwei hauptsächliche Modelle des Verlaufs der Tumorerkrankungen vorgeschlagen: das klonale Evolutions- sowie das Krebsstammzellen Modell. Das erste basiert auf der Annahme, dass Krebs ausschliesslich eine Krankheit der Gene darstellt. Stochastisch auftretende genetische Ereignisse führen demnach zu einem genetisch heterogenen Tumor in welchem die Zellen natürlicher Selektion nach Darwinunterliegen. Alle Tumorzellen haben dabei eine ähnliche Fähigkeit, neues Tumorwachstum in Xenotransplantationen zu initiieren. Diese sind durch genetische Läsionen charakterisiert. Dem gegenüber steht das Krebsstammzellen Modell, welches Krebs als eine Krankheit betrachtet, die hierarchisch organisiert ist und den Regeln der Organogenese folgt. Hier wird postuliert, dass eine seltene Population von Zellen für das tumorigene Verhalten verantwortlich ist. Durch neue Sequenziermethoden wird zunehmend auch klar, dass sich die beiden Modelle nicht unbedingt ausschliessen müssen.

Die Untersuchungen, welche in dieser Arbeit vorgestellt werden, haben die zelluläre Organisation des häufigsten kindlichen Sarkomas, des Rhabdomyosarkoms (RMS), charakterisiert. RMS zeigt sich klinisch in zwei Hauptgruppen – embryonal (ERMS) und alveolär (ARMS). ERMS ist verantwortlich für 70% aller Fälle und weisen ein verhältnismässiges komplexes Genom auf. ARMS auf der anderen Seite hat weniger Mutationen und ist in ca. 80% der Fälle durch eine chromosomale Translokation charakterisiert, die zur Expression eines onkogenenFusionsprotein führt, PAX3/7-FOXO1. Wir konnten nun erstmals durch Bildung von Sphären und Xenotransplantationenzeigen, dass ERMS Tumorzellen eine kleine Population von

Krebsstammzellen aufweisen.Wir zeigen, dass diese Population mittels aktivem Hedgehog Signalweg gesteuert wird, und dass ihre Anwesenheit von prognostischer Bedeutung ist. Daher ist ERMS ein hierarchisch organisierter Tumor. Auf der anderen Seite zeigen unsere Untersuchungen an ARMS, dass die Mehrheit der Tumorzellen dieser RMS Gruppe Eigenschaften einer Stammzelle aufweisen, welche ultimativ durch das Fusionsprotein PAX3/FOXO1 gesteuert werden.

Obwohl ähnliche Untersuchungen schon funktionelle Heterogenität in verschiedenen kindlichen Sarkomen nachgewiesen haben, konnten diese Erkenntnisse bis jetzt klinisch nicht genutzt werden. Unsere Untersuchungen heben nun den Hedgehog Signalweg als mögliche therapeutische Option hervor. Dies zeigt, dass sinnvoll ausgesuchte neue Therapien nicht nur den Mutationshintergrund sondern auch die hierarchische Organisation des Tumors berücksichtigen müssen. Die beiden histologischen RMS Untergruppen, welche bis anhin mit ähnlichen Protokollen behandelt werden, weisen demnach eine unterschiedliche zelluläre Organisation auf und brauchen in Zukunft möglicherweise unterschiedliche Behandlungsstrategien. Deshalb haben unsere Untersuchungen über die Krebsstammzellen nicht nur das Verständnis zur Tumororganisation signifikant verbessert, sondern implementieren auch wichtige klinische Konsequenzen. Sie zeigen zudem, dass der Tumorheterogenität in pädiatrischen Sarkomen eine Schlüsselrolle auf dem Weg zu einer langfristigen Heilung zukommt.

3. List of Abbreviations

ABCG2	ATP-binding cassette sub-family G member 2
ALK	Anaplastic Lymphoma Kinase
AKT	AK – mouse strain, T – Thymoma; also called Protein Kinase B (PKB)
ARF	Alternate Reading Frame; part of CDKN2A gene locus
CCND1	Cyclin D1
CDK	Cyclin-dependent kinase
CD[number]	Cluster of Differentiation
cDNA	complementary Deoxyribonucleic acid
CI	Confidence Interval
CK1	Casein Kinase 1
c-KIT	cellular Tyrosine protein KInase; also called CD117 or Stem Cell growth Factor Receptor (SCFR)
c-MET	cellular Mesenchymal-Epithelial Transition factor; also called Hepatocyte Growth Factor Receptor (HGFR)
CMV	Cytomegalovirus
DAPI	4',6-Diamidino-2-Phanylindole
DMEM	Dulbecco's Minimum Essential Medium
DMSO	Dimethylsulphoxide
EDTA	Ethylene diamine tetraacetic acid
ERK	Extracellular signal Regulated Kinase
FBS	Fetal Bovine Serum
FOS	Finkel-Biskis-Jinkins murine Osteogenicsarcoma
FOXO	Forkhead box O
GLI	Glioma-associated
GSK3β	Glycogen synthase kinase-3 beta
GTPase	Guanosine triphosphate hydrolase
HES	Hairy and Enhancer of Split
HHIP	Hedgehog interacting protein
HIF	Hypoxia inducible factor
h-TERT	human telomerase reverse transcriptase
INK4	Inhibitor of cyclin-dependent kinase 4
qRT-PCR	quantitative Real-Time Polymerase Chain Reaction
LGR5	Leucine-rich G-coupled Receptor 5

MAPK	Mitogen-Activated Protein Kinase
MDM2	Mouse double minute 2 homolog
MDR1	Multidrug resistance protein 1; also called Permeability-glycoprotein 1 (P-gp)
MEK	MAPK/ERK Kinase; also called mitogen-activated protein kinase kinase (MKK; MAP2K)
MSC	Mesenchymal Stem Cell
mRNA	messenger ribonucleic acid
mTOR	mammalian Target of Rapamycin
MYC (C-, N-)	Myelocytomatosis oncogene (C-cellular, N-neuroblastoma)
MYF	Myogenic factor
NANOG	Tír na nÓg
NF1	Neurofibromatosis 1
NGS	Next-generation sequencing
NOD	Non-Obese Diabetic
OCT4	Octamer-binding transcription factor 4
P53	Protein 53; also called Transformation-related protein 53 (TRP53)
PARP	Poly (ADP-ribose) polymerase
PAX	Paired box protein
PI3K	Phosphoinositide-3-kinase
PKC	Protein Kinase C
PTEN	Phosphatase and tensin homolog
RAS	Renin-Angiotensin System
ROS	Reactive Oxygen Species
Sca-1	Stem cell antigen-1
SCID	Severe combined immunodeficiency
SDF1α	Stromal derived factor-1 alpha
SEER	Surveillance, Epidemiology, and End Results
shRNA	short hairpin RNA
siRNA	small interfering RNA
SOX2	SRY (sex determining region Y)-box 2
Stro-1	Stromal precursor antigen-1
VEGF	Vascular Enodthelial Growth Factor
Wnt	Wingless related integration site; a combination of Wingless (Wg) and Int1

4. Introduction[1]

4.1. Cancer: A brief introduction

Cancer is a group of diseases characterized by uncontrolled proliferation of atypical cells that eventually develop the ability to invade surrounding normal tissues and spread to other organs in the body. It is the second most common cause of death worldwide, after heart disease [3]. Cancers are histologically classified based on the embryonic origin of the normal tissue they most closely resemble: carcinomas (epithelial tumors), sarcomas (mesenchymal tumors), neuroectodermal tumors (occurring in tissues derived from outer cell layer of early embryo) and hematological tumors (blood cancers).

The relative incidence of cancer types changes remarkably across different population age groups (Fig. 1A; [1]). Carcinoma is the most commonly diagnosed cancer types in the world; accounting for 80% of all cancer-related deaths and occurs mainly in adults. Children (0-14 years) develop primarily hematological malignancies, neuroectodermal tumors and sarcomas. The distribution of cancer entities diagnosed in children also changes with increasing age (Fig. 1B; [2]). The cancer incidence and observed survival in 0-14 year age group in Switzerland is depicted in Fig. 1, C and D.

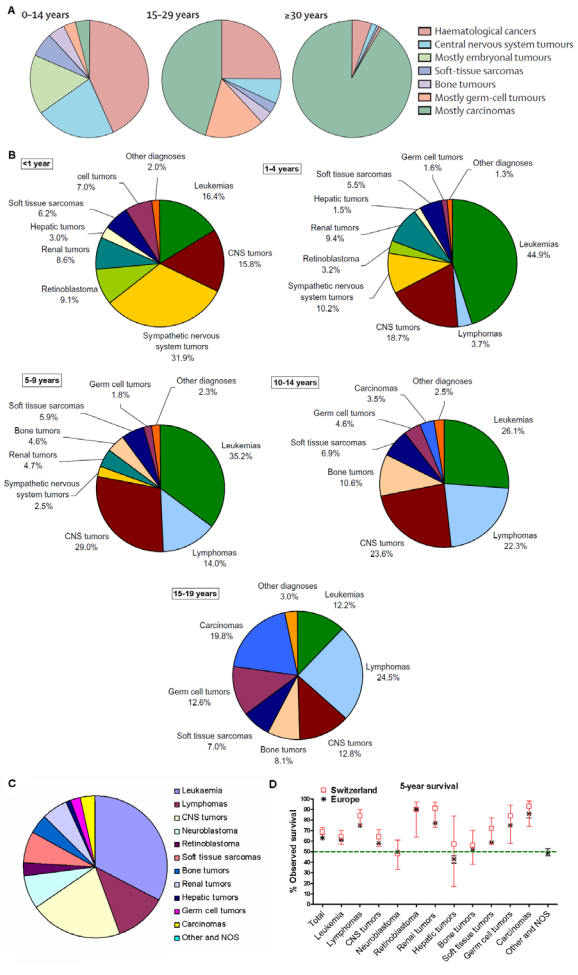

Figure 1. Cancer incidence by type in European populations. (**A**) Data derived from a total of 53,717 cases for age 0–14 years, 282,042 cases for age 15–29 years, and 5,950,220 cases for age 30+ years; obtained from cancer registries. Adapted from [1]. (**B**) Relative frequencies for the main International Classification of Childhood Cancer-3 diagnostic groups by indicated age groups. Adapted from [2]. (**C**) Incidence of cancer types in 0-14 year age group in Switzerland standardized to world standard population reported by Automated Childhood Cancer Information System (ACCIS; International Agency for Research on Cancer, World Health Organization). (**D**) Estimate of five-year observed cumulative survival for Switzerland and Europe for 0-14 age group, reported by ACCIS. Error bars represent 95% C.I. Graphs for (**C**) and (**D**) were constructed using data available at http://acciss.iarc.fr (Last updated on: 11/03/2003; accessed 3 March 2014, 17:37)

[1] Many sections within the *Introduction* have been adapted from the published book chapter:
Satheesha, S. and Schäfer, B.W., *Cancer Stem Cells in Pediatric Sarcomas*, in *Stem Cells and Cancer Stem Cells: Therapeutic Applications in Disease and Injury*, M.A. Hayat, Editor. 2014, Springer: Dordrecht. p. 111-126.

The cancer-causing or etiological factors can be broadly classified as *Intrinsic* or *Extrinsic*, based on their source. Intrinsic factors primarily include inherited or acquired genetic mutations. Extrinsic factors could be chemical (such as asbestos, tobacco etc.), physical (ionising and non-ionising radiation) or biological (viruses, bacteria and other parasites). Other risk factors that contribute to cancer have also been identified such as age, lifestyle (exercise, diet, alcohol consumption) and geographical location (pollution, parasite prevalence). The causative factor for most pediatric tumor types is unknown and the risk factors are unclear.

Cancer initiates as a monoclonal disease following a genetic mutation. The development of cancer is a multi-step process in which normal cells accrue genetic and epigenetic alterations that progressively leads to their conversion into a pre-neoplastic, and finally a highly malignant state (Fig. 2A) [4-5]. Normal cellular machinery maintains homeostasis by employing evolutionarily conserved signaling networks that are extensively inter-linked and possess intricate feedback mechanisms. The genetic mutation and loss of epigenetic identity of normal cells has a cascading effect on cell transcriptional profiles which translates to altered protein expression and function. The mutations that initiate ('gatekeeper' mutations) and cause cancer progression ('driver' mutations) occur in key nodes that affect cellular genome maintenance, cell fate or cell proliferation (Fig. 2B). This culminates in a cancer cell acquiring functional features that makes it resourceful, versatile, labile and hence difficult to kill. The features possessed by a cancer cell have been codified as the 'Hallmarks of Cancer' (Fig. 2, C and D) [6-7]. Also, cell extrinsic factors such as the tumor cell microenvironment have been recently identified as an important determinant of cancer cell behavior.

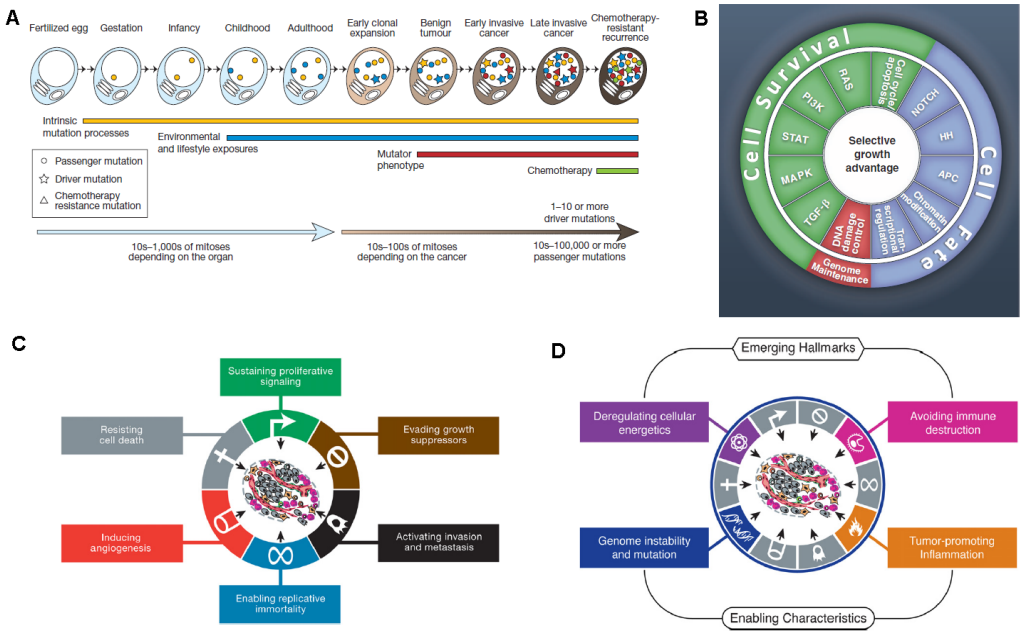

Figure 2. Current understanding of the molecular and cellular biology of cancer. (**A**) The concept of the multi-step nature of carcinogenesis depicted as a lineage of mitotic cell division from fertilized egg to a single cell within a cancer, which is applicable to most adult cancers and specifically proven in the case of colorectal cancer development. While driver mutation leads to cancer progression a cancer cell possesses many 'passenger' mutations that do not

contribute to cancer cell function. Adapted from [4]. (**B**) The driver genes identified from cancer sequencing studies can be classified into one or more of the 12 pathways (middle ring) that confer a selective growth advantage (inner circle). These affect major cellular processes (outer ring). Detailed explanation in [5]. (**C**) The first described six 'core' acquired functional capabilities of cancer cells. Adapted from [7]. Detailed explanation in [6] (**D**) Two additional hallmarks yet to be generalized and therefore referred to as 'emerging': altered cellular metabolism and evasion of immune surveillance seem to support neoplastic progression. Two consequential characteristics of cancer: genomic instability and inflammation facilitate acquisition of 'core' and 'emerging' hallmarks and have been described as 'enabling' hallmarks [7].

4.2. Sarcoma

4.2.1. Diagnosis

Sarcomas comprise a heterogeneous group of rare malignancies (5.9 cases per 100,000 inhabitants) with features of mesodermal or neural crest origin [8]. They consist of a large number of histological variants with differing clinical behavior [9]. Sarcomas usually present as enlarging mass lesions, deep within tissues, without any characteristic clinical symptoms. The patient experiences physical symptoms only if the lesion is compressing adjacent structures and hence making early detection problematic. They do not seem to be associated with a particular organ system like carcinomas and can occur in any part of the body, most commonly in the extremities, followed by the trunk and intra-abdominal sites. However some histological variants seem to show a predilection to certain sites and gender, the reasons for which is still unclear.

Certain broad classification principles are used in sarcoma biology; i) based on the closest immunotypic and cellular resemblance to an adult mesenchymal tissue (e.g. smooth or skeletal muscle, vasculature, fibrous tissue, adipose or chondro-osseous tissue), ii) based on cellular morphology (e.g. small round blue cells, spindle cells, pleomorphic or epithelioid cells), iii) based on genetic lesions (e.g. chromosome translocation-positive or –negative) and iv) based on clinical behavior determined retrospectively (e.g. benign, locally invasive or rarely metastasizing intermediate or malignant). Over the past two decades molecular genetics has played an increasingly important role in correct diagnosis of sarcomas as a significant number of them possess characteristic chromosome translocations (Table 1); encoding for either aberrant transcription factors, for example alveolar rhabdomyosarcoma (ARMS), Ewing sarcoma and primitive neuroectodermal tumors (PNETs) and synovial sarcoma or leading to constitutive growth factor signaling as in dermatofibrosarcoma pertuberans (DFSP) [10].

Table 1. Chromosomal translocations in sarcomas. [9]

Tumour	Main translocations	Involved genes
Alveolar rhabdomyosarcoma	t(2;13)(q35;q14)	*PAX3, FOX01*
	t(1;13)(p36;q14)	*PAX7, FOX01*
Alveolar soft part sarcoma	t(X;17) (p11;q25)	*TFE3, ASPL*
Angiomatoid fibrous histiocytoma	t(12;16)(q13;p11)	*ATF1, FUS*
	t(12;22)(q13;q12)	*ATF1, EWSR1*
	t(2;22)(q33;q12)	*CREB1, EWSR*
Clear cell sarcoma	t(12;22)(q13;q12)	*ATF1, EWSR1*
Dermatofibrosarcoma protuberans	t(17;22)(q22;q13)	*COL1A1, PDGFB*
Desmoplastic small round cell tumour	t(11;22)(p13;q12)	*WT1, EWSR1*
	t(21;22)(q22;q12)	*ERG, EWSR1*
Endometrial stromal sarcoma	t(7;17)(p15;q21)	*JAZF1, JJAZ1*
	t(6p;7p)	*JAZF1, PHF1*
	t(6p;10q;10p)	*EPC1, PHF1*
Ewing sarcoma/primitive neuroectodermal tumour	t(11;22)(q24;q12)	*FLI1, EWSR1*
	t(21;22)(q22;q12)	*ERG, EWSR1*
	t(7;22)(p22;q12)	*ETV1, EWSR1*
	t(2;22)(q33;q12)	*FEV, EWSR1*
	t(17;22)(q12;q12)	*ETV4, EWSR1*
Extraskeletal myxoid chondrosarcoma	t(9;22)(q21−31;q12)	*NR4A3, EWSR1*
	t(9;17)(q22;q11)	*NR4A3, TAF15*
Infantile fibrosarcoma	t(12;15)(p13;q26)	*ETV6, NTRK3*
Inflammatory myofibroblastic tumour	2p23	*ALK* fusions
Low-grade fibromyxoid sarcoma	t(7;16)(q32−34;p11)	*FUS, CREB3L2*
	t(11;16) (p11;p11)	*FUS, CREB3L1*
Myxoid round cell liposarcoma	t(12;16)(q13;p11)	*DDIT3, FUS*
	t(12;22)(q13;q11−q12)	*DDIT3, EWSR1*
Synovial sarcoma	t(X;18)(p11.2;q11.2)	*SSX1, 2 or 4, SYT*

4.2.2. Epidemiology

Sarcomas pose a unique challenge to researchers and clinicians alike as they cross the age spectrum. Although in total numbers more adults are diagnosed with sarcoma its relative incidence is higher in the pediatric populations, accounting for 7.4% of all pediatric malignancies. Significant differences have been noted in the occurrence pattern with age (Fig. 3A). The incidence of sarcomas in infants (<1 year old) was found to be higher than in older children [11]. Congenital fibrosarcoma and hemangiopericytoma are peculiar to infants while RMS is the most common sarcoma in the first two decades of life (median age of 15 years). In children <10 years of age the embryonal RMS (ERMS) is more common followed by malignancies of fibroblastic histologies such as UPS (previously referred to as malignant fibrous histiocytoma or MFH) and fibrosarcoma [8]. In young adolescents (age 10-14 years) ARMS becomes more common and in older patients the pleomorphic subtype is the most often diagnosed RMS [12]. In the second decade of life non-RMS sarcomas occur more frequently and eventually become the most common sarcomas diagnosed in adults. These include osseous tumors such as Ewing sarcoma and osteosarcoma, fibroblastic tumors such as DFSP and UPS, chondrosarcoma, synovial sarcoma, malignant peripheral nerve sheath tumor (MPNST) and desmoplastic small round cell tumor (DSRTC). In young adults (age 20-39 years) Kaposi sarcoma is the most frequent sarcoma since the dominant causal mechanism requires HIV infection [13]. Synovial sarcoma, Ewing sarcoma, DFSP and alveolar soft parts sarcoma (AFPS) could be considered as transitional tumor types as they overlap the pediatric and young adult age groups [8, 14-15]. Older adults (>40 years old) have increased propensity for leiomyosarcoma, liposarcoma and blood vessel tumours. Osteosarcoma has its second incidence peak in people above 60 years of age as a consequence of treatment for a different cancer or secondary to Paget's disease [16].

Within a sarcoma histotype predilection to site of occurrence also changes with age. Ewing sarcoma in children is predominantly diagnosed in the bone while in adults it manifests itself in the soft tissues [14]. Embryonal RMS the predominant histology in children shows a preference for the head and neck regions and the adult pleomorphic RMS occurs in the extremities [8]. In the case of osteosarcoma, children develop sarcoma in the lower long bones during the growth spurt and in adults the pelvic region is more commonly afflicted than in children [16]. Survival of sarcoma patients decreases with advancing age (Fig. 3B).

A

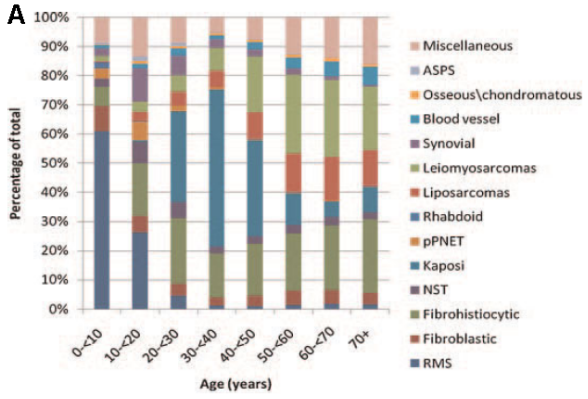

B

	Number of patients	5-year survival rate, %
RMS		
Adults	113	26
	171 (1975–2001)	40
	1,071 (1973–2005)	27
Children	1,248 (1984–1997, IRS-III and IV study)	83
	1,529 (1973–2005)	61
EWS/PNET		
Adults	59 (1980–1995)	38
	182 (1982–1992)	54
	27 (1979–2002)	58
	24 (1990–2005), localized disease	3-year survival: 59
	25 (1991–2002), axial location	2-year survival: 33
	372 adults and 353 children (1989–2007)	53.8
Children	220 (1979–2004)	63.5
DSRCT		
Adults	18 (1998–2006)	27.92
Children	11	21.2

Figures in parentheses show observation periods of the studies.

Figure 3. Sarcoma incidence and survival pattern in different age groups. (**A**) Distribution of histological subtypes in 10-year age groups determined from 48,012 cases collected from the SEER database (1973-2006) [8]. (**B**) Reported survival rate of pediatric-type sarcomas for adult and pediatric patients. Table adapted from [17].

Whether age is a prognostic factor is under discussion and is critically reviewed for Ewing sarcoma family of tumors [14]. The difference in survival could be due to the dissimilar clinical management strategies used for adult and pediatric sarcoma patients. There may additionally be inherent differences in the tumor biology but the data is too limited to draw conclusions [8, 14, 18-19].

Since the experimental work performed for the present doctoral thesis focuses on pediatric rhabdomyosarcoma the following sections will focus and elaborate on sarcoma histotypes and sub-histotypes which are most common in the pediatric population or are in the transitional zone between children and young adults. These include ERMS, ARMS, UPS, osteosarcoma, Ewing sarcoma and synovial sarcoma.

4.2.3. Treatment of pediatric sarcomas

Treatment approach to sarcomas is multimodal and includes surgery, conventional anti-mitotic combinatorial chemotherapy and optional radiotherapy (Fig. 4).

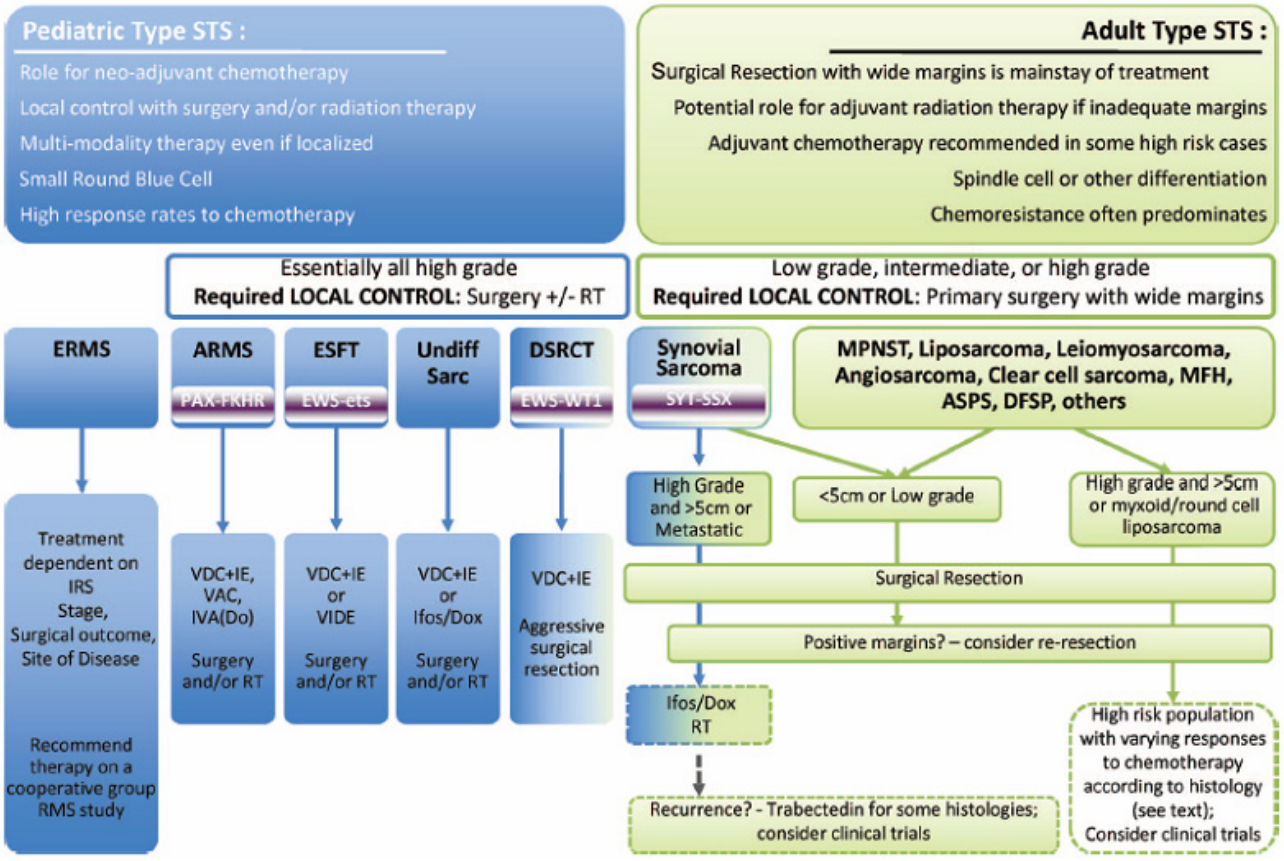

Figure 4. Current multimodal treatment approach in sarcomas based on histology [15]. Solid boxes represent standard of care whereas dotted lines may not apply to all or are still in clinical trials. Dotted lines represent possible recurrence. DSRCT and synovial sarcoma are represented with a gradient because they have features of both pediatric type and adult-type sarcomas.
ESFT, Ewing Sarcoma Family of Tumors (Ewing sarcoma and PNETs); Ifos/Dox, ifosfamide and doxorubicin; IRS, Intergroup Rhabdomyosarcoma Study; IVA, ifosfamide, vincristine, and actinomycin; IVA(Do), IVA plus doxorubicin, RT, radiotherapy; STS, Soft-tissue Sarcoma; VAC, vincristine, actinomycin-D, and cyclophosphamide; VDC_IE, vincristine, doxorubicin, and cyclophosphamide plus ifosfamide and etoposide; VIDE, vincristine, ifosfamide, doxorubicin, and etoposide. Also see text.

Although pediatric sarcomas are generally considered as chemosensitive and radiosensitive tumors surgery with negative margins is the only way to achieve complete remission. Local control is the major cause of treatment failure. In case of synovial sarcoma it was noted that positive margin was an independent predictor of local recurrence [20]. Surgery is performed after chemotherapy in some European protocols to ensure better local control. If complete resection is possible for a low-grade or low-risk tumor type only then radiotherapy is avoided. However RMS occurs mainly in sites where surgery is either unfeasible or would lead to severe cosmetic consequences, in which case radiotherapy and chemotherapy are the only hopes for local and systemic control [21-22].

The treatment of RMS has improved over the past decades by the implementation of multi-institutional co-operative risk-adapted trials. The groups conducting these trials are the Soft tissue Sarcoma committee of the Children's Oncology Group (STS-COG, formerly Intergroup RMS

Study Group, IRSG) in the United States, and the recently formed European pediatric Soft tissue Sarcoma Study Group (EpSSG). The latter was formed by the joining of International Society of Pediatric Oncology-Malignant Mesenchymal Tumor committee (SIOP-MMT), the German Soft tissue co-operative study (CWS) and the Italian Co-operative Group (ICG; Associazione Italiana Ematologia Oncologia Pediatrica-Soft Tissue Sarcoma Committee, AIEOP-STSC). Based on clinical parameters at the time of diagnosis RMS patients are divided into clinical groups. The clinical groups are then used as prognostic indicators to divide the patients into 'risk groups'. The intensity of treatment is predicated on the risk stratification since the staging system closely relates to outcome. The clinical grouping and risk-based staging systems are not uniform across the two trial leaders making comparisons difficult (Table 2).

Table 2. Risk stratification used in Soft tissue sarcoma co-operative groups with concurrent treatment and estimated survival. [18]

Risk group	Group	Histology	Site	Size	*N*	Metastases	Stage	Postsurgical group*	Age	Treatment	EFS/OS (%)
European cooperative group (EpSSG)											
Low	A	ERMS/NOS	Any	<5 cm	N0	M0		I	1 < age ≤ 10	VA	90–95
Standard	B	ERMS/NOS	Any	>5 cm	N0	M0		I	Age > 10	IVA + VA or IVA with or without RT	78–90
	C	ERMS/NOS	Favourable		N0	M0		II–III	<21		72–88
	D	ERMS/NOS	Unfavourable	<5 cm	N0	M0		II–III	1 < age ≤ 10		80–85
High	E	ERMS/NOS	Unfavourable	>5 cm	N0	M0		II–III	Age > 10	IVA versus IVADo plus RT plus VC	55–60
	F	ERMS/NOS	Any		N1	M0		II–III	<21		50–60
	G	ARMS	Any		N0	M0		I–II–III	<21		50–60
Very high	H	ARMS	Any		N1	M0		I–II–III	<21	IVADo plus RT plus VC	40–50
Metastatic disease	*Not included in EpSSG protocol*				M1		IV				
IRS-V (COG) cooperative group											
Low risk											88
	Low-A	ERMS	Favourable	Any	N0	M0	1	I	<50	VA	
	D9602	ERMS	Favourable	Any	N0	M0	1	II	<50	VA + RT	
		ERMS	Orbit only	Any	N0	M0	1	III	<50	VA + RT	
		ERMS	Unfavourable	<5 cm	N0 or NX	M0	2	I	<50	VA	
	Low-B	ERMS	Favourable	Any	N1	M0	1	II	<50	VAC + RT	
	D9602	ERMS	Orbit only	Any	N1	M0	1	III	<50	VAC + RT	
		ERMS	Favourable	Any	Any	M0	1	III	<50	VAC + RT	
		ERMS	Unfavourable	<5 cm	N0 or NX	M0	2	II	<50	VAC + RT	
		ERMS	Unfavourable	<5 cm	N1	M0	3	I or II	<50	VAC (+RT, GpII)	
		ERMS	Unfavourable	>5 cm	Any	M0	3	I or II	<50	VAC (+RT, GpII)	
Intermediate	D9803	ERMS	Unfavourable	<5 cm	N0 or NX	M0	2	III	<50	VAC ± Topo + RT	55–76
		ERMS	Unfavourable	<5 cm	N1	M0	3	III	<50	VAC ± Topo + RT	
		ERMS	Unfavourable	>5 cm	Any	M0	3	III	<50	VAC ± Topo + RT	
		ARMS/NOS	Any	Any	Any	M0	1 or 2 or 3	I or II or III	<50	VAC ± Topo + RT	
		ERMS	Any	Any	Any	M1	4	I or II or III or IV	<10	VAC ± Topo + RT	
High	D9802	ERMS	Any	Any	Any	M1	4	IV	≥10 to <50	CPT-11, VAC + RT	<30
		ARMS/NOS	Any	Any	Any	M1	4	IV	<50	CPT-11, VAC + RT	

NOS: not otherwise specified. Favourable sites include: urogenital (non-bladder, non-prostate), head and neck (non-parameningeal), orbit, unfavourable includes all other sites. N0: lymph node involvement absent; N1: positive lymph nodes; and Nx: unknown involvement lymph nodes. M0: no distant metastases; and M1: distant metastases present. I: ifosfamide; Do: doxorubicin; V: vincristine; A: d-actinomycin; C: cyclophosphamide; Topo: topotecan; CPT-11: irinotecan; and RT: radiotherapy. *Post-surgical clinical grouping system

Despite the initial successes of the multimodal treatment strategies in childhood solid cancers there has been little improvement on mortality in recent years [23]. It seems that 30-40% of children and young adults with sarcoma, irrespective of histology and regimens used, will develop recurrent or metastatic disease and <25% of them will survive in the recurrent setting [15]. About 50% of ERMS cases are considered low risk with a majority having long term event-free survival at 85-95% even with reduced therapy intensity. However there is a minority of low risk patients that still require high-dose chemotherapy and have lower survival. The intermediate risk ERMS patients

consisting of about 40% of ERMS cases have an event-free survival of about 75% which has not improved with either dose intensification or changing therapy agents. The situation is dismal for the high risk metastatic ERMS patients and patients with progressive or recurrent disease, with a five year survival estimate at 35% and 17% respectively [24-25]. At present 30% of osteosarcoma patients do not survive the disease and there has been no significant improvement in the treatment of metastatic disease [16]. The scenario is similar for Ewing sarcoma [26].

Additionally the high cure rates for pediatric sarcomas come at a high cost since severe treatment-related morbidity has been associated with the current regimens [21]. Pediatric patients are treated with high dose systemic chemotherapy, which is not tolerated by adult patients. There is greater than 80% chance of having at least one drug-related side-effect that is severe, life-threatening or fatal during the course of therapy [27]. The VAC protocol which is the mainstay in RMS treatment is associated with considerable acute toxicity [22]. The alkylating drugs such as ifosfamide and cyclophosphamide cause gonadal toxicity, ifosfomide can cause acute neurologic complications, anthracycline drugs such as doxorubicin cause cardiotoxicity, d-actinomycin can cause hepatotoxicity (especially in infants) and vincristine induces peripheral neuropathies. There is a significant risk of late effects such as cardiac dysfunction and coronary heart disease, cognitive impairment, renal insufficiency, endocrinopathies, including infertility, and secondary malignant neoplasms such as leukemia, which are not clinically evident until many years later [23, 28-29]. The late effects of radiotherapy are staggering. The survivors of childhood cancers treated with direct abdominopelvic irradiation have a risk of developing colorectal cancer that is comparable to that of individuals with a strong family history of colorectal cancer [30]. Radiotherapy also causes bone growth arrest, muscle atrophy, bladder dysfunction and infertility in childhood RMS survivors [22, 31]. Recent EpSSG-led trials seeking to reduce or even omit radiation modality showed that although this led to slightly higher relapse risk the overall survival was comparable to the COG trials [32]. These recurrent tumors seem to be amenable to re-treatment; however the effect of increased hospitalization on patient quality of life and morbidity in the long-term needs further investigation.

Due to the aforementioned inadequacies and limitations of current modalities there has been an emphasis on understanding the molecular biology of pediatric sarcomas to tailor personalized rationale-based therapies. To do so, one would need to answer three important interrelated questions,

- What causes sarcomas? – etiological factors that could provide targeting options
- Where do sarcomas originate? – ‘cell of origin’ to design efficient models for drug testing
- How do sarcomas develop? – models of sarcomagenesis to delineate targeting strategies

These questions will be briefly discussed in the following sections.

4.2.4. Etiology

The etiology of sarcomas is under extensive investigation which has led to the identification of many important oncogenic drivers [33]. Interestingly pediatric cancer contain very few mutations compared to adult cancer entities and are therefore considered as genetically simple tumors to study (Fig. 5) [5]. Even so, the 'magic bullet' to completely cure the disease is elusive.

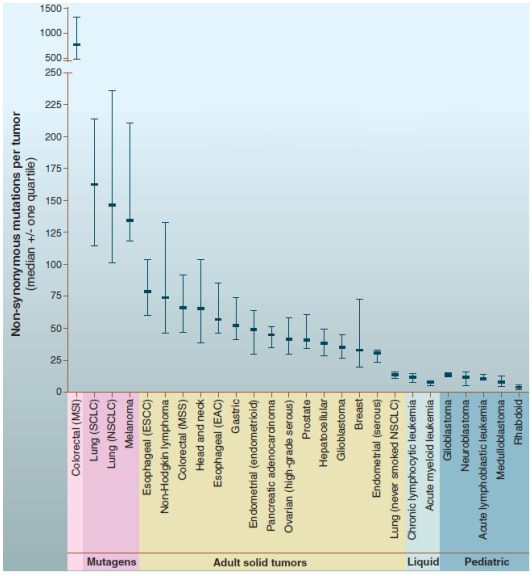

Figure 5. The median number of non-synonymous mutations per tumor in a variety of tumor types. Horizontal bars indicate the 25 and 75% quartiles. MSI, microsatellite instability; SCLC, small cell lung cancers; NSCLC, non–small cell lung cancers; ESCC, esophageal squamous cell carcinomas; MSS, microsatellite stable; EAC, esophageal adenocarcinomas. Adapted from [5].

Many pediatric sarcomas contain chromosomal translocations (Table 1) which are necessary for the survival of the cancer cell but they seem not be sufficient for tumorigenicity in most cases; synovial sarcoma being a key exception [34-35]. Usually additional secondary mutations are necessary to fully transform cells [33, 36-37]. For instance, for complete transformation of skeletal myoblasts into ARMS *in vitro*, the initial hit of PAX3-FOXO1 expression needed to be coupled with loss of INK4A pathway, N-MYC amplification and stabilization of h-TERT [38] and disruption of p53 or p16Ink4a pathway was required *in vivo* [39-40]. The translocation-positive sarcoma have a near-diploid karyotype which is in mark contrast to the relatively more complex karyotypes found in the translocation-negative sarcoma subtypes (ERMS, osteosarcoma and UPS). Recent NGS studies in RMS could reliably quantify this difference between fusion positive and negative RMS [41-42].

Certain congenital syndromes and birth defects seem to be significantly associated with risk of developing translocation-negative sarcomas (Fig. 6). Many of the genetic syndromes associated with sarcoma development disrupt genes involved in genome maintenance. Additionally mice deficient in DNA repair mechanism with an Ink4a mutant background were shown to develop

ERMS, fibrosarcoma and UPS [43]. These observations have led to improved disease modeling and identification of tumor initiating lesions important in sporadic sarcomas.

A

Disorder	Genetic aberration
Beckwith-Weidemann syndrome	Deletions and loss of heterozygosity at chromosome 11p15, particularly affecting *IGF2, CDKA1C, H19,* and/or *LIT1*
Gorlin syndrome (basal cell nevus syndrome)	*PTCH* gene mutation
Costello syndrome	*H-RAS* mutation
Neurofibromatosis 1	*NF1* mutation
Li-Fraumeni syndrome	*TP53* mutation
Mosaic variegated aneuploidy syndrome	*BUB1B* mutation
Nijmegen breakage syndrome (ataxia-telangectasis syndrome variant 1)	*NBS* mutation
Rubinstein-Taybi syndrome	*CREBBP* mutation
Constitutional mismatch-repair/deficiency syndrome	*PSM2* mutation
Adenomatous polyposis coli	*APC* mutation
Hereditary retinoblastoma	*RBI* mutation
Familial pleuropulmonary blastoma syndrome	*DICER* mutation
Noonan syndrome	*PTPN11* mutation
Werner syndrome	*RECOL2* mutation

B

Disorder	Gene
Li-Fraumeni Syndrome	*TP53*, tumor protein p53
Retinoblastoma	*RB1*, retinoblastoma 1
Rothmund Thomson Syndrome	*REQL4*, RecQ protein-like 4, DNA helicase
Werner Syndrome	*WRN*, Werner syndrome, RecQ helicase-like
Bloom Syndrome	*BLM*, Bloom syndrome, RecQ helicase-like
Diamond Blackfan Anemia	Ribosomal protein genes, including *RPS19, RPL5, RPL11, RPL35A, RPS24, RPS17,* and *RPS7*

Figure 6. Congenital disorders associated with (**A**) rhabdomyosarcoma (Adapted from [44]) and (**B**) osteosarcoma [16].

Loss of cell cycle checkpoints seems to be a recurrent theme in sarcomagenesis, including mutation of Retinoblastoma (RB1), deletion of CDKN2A (INK4A locus), PTEN mutations and amplification of CDK4. Loss of p53 activity has been widely reported in various sarcoma subtypes through different mechanisms. Almost all transgenic sarcoma mouse models require p53 (homozygous or heterozygous) mutation, Ink4a mutation and/or disruption of the Rb pathway to initiate tumor formation or improve phenotype penetrance. Interestingly mice with p53 or Ink4a null mutation alone developed sarcomas with relatively lower penetrance. The most penetrant osteosarcoma mouse models involve the co-operative effect of p53 and Rb1 mutations [45-46]. In case of ERMS mouse models loss of Rb1 seems to act a genetic modifier by de-differentiating the tumor phenotype [47]. It is important to acknowledge and factor in the difference between mouse models of sarcomagenesis and the human situation. Human RB1 loss of function mutations translates to some residual activity unlike in the mouse where the entire gene is lost. Also p53 mutations in humans have gain of function phenotype but in mouse they are null mutations.

Commonly found activated oncogenic pathways include MYC (osteosarcoma and RMS), RAS (synovial sarcoma and RMS) and FOS (osteosarcoma and ERMS). RAS pathway has now been unequivocally identified as the most commonly activated oncogenic pathway in RMS [41-42]. RAS activation led to ERMS formation in zebrafish [48]. KRAS activation in mice with p53 null background leads to UPS formation [49-50]. Various growth factor receptors are either amplified or the signaling pathways have been shown to be activated in different sarcoma subtypes [35-37, 51]. These include Epidermal Growth Factor Receptor (EGFR) in ERMS, UPS and osteosarcoma; Insulin Growth Factor Receptor (IGFR) and Fibroblast Growth Factor Receptor (FGFR) in RMS and osteosarcoma; Platelet Derived Growth Factor Receptor (PDGFR) in RMS, Connective Tissue Growth Factor (CTGF) in osteosarcoma and Hepatocyte Growth Factor Receptor (HGFR or c-MET) in ERMS, synovial sarcoma and osteosarcoma. Epigenetic changes such as Loss of

Heterozygosity at 11p15.5, which includes the IGF2 locus, are commonly observed in ERMS tumors.

Lately the importance of developmental pathways such as Wnt (canonical and non-canonical), Hedgehog, Notch and Transforming Growth Factor β (TGFβ) in tumor initiation and differentiation has been shown in diverse sarcomas [51-52] (discussed later). Other cellular processes that play critical roles in maintaining cancer cell functions such as epigenetic regulation of gene expression, apoptotic pathway regulation, post-transcriptional regulation of RNA via non-coding RNAs, protein translation regulation (mTOR pathway), protein post-translational regulation (protein folding, ubiquitination, phosphorylation), metabolism (ROS generation), angiogenesis induction (VEGF production) seem to aid in sarcomagenesis and are also being actively scrutinized for targeting options in pediatric sarcomas [37, 41-42, 51, 53-57]. Overall it is apparent that pediatric sarcoma cells despite harboring few mutations are successful in possessing many of the cancer hallmarks. Apart from the fusion proteins in the translocation positive sarcomas, it is not yet clear which of the aforementioned node(s) is central to the sarcoma phenotype. A bottom-up way of addressing this quandary would be to establish a faithful sarcoma model that would recapitulate the tumor phenotype. To do so, we would need to know the sarcoma 'cell of origin'.

4.2.5. Sarcoma 'cell of origin'

Improved gene targeting methods in mice which allow for spatial and temporal control of gene expression and gene expression profiling have made it possible to rigorously interrogate the 'cell of origin' for different sarcomas (Fig. 7).

4.2.5.1. Multi-lineage stem cell origin

It was postulated decades ago that mesenchymal neoplasms could have a stem cell origin based on ultrastructural and immunophenotyping studies [58]. Accordingly, results from *in vitro* experiments and gene expression profiling and also extrapolations from clinical presentations have led researchers to postulate mesenchymal stem cell (MSC) as the 'cell of origin' for many of the pediatric sarcoma entities, including osteosarcoma, Ewing sarcoma, ARMS, UPS and synovial sarcoma [45, 59-64]. This has been successfully established *in vivo* for osteosarcoma, where tumors arose from mesenchymal progenitor lineage upon homozygous p53 deletion and Rb1 deletion [65]. Interestingly, the authors describe a large percentage of sarcoma entities in the mesenchymal lineage model as 'poorly differentiated soft tissue sarcoma' which could be a UPS phenotype. Ewing sarcoma cells seem to possess features of MSCs [66]. However when EWS-FLI1 expression was introduced in the mesenchymal progenitor compartment it led to increased incidence of 'poorly differentiated sarcoma' with high expression of EWS-FLI1 specifically in the tumor cells but it is

unclear how much this model resembles the human situation [67]. In general, the expression of EWS-FLI1 alone has been found to be insufficient to completely transform MSCs *in vivo*.

A neural crest-derived (pre-myogenic) stem cells compartment has been propounded as a possible origin for ERMS since it is known to occur in body parts where no known skeletal muscle cells are present. Indirect evidence has also been provided by ERMS development in mice with NF1 mutation [68]. Recent efforts to identify the 'cell of origin' in Ptch1 mutant mouse model of ERMS revealed that a prenatal activation of the hedgehog pathway in a pre-somitic compartment rather than the muscle lineage is required for tumor formation [69]. Additionally, a rare sarcoma entity, Ectomesenchymoma, intriguingly and most commonly, presents with intermixed areas of neuronal and rhybdomyosarcomatous differentiation and is thought to arise from a multipotent neural crest cell [70-71]. A neural crest origin has also been posited for Ewing sarcoma due to the presence of primitive neuroectodermal features within the tumors [72]. Recently it was shown that EWS-FLI1 expression was tolerated by human neural crest stem cells and their MSC progeny; however, the tumorigenic capacity of these cells has not been reported [73].

4.2.5.2. Lineage-restricted stem cell and progenitor origin

Adipocyte stem cells could be chemically transformed to give rise to sarcomas with synovial sarcoma or UPS histology [74]. Recently hedgehog activated ERMS (restricted to the head and neck region) were shown to arise from the adipocytic lineage [75]. The adipocyte stem cells however seem not be conducive to osteosarcoma formation [76]. Instead osteosarcomas develop with high penetrance when tumor suppressors were ablated in the osteoblast lineage-restricted cellular compartments [45-46].

The ERMS 'cell of origin' has been investigated by targeted ablation of Ptch1, p53 and Rb1 activities in a range of cells in the myogenic lineage [47]. These studies showed that ERMS arose from the more differentiated compartments, while UPS arose from the undifferentiated compartments (satellite cell) showing that these two major sarcoma subtypes could lie in a continuum. Also activation of hedgehog signaling in Myogenin (committed muscle progenitor) expressing cells led to formation of ERMS in the tongue. When the oncogenic insults were altered to activate Kras and ablate Tp53 then the undifferented muscle stem cell compartment ($Pax7^{+}MyoD^{-}$) gave rise to mostly RMS and some UPS but the more differentiated compartment ($Pax7^{+}MyoD^{-}$) gave rise to exclusively UPS tumors. Intramuscular origin for UPS has been reported previously [49-50]. Interestingly, osteosarcomas can also arise from Myf5 (activated muscle stem cell) expressing compartment upon homozygous p53 knockout [47].

UPS has also been shown to arise from other mesenchymal lineages. UPS could also be induced from mouse embryonic fibroblasts reprogrammed by homozygous knockout of Rb1 [77]. In the

various models of osteosarcoma UPS incidence has also noted, in particular when p53 was ablated in pre-osteoblasts. It is unclear if the molecular features of the UPS in all these different lineage models are similar.

The mature myoblasts expressing Myf6 were reported as the origin of fusion positive ARMS. The compartment seems to de-differentiate upon expression of Pax3-Foxo1, but this was possible only in a p53 or Ink4a null background [39]. Synovial sarcomas have uncertain differentiation but their origin seems to be from the Myf5 expressing myogenic compartment [34].

It should be noted that the characterization of sarcomas modeled *in vivo* has mainly included histological analysis and gene expression profiling. However relevance to the human situation in clinically important aspects such as latency of the tumor model, which is especially important when studying childhood cancers, and site of incidence has not been taken into account. Additionally, single sarcoma histological entities have been shown to have different 'cell of origin' but it is as of yet unknown if the sarcomas of similar histologies generated from different cellular compartments in different studies are also similar at the molecular level.

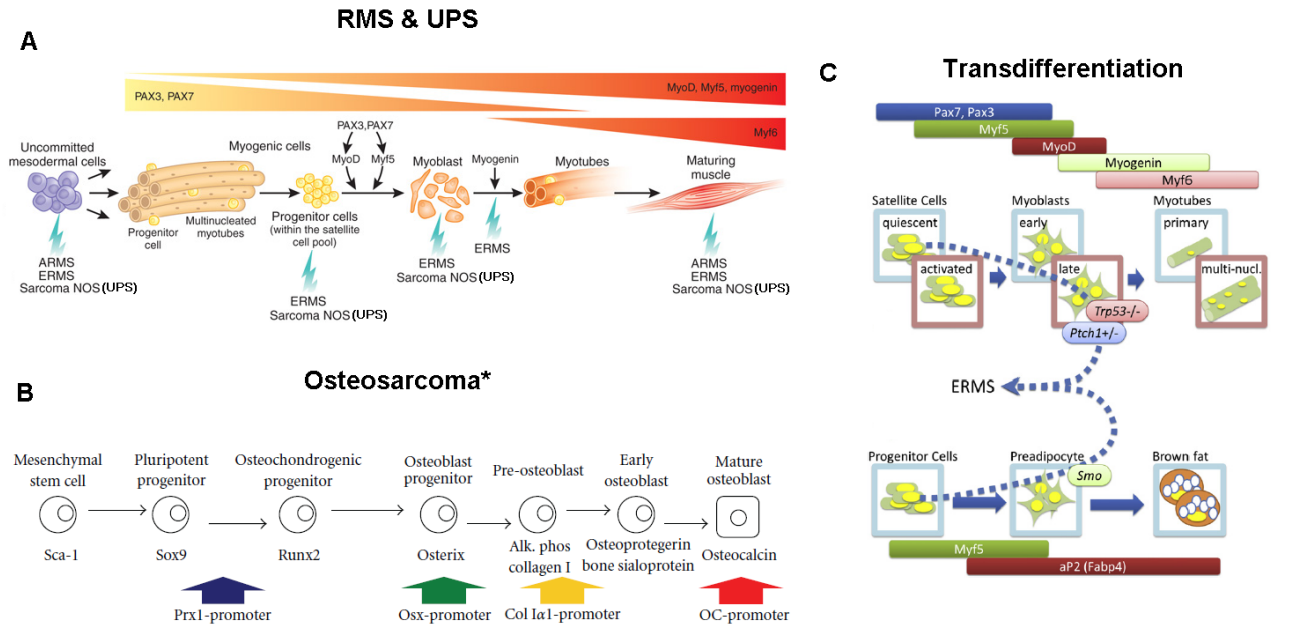

Figure 7. Current understanding of the origins of RMS, UPS and osteosarcoma. (**A**) RMS and UPS can arise from mutli-potent mesodermal cells and also various compartments committed to the muscle lineage. ERMS and UPS are thought to be at different ends of the differentiation spectrum within the same tumor phenotype since UPS tumors can originate from the muscle lineage. ARMS can develop from differentiated muscle through 'de-differentiation'. Adapted from [78]. (**B**) Osteosarcoma mainly initiate from the osteogenic-committed lineage. *Some of the models also presented with multiple tumor types for example – 'poorly differentiated soft tissue sarcoma' (UPS?), adipogenic tumors, RMS. Adapted from [46]. (**C**) Transdifferentiation seen in ERMS development. Activation of the hedgehog pathway by different oncogenic hits (Ptch1 mutation or Smo activation) leads to ERMS development from different mesodermal lineages. Adapted from [79].

Taken together it is clear that single sarcoma entities could have multiple cells of origin depending on the oncogenic hit since the cell differentiation status would confer different permissive states. Conversely the same cell type can give rise to different sarcomas based on the

mutational profile. Although specific lineages are targeted in the tumor-initiation studies the effect of the tumor-initiating lesion on cell fate/differentiation (either de-differentiation or transdifferentiation; Fig 7C) could finally determine the tumor phenotype. Taken together this implies that the final tumor phenotype is not indicative of the 'cell of origin' for many sarcomas. For example, ERMS tumors have an activated satellite cell profile even though the cell of origin need not be a muscle stem cell [47-48, 80]. These principles seem to be universally applicable in cancer biology [81].

Once a causative hit has initiated a lesion the question remains as to how it progresses to form the heterogeneous malignant tumor mass which is encountered in the clinics. Different models of tumor development have been postulated which could also be applied to sarcoma progression.

4.3. Models of sarcomagenesis

Initially tumor development was thought to be a product of genetic clones of cancer cells following the Darwinian laws of natural selection; however, experimental and clinical evidence gathered over past couple of decades has made researchers and clinicians refine this model to also explain features of tissue hierarchy observed within heterogeneous masses of certain cancer entities (Fig. 8).

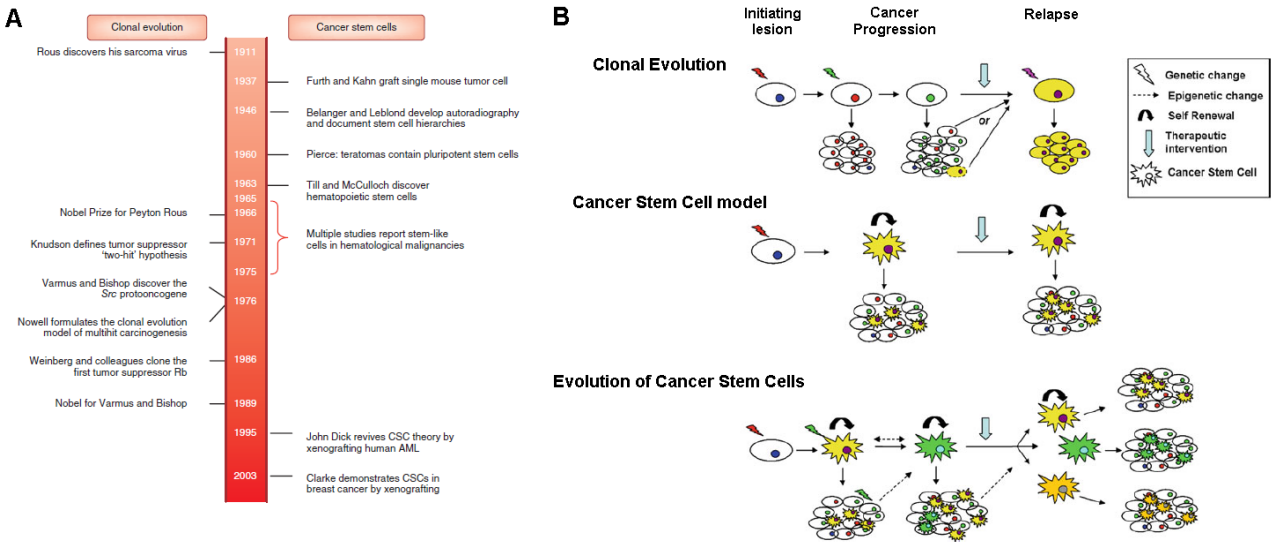

Figure 8. Models of tumor development. (**A**) Timeline highlighting the major discoveries in the development of the clonal evolution (right) and cancer stem cell (left) models [82]. (**B**) Schematic representation of the tumor development models. *Clonal evolution*: Sarcoma formation could be modeled based on selection of the 'fittest' clone. Upon the primary genetic disruption the 'cell of origin' becomes neoplastic and forms a homogeneous tumor mass which increases in heterogeneity, albeit with the persistence of a dominant clone. Therapeutic intervention leads to a selective sweep of a pre-existing or *de novo* drug resistant mutant that initiates tumor growth. *Cancer Stem Cell model:* Sarcomas could also be hierarchically arranged where the initiating oncogenic change causes the 'cell of origin' to assume a stem cell-like phenotype that is able to divide asymmetrically to give rise to the heterogeneous tumor bulk. Upon therapeutic intervention the cancer stem cells (CSCs) persist and reform a heterogeneous tumor which is identical to the primary tumor. The genetic and functional heterogeneity of sarcoma cells could be explained by considering an evolutionary model of CSCs where genetic and epigenetic changes lead to a co-existence of different CSC populations that respond to selective pressures. Adapted from [83].

4.3.1. Clonal evolution model

The widely accepted model of oncogenesis was posited by Peter C. Nowell in 1976 where he described the evolution of a tumor at clonal level in response to selective pressure, making it more aggressive with time by stochastic accumulation of genetic lesions that confer the cells a selective growth advantage (Fig. 8B; Top panel) [84]. The evidence for the clonal evolution in solid tumors has largely been gathered using cytogenetic analysis. Although mesenchymal tumors are thought to follow this model the evidence has been mostly gathered from adult sarcomas wherein mutational burden has the possibility to increase with time [85-87]. But pediatric sarcomas are diagnosed very early in life which leaves a very narrow window for extensive clonal evolution but the genetic instability inherent in pediatric sarcomas could account for the genetic clonal heterogeneity [33, 88]. Although increased karyotypic complexity is seen as sarcomas progress it is unclear if this altered karyotype is what drives the progression [89-90]. The most telling evidence of clonal evolution in disease progression would involve cytogenetic analysis of multiple samples of primary lesion, local recurrences and metastasis. Such longitudinal sampling of clonal aberrations has rarely been done for pediatric sarcomas and, the few studies that did so in the past, fail to show direct clonal evolution due to extensive intratumoral genetic heterogeneity which cannot be covered by traditional cytogenetic methods [85]. The use of NGS technologies with their potential for in-depth genomic coverage could offer novel insights. Accordingly a recent NGS study of ERMS tumors could reliably demonstrate clonal evolution in disease progression whereupon the relapsed and metastatic lesions were genetically different from the primary tumors [41]. However, to date, no specific genetic change has been shown to be necessary for recurrence or relapse in sarcomas.

4.3.2. Cancer Stem Cell models

The Cancer Stem Cell (CSC) hypothesis postulates that analogous to normal regenerating organs tumors are hierarchically organized containing a subset of undifferentiated multipotent self-renewing stem-like cells while the bulk of the tumor consists of differentiated cells incapable of long-term sustenance of tumor growth (Fig. 8B; Middle panel). The model is especially attractive as it seeks to explain tumor relapse through the intrinsic resistance offered by CSCs to anti-mitotic drugs [82, 91-97].The origin of CSCs is under speculation. Initially they were implicitly understood as cells resembling the ‘cell of origin’ of the tumor which in most cases has been thought to be a transformed stem cell that has continued to persist in limited numbers in a progressing tumor [95]. However recent evidence suggests that differentiated cells could reacquire properties of stem cells due to epigenetic changes or oncogenic hits. It is also possible that CSCs emerge as a tumor progresses from a benign lesion to a malignant one. Currently CSCs are considered to be only phenotypically different from their non-CSC counterparts; investigations into the genetic or

epigenetic differences between these populations have begun [96-97]. The CSC phenotypes need not be stable and could be a purely epigenetic phenomenon based on niche factors. Also there might not be just one CSC phenotype but multiple which are either selected depending on the need of the tumor or are generated *de novo*. This latest, more complex notion, is an amalgamation of the clonal evolution and CSC models where CSCs obey Darwinian rules of evolution (Fig. 8B; Bottom panel). This latter model confers versatility to a progressing tumor, explaining many of the clinical phenomena observed and additionally accounting for the multi-functional heterogeneity within tumors [82, 97]. The surge in studies exploring the CSC model of disease progression has led to many controversies in the field, especially with regards to the immunophenotype markers of CSCs [92, 94]. Researchers have begun to standardize the ideas and terminologies associated with the 'CSC field' in order to streamline interpretations [91]. Thus, the model is a work in progress which in itself is likely to evolve with time. Studies in various cancers reveal that the type of tumor model followed could be dependent on the cancer entity and hence the validity of the CSC model would need to be empirically determined on a case-by-case basis [96].

There is biological and clinical circumstantial evidence for the presence of CSCs in pediatric sarcomas. The presence of undifferentiated multipotent cells was noted in sarcomas long before the CSC concept took shape [58]. Pediatric sarcomas have an extensively phenotypically heterogeneous cellular milieu with often a clear differentiation hierarchy irrespective of the genetic background. Osteosarcomas have been known to possess areas of 'dedifferentiation' that can emerge de novo with an abrupt transition from the differentiated areas [9]. Osteosarcoma tumor cells show similarities to primitive osteoblasts and the aggressiveness of the disease seems to correlate with the osteogenic differentiation status of the tumors [98]. Ewing sarcoma cells seem to have a potential for multidirectional differentiation [72]. RMS tumors have features of halted skeletal muscle differentiation [99]. Synovial sarcomas, although of mesodermal origin, also present with co-expression of epithelial markers [35].

Clinical data suggests that osteosarcoma tumors consist of chemoresistant cellular populations since when patients are treated only with conventional chemotherapy the survival rate is only 20% [100]. In case of synovial sarcomas, even though the tumor entity is considered to be chemosensitive the early benefits from therapy seem to dissipate over time and there is also high likelihood of late metastasis [101]. Recent clinical effort in the treatment of metastatic childhood sarcoma showed that while the high-dose therapy was unsuccessful an oral maintenance therapy with lower drug dose showed a high efficacy; which raised the possibility of slow cycling long-living stem cell-like cells being present within sarcomas [102].

Recently efforts have been made towards validating the CSC hypothesis in pediatric sarcomas. These primitive stem cell-like cellular compartments will henceforth be referred to as sarcoma or cancer initiating cells (CICs) to better define their function.

4.4. Identification of sarcoma initiating cells

Sarcoma initiating cells have been isolated using different methods which either employ a phenotypic trait such as cell surface antigen or a functional property such as self-renewal [100, 103-107]. Specifically the CSC model has been most widely studied in osteosarcoma [100, 104].

4.4.1. Cell surface markers

4.4.1.1. CD133

CD133 (Prominin 1) is the most promiscuous CIC marker. It has been used to isolate CICs in colon neoplasia, brain cancer and many other epithelial cancers [92, 96]. CD133 is known to exist in different glycosylated forms of unknown functional significance [108]. Similarly its expression has been documented in many pediatric sarcomas such as ERMS, osteosarcoma, Ewing sarcoma and synovial sarcoma [109-117]. CD133 expression was found to be variable between patients with the same tumor type and there was no specific correlation with pediatric or adult origin of the cell line or tumor [109-110, 112, 118].

The most commonly used glycosylated epitope of CD133 in epithelial cancers is CD133/1 or AC133. Accordingly in Ewing sarcoma AC133 has been used to isolate a self-renewing tumorigenic subpopulation from primary patient tumors [116]. However, the applicability of CD133 as a single marker of Ewing sarcoma stem cells has not been unequivocally established [105]. In ERMS CD133/2 or AC141 was found to be enriched in the sphere cultures and was subsequently used for isolating ERMS stem cells from human cell lines [114]. In studies where only polyclonal CD133 antibodies were used the reconciliation with previous publications is difficult. Interestingly it was noted by Sana *et al.* that the total CD133 expression was rare in primary embryonal and alveolar RMS tumors but increased in the corresponding tumor derived cell lines [112]. Importantly the proportion of total CD133 did not change during the progression of ARMS from primary lesion to recurrence and relapse, even under the influence of chemotherapeutics. The CD133/2 epitope was expressed in synovial sarcoma cell lines and tumor samples, although most of the samples were from adult patients [110, 119]. Naka *et al.* studied primary synovial sarcoma derived cell lines that possessed a high degree of self-renewing capacity *in vivo* but sparse CD133/1 expression [120]. The expression level of CD133/2 was not evaluated however CD133/2 expression seems to reduce tumorigenecity of synovial sarcoma cells [121]. Tirino *et al.* have specifically shown that the CD133/2 epitope is expressed in pediatric osteosarcoma cell lines and in pediatric and adult

osteosarcoma tumor biopsies [109-110]. However, in many studies involving osteosarcoma the epitope status of CD133 has not been mentioned [111, 115, 122] or total CD133 expression is evaluated [113].

4.4.1.2. Others

CD117 (c-kit), in combination with Stro-1, was found to enrich for CICs in osteosarcoma mouse and human cell lines [123]. However, other studies have found primary bone sarcomas and osteosarcoma cell lines to be negative for CD117 expression [110, 124]. Interestingly Stro-1 was initially found to be expressed by osteosarcoma spheres [125]. More recently, work by Zhang *et al.* has shown that osteosarcoma spheres were in fact CD117 and Stro-1 positive [126].

Another potential surface marker that needs further assessment in osteosarcoma is the primitive mesenchymal marker Sca-1. It was observed in a transgenic mouse model that a small population of tumor cells expressed Sca-1 which correlated with increased tumorigenicity [127]. Sca-1 is in fact expressed in early mesenchymal progenitors and it appears that some committed progenitors regain the expression of Sca-1 to accelerate tumor formation. The self-renewal property of the Sca-1^+ population was not addressed and it is yet to be studied in human samples.

In the case of ERMS it was shown that FGFR3 could be a candidate marker to isolate CICs. FGFR3 positive cells were capable of tumor formation at lower cell numbers than the FGFR3 negative cells [128]. But FGFR3 expression was not enriched in ERMS sphere cultures which were shown to have increased tumorigenicity [114]. Additionally, Pressey *et al.* have reported that most of the $FGFR3^+$ cells from RMS cell lines of ERMS and ARMS origin were also positive for CD133 [129].

The expression of neural crest marker CD57 (HNK-1; Human Natural Killer-1) was found to identify population of highly self-renewing tumorigenic cells in Ewing sarcoma [130]. The expression of CD57 did not correlate with CD133 expression.

It has also been recently highlighted that the somatic stem cell marker LGR5 is heterogeneously expressed among different Ewing sarcoma cell lines and patient samples but it is still not clear if it marks a self-renewing population [131]. It is a very interesting marker for further investigation since the functional role of LGR5 in development and in the CSC research field has been firmly established [132-133].

4.4.2. Assays based on functional properties

4.4.2.1. Self-renewal in vitro and in vivo

Developed as a method to isolate neural stem cells, the neurosphere assay has also been used to enrich for primitive long term self-renewing cells from solid cancers. Tumor cells are allowed to

form clonal spherical colonies in suspension in serum-deprived media containing specific growth factors and maintained in long-term cultures. Spheres are thought to arise from primitive cells and although are generally enriched for CICs they are considered to be heterogeneous [134]. In sarcoma stem cell research sphere assay (sarcosphere formation) has been primarily used to indicate the presence of primitive cells in osteosarcoma, ERMS, Ewing sarcoma, synovial sarcoma and UPS cell lines of human and animal origin [106, 114, 120, 125-126, 130, 135-137]. Sphere formation efficiency in osteosarcoma cell lines correlated with tumorigenicity *in vivo* and it was noted that osteosarcoma patient tumor cells from pulmonary metastasis formed larger spheres than primary tumor cells [124]. The sarcosphere assay can be used for identification of cell surface markers that could be used to prospectively sort cellular subpopulations from heterogeneous cell lines and primary tumor material as was done for ERMS [114]. Conversely cellular subpopulations sorted using surface antigens can be cultured as sarcospheres to evaluate and compare the self-renewing capacity *in vitro* and consequently validating the utility of the surface antigen as a 'stemness' marker.

Tumor cells with high self-renewal capacity can also be isolated based on their tumorigenic capacity *in vivo* and/or expression of genes known to be important for conferring 'stemness'. Recent work in synovial sarcoma showed that primary tumor derived cell lines (of unspecified patient age) could be serially transplanted in immunocompromised mice. Heterogeneous expression of the embryonic transcription factors Oct4 and Nanog was seen within the tumor. Although no definitive surface marker was found for prospective isolation of the CIC populations, the self-renewal capacity was imparted by the de-differentiation function of the oncogenic fusion protein SS18-SSX [120]. In a zebrafish model of ERMS a subpopulation of tumor cells resembling activated satellite cells was identified based on increased self-renewal capacity *in vivo* [48]. All reports that have studied CIC populations in osteosarcoma note that the pluripotency genes Nanog, Oct4 and Sox2 were enriched in the self-renewing tumorigenic subpopulations [104, 126]. Functionally Oct4 and Sox2 have been validated as maintaining CICs in osteosarcoma by different studies [138-139]. Interestingly, Sox2 expression correlated with the previously described Sca-1 marker. Whether the Sox2 expressing cells are also Oct4 positive has not been investigated.

4.4.2.2. Quiescence

Analogous to most normal stem cells, CICs could be quiescent and hence not affected by drugs that target actively proliferating cells. Quiescent cells can be identified by their retention of lipophilic membrane dyes such as PKH26. It was observed in osteosarcoma cell lines that 8-25% of the total population consisted of quiescent cells that were capable of long-term sphere formation

and *in vivo* tumor formation at lower numbers. However drug resistance was not directly addressed [124].

4.4.2.3. Drug resistance

Clinically relevant cancer stem cells could express membrane proteins that are able to efflux drugs or enzymes that are capable of drug detoxification. Therefore the property of drug resistance could be used to identify CIC populations.

Side Population analysis

Cells that express the drug efflux protein family including ABCG2 and MDR1 can be isolated by their property to efflux the DNA binding dye Hoechst 3342 using flow cytometry. These cells are labeled as 'Side Population' (SP) and have been shown to have stem cell-like properties. Although isolation of SP cells has been carried out in various sarcoma entities of pediatric and adult origin their stem cell characteristics have not been proven in all cases [140-144]. This could be due to the various technical aspects of SP analysis which makes reproducibility difficult, for example Ewing sarcoma cell line SK-ES-1 was shown to contain 1.2% SP cells in one study [143] which is ten times greater than what was previously reported [142]. Also the inherent toxicity of the Hoechst dye labeling skews the read out of tumorigenicity *in vivo*. Recently, using primary osteosarcoma cells from an undefined age group Yang *et al.* showed that the isolated SP cells were capable of higher tumorigenicity *in vivo* and more resistant to commonly used chemotherapeutics such as doxorubicin, cisplatin and methotrexate [122]. The SP cells have been reported to be heterogeneous in their tumor initiating capacity indicating that there could be room for further enrichment by combining with other CIC markers and features [109, 145-146]. However none of the previously identified osteosarcoma CIC markers, such as CD133 and CD117, segregated with the SP cells [122].

Aldehyde dehydrogenase activity

A method to identify cellular populations that would be resistant to alkylating drugs measures the activity of a detoxification enzyme Aldehyde Dehydrogenase 1 (ALDH1) using flow cytometry. Recently, a population with high activity of ALDH1 ($ALDH1^{high}$) was identified in pediatric OS99-1 osteosarcoma cell line which was tumorigenic at lower numbers than the low ALDH1 activity cells and could additionally self renew *in vivo* [147]. Interestingly it was shown that the proportion of $ALDH1^{high}$ population increased in xenotransplanted tumor in comparison to cell lines which highlights the importance of *in vivo* niche-dependent effects. In Ewing sarcoma cell lines and early passage primary xenografts a small population of $ALDH1^{high}$ cells was noted. When the cells with high and low ALDH1 activity were isolated and injected in immunocompromised mice only 0.6%

of the ALDH1^{high} cells were capable of tumor formation [117]. Similar to SP analysis not all ALDH1^{high} cells were capable of tumor initiation. The authors also used CD133/2 to isolate tumorigenic population and concluded that ALDH1 activity was a better marker. However, the CD133/1 epitope has been established as a Ewing sarcoma stem cell marker and hence it is still unclear whether CD133/1 expression or ALDH1 activity marks stem cell-like cells. Interestingly the ALDH1^{high} cells were shown to be resistant to doxorubicin, a characteristic which has not yet been proven for CD133/1^{+} cells.

Selection under drug treatment

Drug treatment could also be used to enrich for tumor cells with resistance capacity, and consequently responsible for tumor relapse [148]. Therefore to select for cells with drug resistance properties osteosarcoma cell line MG63 was treated with a PARP inhibitor [149] or grown as spheres in media containing vincristine, a commonly used drug in clinics [111]. Treatment with PARP inhibitor led to the formation of a heterogeneous cell line with high sphere forming capacity and differentiation potential. The spheres formed under vincristine selection were enriched for total CD133 and drug efflux proteins. A non-tumorigenic pediatric osteosarcoma cell line HOS and ARMS cell line Rh4 were selected for cisplatin resistance and it was found that the resistant cells had an increased SP profile. Interestingly cisplatin treated HOS SP cells were capable of tumor formation *in vivo* [146]. Similarly, the SP proportion within UPS xenotransplanted tumors increased considerably when treated with conventional chemotherapeutics *in vivo* [144].

Motility and hypoxia

It is also possible that the CIC property is a function of the environment and hence recreating an appropriate niche could select for cells with self-renewal capacity. Side population cells were collected from ARMS cell line Rh4 and allowed to migrate to media containing high levels of SDF1α. The cells were found to have higher migration capacity and also increased tumorigenicity in mice. Also the migratory SP fraction increased when cells were briefly exposed to hypoxia. Interestingly the tumorigenicity of the migratory hypoxic SP cells was increased by 4000 fold [145]. Simulation of bone hypoxic environment led to increased osteosarcoma sphere formation [126].

4.5. Characterization of sarcoma initiating cells

The primitive cellular subpopulations, once identified and isolated, must fulfill certain functional criteria before being designated as bona fide stem cell-like CIC population.

4.5.1. Tumor initiation and self-renewal *in vivo*

One of the key properties that a CIC population must possess is that of long-term self-renewal. Although the *in vitro* sphere formation assay is indicative of a self-renewing population it is not always definitive [81, 110, 134]. Therefore higher propensity for tumor initiation must be shown *in vivo* by limiting dilution and preferably the self-renewing capacity of the subpopulation elucidated by serial transplantation. Earlier studies on osteosarcoma stem cells did not include *in vivo* validation [125]: either the experiments were not attempted or the tumor cells were deemed to be graft resistant [109]. However recent work has shown that it is indeed possible to grow osteosarcoma cell lines and even primary cells in immunocompromised mice [122-124, 139, 146, 150]. Importantly some of these studies also showed that the subpopulations could self-renew *in vivo* [122-123, 139, 150]. Similar results have been obtained for ERMS [48, 114], ARMS [145-146], Ewing sarcoma [116-117, 130], and UPS [144].

4.5.2. Stem cell phenotype and differentiation potential

Osteosarcoma, Ewing sarcoma and synovial sarcoma initiating cells have been shown to possess mesenchymal stem cell features [104, 107, 120]. The gene expression profile of ERMS spheres resembled that of neurospheres and glioma patient samples indicating a neural background [114]. ERMS stem cells have also been known to possess a more lineage restricted phenotype. ERMS sarcospheres were enriched for neural crest and myogenic lineage-specific stem cell genes such as PAX3 and PAX7 while downregulating genes important in myogenic differentiation [114] and similar results observed for the $CD133^+$ ERMS cells [129]. The ERMS stem cells identified from RAS-dependent sarcomas were noted to have an activated satellite cell gene expression profile.

Sarcoma initiating cells have been shown to be enriched for various genes that are important for embryonic stem cell self-renewal including Oct3/4, Nanog and Sox2. These transcription factors are enriched in sarcospheres and in sorted CIC populations from various sarcoma entities. Although Oct4 expressing cells were specifically shown to have CIC properties in osteosarcoma the role of Oct4 in sarcoma biology has not been established due to experimental and biological limitations [100]. Sox2 expression in osteosarcoma seems to maintain Sca-1 expression and the undifferentiated state of the tumor-initiating population [138]. In Ewing sarcoma it was shown that expression of Sox2 had a functional consequence in tumorigenicity of cell lines and that Sox2 is a target gene of EWS-FLI1 [151]. The fusion protein in synovial sarcoma seems to also confer

'stemness' to the tumor cells [120]. The expression level of PAX3-FOXO1 determined the tumorigenicity capacity of ARMS cells [40, 152]. Thus in the case of the translocation-positive sarcomas the oncogenic fusion proteins could orchestrate the stem cell phenotype in tumor cells. Other stem cell associated genes used to characterize sarcoma stem cells are Bmi-1, Stat3, Nucleostemin, Msx1 and Nestin [106].

Functionally, a stem cell possesses the ability to differentiate into various lineages. The multi-potential characteristic of sarcoma initiating cells could explain the observed heterogeneous cellular populations within the tumor that display immunophenotype of different germ layers. Accordingly many reports have shown that sarcospheres are capable of differentiating into multiple lineages [114, 116, 123, 125].

4.5.3. Quiescence and rarity

These properties of CSCs are not directly implied by the CSC model [94]. CICs could boast higher proliferation in order to increase tumor aggressiveness. The $CD133^{+}$ cells from osteosarcoma cell lines were shown to have a higher rate of proliferation [109]. The pediatric sarcoma fusion proteins, that mediate 'stemness', are intrinsically necessary for cancer cell proliferation. The rarity of CICs has also been questioned. Contextual factors such as genetic heterogeneity, depth of differentiation hierarchy and microenvironment could influence the proportion of CICs within a tumor. The large proportion (45%-75%) of osteosarcoma cells was found to be Sox2-Sca-1^{high} [138].

4.5.4. Drug resistance

The clinically relevant property of CICs is their acquired resistance to conventional drug onslaught. This has been shown conclusively in a variety of adult cancer entities (Fig. 9).

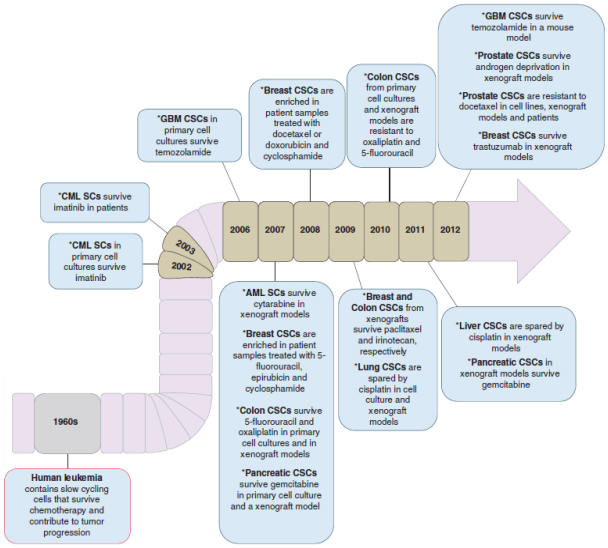

Figure 9. Timeline of milestone studies that demonstrate how CSCs (CICs) contribute to the acquisition of chemotherapy resistance: first shown in leukemia (red box) and consequently demonstrated in a

variety of tumor types (black box). AML, acute myeloid leukemia; CML, chronic myeloid leukemia; GBM, glioblastoma multiforme. Adapted from [153].

In pediatric sarcomas: osteosarcoma, Ewing sarcoma and ERMS initiating cells isolated using different techniques have been reported to be resistant to commonly used therapeutics such as cisplatin, doxorubicin, daunorubicin, methotrexate, etoposide, vincristine and chlorambucil [114, 117-118, 122-123, 135, 143, 154-155]. The use of conventional chemotherapy decreased UPS tumor growth *in vivo* but it did not affect the ability of the cells to form tumors upon serial transplantation [144]. Stro-1^+ human osteosarcoma cells were specifically found to be enriched for the drug efflux protein ABCG2 [123]. The theoretical consideration earlier was that a stem cell nature implied quiescence and hence only a minimal effect of a DNA damaging agent. However most reports on sarcoma initiating cells have not specifically highlighted a slower cell cycle kinetic for the CIC compartment. An alternative explanation for resistance to replication stress inducing drugs could be efficient DNA repair mechanisms. It was shown that osteosarcoma and Ewing sarcoma sphere cells over-express DNA mismatch repair genes MLH1 and MSH2 [135]. Gene ontology analysis of ERMS spheres showed that DNA mismatch repair pathway was significantly overrepresented (Satheesha S., unpublished data). Anti-apoptotic pathways have also been shown to be activated in osteosarcoma cell line selected for resistance to PARP inhibition [115].

There are some limitations and caveats to the studies discussed above. Since pediatric sarcomas are rare malignancies most of the data collected have been from cell lines or their xenografts in immunocompromised mouse models. However, wherever possible the existence of sarcoma initiating cells needs be directly validated using primary patient material and/or transgenic animal models. Alternatively the identified marker or pathway could also be validated retrospectively on a large cohort of patient samples as was done for CD133 in ERMS where high CD133 expression significantly associated with lower overall survival [114] and in osteosarcoma where CD133 expression positively correlated with lung metastasis and proved to be an independent prognostic marker [156]. Technical caveats such as limited reproducibility of the SP analysis or lack of adherence to the CD133 epitope status across studies makes generalizations difficult at the moment. Also, care must be taken as to the use of the most stringent mouse model. It is interesting to note that the site and media composition of tumor cell engraftment had a critical role in not only primary tumor generation but also formation of metastasis, especially in osteosarcoma [124, 149]. This highlights the importance of niche factors in the tumorigenicity of cells and consequently the significance of orthotopic engraftment routes. Technical aspects of primary tumor tissue handling, such as enzymatic digestion and engraftment media composition, could have profound effects on tumor formation *in vivo* and therefore affect the robustness and reproducibility of the CIC marker.

Despite these concerns, the data taken together seem to indicate that many pediatric sarcoma entities contain a subpopulation of highly tumorigenic cells that are multipotent and capable of self-renewal *in vitro* and *in vivo*. It is possible that the property of quiescence cannot be universally applied to all sarcoma initiating cell populations and the proportion of cells within a tumor that possess stem cell-like properties is unclear as this appears to depend on the isolation technique used. Along with intra-tumoral, inter-tumoral heterogeneity will play an important role in dissecting the sarcoma stem cell biology and also establish its clinical significance [157]. Nonetheless, researchers have already begun to analyze pathways that are activated in the sarcoma initiating cells in order to present novel targeting options.

4.6. Targeting sarcoma initiating cells

4.6.1. Pathways conferring growth advantage

Oncogenic pathways that provide the sarcoma initiating cells with their increased tumorigenic capacity are largely unresolved. Most commonly cell cycle and DNA repair regulatory pathways have been identified as being important. In osteosarcoma and Ewing sarcoma sphere cells it was noted that the expression of p14INK4a/p19ARF was reduced [135]. Also pediatric MSCs had a decreased expression of p14INK4a which could account for the higher cellular proliferation and possibly the permissiveness for EWS-FLI1 expression [151]. The expression of enzyme RECQL involved in DNA repair was downregulated in the quiescent osteosarcoma stem cell population implying higher genetic instability within this population [124]. Patients with loss of function mutations in RECQL have a higher incidence of osteosarcoma than the general population but as of yet the role of RECQL in sporadic osteosarcoma has not been established.

Growth factor pathways have also been implicated in sarcoma initiating cell maintenance. Cisplatin resistant osteosarcoma and ARMS SP cells displayed autocrine VEGF signaling which was dependent on increased MAPK-ERK pathway activity and therefore sensitive to MAPK or VEGF inhibition [146]. Also RAS-dependent ERMS initiating cells were shown to express high levels of c-MET/HGFR. Ewing sarcoma stem cells have been shown to employ microRNAs (miRNA) to sustain a stem cell phenotype [158-159]. The expression of EWS-FLI1 in pediatric MSCs led to reprogramming of the cells to assume a primary Ewing sarcoma phenotype by repressing the expression of miRNA-145 [107]. Further investigations revealed that the CD133/1^{+} fraction of Ewing sarcoma cells show disrupted TARBP2-depedent miRNA processing which seems to be important for the CIC-like nature of the cells [158]. By increasing the activity of TARBP2 using enoxacin, an antibacterial agent of the fluoroquinolone family, the *in vitro* spherogenicity and *in vivo* tumor growth of Ewing sarcoma xenografts was reduced. Alternatively

the fusion protein activity or expression could be directly inhibited to attenuate the CIC phenotype [117, 135].

4.6.2. Developmental pathways affecting differentiation and survival

The course of organ development seems to be closely linked with tumorigenesis [160] and therefore pathways playing important roles in organismal development such as Wnt, Hedgehog, Notch and TGFβ have now been linked to initiation and progression of different cancer entities. It is becoming increasingly apparent that these pathways could affect tumor cell differentiation and thereby modulate CIC properties [161-170].

4.6.2.1. Wnt signaling pathway

Wnt signaling dictates cell fate determination, polarity and adhesion and development of various organ systems and tissue self-renewal in certain adult organ systems [171]. In mammals Wnt proteins consists of 19 highly conserved glycoproteins that serve as secreted ligands for the Frizzled (Fz 1-10) receptors. Depending on the combination of Wnt-Fz receptor complex formed receptor could initiate two signaling cascades (Fig. 10): canonical (Wnt/β-catenin) and non-canonical (Wnt/Ca^{2+} or planar cell polarity; PCP).

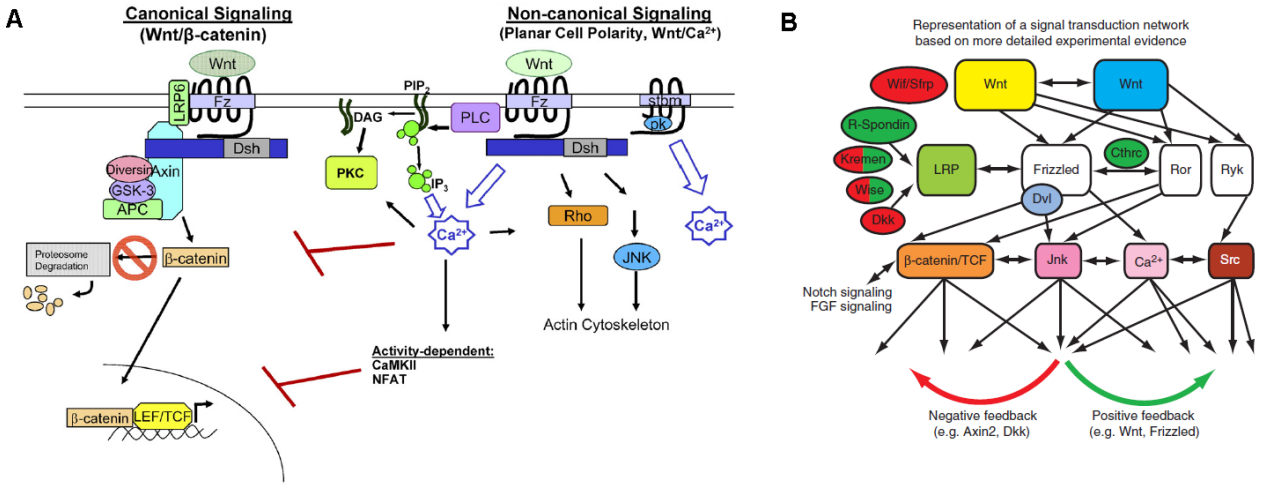

Figure 10. Schematic representation of the Wingless/Wnt signaling network. (**A**) Major arms of the Wnt signaling system. Adapted from [172]. (**B**) Recent studies show that the seemingly distinct Wnt pathways behave as a network. Adapted from [170].

In the canonical pathway binding of ligand to receptor complex of Fz and LRP5/6 (member of the LDL receptor family) leads to stabilization of β-catenin whereupon it translocates to the nucleus to form a transcription activator complex with T-cell factor/lymphois-enhancer factor (TCF/LEF). The target genes include MYC, CCND1 among others. In the absence of the ligand β-catenin is phosphorylated by GSK3β and CK1 within the 'destruction' complex formed by Adenomatous polyposis coli (APC) and Axin proteins. The phosphorylation primes β-catenin for proteosomal

degradation. The ligand binding inhibits the activity of GSK3β via Dishevelled (DSH). The non-canonical pathway is considered to be β-catenin independent. It involves signaling via receptor tyrosin kinases (RTKs) such as Ror and Ryk, small Rho GTPases, c-Jun N-terminal Kinase (JNK) and induction of intra-cellular Ca^{2+} fluxes to affect organ morphogenesis. Recent data shows that the two seemingly distinct pathways could behave as an integrated network fine-tuned to the demands of the environmental context [170].

4.6.2.2. TGFβ signaling pathway

TGFβ plays an important role in, germ layer specification, vertebrate patterning, and organogenesis during embryonic development, and in the homeostatsis and regeneration of adult tissues [165]. The ligand families that can activate the TGFβ superfamily include TGFβ (1-3), bone morphogenetic proteins (BMPs), growth and differentiation factors (GDFs), anti-Müllerian hormone (AMH), Activins and Nodal (Fig. 11). The secreted ligands bind and bring together two transmembrane serine-threonine kinases, known as receptor types I (also called Activin-receptor like kinases, ALKs; 1-7) and II (5 types). Upon ligand activation type II receptor phosphorylates type I receptor, which then leads to phosphorylation of regulatory Smads (1, 2, 3, 5 and 8). The type of Smad phosphorylated is again specific to the ligands that initiate the signal. The phosphorylated Smads generally complex with a common mediator, Smad4, translocate to the nucleus and bind to other transcription factors and nuclear co-factors for context-specific gene expression [162].

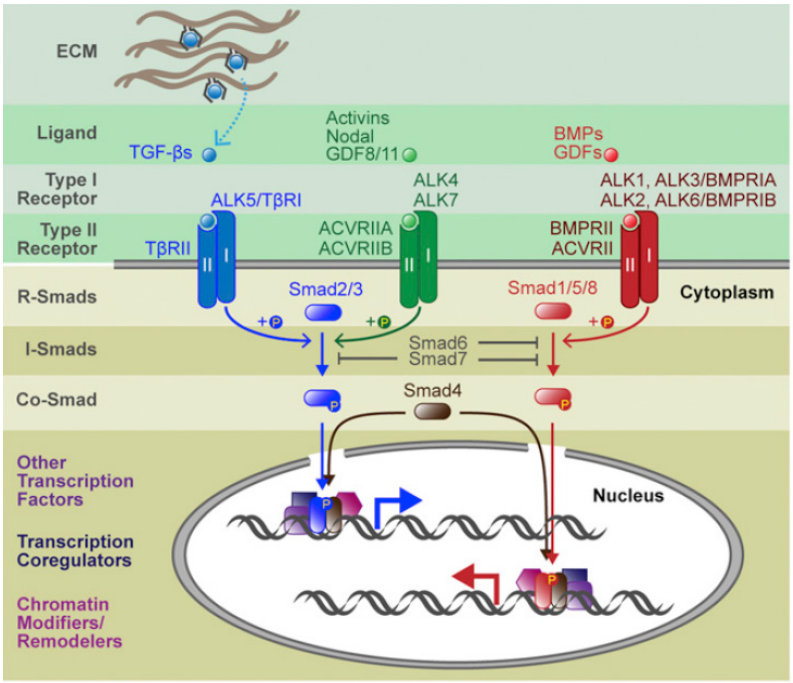

Figure 11. Canonical signaling pathways of the TGFβ supefamily. [165]
ECM, extracellular matrix; R-Smads, Regulatory Smads; I-Smads, Inhibitory Smads

4.6.2.3. Notch signaling pathway

Notch signaling is evolutionary conserved pathway with critical roles during embryogenesis and development of various organ systems; in cell communication, differentiation, proliferation and survival [163]. The pathway is activated via cell-cell contact mediated though ligand-receptor binding. Mammalian membrane-bound Notch ligands occur is two distinct families: Delta-like ligands (DLLs -1, 3 and 4) and Jagged (JAGs: 1 and 2) (Fig. 12). There are four Notch receptors (NOTCH 1-4) that bind to the ligands via extracellular domain with EGF-like repeats. Upon ligand binding, proteolytic cleavages by metalloprotease and gamma.secretase lead to the release of active Notch intra-cellular domain (NICD) into the cytoplasm. NICD translocates to the nucleus and binds to CSL (CBF1/Suppressor of Hairless/LAG1)/RBPJ transcription factor complex to activate or derepress via binding of mastermind-like proteins (MAMLs 1-3) to transcribe of target genes. The downstream targets include HES family of transcription factors, PI3K, AKT, MYC, p21 among others.

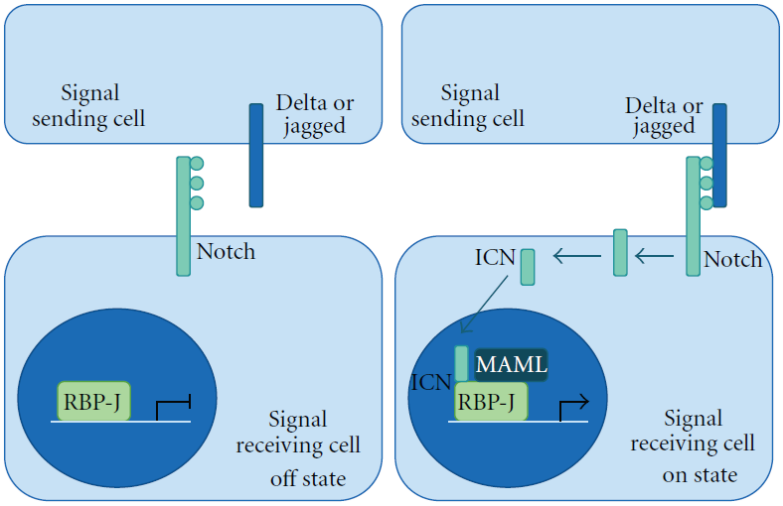

Figure 12. Overview of the Notch pathway. [52]
ICN: Intra-cellular Notch (referred to as NICD in the text)

4.6.2.4. Hedgehog signaling pathway

The hedgehog pathway plays an important role in tissue patterning and stem cell maintenance during embryogenesis. It is essential for the development of epidermal and neural tissues [173]. The hedgehog signaling pathway outcome is determined by balance between the activator and repressor functions of the GLI transcription factors – GLI1, GLI2 and GLI3 (Fig. 13). GLI1 is the most potent transactivator without a repressor function, GLI2 can act as an activator or repressor and GLI3 is mainly a repressor with weak transactivating potential. The pathway is activated by binding of secreted ligands – Sonic (SHH), Indian (IHH) or Desert (DHH) – to the inhibitory transmembrane receptor Patched (PTCH1/2) which causes its internalization and thereby allowing the translocation of Smoothened (SMO) to the primary cilium. Once SMO is in the primary cilium it initiates

downstream events, that are not yet fully characterized, which finally culminate in the dissolution of the inhibitory Suppressor of Fused (SUFU)-GLI complex leading to the formation and stabilization of transactivated GLI transcription factors. The target genes of the pathway include GLI1, GLI2, PTCH1, HHIP, CCND1 and others.

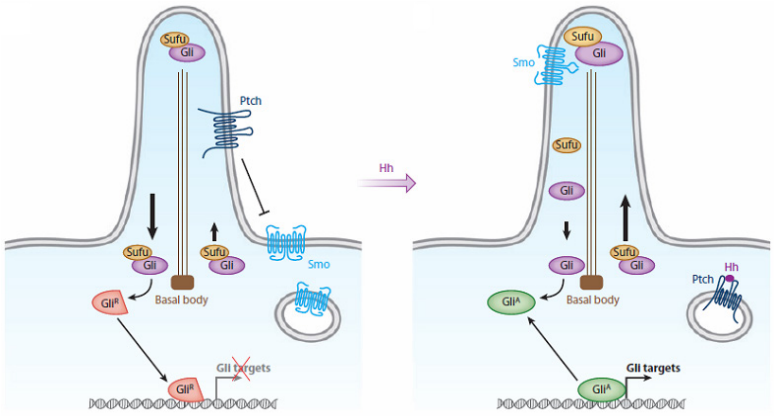

Figure 13. Overview of the hedgehog signaling in mammals. [173]

The effect of these pathways has been better established in adult CICs than pediatric (Table 3); although the signaling systems have been shown to be active and functionally important in pediatric cancers.

Recently, activation of canonical Wnt pathway across the sarcoma spectrum was reported [174]. The study concluded that the effect of Wnt signaling in initiating a stem cell-like phenotype was overshadowed by other mutations within the cells; however this was not directly addressed. In Ewing sarcoma it was recently shown that canonical Wnt signaling pathway can be activated using Wnt ligands and further potentiated by R-spondin which is known to bind LGR5. Activation of Wnt signaling or LGR5 overexpression had no effect on proliferation; however it remains to be seen if it could enhance self-renewal [131]. On the other hand, activation of canonical Wnt signaling seemed to differentiate osteosarcoma stem cells [104, 138]. Recently it was shown that in osteosarcoma the switch from canonical Wnt signaling to non-canonical Jun-based signaling by secretion of DKK1 (Dickkopf-related protein 1) led to the upregulation of CIC marker ALDH1 [175]. Activation of non-canonical Wnt signaling was necessary for derivation of UPS from MSCs [61, 64]. The upregulation of receptors for non-canonical Wnt signaling, FZD2 and FZD3, was observed in ERMS sphere cells [114]. Recently, inhibition of canonical Wnt signaling using GSK3β inhibitors was shown to suppress ERMS self-renewal and tumor growth [176].

Table 3. Developmental pathways shown to be important for adult CICs and pediatric cancers.

Developmental pathway	Adult CICs*	Pediatric sarcomas		Other pediatric solid cancers	
		Associated	*CIC*	*Associated*	*CIC*
Wnt ***Canonical***	Breast, CRC, GBM, CML, AML, cutaneous cancers [153, 167-168, 177]	Sarcoma in general [174], subset of ERMS [41-42, 178], pro-differentiation in RMS and OS [52, 98, 178-181], ES [131, 182], SS [183]	Pro-differentiation in OS [104, 138] and ERMS [176]	Subset of MB, Wilms' tumor, ependymoma, hepatoblastoma, PNETs [184-185]	*Not reported*
Non-canonical		UPS** [61]	OS [175]		
TGFβ	Breast, CML, pancreas, Pro-differentiation in SCC, GBM and CRC [153, 165]	RMS [186], Pro-differentiation in OS [98], SS [187], ES [37]	OS [126]	Subset of MB [188], ependymoma, PNETs [189], Wilms' tumor [190]	*Not reported*
Notch	GBM, breast, NSCLC, prostate, CRC [153, 166, 168]	RMS [52, 181, 191-192], UPS** [193], OS [194-195], ES [37], SS [196]	UPS** [144]	Ependymoma, MB, NB [197]	MB [184]
Hedgehog	Multiple myeloma, GBM, breast, prostate, CML, CRC, melanoma, pancreas [153, 164, 168, 198]	ES [37], ERMS [52, 181], OS [98, 199-200]	UPS** [144]	Ependymoma, hepatoblastoma, Wilms' tumor, subset of MB, NB [106, 185, 199-201]	MB [184], NB [201], DIPG [202]

* Primary studies within the referenced reviews

** Relevance to pediatric UPS unclear

AML, acute myeloid leukemia; CML, chronic myeloid leukemia; CRC, colorectal cancer; DIPG, diffuse intrinsic pontine glioma; ES, Ewing sarcoma; GBM, glioblastoma multiforme; MB, medulloblastoma; NB, neuroblastoma; NSCLC, non-small cell lung cancer; OS, osteosarcoma; PNETs, primitive neuroectodermal tumors; SCC, squamous cell carcinoma; SS, synovial sarcoma

TGFβ signaling has been shown to be an important mediator of self-renewal in osteosarcoma [104]. Osteosarcoma ALDH1^{high} cells overexpressed BMP receptors and BMP-2 treatment led to a decrease in tumorigenicity of ALDH1^{high} cells *in vivo* [150]. Furthermore TGFβ1-induced dedifferentiation of osteosarcoma cells led to the upregulation of various components of the Notch, IGF and PDGF pathways, making it a very interesting signaling node for future studies [126]. The gene expression profiling of osteosarcoma stem cells isolated based on their property of quiescence also revealed upregulation of IGF1 and IHH [124]. The importance of IGF, Hedgehog and TGFβ pathways has been previously implicated in osteosarcomagenesis [98]. Wang *et al.* have observed that SP cells from primary UPS samples expressed higher levels of Hedgehog and Notch pathway components. Inhibition of these pathways *in vivo* decreased the tumor growth and also markedly reduced the tumor initiation capacity of these cells upon serial transplantation in secondary and tertiary recipients [144]. Studies on the roles of Notch and hedgehog signaling in muscle differentiation and RMS tumorigenesis have revealed that their targeting could offer clinical benefit; however their effect on RMS 'stemness' has not been directly investigated [52, 181]. Overall, the function of developmental pathways in sarcoma initiating cells is slowly being elucidated and is a prime avenue for future research. The study of such pathways not only offers rationale for CIC-appropriate treatment but also presents insights into the origins of sarcoma initiating cells.

5. Subject of Investigation

Rhabdomyosarcoma is the most common pediatric soft tissue cancer which is currently treated using conventional multimodal strategies that entail severe acute and chronic morbidity. Furthermore under recurrent and metastatic setting these treatments are ineffective. Therefore there is an urgent need to find rationale-based novel treatment avenues to ensure a long-term cure for the patients with minimal impact on quality of life. Our main aim was to understand the biology of RMS initiation, maintenance and progression to offer new perspectives for translational medicine. To this end we set out the following aims,

1. To elucidate if RMS tumors were hierarchically organized.

2. To characterize the signaling mechanism(s) and/or genes that could contribute to the maintenance of self-renewal and tumor initiating capabilities of the cancer initiating populations.

It would be important to understand if RMS tumors contained tumor cell compartments with enhanced ‘stemness’ and tumorigenic potential since clinical intervention would then need to include drugs that could specifically target these populations. The immunophenotype of the RMS stem cell-like CICs could be used for prognostic risk stratification and as biomarkers during clinical trials. Furthermore the developmental hierarchy of RMS could also provide insight into its origins, which would have significant impact on disease modeling.

6. Results

6.1. CD133 Positive Embryonal Rhabdomyosarcoma Stem-Like Cell Population Is Enriched in Rhabdospheres

Dagmar Walter, **Sampoorna Satheesha**, Patrick Albrecht, Beat C. Bornhauser, Valentina D'Alessandro, Susanne M. Oesch, Hubert Rehrauer, Ivo Leuschner, Ewa Koscielniak, Carole Gengler, Holger Moch, Michele Bernasconi, Felix K. Niggli and Beat W. Schäfer. Part of this study was conducted in cooperation with the CWS Study Group

PLoS ONE e6(5): e19506 (2011)

Summary

We show that highly tumorigenic stem cell-like cells could be enriched from human ERMS cancer cell lines using the neurosphere assay. In an orthotopic tumor model 100 fold less sphere cells were required for tumor initiation compared to adherent cells. The expression of stem cell genes like OCT4, NANOG, SOX2 and C-MYC was increased in the sphere cultures (rhabdospheres). The sphere cells were capable of differentiation into mesenchymal and neuronal lineages. The gene expression profile of rhabdospheres was more similar to that of neural stem cells and glioma patients than mesenchymal stem cells. Rhabdospheres contained a greater number of CD133 expressing cells compared to the adherent cells. Adherent ERMS cell expressing CD133 were more chemoresistant *in vitro* and more tumorigenic *in vivo*. The expression of CD133 in ERMS patient samples predicted worse overall survival.

Conclusions and significance

ERMS tumors seem to be hierarchically organized wherein a subpopulation of cells have enhanced self-renewal and tumor initiation capacity. The optimized rhabdosphere culture system, described here for the first time, provides an easy method evaluate and enrich for self-renewing cells. The neural crest phenotype of rhabdospheres indicates a pre-myogenic origin for ERMS. The report is also the first to show that CD133 expression could be used prospectively to isolate functionally important cells in ERMS. Additionally CD133 expression could be used as a prognostic marker in ERMS. Overall, the report presents novel insight into the biology of ERMS. Its findings have been reproduced and expanded upon by an independent study [129].

For contribution and detailed information see attached manuscript (section 11).

6.2. Targeting hedgehog signaling reduces self-renewal in Embryonal Rhabdomyosarcoma

Sampoorna Satheesha, Amandine Bovay,* Gabriele Manzella,* Elisa A. Casanova, Peter Bode, Réka Belle, Simone Feuchtgruber, Patricia Jaaks, Nurhak Dogan, Ewa Koscielniak, and Beat W. Schäfer

Manuscript under review at *Stem Cells* (submitted April 2014). * Equal contribution

Summary

Using clinically relevant synthetic small molecules and genetic loss- and gain-of-function approaches we show that active hedgehog pathway is necessary for self-renewal *in vitro* and *in vivo* tumor initiation. We provide novel mechanistic insights into ligand-based activation of hedgehog signaling in sporadic ERMS. Additionally we describe novel roles for hedgehog pathway in determining ERMS cell motility, differentiation status and chemoresistance to anti-proliferative drugs currently used in ERMS clinical management. Our data provides the first indications of novel cross-talk between hedgehog pathway and other developmentally important pathways, such as Notch, TGFβ-BMP and Wnt in ERMS. We identify NANOG as a key downstream effector for hedgehog pathway-mediated stemness, previously unknown in any soft tissue sarcoma. Importantly we could demonstrate translational relevance of our findings by showing that functional intra-tumoral heterogeneity measured by the presence of hedgehog-active CICs ($GLI1^+$ and $NANOG^+$) in ERMS patients has significant prognostic impact.

Conclusions and significance

Our study identifies the hedgehog pathway as being instrumental in maintaining the stem cell functions of ERMS CICs. This pathway has been implicated in ERMS tumorigenesis previously [52]; however its specific function was unknown. This is the first report to show that the hedgehog pathway could control CIC properties in a pediatric sarcoma. Also, our data suggests that a combinatorial approach using hedgehog inhibitors would increase treatment efficacy. SMO targeting for progressive rhabdomyosarcoma is already in clinical trial as a single agent (clinicaltrials.gov; NCT01125800). Additionally, ERMS patients are currently stratified for risk of relapse based on clinical parameters only. We present evidence that evaluating the presence of hedgehog-driven CIC populations within ERMS patients can offer better means of risk stratification which has not yet been possible with mutational status. Our study also emphasizes that novel rationally selected treatment strategies need to take into account not only the mutational background but also the hierarchical organization of the tumor. Furthermore, CIC-targeting requires updating the current clinical trial management protocols since the biomarkers and end points used to estimate treatment efficacy would be conceptually altered. Therefore our findings not only advance our

perceptions on the functional role of hedgehog pathway in ERMS but are highly relevant to the current and future clinical management of ERMS patients.

For contribution and detailed information see attached manuscript (section 11). *For the purposes of the present thesis the 'long form' of the manuscript is attached which includes a more in-depth description and discussion of the study results.*

6.3. PAX3-FOXO1 increases fibroblast reprogramming efficiency and drives self-renewal in alveolar rhabdomyosarcoma

Elisa A. Casanova, Melanie Generali, **Sampoorna Satheesha**, Peter K. Bode, Paolo Cinelli, Beat W. Schäfer

Manuscript in preparation

Summary

Multiple ARMS cell lines were analyzed using common CSC assays such as tumorsphere formation, ALDH activity and stem cell surface marker expression. However we were unable to identify de-differentiated, self-renewing subpopulations. ARMS cell lines expressed all core stem cell factors (OCT4, SOX2 and NANOG) but surprisingly the alteration in the expression of these stem cell genes has minimal effect on ARMS pathophysiology; which is in mark contrast to the dramatic effect of altering the levels of PAX3-FOXO1 – the key oncogenic fusion protein in ARMS. Interestingly, PAX3-FOXO1 expression increases the efficiency of reprogramming human fibroblasts into induced pluripotent stem (iPS) cells and could also impede the differentiation ability of iPS cells *in vitro* and *in vivo* indicating that PAX3-FOXO1 could promote stem cell behavior. Furthermore, RH30 ARMS cells were capable of tumor initiation at limiting dilutions and RH30 single cell clones had equal capacity to initiate tumors highlighting that probably all ARMS cells behave as cancer stem/initiating cells.

Conclusions and significance

In this study we present evidence that fusion-positive ARMS, contrary to ERMS, does not possess an exclusive subpopulation of CICs but rather each ARMS cell exhibits similar tumorigenic potential that is strictly PAX3-FOXO1 dependent. The effects of the PAX3-FOXO1 on iPS generation and differentiation indicate that the fusion protein controls mechanisms that can confer de-differentiated self-renewal phenotype to all cancer cells. Our study suggests that all ARMS cells would need to be targeted by inhibiting the activity of PAX3-FOXO1 to ensure a cure. This has immense implications for ARMS treatment strategies and additionally underscores the biological difference between the two RMS histotypes. Our study also presents a novel disease model to study the function of PAX3-FOXO1 without the transcriptional noise that is usually present within a cancer cell. Even though the PAX3-FOXO1 iPS cells do not form true ARMS tumors *in vivo*, the model system could be used to verify the genetic or epigenetic hits that are further required to completely transform the cells.

For contribution and detailed information see attached manuscript (section 11).

7. Discussion and outlook

7.1. The hierarchical organization of RMS tumors

In our studies we used *in vitro* self-renewal assays and *in vivo* xenograft formation to assess the presence of functional heterogeneity within RMS tumors. The data presented in articles 1 and 2 indicate that ERMS tumors seem to the follow the cancer stem cell model of tumor progression. ERMS cell lines having a common genetic background contain phenotypically distinct subpopulations of primitive, multi-potential cells with enhanced self-renewal, tumorigenicity and chemoresistance. Additionally we show that the heterogeneous activation of hedgehog pathway within ERMS cell lines and patient samples has functional and clinical consequence. Active hedgehog pathway is necessary to maintain ERMS self-renewal while pathway inhibition leads to ERMS cell differentiation, reduction in tumorigenic potential and increase in sensitivity to conventional chemotherapeutics. Overall our studies show that ERMS tumors possibly present with a 'steep' hierarchical organization, with a minority of primitive/de-differentiated CICs forming the apex while cells with early and late progenitor phenotype contributing to the majority of the tumor bulk (Fig. 14A). On the contrary, the translocation-positive ARMS tumors are composed of a majority of tumorigenic cells with equal propensity for tumor initiation (article 3). The expression of PAX3-FOXO1 within ARMS tumors de-differentiates the cells; determining self-renewal and tumor initiation. Since PAX3-FOXO1 is ubiquitously expressed in majority of ARMS cells the hierarchy is either 'shallow' (determined by PAX3-FOXO1 expression gradient) or non-existent altogether (Fig. 14B).

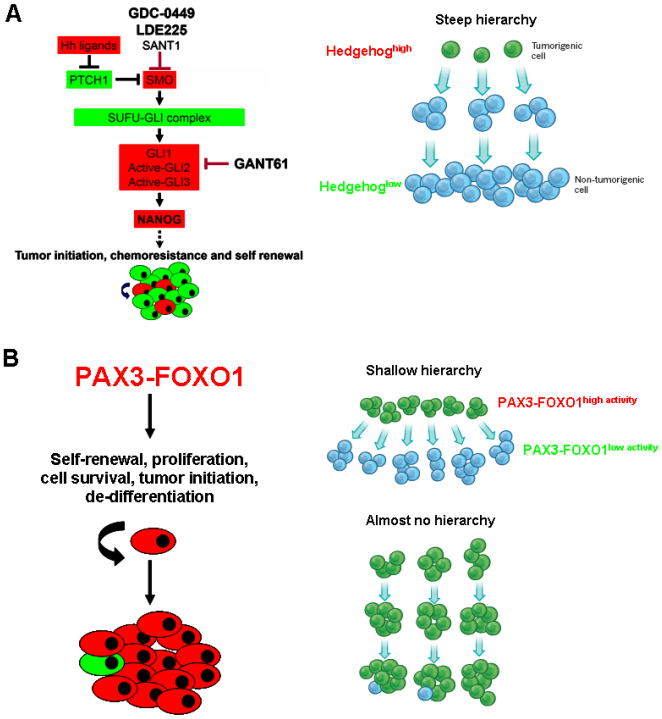

Figure 14. Summary of the RMS tumor progression models elucidated by our studies. (**A**) ERMS tumors contain a subpopulation of hedgehog^{high} compartment characterized by GLI1 and NANOG expression which are

important for tumor maintenance. Thus ERMS tumors could be sustained by a steep hierarchy where majority of tumor cells which are hedgehog^{low} and therefore non-tumorigenic. Drugs indicated in bold are small-molecule inhibitors used in our study. (**B**) ARMS tumors are maintained by PAX3-FOXO1 activity which confers all cells with tumor-initiating features. Thus ARMS tumors could present with either shallow hierarchy based on PAX3-FOXO1 activity or no hierarchy at all. Images on the right side depicting hierarchy adapted from [96].

7.1.1. Markers for ERMS CICs and their regulation

7.1.1.1. GLI1-NANOG

We identified GLI1-NANOG axis as a key determinant of hedgehog-driven ERMS CICs (article 2). GLI1 is considered to be the most reliable marker for active hedgehog signaling [173]. This particular signaling node has been shown to be functionally important in the self-renewal of normal neural, glioma and medulloblastoma stem cell [203-204]. NANOG is part of the core transcriptional factor network, including OCT4 and SOX2, which is essential for the establishment of pluripotency in embryonic stem (ES) cells. These three genes regulate each others' expression and thereby are maintained at defined expression levels leading to an optimal self-renewal phenotype [205]. Interestingly, although the expression of OCT4 and SOX2 is uniform across all ES cells, NANOG expression seems to be heterogeneous – similar to what we have noted in ERMS cells and tumors. It appears that ES cells with lower NANOG expression have a greater propensity to differentiate allowing for important cell fate decisions [206-207]. Navarro *et al.* reported that NANOG heterogeneity in ES cells is mediated by an auto-repression mechanism through unknown binding sites which is OCT4/SOX2 independent [208]. However recent work has shown that heterogeneous expression of NANOG may be a cell culture artifact with little effect on *in vivo* cell fate decisions for ES cells [209]. Even so, heterogeneous expression of NANOG has been noted in multiple cancer types and therefore could be specifically important for CIC functions [210-211].

With the increasing evidence for the important role for NANOG function in cancer it has become imperative to understand NANOG regulation and downstream targets. Embryonic genes are subject to transposition and therefore apart from the embryonic NANOG gene (*NANOG1*; Chr. 12) eleven pseudogenes have been reported in the human genome [212]. Of these only one psuedoegene (*NANOGP8*; Chr. 15) possesses a complete open reading frame and gives rise to a functional protein with one amino acid different (Q253H) from embryonic NANOG. In ES and teratoma cells NANOG protein is derived from *NANOG1* mRNA, however in carcinomas and glioblastoma it seems to be derived either predominantly from *NANOGP8* or from both loci [204, 213-214]. The determination of the loci contributing to the expressed NANOG protein becomes important when investigating gene expression regulation: since the *cis* and *trans* genomic elements associated with either loci would be different. Moreover a recent study in ES cells suggests that the *NANOG1* locus itself is involved in genome-wide chromatin interaction that has functional consequences [215]. Our efforts to identify the mRNA variant expressed in ERMS revealed that *NANOG1* could contribute to the majority of NANOG protein expressed (data not shown). Although it is assumed that *NANOG1*

regulation could be important in ES cells and *NANOGP8* is important in tumorigenesis the regulation of NANOG expression in cancer seems to have been largely centered on the *NANOG1* locus leading to elucidation of many upstream regulators of unclear significance (Fig. 15A). However, in the context of hedgehog signaling GLI binding elements are present in the promoter region of *NANOG1* and *NANOGP8* [204]. Therefore, at least in the system that we describe, NANOG protein expression need not be subject to differential gene loci regulation.

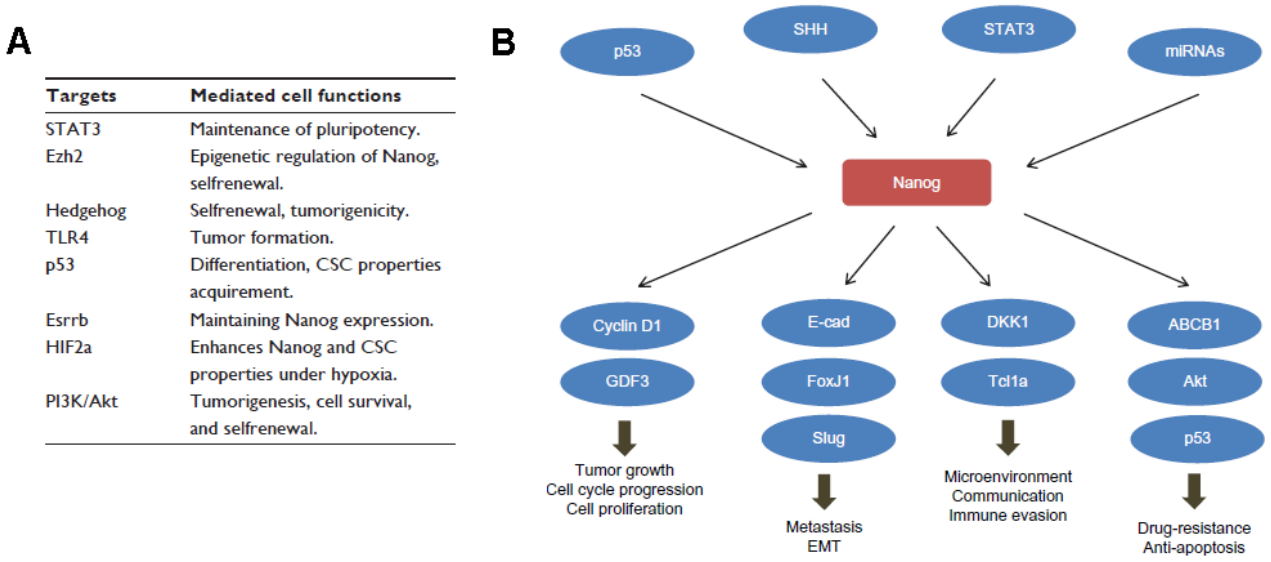

Figure 15. Pathways converging on NANOG. (**A**) Upstream regulators of NANOG. (**B**) Schematic representation of the central role of NANOG in signaling networks perpetuating many cancer hallmarks. Figures adapted from [211]. E-cad, E-cadherin; Esrrb, estrogen-related receptor β; GDF3, growth differentiation factor-3; STAT3, signal transducer and activator of transcription 3; Ezh2, enhancer of zeste homolog 2; Tcl1a, T-cell leukemia/lymphoma protein 1A; TLR4, toll-like receptor 4.

Investigation into the biochemical differences between the proteins encoded from the two loci indicated that NANOG1 and NANOGP8 proteins possibly assume different conformations [216]; however there seem to be no major functional differences between them. Currently available antibodies detect total NANOG protein and therefore for functional analysis most studies do not make a distinction between the two forms. NANOG controls the expression of various genes in cancers that are known to contribute to the acquisition of different cancer hallmarks leading to tumor progression (Fig. 15B; [210-211]). Specifically in hedgehog signaling NANOG regulates the expression of GLI1 and GLI2 and thereby creating a feedforward loop ([203-204] and our study) to maintain ‘stemness’. Additionally we observed a GLI1-independent regulation of the hedgehog pathway by NANOG (data not shown) and therefore it is possible that other genes within the pathway could be affected by NANOG. Also, we were unable to generate a stable NANOG over-expression cell line while hedgehog-activated cell lines could be easily produced; highlighting that NANOG could have additional hedgehog-independent functions within ERMS. Since the role and targets of NANOG seem to be cancer cell-context specific it would be important to further

characterize the functional importance of NANOG in ERMS. Recently developed transgenic mouse models that allow temporal and spatial control of NANOG expression [217-219] could be used in conjunction with the plethora of ERMS mouse models [220] for a thorough investigation of the importance of NANOG in ERMS.

7.1.1.2. CD133

The use of CD133 as a sarcoma stem cell marker has been previously described in section 4.4.1.1. However there have been no studies examining the regulation or function of CD133 in sarcomas. Most studies, including in adult cancer entities, which describe alteration in CD133 expression by cell extrinsic or intrinsic factors do not demonstrate direct transcriptional regulation. For instance, in Ewing sarcoma CIC modeling, expression of EWS-FLI1 in pediatric human MSCs led to increased CD133/AC133 expression but no direct regulation was described [151]. Additional analysis using Ewing sarcoma patient samples and cell lines revealed a cell-context specific expression [118]. Higher expression of hedgehog pathway components has been noted in $CD133^+$ compartment of glioblastoma and medulloblastoma samples [203-204, 221]. Similar results were obtained in ERMS cells [129]; however we were unable to confirm this (data not shown). Although CD133 and GLI2 (but not GLI1 or GLI3) mRNA expression correlated significantly in ERMS patients (data not shown), we could not find evidence for positive regulation of CD133 expression by the hedgehog pathway. On the contrary CD133 (protein) expression was highest in the hedgehog-inhibited ERMS cells lines. Studies in other cancer types which show a positive correlation between CD133 and hedgehog pathway expression, do not address direct regulation. There has been increasing evidence supporting epigenetic and niche-dependent regulation of CD133, which could explain the cell-context dependent expression patterns [222-228].

We and others have described that the ERMS $CD133^+$ population is more chemoresistant to conventional therapies that affect DNA replication although the populations did not proliferate differently (article 1 and [129]). The $CD133^+$ populations in glioma and colon cancer cell lines, upon therapeutic insult (radiation/chemotherapy), seem to preferentially activate DNA repair pathways highlighting a mechanism for their treatment resistance [229-230]. Although we did not directly assess the expression of DNA repair pathway components in the $CD133^+$ population, DNA repair was noted to be the most highly represented upregulated pathway upon gene ontology analysis of ERMS spheres expression profiles (data not shown).

CD133 can be phosphorylated by Src proteins. A recent study in glioma cells has shown that phosphorylated CD133 interacts with p85 subunit of PI3-kinase to activate Akt leading to increased ‘stemness’ [231]. Activated Akt has been previously noted in hepatocellular and neuroblastoma $CD133^+$ populations [231]. Interestingly Akt pathway was shown to be preferentially activated in

the synovial sarcoma CD133$^-$ (AC141$^-$) population [121]. It would be interesting to determine if Akt activation is heterogeneous in other sarcoma types and/or preferentially associated with CIC markers since it is a key node for therapeutic intervention.

7.1.1.3. FGFR3

The role of FGFR3 has been mainly described in bone and connective tissue development. Its transcription has been shown to be positively regulated by Sp1 family of transcription factors, AP2δ and E2F-1 [232-234]. It has been postulated that majority of FGFR3 expression, at least in chondrocytic cells, is due to Serum Response Factor (SRF) transcriptional activity. Consequently FGFR3 expression could be increased by the addition of serum or cytoskeletal changes [235]. However in ERMS cells FGFR3 expression was highest in media without serum [236]. FGFR3 expression could also be controlled by the microenvironment: FGFR3 expression was induced in hypoxic conditions in a HIF1α-dependent manner [237]. Binding sites for other transcriptional regulators have been identified, although not functionally characterized [235], and could mediate cell-context specific regulation.

FGFR3 was found to be part of the RAS signature that could be used to predict drug sensitivity in zebrafish ERMS model [53]. Functionally FGFR3 can trigger MAPK and Akt pathways [235]; however this has not been directly addressed in ERMS cells. The use of FGFR3 expression as ERMS CIC marker has been established mainly using an obscure ERMS cell line, KYM-1 [128]. The expression of survivin, an apoptosis regulator, has been noted to be higher in FGFR3 expressing KYM-1 cells and the use of oncolytic adenovirus to target survivin expression reduced tumor growth [236]. It is unclear if survivin is a robust marker correlating with FGFR3 expression or stem cell activity. It is equally likely that survivin affects ERMS pathogenesis by inducing apoptosis without affecting 'stemness'. We noted FGFR3 expression to be positively regulated by hedgehog pathway in RD cells and negatively regulated in RH36 cells (data not shown). Therefore FGFR3 could mark active hedgehog phenotype depending on ERMS cell-context. In the commonly used ERMS cell lines majority of FGFR3 expressing cells co-expressed CD133 [129]. Furthermore, FGFR3 expression was not enriched in ERMS sphere cells (article 1). It would be useful to assess if combinatorial use of the markers would improve ERMS CIC detection.

7.1.1.4. MYF5

Extensive investigations in skeletal myogenesis using transgenic mouse models have revealed the key roles played certain basic helix-loop-helix (bHLH) transcription factors which are now referred to as muscle regulatory factors (MRFs). These MRFs control muscle stem cell specification (early MRFs) and differentiation (late MRFs) [238]. Myf5 is an early MRF expressed in activated

muscle stem cell. It transcribes MyoD (an early and late MRF) and Myogenin (a late MRF) which together with other transcription factors, epigenetic regulators and miRNAs lead to muscle cell commitment and terminal differentiation [238-239]. Myf5 expression is regulated through different lineage-specific enhancers, minimal promoters and transcription balancing sequences. During myogenesis exogenous signaling pathways such as hedgehog, Wnt (β-catenin-mediated and PCP pathways) and BMP control the expression of Myf5 spatially and temporally. Specifically transcription factors such as Gli2, Gli3, β-catenin, Pax3 (directly and indirectly via Dmrt2), Pax7 (in complex with histone methyltransferases), Six1/Six4 (with Pax3) have been shown to bind to various Myf5 enhancers to initiate expression [238-244]. Recently post-transcriptional regulation of Myf5 expression by miR-31 has been documented in adult myogenesis adding another facet to the complex and intricate regulation of myogenesis [245].

The effect of individual Gli proteins on Myf5 expression and/or myogenic processes in general seem to be dependent on experimental context, such as, *in vitro* vs. *in vivo*, embryonic myogenesis vs. postnatal/adult muscle regeneration and normal vs. pathological conditions [243, 246-250]. For instance, hedgehog inhibition during *in vitro* muscle stem cell activation did not affect Myf5 expression [250], however, hedgehog inhibition and specifically loss of Gli3 reduced Myf5 expression, attenuated muscle regeneration and associated angiogenesis *in vivo* [248-249]. Also in normal myogenesis hedgehog signaling, primarily via Gli2 and (activated) Gli3, is required for Myf5 expression and myotome patterning but in pathological conditions, such as ERMS, Gli1 and Gli2 (but not Gli3) seem to de-differentiate the cells by inhibiting the activity of MyoD and Myf5 [243, 247].

Myf5 has been identified as a component of the ERMS signature from transgenic mouse models and CIC marker in the RAS-activated zebrafish model of ERMS [47-48, 251]. We could not detect Myf5 expression in ERMS cells lines used in our study (data not shown) indicating that Myf5 activity was not necessary for human ERMS cell survival or hedgehog-driven self-renewal, at least *in vitro*. Myf5 mRNA expression level was noted to be higher in ERMS patient samples with high Gli1 mRNA expression [252] and increased Gli3 expression, along with Myf5 expression, was reported in the self-renewing zebrafish ERMS cell compartment [48]. However we did not find a correlation between expression of Myf5 and any of the Gli transcription factors within our cohort of patients. Although this maybe due to the small sample size, it is also possible that Myf5 expression is controlled by hedgehog-independent mechanisms in ERMS.

7.1.2. Novel hedgehog-modulated genes in ERMS

Our study identified transcription factors PITX2, LMX1B and PAX6 as being positively regulated by the hedgehog pathway in ERMS cells (article 2). PITX2 is expressed in cranial tissues

derived from the neural crest and mesoderm [253]. PITX2 has been identified as the master regulator of myogenesis in the head and neck region: extraocular, tongue, laryngeal and other muscles derived from the branchial arches [238]. LMX1B is expressed in the mesenchyme where it integrates signals from different pathways (including hedgehog signaling) to affect dorsal-ventral patterning during limb development [254-255]. It is also known to play a role in kidney and brain development [256]. The expression and function of LMX1B seems to be imperative in the development of neural crest derived-periocular mesencyme which affects the anterior segment of the vertebrate eye [257]. Intriguingly the investigators also noted the expression of LMX1B in the posterior periocular mesenchyme resembling nascent muscle masses derived from the mesoderm. The function of LMX1B in extraocular muscle development has not been further studied. PAX6 plays an important role in the development of neuroectoderm and endocrine lineages. In the retina, PAX6 is required for the maintenance of multi-potential status of stem cells. It is expressed in cerebellar precursors and prepancreatic endoderm [258].

Both PITX2 and LMX1B have been implicated in ovarian cancer progression [259-260]. PAX6 expression has been noted in breast cancer, pancreatic cancer, astrocytic glioma, glioblastoma and medulloblastoma [261-262]. In glioma and glioblastoma PAX6 expression correlates with favorable outcome [263] while its ectopic expression leads to the development of pancreatic cystic adenoma [264]. During development a negative feedback exists between hedgehog signaling and PAX6; similar to the regulation noted in astrocytic glioma cells [258, 265]. However in medulloblastoma PAX6 expression is positively regulated by the hedgehog pathway [265]. Therefore the regulation and function of PAX6 in cancer seems to be cell-context dependent.

There have been no previous indications of oncogenic roles for these genes in ERMS. However, interestingly, majority of ERMS develop in the anatomical sites wherein the expression and/or function of PITX2 and LMX1B have been previously reported. In renal cancer PITX2 seems to protect the cells from doxorubicin mediated toxicity by upregulating multidrug transporter ABCB1 [266]. We also observed increased resistance to doxorubicin in the PITX2-expressing hedgehog-activated ERMS cells. Overall it would be highly informative to further characterize the importance of these novel genes as they could help unravel mechanisms of hedgehog-driven CIC functions in ERMS.

7.1.3. Novel cross-talk between developmental pathways in ERMS and possible lineage relationships within CIC markers

There is emerging evidence of cross-talk between developmental pathways in sustaining different cancer entities. The means of regulation and the final outcome on the activity of the pathways involved seem to depend on the type of cancer studied. For instance, in breast cancer,

Wnt, Notch and hedgehog pathways collaborate to maintain breast CICs [267], while in gastric cancer hedgehog pathway inhibits Wnt signaling to exert a pro-tumorigenic effect [268]. In RMS these pathways have been studied independently (Table 3). Our study (article 2) shows for the first time that activation of the hedgehog pathway in ERMS cells inhibits pathways associated with the myogenic lineage: Notch, Wnt and TGFβ-BMP. Antagonistic regulation between hedgehog signaling and these pathways has been previously reported also in other cell types [269-272]. It was unexpected to find that de-differentiated (hedgehog-active) ERMS cells downregulated Notch (RD cells; data not shown) and TGFβ pathways since inhibition of these pathways in known to differentiate ERMS cells [186, 273]. Wnt pathway activation seems to promote RMS differentiation [52, 178]. Concordantly we observed increased expression of Wnt pathway components in the differentiated hedgehog-inhibited cells. Recently activation of canonical Wnt signaling in ERMS using GSK3β inhibitors was shown to decrease ERMS self-renewal primarily by inducing differentiation [176]. These new insights are highly instructive since pro-differentiation strategies are a key area of interest in RMS and myopathies. Therefore it would be worthwhile to mechanistically characterize these interactions further under pathological conditions [274].

Based on the data and known regulatory mechanisms in myogenesis we can formulate a hypothetical lineage hierarchy within ERMS tumors (Fig. 16).

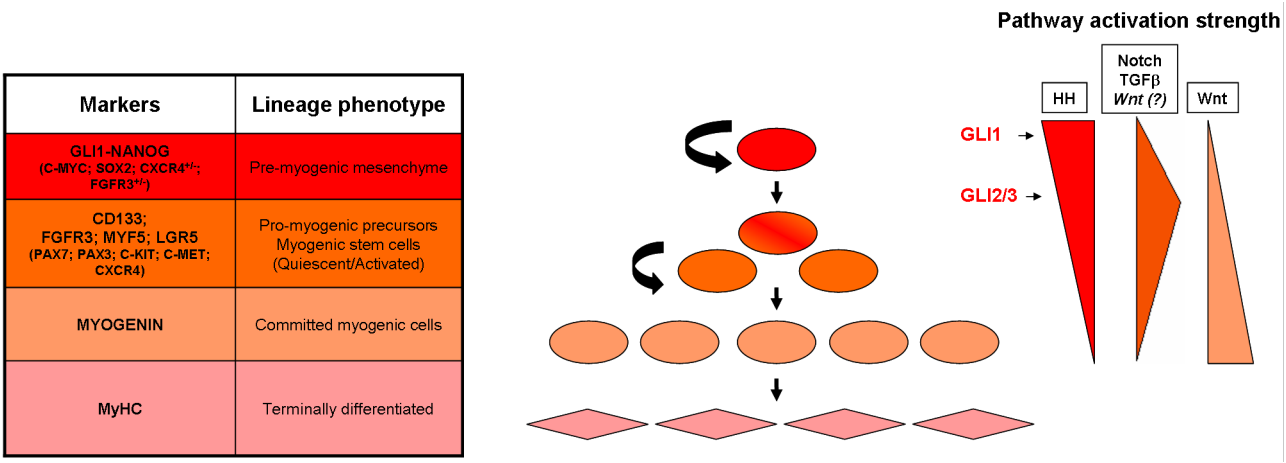

Figure 16. Hypothetical lineage hierarchy in ERMS. GLI1-NANOG expressing cells could possess a pre-myogenic mesenchymal phenotype occupying the apex of the hierarchy with the highest hedgehog pathway activity and self-renewal function. Activity of pro-myogenic developmental pathways (Notch, TGFβ and Wnt) is low. We observed cell line-specific regulation of certain markers by hedgehog signaling: CMYC and SOX2 were positively regulated in RD and RH36 cells respectively by the hedgehog pathway. Also, the expression of CXCR4 and FGFR3 was positively regulated by the hedgehog pathway in RD cells and negatively regulated in RH36 cells. Although we observed upregulation of CXCR4 expression in RD GLI1 over-expressing cells the reduction upon hedgehog inhibition was minor indicating a hedgehog-independent regulation. The transient amplifying population could be characterized by high Notch, TGFβ, GLI2/GLI3-mediated moderately active hedgehog signaling and possibly R-spondin-LGR5-Wnt signaling. It could be marked by the expression of CD133, FGFR3, MYF5 and LGR5. We found the expression of muscle stem cell markers C-KIT and C-MET to be highest in the hedgehog-inhibited RD cells (data not shown). It is possible that different ERMS CIC phenotypes with varying differentiation potentials are concomitantly present within tumors. It is likely that, GLI transcription factors could play non-redundant roles in determining ERMS CIC phenotype and tumor differentiation status, similar to what is seen during normal development. Importantly, if the hypothesis holds true then hedgehog pathway inhibition could affect both apical and transient-amplifying ERMS CICs. Myogenin expressing cells comprise the majority of ERMS cell population and these cells are considered to be lineage-committed. The terminally differentiated cells express myosin fibres. *See text for further details*. HH, Hedgehog signaling; MyHC, Myosin Heavy Chain

Hedgehog signaling is important for myogenesis ([241, 246-247, 249-250]) but functionally the GLI transcription factors seem to play non-redundant, context-dependent and marginally compensatory roles, with GLI2 and GLI3 in general being important for myogenesis than GLI1 [243, 248]. Our study shows that particularly when GLI1 is over-expressed ERMS cells downregulate pathways necessary for myogenic lineage specification and rather express genes that are commonly found in neural crest-derived mesenchyme and neuroectoderm. Therefore hedgehog-active compartment that expresses GLI1 could possess a pre-myogenic mesenchymal phenotype; probably occupying the apex of the hierarchy. Furthermore, the induction of NANOG expression by GLI1 in ERMS cells could potentiate the pre-myogenic phenotype [275-276]. Our analysis for the expression of known ERMS CIC markers and other candidate markers revealed that GLI1 and NANOG expressions appear to the most reliable marker for hedgehog-active pre-myogenic phenotype (discussed above).

The pathways repressed by GLI1 over-expression in ERMS play important roles in skeletal muscle specification and differentiation. Notch activation is necessary during myogenesis for specification, self-renewal and maintenance of muscle stem cells [163]. During postnatal myogenesis BMP signaling co-operates with Notch pathway to maintain quiescence of stem cells and block terminal differentiation [163, 277-278]. BMP signaling in particular has been shown to increase the number of fetal muscle progenitor cells and adult satellite cells [279-280]. Positive interactions between TGFβ and Notch signaling have been documented in other tissues as well [269]. We found CD133 expression to be highest in ERMS cells with a more myogenic background. $CD133^{+}$ cells isolated from blood and skeletal muscle have been used to regenerate muscle in dystrophic muscle mouse models [281] and $CD133^{+}$ ERMS cells are reported to have higher expression of muscle stem cell markers [129]. Therefore CD133 could be marker for early pro-myogenic precursors in ERMS tumors. FGFR3 is expressed in quiescent muscle stem cells [282] and concordantly $FGFR3^{+}$ ERMS cells were reported to show increased expression of quiescent muscle stem cell markers CD34 and PAX3 [128]. Myf^{high} ERMS CIC compartment showed increased expression of muscle stem cell genes, c-met and m-cadherin and also bmp3 [251]. Expression of Notch2 and GIi3, along with Myf5, was found to be highest in the self-renewing ‘activated stem cell’-like CIC compartment in the RAS-activated zebrafish ERMS model [48]. As previously discussed Myf5 is a Gli2/Gli3 target gene during myogenesis. The mRNA expression of GLI2 and CD133 correlated within ERMS patients. In several cancer types TGFβ2/Smad3 induces GLI2 expression [283].

Wnt signaling plays different roles in the various stages of myogenesis [284]. During embryonic myogenesis Wnt signaling is required for specification of muscle progenitor cells while in adult myogenesis a temporal switch from active Notch to Wnt is required for terminal differentiation

[285]. However a positive regulation between Wnt and Notch signaling is also possible and has been noted in other cell systems and cancers [181]. We also analyzed LGR5 expression, a Wnt target gene and pathway component [286], which was enriched in ERMS spheres and heterogeneously expressed within cell lines (data not shown). Similar to what we observed for other Wnt pathway components: the expression of LGR5 was increased in the more differentiated compartment. Interestingly, Wnt-β-catenin signaling through R-spondin (an LGR5 ligand) increased Myf5 expression in myoblasts [242, 286]. Therefore Notch, TGFβ, GLI2/GLI3-mediated hedgehog signaling and possibly Wnt signaling could control the self-renewal of the transient amplifying population which is characterized by a myogenic lineage phenotype and could be identified by CD133, FGFR3, MYF5 and LGR5 expression status. Upon inhibition of hedgehog, Notch, TGFβ or activation of Wnt signaling ERMS cells seem to increase the expression of myogenin which signifies commitment to differentiation (this study and [176, 178, 186, 273]) and eventually leads to terminal differentiation as assessed by the expression of myosin fibers.

So far our knowledge about the hierarchical organization in ERMS is elucidated from the 'potential' of various cell types to initiate tumor formation. However this may not be the actual 'fate' of the cell type during tumor growth *in vivo* [96]. Therefore lineage tracing experiments using ERMS mouse models should be able to not only concretely prove the application of the CSC model in ERMS progression but also clarify the hierarchy of the CIC markers. Further progress in understanding the developmental biology of the neural crest, mesoderm and skeletal muscle could shed more light on CIC regulation in ERMS and in general improve disease modeling [287].

7.2. Factors that could influence sarcoma hierarchical organization

7.2.1. Non-genetic determinants

Studies in several cancer types show that the CIC phenotype is not a static entity. The plasticity of CIC phenotype may be determined by epigenetic modulators, niche factors such as hypoxia, inverse-paracrine pathway activation and genotypic background of the mouse strain used for xenograft studies; and noisy cellular gene expression leading to stochastic state transitions [96-97]. It is possible that some, if not all, of these factors put pressure on cell fate decisions and therefore could determine the CIC phenotype. Additionally the efficiency of the interconversions between the CIC and non-CIC state would influence the functional readouts in CIC assays and impact clinical outcome (Fig. 17 and 18). In ERMS we have shown that hedgehog pathway can be modulated leading to alteration in cellular differentiation states. Therefore the hierarchy in ERMS is clearly not static. However under basal conditions we detect only rare cells expressing high levels of GLI1-NANOG indicating that the interconversion between the GLI1-NANOG^{high} and GLI1-NANOG^{low} may be inefficient. In osteosarcoma hypoxia seems to play a major role in determining

differentiation status of CICs indicating a more dynamic regulation of this population than previously appreciated [126]. Although our study shows that ARMS does not present with a 'steep' hierarchical organization hypoxic conditions could induce phenotypic alteration in cells to increase their tumorigenicity [145].

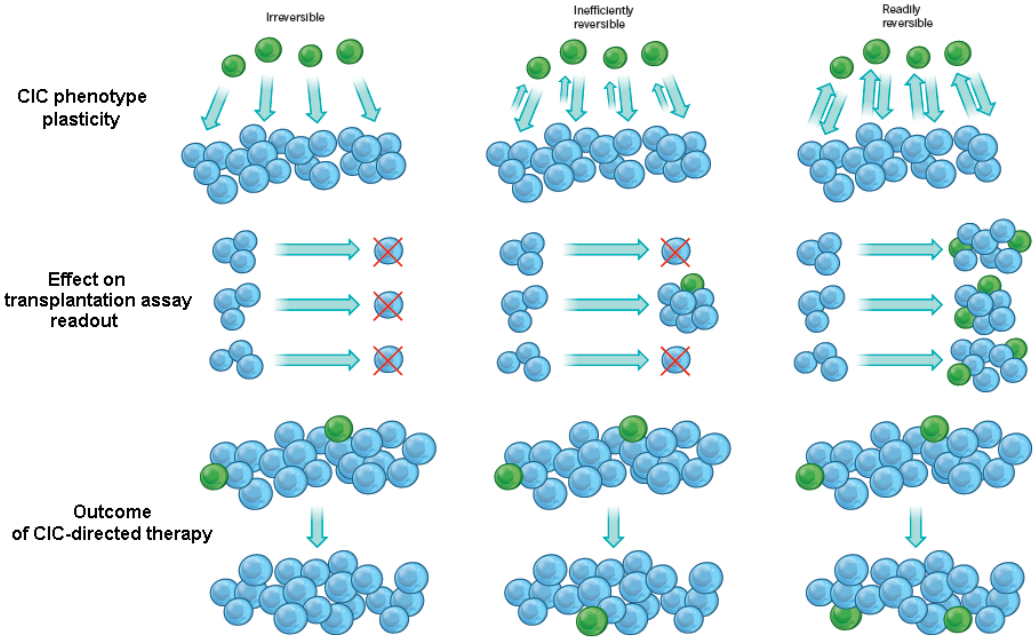

Figure 17. Impact of cell plasticity on sarcoma stem cell modeling. If the CIC phenotype is static then non-CIC cells will not be capable of tumor initiation in transplantation assays and CIC-directed therapies will not lead to tumor shrinkage but will not allow tumor relapse. However if the CIC phenotype is reversible, either due to cell intrinsic or extrinsic factors, then some or many tumors will form when non-CIC cells are xenotransplanted and importantly the CIC-directed therapies will not be beneficial. Adapted from [96]

7.2.2. Genetic determinants

7.2.2.1. Mutations in oncogenes and tumor suppresors

The effect of genotypic insult on the functionality of CIC markers has been shown in lung cancer mouse models where Sca-1^{+} cells were shown to have enriched tumorigenic properties in Kras and p53 mutant background but not when Kras was mutated alone [288]. Recent studies show that oncogenes, such as Pten, Ras, Rb1 and Myc, also play an important role in self-renewal and/or transformation of normal cells into cancer stem cell-like cells [77, 289-291]. Specifically, p53 - the most commonly mutated tumor suppressor in sarcoma models, plays complex context-dependent roles in the maintaining mesenchymal lineage phenotypes [292]. Rb1 has been identified a modifier of the sarcoma phenotypes generated in osteosarcoma and RMS mouse models [45, 47]. Overall genetic alterations could influence the sarcoma 'cell of origin' (summarized in section 4.2.5) and consequently also the sarcoma CIC markers and lineage phenotypes (Fig. 18).

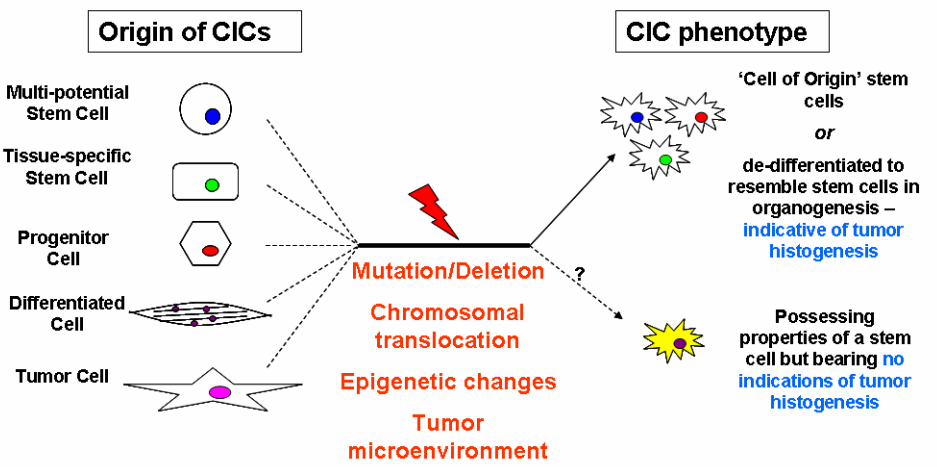

Figure 18. Impact of genetic and non-genetic determinants on sarcoma CIC phenotypes. Sarcoma stem/initiating cells could be persistent clones of the 'cell of origin' which could be a neoplastic stem cell or a de-differentiated mature cell. Sarcoma stem cells could also be tumor cells that have acquired the stem cell properties to either resemble the 'cell of origin' or other stem cells within the tumor histogenic lineage. However it is also possible that the sarcoma stem cell phenotype resembles a stem cell that has no direct bearing on the lineage of tumor development (transdifferentiation). Genetic, epigenetic and cell extrinsic factors could affect cell fat decisions and thereby alter CIC phenotypes. Adapted from [83].

Recent NGS studies found that the RAS pathway is most commonly de-regulated in ERMS [41-42]. The cell lines used in our study also possess activating RAS mutations (RD -NRAS Q61H and RH36 -HRAS Q61K). Interestingly RAS pathway activation is known to increase hedgehog signaling strength [293]. RD cells also possess p53 mutation (R248V) and disruption of the p53 pathway has been documented in sporadic ERMS tumors [41-42]. Rubin *et al.* reported that 59% of ERMS patients in their cohort had a mutant p53 signature and majority of patients with hedgehog-active signature (29% of total) also possessed a mutant p53 signature [47]. p53 has been known to repress NANOG expression and loss of p53 increases hedgehog-NANOG signaling strength [203-204, 211]. Therefore it is likely that the hedgehog-active CIC phenotype may be a common feature in sporadic ERMS cancer.

In case of ARMS PAX3/PAX7-FOXO1 is the main oncogenic mutation in the tumor accompanied by very few additional mutations [41-42]. Our study (article 3) shows that PAX3-FOXO1 can confer 'stemness' to cells. Apart from being necessary for tumor initiation it is also necessary for cell survival and proliferation. Furthermore it blocks differentiation and thereby keeps all PAX3-FOXO1 expressing cells (majority of the tumor) in an undifferentiated state. The de-differentiation function of PAX3-FOXO1 that we observed across various lineages in PAX3-FOXO1 expressing iPS cells implies that a non-skeletal muscle origin could be envisioned for ARMS [60]. Also in other fusion-positive sarcomas it is the fusion oncogenes that provide the cues for 'stemness' [120, 151]. However in contrast to our findings in ARMS, Ewing sarcoma tumors have been determined to contain functionally distinct subpopulations [107].

Also it is possible that only a subset of sarcomas, depending on the genotype, present with hierarchical organization. Wnt pathway activating mutations have been recently identified in a

subset of ERMS patients; however nuclear β-catenin accumulation is heterogeneous among the tumor cells [41, 294]. Wnt pathway activation as discussed earlier has a pro-differentiation consequence in ERMS cells. Therefore further studies are needed to characterize the nature of these tumors and if they are also hierarchically organized.

7.2.2.2. Intra-tumoral genetic heterogeneity

Deep sequencing and data analysis with improved bioinformatic methods show that tumor entities are often composed of a dominant genetic clone and minor genetically distinct subclones [295]. Extensive genetic heterogeneity within tumors could obscure isolation of truly functionally distinct cellular populations since cellular compartments isolated for enriched tumorigenicity could be endowed with such a property due to their mutational background [96-97]. Combining functional studies, such as clonal xenografting and sphere formation, with deep sequencing could test if functional heterogeneity is present within subclones and also amongst them [296-297]. ERMS and ARMS tumors have considerable genetic heterogeneity. Clonal evolution of subclones in ERMS tumors has been documented during tumor progression [41]. However NGS data alone cannot directly test the cancer stem cell model. Given the evidence for hierarchical organization in ERMS tumors we predict that ERMS CICs undergo clonal evolution during tumor progression to generate relapse and metastasis. Therefore future studies would need to incorporate genetic analysis and functional assays using patient material wherein the genetic heterogeneity is maintained. In ARMS we show that single cell clones had equal propensity for tumor initiation despite presenting with phenotypic heterogeneity. Therefore, although it remains to be determined using primary tumors, intra-tumoral genetic heterogeneity possibly has little effect on CIC properties which seem to be mainly determined by PAX3-FOXO1 activity.

7.3. Treatment implications and impact on clinical care

Understanding the hierarchical organization, or lack thereof, in RMS tumors has significant implications for therapeutic strategies. At present E- and ARMS patients are treated with similar drugs regimens; with just therapy ‘intensity’ being altered based on clinically determined parameters. Our studies show that although RMS tumors present with markers of halted skeletal muscle differentiation, the fusion-negative and fusion-positive RMS tumors are in fact very different in their cellular organization. Therefore our studies add to the increasing weight of evidence that the histological subtypes should be treated as distinct molecular and biological entities. Recently the RAS pathway has been proposed as a common therapeutic target axis across the histological subtypes [42]; however our data argues against similar treatment of the RMS variants. Instead we propose that therapies against ERMS tumors should include hedgehog

inhibitors to debilitate the hierarchical organization of the tumor while in fusion-positive ARMS tumors the need of the hour would be to target the fusion protein activity [298].

7.3.1. Targeting hedgehog signaling

Several means of hedgehog pathway activation has been noted in cancers [161] and in order to target it effectively it would be important to elucidate the mechanism of pathway activation that is prevalent in ERMS. To this end, we show for the first time in ERMS that autocrine ligand-based signaling via IHH and DHH occurs in ERMS. We detected increased stromal ligand expression within xenografts compared to normal mouse muscle indicating a minor contribution from inverse-paracrine activation. Also we clarified that the contribution of SMO-independent GLI activation is minor within ERMS. Therefore using SMO inhibitors would be effective in ERMS.

The targeting of hedgehog pathway in RMS xenografts has been previously reported however there are serious concerns regarding their validity for interpreting treatment efficacy. Two of the studies use non-specific drugs: Betulinic acid [299] and Forskolin [300]. Importantly betulinic acid was shown to induce regression in GLI1 amplified ARMS xenografts. In ERMS, although administration of forskolin led to reduced tumor growth, the specific inhibition of hedgehog pathway was not reported either *in vitro* or *in vivo*. The use of SMO inhibitor cyclopamine in Ptch1 mutant ERMS tumors *in vivo* did not induce tumor regression leading the authors to conclude that hedgehog signaling is important for tumor initiation but not maintenance [301]. However the efficacy of the drug was found to be low and severe toxicities were associated with cyclopamine treatments. Recently a chemical screen conducted by an independent study group to identify drugs that could inhibit ERMS self-renewal also identified cyclopamine as a potent tumor inhibitor *in vivo* [176]. Evidence from clinics shows that cyclopamine has low affinity for SMO, poor oral bioavailability, suboptimal pharmacokinetics and low metabolic stability and hence studies performed using this drug could give spurious results [161, 302]. Therefore new studies are required to assess the effect of using clinically relevant hedgehog inhibitors on ERMS tumors *in vivo*.

There are some additional key issues to consider before using SMO inhibitors in ERMS,

1. In hedgehog-dependent cancers where mutational activation has been noted, the use of SMO inhibitor as a single therapeutic agent has led to the development of SMO activating mutations which render the patients insensitive [161]. Since the activity of GLI transcription factors could be increased in the absence of SMO signaling it is possible that tumor cells could compensate for SMO inhibition by activating other pathways that directly regulate the GLI code [303]. Therefore it would be more prudent to test combination treatment strategies, preferably using GLI inhibitors rather than SMO inhibitors, to avoid compensatory mechanisms. Many of the oncogenic pathways that have

been reported to increase ERMS tumor aggressiveness also could positively influence GLI activity (Fig. 19).

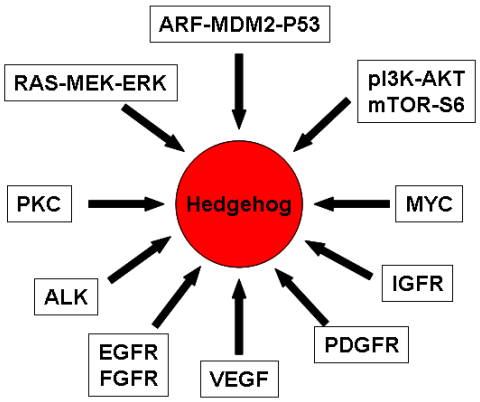

Figure 19. Crosstalk between hedgehog signaling and oncogenic pathways. Details of the studies documenting the activation of the depicted pathways in ERMS are presented in reference [55]. The crosstalk mechanisms have been reviewed in [303-304]. Additional references: [305-308]

2. Importantly our studies present hedgehog inhibition as means to reduce self-renewal in ERMS. Therefore measuring the efficacy of hedgehog inhibitors on tumor regression as primary treatment endpoint could lead to erroneous interpretations. Strategies that are directed against self-renewal of a cellular subpopulation rather than tumor bulk would imply that the treatment efficacy should measure long-term disease-free survival and not just short-term effects on tumor growth. Hence translational research in ERMS evaluating hedgehog inhibitors need to have an altered design that would accommodate the cancer stem cell model. A possible strategy of how we could assess hedgehog inhibition in combination with other treatment options as an anti-CIC therapy in experimental laboratory and clinical trial situation has been depicted in Fig. 20.

Our study presents GLI1 and NANOG expression as biomarkers to assess hedgehog-driven self-renewal in ERMS. Expression of GLI1 and NANOG within sporadic ERMS patients could predict worse overall and event-free survival. Although high CD133 expression seems to predict worse overall survival in ERMS its dynamic regulation and unclear function in self-renewal limits its use as a CIC biomarker [108, 309]. So far the importance of FGFR3 or MYF5 expression for ERMS patient outcome has not been established. Importantly mutational status or signatures have not been successful in prospectively stratifying patients to predict outcome [41, 47]. Therefore combining genetic information with CIC biomarkers could offer improved insight for patient recruitment in trials, combinatorial treatment options and efficacy endpoint evaluations.

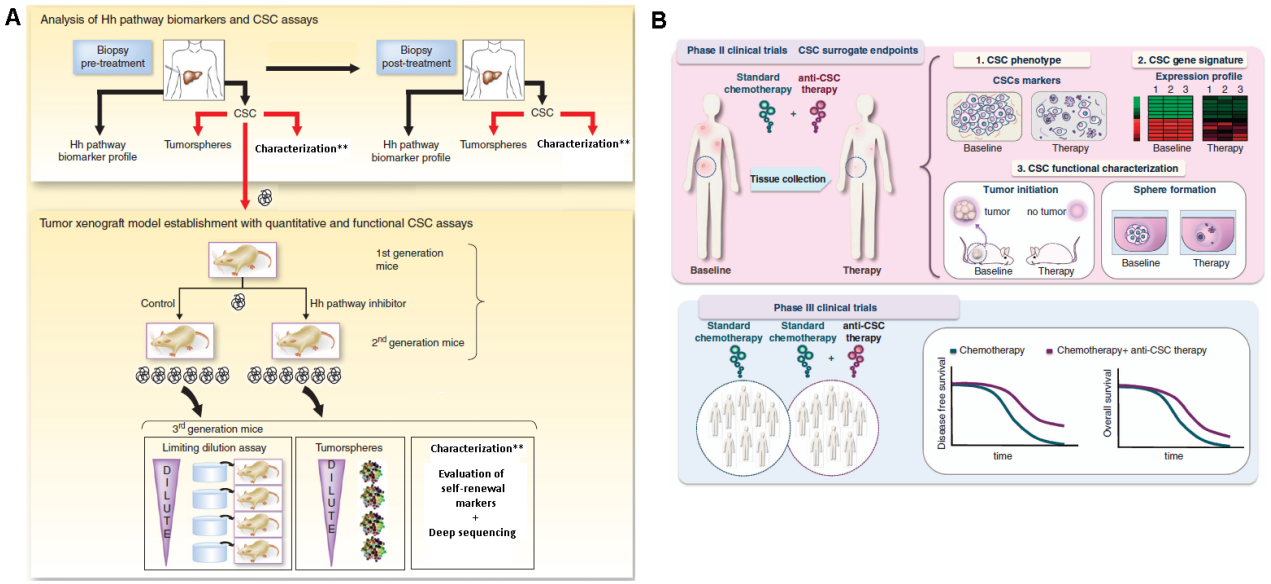

Figure 20. Hedgehog inhibition to reduce self-renewal in pre-clinical and clinical settings. (**A**) Treatment-naïve and post-treatment biopsies from patients could be used for *in vitro* (sphere assay) and *in vivo* (patient-derived xenograft) studies that assess hedgehog-driven self-renewal. **Characterization of tumor biopsies would involve analysis of self-renewal marker expression (such as GLI1 and NANOG) and genome sequencing to evaluate effects on mutational spectra and subclonal architecture. Adapted from [310]. (**B**) During clinical trials surrogate end points that involve genetic, phenotypic and functional analyses would need to be used to assess the effectiveness of combination strategies involving standard treatment with hedgehog inhibitors (anti-CSC therapy) [153].

3. The use of SMO inhibiting drugs systemically in growing children could lead to premature dwarfism since bone growth plate development depends on IHH signaling [311]. In infants less than six months old hedgehog inhibition could affect cerebellar development [312]. Clinical trials are ongoing to assess the optimal therapeutic dosage for SMO inhibitor LDE225, as a single agent, in medulloblastoma and other refractory solid tumors in children (including RMS). The safety profiles generated from these trials should be helpful in making treatment decisions in children. Even so, it would be useful to identify ways in which hedgehog inhibitors could be targeted to the tumor site instead of systemic application. Issues with drug-targeting in children are not unique to hedgehog inhibition: a developing child would be much more vulnerable to developmental side-effects of any targeted drug compared to adult patients [23, 313]. Therefore apart from novel targeting agents we would also need efficient targeted-delivery modes to improve patient quality of life.

Current treatment modalities entail severe side-effects (discussed in section 4.2.3). Our data shows that using hedgehog inhibitors not only reduces self-renewal but also sensitizes ERMS cells to normal chemotherapeutics, thereby allowing a reduction in standard therapy length and dosage. Other pro-differentiation strategies could be combined with hedgehog inhibition to terminally differentiate ERMS cells. This would especially be beneficial in reducing the chance for metastasis since non-CIC committed progenitor cells possess higher invasiveness (article 2 and [251]). These principles could be extended to other pediatric sarcoma entities (Fig. 21A).

The clinical benefit from conventional treatment of childhood sarcomas has reached a plateau [23]. Local recurrence and its refractoriness is still a major problem for sarcoma patients. Therefore the need of the hour in the sarcoma stem cell research field is not only identification of tumor sustaining subpopulations but also the mechanisms that are necessary for the survival of these cells, be it cell intrinsic or extrinsic, in order to target them efficiently. Overall, research and development in sarcoma stem cell modeling promises to have an impact in all aspects of patient care (Fig. 21B).

A

Pediatric sarcoma	Pathways/Drugs targeting pediatric sarcoma CICs	Combinatorial options for pro-differentiation strategy
Osteosarcoma	FGF signaling	TGFβ inhibition + activating Wnt signaling
Embryonal RMS	Hedgehog signaling	Notch+TGFβ inhibition + activating Wnt signaling
UPS**	Hedgehog+Notch signaling	Activating Wnt signaling
Alveolar RMS	PAX3-FOXO1 activity	Notch inhibition
Synovial sarcoma	SS18-SSX activity	
Ewing sarcoma	EWS-FLI1 activity (YK-4-279) Enoxin (TARBP2 activity)	

B

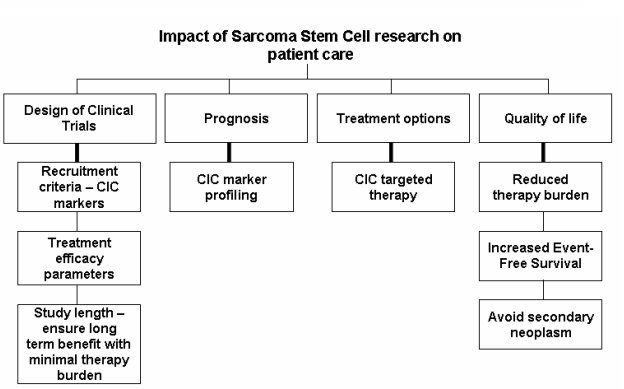

Figure 21. Translational relevance of sarcoma stem cell research. (**A**) Sarcoma CIC-inhibiting pathways/drugs which could be combined with the inhibition of other pro-differentiation pathways. **relevance to pediatric UPS is unclear. [104, 117, 120, 158, 176] Other references are listed in Table 3. (**B**) Perceived impact of sarcoma stem cell research in clinical management of patients [83].

7.4. Conclusion

It is becoming increasingly apparent that tumor heterogeneity is an important factor that impedes successful treatment in the clinics [7]. Genetic, epigenetic and/or tumor microenvironment collude to generate not just intra-tumoral heterogeneity but also contribute to inter-tumoral heterogeneity [97]. The heterogeneity determines 'stemness' features of cancer cells, which has significant impact on clinical outcome and provides novel therapeutic options. In certain cancer entities, like ERMS, functional heterogeneity is in a steep hierarchy where rare primitive tumorigenic cells, akin to normal stem cell behavior, would give rise to many phenotypically distinct non-tumorigenic cells. In other cancer types, like ARMS, shallow or no hierarchy is observed despite being a phenotypically heterogeneous tumor mass and therefore tumorigenic cells are common. In the latter scenario usually genetic determinants (for example PAX3-FOXO1) provide 'stemness' characteristics to cancer cells and inter-tumoral differences could be attributed to varying PAX3-FOXO1 transcriptional signatures. In conclusion our studies incorporate the latest models of tumor progression to provide novel perspectives to RMS tumor biology which will aid in designing optimum therapeutic strategies against these deadly childhood cancers.

8. Bibliography

1. Pritchard-Jones, K. and R. Sullivan, *Children with cancer: driving the global agenda.* Lancet Oncol, 2013. **14**(3): p. 189-91.
2. Kaatsch, P., *Epidemiology of childhood cancer.* Cancer Treat Rev, 2010. **36**(4): p. 277-85.
3. American Cancer Society. *Global Cancer Facts & Figures 2nd Edition*. 2011, American Cancer Society: Atlanta.
4. Stratton, M.R., P.J. Campbell, and P.A. Futreal, *The cancer genome.* Nature, 2009. **458**(7239): p. 719-24.
5. Vogelstein, B., N. Papadopoulos, V.E. Velculescu, S. Zhou, L.A. Diaz, Jr., and K.W. Kinzler, *Cancer genome landscapes.* Science, 2013. **339**(6127): p. 1546-58.
6. Hanahan, D. and R.A. Weinberg, *The hallmarks of cancer.* Cell, 2000. **100**(1): p. 57-70.
7. Hanahan, D. and R.A. Weinberg, *Hallmarks of cancer: the next generation.* Cell, 2011. **144**(5): p. 646-74.
8. Ferrari, A., I. Sultan, T.T. Huang, C. Rodriguez-Galindo, A. Shehadeh, C. Meazza, K.K. Ness, M. Casanova, and S.L. Spunt, *Soft tissue sarcoma across the age spectrum: A population-based study from the surveillance epidemiology and end results database.* Pediatr Blood Cancer, 2011. **57**(6): p. 943-9.
9. Thway, K., *Pathology of soft tissue sarcomas.* Clin Oncol (R Coll Radiol), 2009. **21**(9): p. 695-705.
10. Mertens, F., C.R. Antonescu, P. Hohenberger, M. Ladanyi, P. Modena, M. D'Incalci, P.G. Casali, M. Aglietta, and T. Alvegard, *Translocation-related sarcomas.* Semin Oncol, 2009. **36**(4): p. 312-23.
11. Sultan, I., M. Casanova, U. Al-Jumaily, C. Meazza, C. Rodriguez-Galindo, and A. Ferrari, *Soft tissue sarcomas in the first year of life.* Eur J Cancer, 2010. **46**(13): p. 2449-56.
12. Perez, E.A., N. Kassira, M.C. Cheung, L.G. Koniaris, H.L. Neville, and J.E. Sola, *Rhabdomyosarcoma in children: a SEER population based study.* J Surg Res, 2011. **170**(2): p. e243-51.
13. Soliman, H., A. Ferrari, and D. Thomas, *Sarcoma in the young adult population: an international view.* Semin Oncol, 2009. **36**(3): p. 227-36.
14. Scurr, M. and I. Judson, *How to treat the Ewing's family of sarcomas in adult patients.* Oncologist, 2006. **11**(1): p. 65-72.
15. Merchant, M.S. and C.L. Mackall, *Current approach to pediatric soft tissue sarcomas.* Oncologist, 2009. **14**(11): p. 1139-53.
16. Savage, S.A. and L. Mirabello, *Using epidemiology and genomics to understand osteosarcoma etiology.* Sarcoma, 2011. **2011**: p. 548151.
17. Ahn, H.K., J.E. Uhm, J. Lee, H. Lim do, S.W. Seo, K.S. Sung, S.J. Lee, D.J. Lee, K.K. Baek, W.S. Kim, and J.O. Park, *Analysis of prognostic factors of pediatric-type sarcomas in adult patients.* Oncology, 2011. **80**(1-2): p. 21-8.
18. Van Gaal, J.C., E.S. De Bont, S.E. Kaal, Y. Versleijen-Jonkers, and W.T. van der Graaf, *Building the bridge between rhabdomyosarcoma in children, adolescents and young adults: the road ahead.* Crit Rev Oncol Hematol, 2012. **82**(3): p. 259-79.
19. Murphy, M.F., J.F. Bithell, C.A. Stiller, G.M. Kendall, and K.A. O'Neill, *Childhood and adult cancers: contrasts and commonalities.* Maturitas, 2013. **76**(1): p. 95-8.
20. Eilber, F.C. and S.M. Dry, *Diagnosis and management of synovial sarcoma.* J Surg Oncol, 2008. **97**(4): p. 314-20.
21. Stevens, M.C., *Treatment for childhood rhabdomyosarcoma: the cost of cure.* Lancet Oncol, 2005. **6**(2): p. 77-84.
22. Walterhouse, D. and A. Watson, *Optimal management strategies for rhabdomyosarcoma in children.* Paediatr Drugs, 2007. **9**(6): p. 391-400.
23. Norris, R.E. and P.C. Adamson, *Challenges and opportunities in childhood cancer drug development.* Nat Rev Cancer, 2012. **12**(11): p. 776-82.
24. Hawkins, D.S., S.L. Spunt, and S.X. Skapek, *Children's Oncology Group's 2013 blueprint for research: Soft tissue sarcomas.* Pediatr Blood Cancer, 2013. **60**(6): p. 1001-8.
25. Malempati, S. and D.S. Hawkins, *Rhabdomyosarcoma: review of the Children's Oncology Group (COG) Soft-Tissue Sarcoma Committee experience and rationale for current COG studies.* Pediatr Blood Cancer, 2012. **59**(1): p. 5-10.
26. Esiashvili, N., M. Goodman, and R.B. Marcus, Jr., *Changes in incidence and survival of Ewing sarcoma patients over the past 3 decades: Surveillance Epidemiology and End Results data.* J Pediatr Hematol Oncol, 2008. **30**(6): p. 425-30.
27. Crist, W.M., J.R. Anderson, J.L. Meza, C. Fryer, R.B. Raney, F.B. Ruymann, J. Breneman, S.J. Qualman, E. Wiener, M. Wharam, T. Lobe, B. Webber, H.M. Maurer, and S.S. Donaldson, *Intergroup rhabdomyosarcoma study-IV: results for patients with nonmetastatic disease.* J Clin Oncol, 2001. **19**(12): p. 3091-102.

28. Oeffinger, K.C., A.C. Mertens, C.A. Sklar, T. Kawashima, M.M. Hudson, A.T. Meadows, D.L. Friedman, N. Marina, W. Hobbie, N.S. Kadan-Lottick, C.L. Schwartz, W. Leisenring, and L.L. Robison, *Chronic health conditions in adult survivors of childhood cancer.* N Engl J Med, 2006. **355**(15): p. 1572-82.
29. Bhatia, S. and A.T. Meadows, *Long-term follow-up of childhood cancer survivors: future directions for clinical care and research.* Pediatr Blood Cancer, 2006. **46**(2): p. 143-8.
30. Reulen, R.C., C. Frobisher, D.L. Winter, J. Kelly, E.R. Lancashire, C.A. Stiller, K. Pritchard-Jones, H.C. Jenkinson, and M.M. Hawkins, *Long-term risks of subsequent primary neoplasms among survivors of childhood cancer.* JAMA, 2011. **305**(22): p. 2311-9.
31. Hawkins, D.S., A.A. Gupta, and E.R. Rudzinski, *What is new in the biology and treatment of pediatric rhabdomyosarcoma?* Curr Opin Pediatr, 2014. **26**(1): p. 50-6.
32. Jenney, M., O. Oberlin, G. Audry, M.C. Stevens, A. Rey, J.H. Merks, A. Kelsey, S. Gallego, C. Haie-Meder, and H. Martelli, *Conservative approach in localised rhabdomyosarcoma of the bladder and prostate: results from International Society of Paediatric Oncology (SIOP) studies: malignant mesenchymal tumour (MMT) 84, 89 and 95.* Pediatr Blood Cancer, 2014. **61**(2): p. 217-22.
33. Helman, L.J. and P. Meltzer, *Mechanisms of sarcoma development.* Nat Rev Cancer, 2003. **3**(9): p. 685-94.
34. Haldar, M., J.D. Hancock, C.M. Coffin, S.L. Lessnick, and M.R. Capecchi, *A conditional mouse model of synovial sarcoma: insights into a myogenic origin.* Cancer Cell, 2007. **11**(4): p. 375-88.
35. Haldar, M., R.L. Randall, and M.R. Capecchi, *Synovial sarcoma: from genetics to genetic-based animal modeling.* Clin Orthop Relat Res, 2008. **466**(9): p. 2156-67.
36. De Giovanni, C., L. Landuzzi, G. Nicoletti, P.L. Lollini, and P. Nanni, *Molecular and cellular biology of rhabdomyosarcoma.* Future Oncol, 2009. **5**(9): p. 1449-75.
37. Lessnick, S.L. and M. Ladanyi, *Molecular pathogenesis of Ewing sarcoma: new therapeutic and transcriptional targets.* Annu Rev Pathol, 2012. **7**: p. 145-59.
38. Naini, S., K.T. Etheridge, S.J. Adam, S.J. Qualman, R.C. Bentley, C.M. Counter, and C.M. Linardic, *Defining the cooperative genetic changes that temporally drive alveolar rhabdomyosarcoma.* Cancer Res, 2008. **68**(23): p. 9583-8.
39. Keller, C., B.R. Arenkiel, C.M. Coffin, N. El-Bardeesy, R.A. DePinho, and M.R. Capecchi, *Alveolar rhabdomyosarcomas in conditional Pax3:Fkhr mice: cooperativity of Ink4a/ARF and Trp53 loss of function.* Genes Dev, 2004. **18**(21): p. 2614-26.
40. Nishijo, K., Q.R. Chen, L. Zhang, A.T. McCleish, A. Rodriguez, M.J. Cho, S.I. Prajapati, J.A. Gelfond, G.B. Chisholm, J.E. Michalek, B.J. Aronow, F.G. Barr, R.L. Randall, M. Ladanyi, S.J. Qualman, B.P. Rubin, R.D. LeGallo, C. Wang, J. Khan, and C. Keller, *Credentialing a preclinical mouse model of alveolar rhabdomyosarcoma.* Cancer Res, 2009. **69**(7): p. 2902-11.
41. Chen, X., E. Stewart, A.A. Shelat, C. Qu, A. Bahrami, M. Hatley, G. Wu, C. Bradley, J. McEvoy, A. Pappo, S. Spunt, M.B. Valentine, V. Valentine, F. Krafcik, W.H. Lang, M. Wierdl, L. Tsurkan, V. Tolleman, S.M. Federico, C. Morton, C. Lu, L. Ding, J. Easton, M. Rusch, P. Nagahawatte, J. Wang, M. Parker, L. Wei, E. Hedlund, D. Finkelstein, M. Edmonson, S. Shurtleff, K. Boggs, H. Mulder, D. Yergeau, S. Skapek, D.S. Hawkins, N. Ramirez, P.M. Potter, J.A. Sandoval, A.M. Davidoff, E.R. Mardis, R.K. Wilson, J. Zhang, J.R. Downing, and M.A. Dyer, *Targeting oxidative stress in embryonal rhabdomyosarcoma.* Cancer Cell, 2013. **24**(6): p. 710-24.
42. Shern, J.F., L. Chen, J. Chmielecki, J.S. Wei, R. Patidar, M. Rosenberg, L. Ambrogio, D. Auclair, J. Wang, Y.K. Song, C. Tolman, L. Hurd, H. Liao, S. Zhang, D. Bogen, A.S. Brohl, S. Sindiri, D. Catchpoole, T. Badgett, G. Getz, J. Mora, J.R. Anderson, S.X. Skapek, F.G. Barr, M. Meyerson, D.S. Hawkins, and J. Khan, *Comprehensive Genomic Analysis of Rhabdomyosarcoma Reveals a Landscape of Alterations Affecting a Common Genetic Axis in Fusion-Positive and Fusion-Negative Tumors.* Cancer Discov, 2014.
43. Sharpless, N.E., D.O. Ferguson, R.C. O'Hagan, D.H. Castrillon, C. Lee, P.A. Farazi, S. Alson, J. Fleming, C.C. Morton, K. Frank, L. Chin, F.W. Alt, and R.A. DePinho, *Impaired nonhomologous end-joining provokes soft tissue sarcomas harboring chromosomal translocations, amplifications, and deletions.* Mol Cell, 2001. **8**(6): p. 1187-96.
44. Parham, D.M., R. Alaggio, and C.M. Coffin, *Myogenic tumors in children and adolescents.* Pediatr Dev Pathol, 2012. **15**(1 Suppl): p. 211-38.
45. Janeway, K.A. and C.R. Walkley, *Modeling human osteosarcoma in the mouse: From bedside to bench.* Bone, 2010. **47**(5): p. 859-65.
46. Jones, K.B., *Osteosarcomagenesis: modeling cancer initiation in the mouse.* Sarcoma, 2011. **2011**: p. 694136.
47. Rubin, B.P., K. Nishijo, H.I. Chen, X. Yi, D.P. Schuetze, R. Pal, S.I. Prajapati, J. Abraham, B.R. Arenkiel, Q.R. Chen, S. Davis, A.T. McCleish, M.R. Capecchi, J.E. Michalek, L.A. Zarzabal, J. Khan, Z. Yu, D.M. Parham, F.G. Barr, P.S. Meltzer, Y. Chen, and C. Keller, *Evidence for an unanticipated relationship between undifferentiated pleomorphic sarcoma and embryonal rhabdomyosarcoma.* Cancer Cell, 2011. **19**(2): p. 177-91.

48. Langenau, D.M., M.D. Keefe, N.Y. Storer, J.R. Guyon, J.L. Kutok, X. Le, W. Goessling, D.S. Neuberg, L.M. Kunkel, and L.I. Zon, *Effects of RAS on the genesis of embryonal rhabdomyosarcoma.* Genes Dev, 2007. **21**(11): p. 1382-95.
49. Kirsch, D.G., D.M. Dinulescu, J.B. Miller, J. Grimm, P.M. Santiago, N.P. Young, G.P. Nielsen, B.J. Quade, C.J. Chaber, C.P. Schultz, O. Takeuchi, R.T. Bronson, D. Crowley, S.J. Korsmeyer, S.S. Yoon, F.J. Hornicek, R. Weissleder, and T. Jacks, *A spatially and temporally restricted mouse model of soft tissue sarcoma.* Nat Med, 2007. **13**(8): p. 992-7.
50. Mito, J.K., R.F. Riedel, L. Dodd, G. Lahat, A.J. Lazar, R.D. Dodd, L. Stangenberg, W.C. Eward, F.J. Hornicek, S.S. Yoon, B.E. Brigman, T. Jacks, D. Lev, S. Mukherjee, and D.G. Kirsch, *Cross species genomic analysis identifies a mouse model as undifferentiated pleomorphic sarcoma/malignant fibrous histiocytoma.* PLoS One, 2009. **4**(11): p. e8075.
51. Broadhead, M.L., J.C. Clark, D.E. Myers, C.R. Dass, and P.F. Choong, *The molecular pathogenesis of osteosarcoma: a review.* Sarcoma, 2011. **2011**: p. 959248.
52. Belyea, B., J.G. Kephart, J. Blum, D.G. Kirsch, and C.M. Linardic, *Embryonic signaling pathways and rhabdomyosarcoma: contributions to cancer development and opportunities for therapeutic targeting.* Sarcoma, 2012. **2012**: p. 406239.
53. Le, X., E.K. Pugach, S. Hettmer, N.Y. Storer, J. Liu, A.A. Wills, A. DiBiase, E.Y. Chen, M.S. Ignatius, K.D. Poss, A.J. Wagers, D.M. Langenau, and L.I. Zon, *A novel chemical screening strategy in zebrafish identifies common pathways in embryogenesis and rhabdomyosarcoma development.* Development, 2013. **140**(11): p. 2354-64.
54. Wachtel, M. and B.W. Schafer, *Targets for cancer therapy in childhood sarcomas.* Cancer Treat Rev, 2010. **36**(4): p. 318-27.
55. Sokolowski, E., C.B. Turina, K. Kikuchi, D.M. Langenau, and C. Keller, *Proof-of-concept rare cancers in drug development: the case for rhabdomyosarcoma.* Oncogene, 2013.
56. Hettmer, S., J. Liu, C.M. Miller, M.C. Lindsay, C.A. Sparks, D.A. Guertin, R.T. Bronson, D.M. Langenau, and A.J. Wagers, *Sarcomas induced in discrete subsets of prospectively isolated skeletal muscle cells.* Proc Natl Acad Sci U S A, 2011. **108**(50): p. 20002-7.
57. Rota, R., R. Ciarapica, A. Giordano, L. Miele, and F. Locatelli, *MicroRNAs in rhabdomyosarcoma: pathogenetic implications and translational potentiality.* Mol Cancer, 2011. **10**: p. 120.
58. Katenkamp, D. and N.T. Raikhlin, *Stem cell concept and heterogeneity of malignant soft tissue tumor--a challenge to reconsider diagnostics and therapy?* Exp Pathol, 1985. **28**(1): p. 3-11.
59. Rodriguez, R., R. Rubio, and P. Menendez, *Modeling sarcomagenesis using multipotent mesenchymal stem cells.* Cell Res, 2012. **22**(1): p. 62-77.
60. Charytonowicz, E., C. Cordon-Cardo, I. Matushansky, and M. Ziman, *Alveolar rhabdomyosarcoma: is the cell of origin a mesenchymal stem cell?* Cancer Lett, 2009. **279**(2): p. 126-36.
61. Matushansky, I., E. Hernando, N.D. Socci, J.E. Mills, T.A. Matos, M.A. Edgar, S. Singer, R.G. Maki, and C. Cordon-Cardo, *Derivation of sarcomas from mesenchymal stem cells via inactivation of the Wnt pathway.* J Clin Invest, 2007. **117**(11): p. 3248-57.
62. Xiao, W., A.B. Mohseny, P.C. Hogendoorn, and A.M. Cleton-Jansen, *Mesenchymal stem cell transformation and sarcoma genesis.* Clin Sarcoma Res, 2013. **3**(1): p. 10.
63. Lin, P.P., Y. Wang, and G. Lozano, *Mesenchymal Stem Cells and the Origin of Ewing's Sarcoma.* Sarcoma, 2011. **2011**.
64. Matushansky, I., E. Charytonowicz, J. Mills, S. Siddiqi, T. Hricik, and C. Cordon-Cardo, *MFH classification: differentiating undifferentiated pleomorphic sarcoma in the 21st Century.* Expert Rev Anticancer Ther, 2009. **9**(8): p. 1135-44.
65. Lin, P.P., M.K. Pandey, F. Jin, A.K. Raymond, H. Akiyama, and G. Lozano, *Targeted mutation of p53 and Rb in mesenchymal cells of the limb bud produces sarcomas in mice.* Carcinogenesis, 2009. **30**(10): p. 1789-95.
66. Tirode, F., K. Laud-Duval, A. Prieur, B. Delorme, P. Charbord, and O. Delattre, *Mesenchymal stem cell features of Ewing tumors.* Cancer Cell, 2007. **11**(5): p. 421-9.
67. Lin, P.P., M.K. Pandey, F. Jin, S. Xiong, M. Deavers, J.M. Parant, and G. Lozano, *EWS-FLI1 induces developmental abnormalities and accelerates sarcoma formation in a transgenic mouse model.* Cancer Res, 2008. **68**(21): p. 8968-75.
68. Vogel, K.S., L.J. Klesse, S. Velasco-Miguel, K. Meyers, E.J. Rushing, and L.F. Parada, *Mouse tumor model for neurofibromatosis type 1.* Science, 1999. **286**(5447): p. 2176-9.
69. Nitzki, F., A. Zibat, A. Frommhold, A. Schneider, W. Schulz-Schaeffer, T. Braun, and H. Hahn, *Uncommitted precursor cells might contribute to increased incidence of embryonal rhabdomyosarcoma in heterozygous Patched1-mutant mice.* Oncogene, 2011. **30**(43): p. 4428-36.
70. Boue, D.R., D.M. Parham, B. Webber, W.M. Crist, and S.J. Qualman, *Clinicopathologic study of ectomesenchymomas from Intergroup Rhabdomyosarcoma Study Groups III and IV.* Pediatr Dev Pathol, 2000. **3**(3): p. 290-300.

71. Freitas, A.B., P.H. Aguiar, F.K. Miura, A. Yasuda, J. Soglia, F. Soglia, C.H. Aguiar, F. Vinko, and N.S. Silva, *Malignant ectomesenchymoma. Case report and review of the literature.* Pediatr Neurosurg, 1999. **30**(6): p. 320-30.
72. Pinto, A., P. Dickman, and D. Parham, *Pathobiologic markers of the ewing sarcoma family of tumors: state of the art and prediction of behaviour.* Sarcoma, 2011. **2011**: p. 856190.
73. von Levetzow, C., X. Jiang, Y. Gwye, G. von Levetzow, L. Hung, A. Cooper, J.H. Hsu, and E.R. Lawlor, *Modeling initiation of Ewing sarcoma in human neural crest cells.* PLoS One, 2011. **6**(4): p. e19305.
74. Chen, H., S. Zhang, J.C. Wen, J.K. Zheng, Q. Chen, W.Y. Li, P.P. Wang, L. Ma, T.H. Huang, G. Huang, and L.Y. Yang, *Several types of soft tissue sarcomas originate from the malignant transformation of adipose tissue-derived stem cells.* Mol Med Rep, 2010. **3**(3): p. 441-8.
75. Hatley, M.E., W. Tang, M.R. Garcia, D. Finkelstein, D.P. Millay, N. Liu, J. Graff, R.L. Galindo, and E.N. Olson, *A mouse model of rhabdomyosarcoma originating from the adipocyte lineage.* Cancer Cell, 2012. **22**(4): p. 536-46.
76. Rubio, R., I. Gutierrez-Aranda, A.I. Saez-Castillo, A. Labarga, M. Rosu-Myles, S. Gonzalez-Garcia, M.L. Toribio, P. Menendez, and R. Rodriguez, *The differentiation stage of p53-Rb-deficient bone marrow mesenchymal stem cells imposes the phenotype of in vivo sarcoma development.* Oncogene, 2013. **32**(41): p. 4970-80.
77. Liu, Y., B. Clem, E.K. Zuba-Surma, S. El-Naggar, S. Telang, A.B. Jenson, Y. Wang, H. Shao, M.Z. Ratajczak, J. Chesney, and D.C. Dean, *Mouse fibroblasts lacking RB1 function form spheres and undergo reprogramming to a cancer stem cell phenotype.* Cell Stem Cell, 2009. **4**(4): p. 336-47.
78. Hettmer, S. and A.J. Wagers, *Muscling in: Uncovering the origins of rhabdomyosarcoma.* Nat Med, 2010. **16**(2): p. 171-3.
79. Kikuchi, K. and C. Keller, *The not-so-skinny on muscle cancer.* Cancer Cell, 2012. **22**(4): p. 421-2.
80. Kikuchi, K., B.P. Rubin, and C. Keller, *Developmental origins of fusion-negative rhabdomyosarcomas.* Curr Top Dev Biol, 2011. **96**: p. 33-56.
81. Blanpain, C., *Tracing the cellular origin of cancer.* Nat Cell Biol, 2013. **15**(2): p. 126-34.
82. Clevers, H., *The cancer stem cell: premises, promises and challenges.* Nat Med, 2011. **17**(3): p. 313-9.
83. Satheesha, S. and B.W. Schäfer, *Cancer Stem Cells in Pediatric Sarcomas*, in *Stem Cells and Cancer Stem Cells: Therapeutic Applications in Disease and Injury*, M.A. Hayat, Editor. 2014, Springer: Dordrecht. p. 111-126.
84. Nowell, P.C., *The clonal evolution of tumor cell populations.* Science, 1976. **194**(4260): p. 23-8.
85. Orndal, C., A. Rydholm, H. Willen, F. Mitelman, and N. Mandahl, *Cytogenetic intratumor heterogeneity in soft tissue tumors.* Cancer Genet Cytogenet, 1994. **78**(2): p. 127-37.
86. Tarkkanen, M., R. Huuhtanen, M. Virolainen, T. Wiklund, S. Asko-Seljavaara, E. Tukiainen, M. Lepantalo, I. Elomaa, and S. Knuutila, *Comparison of genetic changes in primary sarcomas and their pulmonary metastases.* Genes Chromosomes Cancer, 1999. **25**(4): p. 323-31.
87. Popov, P., M. Virolainen, E. Tukiainen, S. Asko-Scljavaara, R. Huuhtanen, S. Knuutila, and M. Tarkkanen, *Primary soft tissue sarcoma and its local recurrence: genetic changes studied by comparative genomic hybridization.* Mod Pathol, 2001. **14**(10): p. 978-84.
88. Mertens, F., N. Mandahl, F. Mitelman, and S. Heim, *Cytogenetic analysis in the examination of solid tumors in children.* Pediatr Hematol Oncol, 1994. **11**(4): p. 361-77.
89. Dietrich, C.U., B.B. Jacobsen, H. Starklint, and S. Heim, *Clonal karyotypic evolution in an embryonal rhabdomyosarcoma with trisomy 8 as the primary chromosomal abnormality.* Genes Chromosomes Cancer, 1993. **7**(4): p. 240-4.
90. Manor, E., L. Bodner, P. Kachko, and J. Kapelushnik, *Trisomy 8 as a sole aberration in embryonal rhabdomyosarcoma (sarcoma botryoides) of the vagina.* Cancer Genet Cytogenet, 2009. **195**(2): p. 172-4.
91. Valent, P., D. Bonnet, R. De Maria, T. Lapidot, M. Copland, J.V. Melo, C. Chomienne, F. Ishikawa, J.J. Schuringa, G. Stassi, B. Huntly, H. Herrmann, J. Soulier, A. Roesch, G.J. Schuurhuis, S. Wohrer, M. Arock, J. Zuber, S. Cerny-Reiterer, H.E. Johnsen, M. Andreeff, and C. Eaves, *Cancer stem cell definitions and terminology: the devil is in the details.* Nat Rev Cancer, 2012. **12**(11): p. 767-75.
92. Visvader, J.E. and G.J. Lindeman, *Cancer stem cells in solid tumours: accumulating evidence and unresolved questions.* Nat Rev Cancer, 2008. **8**(10): p. 755-68.
93. Beck, B. and C. Blanpain, *Unravelling cancer stem cell potential.* Nat Rev Cancer, 2013. **13**(10): p. 727-38.
94. Magee, J.A., E. Piskounova, and S.J. Morrison, *Cancer stem cells: impact, heterogeneity, and uncertainty.* Cancer Cell, 2012. **21**(3): p. 283-96.
95. Reya, T., S.J. Morrison, M.F. Clarke, and I.L. Weissman, *Stem cells, cancer, and cancer stem cells.* Nature, 2001. **414**(6859): p. 105-11.

96. Meacham, C.E. and S.J. Morrison, *Tumour heterogeneity and cancer cell plasticity.* Nature, 2013. **501**(7467): p. 328-37.
97. Kreso, A. and J.E. Dick, *Evolution of the Cancer Stem Cell Model.* Cell Stem Cell, 2014. **14**(3): p. 275-291.
98. Wagner, E.R., G. Luther, G. Zhu, Q. Luo, Q. Shi, S.H. Kim, J.L. Gao, E. Huang, Y. Gao, K. Yang, L. Wang, C. Teven, X. Luo, X. Liu, M. Li, N. Hu, Y. Su, Y. Bi, B.C. He, N. Tang, J. Luo, L. Chen, G. Zuo, R. Rames, R.C. Haydon, H.H. Luu, and T.C. He, *Defective osteogenic differentiation in the development of osteosarcoma.* Sarcoma, 2011. **2011**: p. 325238.
99. Saab, R., S.L. Spunt, and S.X. Skapek, *Myogenesis and rhabdomyosarcoma the Jekyll and Hyde of skeletal muscle.* Curr Top Dev Biol, 2011. **94**: p. 197-234.
100. Gibbs, C.P., Jr., P.P. Levings, and S.C. Ghivizzani, *Evidence for the osteosarcoma stem cell.* Curr Orthop Pract, 2011. **22**(4): p. 322-326.
101. Wolden, S.L. and K.M. Alektiar, *Sarcomas across the age spectrum.* Semin Radiat Oncol, 2010. **20**(1): p. 45-51.
102. Cripe, T.P., *Can less really be more? Using lessons from leukemia and cancer stem cells to make sense of oral maintenance for metastatic sarcoma.* Pediatr Blood Cancer, 2008. **50**(4): p. 737-8.
103. Duan, J.J., W. Qiu, S.L. Xu, B. Wang, X.Z. Ye, Y.F. Ping, X. Zhang, X.W. Bian, and S.C. Yu, *Strategies for isolating and enriching cancer stem cells: well begun is half done.* Stem Cells Dev, 2013. **22**(16): p. 2221-39.
104. Basu-Roy, U., C. Basilico, and A. Mansukhani, *Perspectives on cancer stem cells in osteosarcoma.* Cancer Lett, 2012.
105. Dela Cruz, F.S., *Cancer stem cells in pediatric sarcomas.* Front Oncol, 2013. **3**: p. 168.
106. Friedman, G.K. and G.Y. Gillespie, *Cancer Stem Cells and Pediatric Solid Tumors.* Cancers (Basel), 2011. **3**(1): p. 298-318.
107. Riggi, N., M.L. Suva, and I. Stamenkovic, *The cancer stem cell paradigm in Ewing's sarcoma: what can we learn about these rare cells from a rare tumor?* Expert Rev Anticancer Ther, 2011. **11**(2): p. 143-5.
108. Bidlingmaier, S., X. Zhu, and B. Liu, *The utility and limitations of glycosylated human CD133 epitopes in defining cancer stem cells.* J Mol Med (Berl), 2008. **86**(9): p. 1025-32.
109. Tirino, V., V. Desiderio, R. d'Aquino, F. De Francesco, G. Pirozzi, A. Graziano, U. Galderisi, C. Cavaliere, A. De Rosa, G. Papaccio, and A. Giordano, *Detection and characterization of CD133+ cancer stem cells in human solid tumours.* PLoS One, 2008. **3**(10): p. e3469.
110. Tirino, V., V. Desiderio, F. Paino, A. De Rosa, F. Papaccio, F. Fazioli, G. Pirozzi, and G. Papaccio, *Human primary bone sarcomas contain CD133+ cancer stem cells displaying high tumorigenicity in vivo.* FASEB J, 2011. **25**(6): p. 2022-30.
111. Lou, N., Y. Wang, D. Sun, J. Zhao, and Z. Gao, *Isolation of stem-like cells from human MG-63 osteosarcoma cells using limiting dilution in combination with vincristine selection.* Indian J Biochem Biophys, 2010. **47**(6): p. 340-7.
112. Sana, J., I. Zambo, J. Skoda, J. Neradil, P. Chlapek, M. Hermanova, P. Mudry, A. Vasikova, K. Zitterbart, A. Hampl, J. Sterba, and R. Veselska, *CD133 expression and identification of CD133/nestin positive cells in rhabdomyosarcomas and rhabdomyosarcoma cell lines.* Anal Cell Pathol (Amst), 2011. **34**: p. 1-16.
113. Veselska, R., M. Hermanova, T. Loja, P. Chlapek, I. Zambo, K. Vesely, K. Zitterbart, and J. Sterba, *Nestin expression in osteosarcomas and derivation of nestin/CD133 positive osteosarcoma cell lines.* BMC Cancer, 2008. **8**: p. 300.
114. Walter, D., S. Satheesha, P. Albrecht, B.C. Bornhauser, V. D'Alessandro, S.M. Oesch, H. Rehrauer, I. Leuschner, E. Koscielniak, C. Gengler, H. Moch, M. Bernasconi, F.K. Niggli, and B.W. Schafer, *CD133 positive embryonal rhabdomyosarcoma stem-like cell population is enriched in rhabdospheres.* PLoS One, 2011. **6**(5): p. e19506.
115. Di Fiore, R., A. Santulli, R.D. Ferrante, M. Giuliano, A. De Blasio, C. Messina, G. Pirozzi, V. Tirino, G. Tesoriere, and R. Vento, *Identification and expansion of human osteosarcoma-cancer-stem cells by long-term 3-aminobenzamide treatment.* J Cell Physiol, 2009. **219**(2): p. 301-13.
116. Suva, M.L., N. Riggi, J.C. Stehle, K. Baumer, S. Tercier, J.M. Joseph, D. Suva, V. Clement, P. Provero, L. Cironi, M.C. Osterheld, L. Guillou, and I. Stamenkovic, *Identification of cancer stem cells in Ewing's sarcoma.* Cancer Res, 2009. **69**(5): p. 1776-81.
117. Awad, O., J.T. Yustein, P. Shah, N. Gul, V. Katuri, A. O'Neill, Y. Kong, M.L. Brown, J.A. Toretsky, and D.M. Loeb, *High ALDH activity identifies chemotherapy-resistant Ewing's sarcoma stem cells that retain sensitivity to EWS-FLI1 inhibition.* PLoS One, 2010. **5**(11): p. e13943.
118. Jiang, X., Y. Gwye, D. Russell, C. Cao, D. Douglas, L. Hung, H. Kovar, T.J. Triche, and E.R. Lawlor, *CD133 expression in chemo-resistant Ewing sarcoma cells.* BMC Cancer, 2010. **10**: p. 116.
119. Terry, J. and T. Nielsen, *Expression of CD133 in synovial sarcoma.* Appl Immunohistochem Mol Morphol, 2010. **18**(2): p. 159-65.

120. Naka, N., S. Takenaka, N. Araki, T. Miwa, N. Hashimoto, K. Yoshioka, S. Joyama, K. Hamada, Y. Tsukamoto, Y. Tomita, T. Ueda, H. Yoshikawa, and K. Itoh, *Synovial sarcoma is a stem cell malignancy.* Stem Cells, 2010. **28**(7): p. 1119-31.
121. Kimura, T., L. Wang, K. Tabu, H. Nishihara, Y. Mashita, N. Kikuchi, M. Tanino, H. Hiraga, and S. Tanaka, *CD133 negatively regulates tumorigenicity via AKT pathway in synovial sarcoma.* Cancer Invest, 2012. **30**(5): p. 390-7.
122. Yang, M., M. Yan, R. Zhang, J. Li, and Z. Luo, *Side population cells isolated from human osteosarcoma are enriched with tumor-initiating cells.* Cancer Sci, 2011.
123. Adhikari, A.S., N. Agarwal, B.M. Wood, C. Porretta, B. Ruiz, R.R. Pochampally, and T. Iwakuma, *CD117 and Stro-1 identify osteosarcoma tumor-initiating cells associated with metastasis and drug resistance.* Cancer Res, 2010. **70**(11): p. 4602-12.
124. Rainusso, N., T.K. Man, C.C. Lau, J. Hicks, J.J. Shen, A. Yu, L.L. Wang, and J.M. Rosen, *Identification and gene expression profiling of tumor-initiating cells isolated from human osteosarcoma cell lines in an orthotopic mouse model.* Cancer Biol Ther, 2011. **12**(4): p. 278-87.
125. Gibbs, C.P., V.G. Kukekov, J.D. Reith, O. Tchigrinova, O.N. Suslov, E.W. Scott, S.C. Ghivizzani, T.N. Ignatova, and D.A. Steindler, *Stem-like cells in bone sarcomas: implications for tumorigenesis.* Neoplasia, 2005. **7**(11): p. 967-76.
126. Zhang, H., H. Wu, J. Zheng, P. Yu, L. Xu, P. Jiang, J. Gao, H. Wang, and Y. Zhang, *Transforming growth factor beta1 signal is crucial for dedifferentiation of cancer cells to cancer stem cells in osteosarcoma.* Stem Cells, 2013. **31**(3): p. 433-46.
127. Berman, S.D., E. Calo, A.S. Landman, P.S. Danielian, E.S. Miller, J.C. West, B.D. Fonhoue, A. Caron, R. Bronson, M.L. Bouxsein, S. Mukherjee, and J.A. Lees, *Metastatic osteosarcoma induced by inactivation of Rb and p53 in the osteoblast lineage.* Proc Natl Acad Sci U S A, 2008. **105**(33): p. 11851-6.
128. Hirotsu, M., T. Setoguchi, Y. Matsunoshita, H. Sasaki, H. Nagao, H. Gao, K. Sugimura, and S. Komiya, *Tumour formation by single fibroblast growth factor receptor 3-positive rhabdomyosarcoma-initiating cells.* Br J Cancer, 2009. **101**(12): p. 2030-7.
129. Pressey, J.G., M.C. Haas, C.S. Pressey, V.M. Kelly, J.N. Parker, G.Y. Gillespie, and G.K. Friedman, *CD133 marks a myogenically primitive subpopulation in rhabdomyosarcoma cell lines that are relatively chemoresistant but sensitive to mutant HSV.* Pediatr Blood Cancer, 2013. **60**(1): p. 45-52.
130. Wahl, J., L. Bogatyreva, P. Boukamp, M. Rojewski, F. van Valen, J. Fiedler, N. Hipp, K.M. Debatin, and C. Beltinger, *Ewing's sarcoma cells with CD57-associated increase of tumorigenicity and with neural crest-like differentiation capacity.* Int J Cancer, 2010. **127**(6): p. 1295-307.
131. Scannell, C.A., E.A. Pedersen, J.T. Mosher, M.A. Krook, L.A. Nicholls, B.A. Wilky, D.M. Loeb, and E.R. Lawlor, *LGR5 is Expressed by Ewing Sarcoma and Potentiates Wnt/beta-Catenin Signaling.* Front Oncol, 2013. **3**: p. 81.
132. Barker, N. and H. Clevers, *Leucine-rich repeat-containing G-protein-coupled receptors as markers of adult stem cells.* Gastroenterology, 2010. **138**(5): p. 1681-96.
133. Schepers, A.G., H.J. Snippert, D.E. Stange, M. van den Born, J.H. van Es, M. van de Wetering, and H. Clevers, *Lineage tracing reveals Lgr5+ stem cell activity in mouse intestinal adenomas.* Science, 2012. **337**(6095): p. 730-5.
134. Pastrana, E., V. Silva-Vargas, and F. Doetsch, *Eyes wide open: a critical review of sphere-formation as an assay for stem cells.* Cell Stem Cell, 2011. **8**(5): p. 486-98.
135. Fujii, H., K. Honoki, T. Tsujiuchi, A. Kido, K. Yoshitani, and Y. Takakura, *Sphere-forming stem-like cell populations with drug resistance in human sarcoma cell lines.* Int J Oncol, 2009. **34**(5): p. 1381-6.
136. Fujii, H., K. Honoki, T. Tsujiuchi, A. Kido, K. Yoshitani, T. Mori, and Y. Takakura, *Reduced expression of INK4a/ARF genes in stem-like sphere cells from rat sarcomas.* Biochem Biophys Res Commun, 2007. **362**(3): p. 773-8.
137. Wang, L., P. Park, and C.Y. Lin, *Characterization of stem cell attributes in human osteosarcoma cell lines.* Cancer Biol Ther, 2009. **8**(6): p. 543-52.
138. Basu-Roy, U., E. Seo, L. Ramanathapuram, T.B. Rapp, J.A. Perry, S.H. Orkin, A. Mansukhani, and C. Basilico, *Sox2 maintains self renewal of tumor-initiating cells in osteosarcomas.* Oncogene, 2012. **31**(18): p. 2270-82.
139. Levings, P.P., S.V. McGarry, T.P. Currie, D.M. Nickerson, S. McClellan, S.C. Ghivizzani, D.A. Steindler, and C.P. Gibbs, *Expression of an exogenous human Oct-4 promoter identifies tumor-initiating cells in osteosarcoma.* Cancer Res, 2009. **69**(14): p. 5648-55.
140. Murase, M., M. Kano, T. Tsukahara, A. Takahashi, T. Torigoe, S. Kawaguchi, S. Kimura, T. Wada, Y. Uchihashi, T. Kondo, T. Yamashita, and N. Sato, *Side population cells have the characteristics of cancer stem-like cells/cancer-initiating cells in bone sarcomas.* Br J Cancer, 2009. **101**(8): p. 1425-32.
141. Siclari, V.A. and L. Qin, *Targeting the osteosarcoma cancer stem cell.* J Orthop Surg Res, 2010. **5**: p. 78.

142. Komuro, H., R. Saihara, M. Shinya, J. Takita, S. Kaneko, M. Kaneko, and Y. Hayashi, *Identification of side population cells (stem-like cell population) in pediatric solid tumor cell lines.* J Pediatr Surg, 2007. **42**(12): p. 2040-5.
143. Yang, M., R. Zhang, M. Yan, Z. Ye, W. Liang, and Z. Luo, *Detection and characterization of side population in Ewing's sarcoma SK-ES-1 cells in vitro.* Biochem Biophys Res Commun, 2010. **391**(1): p. 1062-6.
144. Wang, C.Y., Q. Wei, I. Han, S. Sato, R. Ghanbari-Azarnier, H. Whetstone, R. Poon, J. Hu, F. Zheng, P. Zhang, W. Wang, J.S. Wunder, and B.A. Alman, *Hedgehog and Notch signaling regulate self-renewal of undifferentiated pleomorphic sarcomas.* Cancer Res, 2012. **72**(4): p. 1013-22.
145. Das, B., R. Tsuchida, D. Malkin, G. Koren, S. Baruchel, and H. Yeger, *Hypoxia enhances tumor stemness by increasing the invasive and tumorigenic side population fraction.* Stem Cells, 2008. **26**(7): p. 1818-30.
146. Tsuchida, R., B. Das, H. Yeger, G. Koren, M. Shibuya, P.S. Thorner, S. Baruchel, and D. Malkin, *Cisplatin treatment increases survival and expansion of a highly tumorigenic side-population fraction by upregulating VEGF/Flt1 autocrine signaling.* Oncogene, 2008. **27**(28): p. 3923-34.
147. Wang, L., P. Park, H. Zhang, F. La Marca, and C.Y. Lin, *Prospective identification of tumorigenic osteosarcoma cancer stem cells in OS99-1 cells based on high aldehyde dehydrogenase activity.* Int J Cancer, 2011. **128**(2): p. 294-303.
148. Chiodi, I., C. Belgiovine, F. Dona, A.I. Scovassi, and C. Mondello, *Drug treatment of cancer cell lines: a way to select for cancer stem cells?* Cancers (Basel), 2011. **3**(1): p. 1111-28.
149. Di Fiore, R., A. Guercio, R. Puleio, P. Di Marco, R. Drago-Ferrante, A. D'Anneo, A. De Blasio, D. Carlisi, S. Di Bella, F. Pentimalli, I.M. Forte, A. Giordano, G. Tesoriere, and R. Vento, *Modeling human osteosarcoma in mice through 3AB-OS cancer stem cell xenografts.* J Cell Biochem, 2012. **113**(11): p. 3380-92.
150. Wang, L., P. Park, H. Zhang, F. La Marca, A. Claeson, J. Valdivia, and C.Y. Lin, *BMP-2 inhibits the tumorigenicity of cancer stem cells in human osteosarcoma OS99-1 cell line.* Cancer Biol Ther, 2011. **11**(5): p. 457-63.
151. Riggi, N., M.L. Suva, C. De Vito, P. Provero, J.C. Stehle, K. Baumer, L. Cironi, M. Janiszewska, T. Petricevic, D. Suva, S. Tercier, J.M. Joseph, L. Guillou, and I. Stamenkovic, *EWS-FLI-1 modulates miRNA145 and SOX2 expression to initiate mesenchymal stem cell reprogramming toward Ewing sarcoma cancer stem cells.* Genes Dev, 2010. **24**(9): p. 916-32.
152. Xia, S.J., D.D. Holder, B.R. Pawel, C. Zhang, and F.G. Barr, *High expression of the PAX3-FKHR oncoprotein is required to promote tumorigenesis of human myoblasts.* Am J Pathol, 2009. **175**(6): p. 2600-8.
153. Vidal, S.J., V. Rodriguez-Bravo, M. Galsky, C. Cordon-Cardo, and J. Domingo-Domenech, *Targeting cancer stem cells to suppress acquired chemotherapy resistance.* Oncogene, 2013.
154. Honoki, K., *Do stem-like cells play a role in drug resistance of sarcomas?* Expert Rev Anticancer Ther, 2010. **10**(2): p. 261-70.
155. Honoki, K., H. Fujii, A. Kubo, A. Kido, T. Mori, Y. Tanaka, and T. Tsujiuchi, *Possible involvement of stem-like populations with elevated ALDH1 in sarcomas for chemotherapeutic drug resistance.* Oncol Rep, 2010. **24**(2): p. 501-5.
156. He, A., W. Qi, Y. Huang, T. Feng, J. Chen, Y. Sun, Z. Shen, and Y. Yao, *CD133 expression predicts lung metastasis and poor prognosis in osteosarcoma patients: A clinical and experimental study.* Exp Ther Med, 2012. **4**(3): p. 435-441.
157. De Sousa, E.M.F., L. Vermeulen, E. Fessler, and J.P. Medema, *Cancer heterogeneity--a multifaceted view.* EMBO Rep, 2013. **14**(8): p. 686-95.
158. De Vito, C., N. Riggi, S. Cornaz, M.L. Suva, K. Baumer, P. Provero, and I. Stamenkovic, *A TARBP2-dependent miRNA expression profile underlies cancer stem cell properties and provides candidate therapeutic reagents in Ewing sarcoma.* Cancer Cell, 2012. **21**(6): p. 807-21.
159. De Vito, C., N. Riggi, M.L. Suva, M. Janiszewska, J. Horlbeck, K. Baumer, P. Provero, and I. Stamenkovic, *Let-7a is a direct EWS-FLI-1 target implicated in Ewing's sarcoma development.* PLoS One, 2011. **6**(8): p. e23592.
160. Kho, A.T., Q. Zhao, Z. Cai, A.J. Butte, J.Y. Kim, S.L. Pomeroy, D.H. Rowitch, and I.S. Kohane, *Conserved mechanisms across development and tumorigenesis revealed by a mouse development perspective of human cancers.* Genes Dev, 2004. **18**(6): p. 629-40.
161. Amakye, D., Z. Jagani, and M. Dorsch, *Unraveling the therapeutic potential of the Hedgehog pathway in cancer.* Nat Med, 2013. **19**(11): p. 1410-22.
162. Gaarenstroom, T. and C.S. Hill, *TGF-beta signaling to chromatin: How Smads regulate transcription during self-renewal and differentiation.* Semin Cell Dev Biol, 2014.
163. Koch, U., R. Lehal, and F. Radtke, *Stem cells living with a Notch.* Development, 2013. **140**(4): p. 689-704.
164. Merchant, A.A. and W. Matsui, *Targeting Hedgehog--a cancer stem cell pathway.* Clin Cancer Res, 2010. **16**(12): p. 3130-40.

165. Oshimori, N. and E. Fuchs, *The harmonies played by TGF-beta in stem cell biology.* Cell Stem Cell, 2012. **11**(6): p. 751-64.
166. Pannuti, A., K. Foreman, P. Rizzo, C. Osipo, T. Golde, B. Osborne, and L. Miele, *Targeting Notch to target cancer stem cells.* Clin Cancer Res, 2010. **16**(12): p. 3141-52.
167. Takahashi-Yanaga, F. and M. Kahn, *Targeting Wnt signaling: can we safely eradicate cancer stem cells?* Clin Cancer Res, 2010. **16**(12): p. 3153-62.
168. Takebe, N., P.J. Harris, R.Q. Warren, and S.P. Ivy, *Targeting cancer stem cells by inhibiting Wnt, Notch, and Hedgehog pathways.* Nat Rev Clin Oncol, 2011. **8**(2): p. 97-106.
169. Takebe, N. and S.P. Ivy, *Controversies in cancer stem cells: targeting embryonic signaling pathways.* Clin Cancer Res, 2010. **16**(12): p. 3106-12.
170. van Amerongen, R. and R. Nusse, *Towards an integrated view of Wnt signaling in development.* Development, 2009. **136**(19): p. 3205-14.
171. Clevers, H., *Wnt/beta-catenin signaling in development and disease.* Cell, 2006. **127**(3): p. 469-80.
172. Slusarski, D.C. and F. Pelegri, *Calcium signaling in vertebrate embryonic patterning and morphogenesis.* Dev Biol, 2007. **307**(1): p. 1-13.
173. Hui, C.C. and S. Angers, *Gli proteins in development and disease.* Annu Rev Cell Dev Biol, 2011. **27**: p. 513-37.
174. Vijayakumar, S., G. Liu, I.A. Rus, S. Yao, Y. Chen, G. Akiri, L. Grumolato, and S.A. Aaronson, *High-frequency canonical Wnt activation in multiple sarcoma subtypes drives proliferation through a TCF/beta-catenin target gene, CDC25A.* Cancer Cell, 2011. **19**(5): p. 601-12.
175. Krause, U., D.M. Ryan, B.H. Clough, and C.A. Gregory, *An unexpected role for a Wnt-inhibitor: Dickkopf-1 triggers a novel cancer survival mechanism through modulation of aldehyde-dehydrogenase-1 activity.* Cell Death Dis, 2014. **5**: p. e1093.
176. Chen, E.Y., M.T. Deran, M.S. Ignatius, K.B. Grandinetti, R. Clagg, K.M. McCarthy, R.M. Lobbardi, J. Brockmann, C. Keller, X. Wu, and D.M. Langenau, *Glycogen synthase kinase 3 inhibitors induce the canonical WNT/beta-catenin pathway to suppress growth and self-renewal in embryonal rhabdomyosarcoma.* Proc Natl Acad Sci U S A, 2014. **111**(14): p. 5349-54.
177. Karamboulas, C. and L. Ailles, *Developmental signaling pathways in cancer stem cells of solid tumors.* Biochim Biophys Acta, 2013. **1830**(2): p. 2481-95.
178. Annavarapu, S.R., S. Cialfi, C. Dominici, G.K. Kokai, S. Uccini, S. Ceccarelli, H.P. McDowell, and T.R. Helliwell, *Characterization of Wnt/beta-catenin signaling in rhabdomyosarcoma.* Lab Invest, 2013. **93**(10): p. 1090-9.
179. Singh, S., C. Vinson, C.M. Gurley, G.T. Nolen, M.L. Beggs, R. Nagarajan, E.F. Wagner, D.M. Parham, and C.A. Peterson, *Impaired Wnt signaling in embryonal rhabdomyosarcoma cells from p53/c-fos double mutant mice.* Am J Pathol, 2010. **177**(4): p. 2055-66.
180. Cleton-Jansen, A.M., J.K. Anninga, I.H. Briaire-de Bruijn, S. Romeo, J. Oosting, R.M. Egeler, H. Gelderblom, A.H. Taminiau, and P.C. Hogendoorn, *Profiling of high-grade central osteosarcoma and its putative progenitor cells identifies tumourigenic pathways.* Br J Cancer, 2009. **101**(12): p. 2064.
181. Roma, J., A. Almazan-Moga, J. Sanchez de Toledo, and S. Gallego, *Notch, wnt, and hedgehog pathways in rhabdomyosarcoma: from single pathways to an integrated network.* Sarcoma, 2012. **2012**: p. 695603.
182. Navarro, D., N. Agra, A. Pestana, J. Alonso, and J.M. Gonzalez-Sancho, *The EWS/FLI1 oncogenic protein inhibits expression of the Wnt inhibitor DICKKOPF-1 gene and antagonizes beta-catenin/TCF-mediated transcription.* Carcinogenesis, 2010. **31**(3): p. 394-401.
183. Pretto, D., R. Barco, J. Rivera, N. Neel, M.D. Gustavson, and J.E. Eid, *The synovial sarcoma translocation protein SYT-SSX2 recruits beta-catenin to the nucleus and associates with it in an active complex.* Oncogene, 2006. **25**(26): p. 3661-9.
184. Manoranjan, B., C. Venugopal, N. McFarlane, B.W. Doble, S.E. Dunn, K. Scheinemann, and S.K. Singh, *Medulloblastoma stem cells: where development and cancer cross pathways.* Pediatr Res, 2012. **71**(4 Pt 2): p. 516-22.
185. Moore, S.W., *Developmental genes and cancer in children.* Pediatr Blood Cancer, 2009. **52**(7): p. 755-60.
186. Wang, S., L. Guo, L. Dong, S. Li, J. Zhang, and M. Sun, *TGF-beta1 signal pathway may contribute to rhabdomyosarcoma development by inhibiting differentiation.* Cancer Sci, 2010. **101**(5): p. 1108-16.
187. Qi, Y., C.C. Wang, Y.L. He, H. Zou, C.X. Liu, L.J. Pang, J.M. Hu, J.F. Jiang, W.J. Zhang, and F. Li, *The correlation between morphology and the expression of TGF-beta signaling pathway proteins and epithelial-mesenchymal transition-related proteins in synovial sarcomas.* Int J Clin Exp Pathol, 2013. **6**(12): p. 2787-99.
188. Aref, D., C.J. Moffatt, S. Agnihotri, V. Ramaswamy, A.M. Dubuc, P.A. Northcott, M.D. Taylor, A. Perry, J.M. Olson, C.G. Eberhart, and S.E. Croul, *Canonical TGF-beta pathway activity is a predictor of SHH-driven medulloblastoma survival and delineates putative precursors in cerebellar development.* Brain Pathol, 2013. **23**(2): p. 178-91.

189. Jennings, M.T., I.T. Kaariainen, L. Gold, R.J. Maciunas, and P.A. Commers, *TGF beta 1 and TGF beta 2 are potential growth regulators for medulloblastomas, primitive neuroectodermal tumors, and ependymomas: evidence in support of an autocrine hypothesis.* Hum Pathol, 1994. **25**(5): p. 464-75.
190. Zhang, L., W. Liu, Y. Qin, and R. Wu, *Expression of TGF-beta1 in Wilms' tumor was associated with invasiveness and disease progression.* J Pediatr Urol, 2014.
191. Belyea, B.C., S. Naini, R.C. Bentley, and C.M. Linardic, *Inhibition of the Notch-Hey1 axis blocks embryonal rhabdomyosarcoma tumorigenesis.* Clin Cancer Res, 2011. **17**(23): p. 7324-36.
192. Nagao, H., T. Setoguchi, S. Kitamoto, Y. Ishidou, S. Nagano, M. Yokouchi, M. Abematsu, N. Kawabata, S. Maeda, S. Yonezawa, and S. Komiya, *RBPJ is a novel target for rhabdomyosarcoma therapy.* PLoS One, 2012. **7**(7): p. e39268.
193. Guijarro, M.V., S. Dahiya, L.S. Danielson, M.F. Segura, F.M. Vales-Lara, S. Menendez, D. Popiolek, K. Mittal, J.J. Wei, J. Zavadil, C. Cordon-Cardo, P.P. Pandolfi, and E. Hernando, *Dual Pten/Tp53 suppression promotes sarcoma progression by activating Notch signaling.* Am J Pathol, 2013. **182**(6): p. 2015-27.
194. Tanaka, M., T. Setoguchi, M. Hirotsu, H. Gao, H. Sasaki, Y. Matsunoshita, and S. Komiya, *Inhibition of Notch pathway prevents osteosarcoma growth by cell cycle regulation.* Br J Cancer, 2009. **100**(12): p. 1957-65.
195. Zhang, P., Y. Yang, P.A. Zweidler-McKay, and D.P. Hughes, *Critical role of notch signaling in osteosarcoma invasion and metastasis.* Clin Cancer Res, 2008. **14**(10): p. 2962-9.
196. Rota, R., R. Ciarapica, L. Miele, and F. Locatelli, *Notch signaling in pediatric soft tissue sarcomas.* BMC Med, 2012. **10**: p. 141.
197. Zweidler-McKay, P.A., *Notch signaling in pediatric malignancies.* Curr Oncol Rep, 2008. **10**(6): p. 459-68.
198. Santini, R., M.C. Vinci, S. Pandolfi, J.Y. Penachioni, V. Montagnani, B. Olivito, R. Gattai, N. Pimpinelli, G. Gerlini, L. Borgognoni, and B. Stecca, *Hedgehog-GLI signaling drives self-renewal and tumorigenicity of human melanoma-initiating cells.* Stem Cells, 2012. **30**(9): p. 1808-18.
199. Oue, T., A. Yoneda, S. Uehara, H. Yamanaka, and M. Fukuzawa, *Increased expression of the hedgehog signaling pathway in pediatric solid malignancies.* J Pediatr Surg, 2010. **45**(2): p. 387-92.
200. Macdonald, T.J., *Hedgehog Pathway in Pediatric Cancers: They're Not Just for Brain Tumors Anymore.* Am Soc Clin Oncol Educ Book, 2012. **32**: p. 605-609.
201. Shahi, M.H., J.A. Rey, and J.S. Castresana, *The sonic hedgehog-GLI1 signaling pathway in brain tumor development.* Expert Opin Ther Targets, 2012. **16**(12): p. 1227-38.
202. Monje, M., S.S. Mitra, M.E. Freret, T.B. Raveh, J. Kim, M. Masek, J.L. Attema, G. Li, T. Haddix, M.S. Edwards, P.G. Fisher, I.L. Weissman, D.H. Rowitch, H. Vogel, A.J. Wong, and P.A. Beachy, *Hedgehog-responsive candidate cell of origin for diffuse intrinsic pontine glioma.* Proc Natl Acad Sci U S A, 2011. **108**(11): p. 4453-8.
203. Po, A., E. Ferretti, E. Miele, E. De Smaele, A. Paganelli, G. Canettieri, S. Coni, L. Di Marcotullio, M. Biffoni, L. Massimi, C. Di Rocco, I. Screpanti, and A. Gulino, *Hedgehog controls neural stem cells through p53-independent regulation of Nanog.* EMBO J, 2010. **29**(15): p. 2646-58.
204. Zbinden, M., A. Duquet, A. Lorente-Trigos, S.N. Ngwabyt, I. Borges, and A. Ruiz i Altaba, *NANOG regulates glioma stem cells and is essential in vivo acting in a cross-functional network with GLI1 and p53.* EMBO J, 2010. **29**(15): p. 2659-74.
205. Chambers, I. and S.R. Tomlinson, *The transcriptional foundation of pluripotency.* Development, 2009. **136**(14): p. 2311-22.
206. MacArthur, B.D., A. Sevilla, M. Lenz, F.J. Muller, B.M. Schuldt, A.A. Schuppert, S.J. Ridden, P.S. Stumpf, M. Fidalgo, A. Ma'ayan, J. Wang, and I.R. Lemischka, *Nanog-dependent feedback loops regulate murine embryonic stem cell heterogeneity.* Nat Cell Biol, 2012. **14**(11): p. 1139-47.
207. Kalmar, T., C. Lim, P. Hayward, S. Munoz-Descalzo, J. Nichols, J. Garcia-Ojalvo, and A. Martinez Arias, *Regulated fluctuations in nanog expression mediate cell fate decisions in embryonic stem cells.* PLoS Biol, 2009. **7**(7): p. e1000149.
208. Navarro, P., N. Festuccia, D. Colby, A. Gagliardi, N.P. Mullin, W. Zhang, V. Karwacki-Neisius, R. Osorno, D. Kelly, M. Robertson, and I. Chambers, *OCT4/SOX2-independent Nanog autorepression modulates heterogeneous Nanog gene expression in mouse ES cells.* EMBO J, 2012. **31**(24): p. 4547-62.
209. Smith, A., *Nanog heterogeneity: tilting at windmills?* Cell Stem Cell, 2013. **13**(1): p. 6-7.
210. Santaliz-Ruiz, L.E., X. Xie, M. Old, T.N. Teknos, Q. Pan, A.G. James, and R.J. Solove, *Emerging role of nanog in tumorigenesis and cancer stem cells.* Int J Cancer, 2013.
211. Wang, M.L., S.H. Chiou, and C.W. Wu, *Targeting cancer stem cells: emerging role of Nanog transcription factor.* Onco Targets Ther, 2013. **6**: p. 1207-1220.
212. Booth, H.A. and P.W. Holland, *Eleven daughters of NANOG.* Genomics, 2004. **84**(2): p. 229-38.
213. Jeter, C.R., M. Badeaux, G. Choy, D. Chandra, L. Patrawala, C. Liu, T. Calhoun-Davis, H. Zaehres, G.Q. Daley, and D.G. Tang, *Functional evidence that the self-renewal gene NANOG regulates human tumor development.* Stem Cells, 2009. **27**(5): p. 993-1005.

214. Jeter, C.R., *Investigating the role of the embryonic stem cell self-renewal gene NANOG in neoplastic process*, in *Stem Cells and Cancer Stem Cells: Therapeutic Applications in Disease and Injury*, M.A. Hayat, Editor. 2014, Springer: Dordrecht.
215. Apostolou, E., F. Ferrari, R.M. Walsh, O. Bar-Nur, M. Stadtfeld, S. Cheloufi, H.T. Stuart, J.M. Polo, T.K. Ohsumi, M.L. Borowsky, P.V. Kharchenko, P.J. Park, and K. Hochedlinger, *Genome-wide chromatin interactions of the Nanog locus in pluripotency, differentiation, and reprogramming.* Cell Stem Cell, 2013. **12**(6): p. 699-712.
216. Liu, B., M.D. Badeaux, G. Choy, D. Chandra, I. Shen, C.R. Jeter, K. Rycaj, C.F. Lee, M.D. Person, C. Liu, Y. Chen, J. Shen, S.Y. Jung, J. Qin, and D.G. Tang, *Nanog1 in NTERA-2 and Recombinant NanogP8 from Somatic Cancer Cells Adopt Multiple Protein Conformations and Migrate at Multiple M.W Species.* PLoS One, 2014. **9**(3): p. e90615.
217. Lu, X., S.J. Mazur, T. Lin, E. Appella, and Y. Xu, *The pluripotency factor nanog promotes breast cancer tumorigenesis and metastasis.* Oncogene, 2013.
218. Badeaux, M.A., C.R. Jeter, S. Gong, B. Liu, M.V. Suraneni, J. Rundhaug, S.M. Fischer, T. Yang, D. Kusewitt, and D.G. Tang, *In vivo functional studies of tumor-specific retrogene NanogP8 in transgenic animals.* Cell Cycle, 2013. **12**(15): p. 2395-408.
219. Yamaguchi, S., K. Kurimoto, Y. Yabuta, H. Sasaki, N. Nakatsuji, M. Saitou, and T. Tada, *Conditional knockdown of Nanog induces apoptotic cell death in mouse migrating primordial germ cells.* Development, 2009. **136**(23): p. 4011-20.
220. Zanola, A., S. Rossi, F. Faggi, E. Monti, and A. Fanzani, *Rhabdomyosarcomas: an overview on the experimental animal models.* J Cell Mol Med, 2012. **16**(7): p. 1377-91.
221. Clement, V., P. Sanchez, N. de Tribolet, I. Radovanovic, and A. Ruiz i Altaba, *HEDGEHOG-GLI1 signaling regulates human glioma growth, cancer stem cell self-renewal, and tumorigenicity.* Curr Biol, 2007. **17**(2): p. 165-72.
222. Gopisetty, G., J. Xu, D. Sampath, H. Colman, and V.K. Puduvalli, *Epigenetic regulation of CD133/PROM1 expression in glioma stem cells by Sp1/myc and promoter methylation.* Oncogene, 2013. **32**(26): p. 3119-29.
223. Calabrese, C., H. Poppleton, M. Kocak, T.L. Hogg, C. Fuller, B. Hamner, E.Y. Oh, M.W. Gaber, D. Finklestein, M. Allen, A. Frank, I.T. Bayazitov, S.S. Zakharenko, A. Gajjar, A. Davidoff, and R.J. Gilbertson, *A perivascular niche for brain tumor stem cells.* Cancer Cell, 2007. **11**(1): p. 69-82.
224. Griguer, C.E., C.R. Oliva, E. Gobin, P. Marcorelles, D.J. Benos, J.R. Lancaster, Jr., and G.Y. Gillespie, *CD133 is a marker of bioenergetic stress in human glioma.* PLoS One, 2008. **3**(11): p. e3655.
225. Li, Z., S. Bao, Q. Wu, H. Wang, C. Eyler, S. Sathornsumetee, Q. Shi, Y. Cao, J. Lathia, R.E. McLendon, A.B. Hjelmeland, and J.N. Rich, *Hypoxia-inducible factors regulate tumorigenic capacity of glioma stem cells.* Cancer Cell, 2009. **15**(6): p. 501-13.
226. Matsumoto, K., T. Arao, K. Tanaka, H. Kaneda, K. Kudo, Y. Fujita, D. Tamura, K. Aomatsu, T. Tamura, Y. Yamada, N. Saijo, and K. Nishio, *mTOR signal and hypoxia-inducible factor-1 alpha regulate CD133 expression in cancer cells.* Cancer Res, 2009. **69**(18): p. 7160-4.
227. Pellacani, D., R.J. Packer, F.M. Frame, E.E. Oldridge, P.A. Berry, M.C. Labarthe, M.J. Stower, M.S. Simms, A.T. Collins, and N.J. Maitland, *Regulation of the stem cell marker CD133 is independent of promoter hypermethylation in human epithelial differentiation and cancer.* Mol Cancer, 2011. **10**: p. 94.
228. Soeda, A., M. Park, D. Lee, A. Mintz, A. Androutsellis-Theotokis, R.D. McKay, J. Engh, T. Iwama, T. Kunisada, A.B. Kassam, I.F. Pollack, and D.M. Park, *Hypoxia promotes expansion of the CD133-positive glioma stem cells through activation of HIF-1alpha.* Oncogene, 2009. **28**(45): p. 3949-59.
229. Bao, S., Q. Wu, S. Sathornsumetee, Y. Hao, Z. Li, A.B. Hjelmeland, Q. Shi, R.E. McLendon, D.D. Bigner, and J.N. Rich, *Stem cell-like glioma cells promote tumor angiogenesis through vascular endothelial growth factor.* Cancer Res, 2006. **66**(16): p. 7843-8.
230. Gallmeier, E., P.C. Hermann, M.T. Mueller, J.G. Machado, A. Ziesch, E.N. De Toni, A. Palagyi, C. Eisen, J.W. Ellwart, J. Rivera, B. Rubio-Viqueira, M. Hidalgo, F. Bunz, B. Goke, and C. Heeschen, *Inhibition of ataxia telangiectasia- and Rad3-related function abrogates the in vitro and in vivo tumorigenicity of human colon cancer cells through depletion of the CD133(+) tumor-initiating cell fraction.* Stem Cells, 2011. **29**(3): p. 418-29.
231. Wei, Y., Y. Jiang, F. Zou, Y. Liu, S. Wang, N. Xu, W. Xu, C. Cui, Y. Xing, B. Cao, C. Liu, G. Wu, H. Ao, X. Zhang, and J. Jiang, *Activation of PI3K/Akt pathway by CD133-p85 interaction promotes tumorigenic capacity of glioma stem cells.* Proc Natl Acad Sci U S A, 2013. **110**(17): p. 6829-34.
232. McEwen, D.G. and D.M. Ornitz, *Regulation of the fibroblast growth factor receptor 3 promoter and intron I enhancer by Sp1 family transcription factors.* J Biol Chem, 1998. **273**(9): p. 5349-57.
233. Perez-Castro, A.V., J. Wilson, and M.R. Altherr, *Genomic organization of the human fibroblast growth factor receptor 3 (FGFR3) gene and comparative sequence analysis with the mouse Fgfr3 gene.* Genomics, 1997. **41**(1): p. 10-6.

234. Tan, C.C., M.J. Walsh, and B.D. Gelb, *Fgfr3 is a transcriptional target of Ap2delta and Ash2l-containing histone methyltransferase complexes.* PLoS One, 2009. **4**(12): p. e8535.
235. Reinhold, M.I., D.G. McEwen, and M.C. Naski, *Fibroblast growth factor receptor 3 gene: regulation by serum response factor.* Mol Endocrinol, 2004. **18**(1): p. 241-51.
236. Tanoue, K., Y. Wang, M. Ikeda, K. Mitsui, R. Irie, T. Setoguchi, S. Komiya, S. Natsugoe, and K. Kosai, *Survivin-responsive conditionally replicating adenovirus kills rhabdomyosarcoma stem cells more efficiently than their progeny.* J Transl Med, 2014. **12**: p. 27.
237. Blick, C., A. Ramachandran, S. Wigfield, R. McCormick, A. Jubb, F.M. Buffa, H. Turley, M.A. Knowles, D. Cranston, J. Catto, and A.L. Harris, *Hypoxia regulates FGFR3 expression via HIF-1alpha and miR-100 and contributes to cell survival in non-muscle invasive bladder cancer.* Br J Cancer, 2013. **109**(1): p. 50-9.
238. Braun, T. and M. Gautel, *Transcriptional mechanisms regulating skeletal muscle differentiation, growth and homeostasis.* Nat Rev Mol Cell Biol, 2011. **12**(6): p. 349-61.
239. Francetic, T. and Q. Li, *Skeletal myogenesis and Myf5 activation.* Transcription, 2011. **2**(3): p. 109-114.
240. Borello, U., B. Berarducci, P. Murphy, L. Bajard, V. Buffa, S. Piccolo, M. Buckingham, and G. Cossu, *The Wnt/beta-catenin pathway regulates Gli-mediated Myf5 expression during somitogenesis.* Development, 2006. **133**(18): p. 3723-32.
241. Gustafsson, M.K., H. Pan, D.F. Pinney, Y. Liu, A. Lewandowski, D.J. Epstein, and C.P. Emerson, Jr., *Myf5 is a direct target of long-range Shh signaling and Gli regulation for muscle specification.* Genes Dev, 2002. **16**(1): p. 114-26.
242. Han, X.H., Y.R. Jin, M. Seto, and J.K. Yoon, *A WNT/beta-catenin signaling activator, R-spondin, plays positive regulatory roles during skeletal myogenesis.* J Biol Chem, 2011. **286**(12): p. 10649-59.
243. McDermott, A., M. Gustafsson, T. Elsam, C.C. Hui, C.P. Emerson, Jr., and A.G. Borycki, *Gli2 and Gli3 have redundant and context-dependent function in skeletal muscle formation.* Development, 2005. **132**(2): p. 345-57.
244. Sato, T., D. Rocancourt, L. Marques, S. Thorsteinsdottir, and M. Buckingham, *A Pax3/Dmrt2/Myf5 regulatory cascade functions at the onset of myogenesis.* PLoS Genet, 2010. **6**(4): p. e1000897.
245. Crist, C.G., D. Montarras, and M. Buckingham, *Muscle satellite cells are primed for myogenesis but maintain quiescence with sequestration of Myf5 mRNA targeted by microRNA-31 in mRNP granules.* Cell Stem Cell, 2012. **11**(1): p. 118-26.
246. Anderson, C., V.C. Williams, B. Moyon, P. Daubas, S. Tajbakhsh, M.E. Buckingham, T. Shiroishi, S.M. Hughes, and A.G. Borycki, *Sonic hedgehog acts cell-autonomously on muscle precursor cells to generate limb muscle diversity.* Genes Dev, 2012. **26**(18): p. 2103-17.
247. Gerber, A.N., C.W. Wilson, Y.J. Li, and P.T. Chuang, *The hedgehog regulated oncogenes Gli1 and Gli2 block myoblast differentiation by inhibiting MyoD-mediated transcriptional activation.* Oncogene, 2007. **26**(8): p. 1122-36.
248. Renault, M.A., S. Vandierdonck, C. Chapouly, Y. Yu, G. Qin, A. Metras, T. Couffinhal, D.W. Losordo, Q. Yao, A. Reynaud, B. Jaspard-Vinassa, I. Belloc, C. Desgranges, and A.P. Gadeau, *Gli3 regulation of myogenesis is necessary for ischemia-induced angiogenesis.* Circ Res, 2013. **113**(10): p. 1148-58.
249. Straface, G., T. Aprahamian, A. Flex, E. Gaetani, F. Biscetti, R.C. Smith, G. Pecorini, E. Pola, F. Angelini, E. Stigliano, J.J. Castellot, Jr., D.W. Losordo, and R. Pola, *Sonic hedgehog regulates angiogenesis and myogenesis during post-natal skeletal muscle regeneration.* J Cell Mol Med, 2009. **13**(8B): p. 2424-35.
250. Voronova, A., E. Coyne, A. Al Madhoun, J.V. Fair, N. Bosiljcic, C. St-Louis, G. Li, S. Thurig, V.A. Wallace, N. Wiper-Bergeron, and I.S. Skerjanc, *Hedgehog signaling regulates MyoD expression and activity.* J Biol Chem, 2013. **288**(6): p. 4389-404.
251. Ignatius, M.S., E. Chen, N.M. Elpek, A.Z. Fuller, I.M. Tenente, R. Clagg, S. Liu, J.S. Blackburn, C.M. Linardic, A.E. Rosenberg, P.G. Nielsen, T.R. Mempel, and D.M. Langenau, *In vivo imaging of tumor-propagating cells, regional tumor heterogeneity, and dynamic cell movements in embryonal rhabdomyosarcoma.* Cancer Cell, 2012. **21**(5): p. 680-93.
252. Pressey, J.G., J.R. Anderson, D.K. Crossman, J.C. Lynch, and F.G. Barr, *Hedgehog pathway activity in pediatric embryonal rhabdomyosarcoma and undifferentiated sarcoma: a report from the Children's Oncology Group.* Pediatr Blood Cancer, 2011. **57**(6): p. 930-8.
253. Gage, P.J., W. Rhoades, S.K. Prucka, and T. Hjalt, *Fate maps of neural crest and mesoderm in the mammalian eye.* Invest Ophthalmol Vis Sci, 2005. **46**(11): p. 4200-8.
254. Duboc, V. and M.P. Logan, *Building limb morphology through integration of signalling modules.* Curr Opin Genet Dev, 2009. **19**(5): p. 497-503.
255. Tzchori, I., T.F. Day, P.J. Carolan, Y. Zhao, C.A. Wassif, L. Li, M. Lewandoski, M. Gorivodsky, P.E. Love, F.D. Porter, H. Westphal, and Y. Yang, *LIM homeobox transcription factors integrate signaling events that control three-dimensional limb patterning and growth.* Development, 2009. **136**(8): p. 1375-85.

256. Dai, J.X., R.L. Johnson, and Y.Q. Ding, *Manifold functions of the Nail-Patella Syndrome gene Lmx1b in vertebrate development.* Dev Growth Differ, 2009. **51**(3): p. 241-50.
257. Liu, P. and R.L. Johnson, *Lmx1b is required for murine trabecular meshwork formation and for maintenance of corneal transparency.* Dev Dyn, 2010. **239**(8): p. 2161-71.
258. Buckingham, M. and F. Relaix, *The role of Pax genes in the development of tissues and organs: Pax3 and Pax7 regulate muscle progenitor cell functions.* Annu Rev Cell Dev Biol, 2007. **23**: p. 645-73.
259. Fung, F.K., D.W. Chan, V.W. Liu, T.H. Leung, A.N. Cheung, and H.Y. Ngan, *Increased expression of PITX2 transcription factor contributes to ovarian cancer progression.* PLoS One, 2012. **7**(5): p. e37076.
260. He, L., L. Guo, V. Vathipadiekal, P.A. Sergent, W.B. Growdon, D.A. Engler, B.R. Rueda, M.J. Birrer, S. Orsulic, and G. Mohapatra, *Identification of LMX1B as a novel oncogene in human ovarian cancer.* Oncogene, 2013.
261. Robson, E.J., S.J. He, and M.R. Eccles, *A PANorama of PAX genes in cancer and development.* Nat Rev Cancer, 2006. **6**(1): p. 52-62.
262. Kozmik, Z., U. Sure, D. Ruedi, M. Busslinger, and A. Aguzzi, *Deregulated expression of PAX5 in medulloblastoma.* Proc Natl Acad Sci U S A, 1995. **92**(12): p. 5709-13.
263. Zhou, Y.H., F. Tan, K.R. Hess, and W.K. Yung, *The expression of PAX6, PTEN, vascular endothelial growth factor, and epidermal growth factor receptor in gliomas: relationship to tumor grade and survival.* Clin Cancer Res, 2003. **9**(9): p. 3369-75.
264. Yamaoka, T., M. Yano, T. Yamada, T. Matsushita, M. Moritani, S. Ii, K. Yoshimoto, J. Hata, and M. Itakura, *Diabetes and pancreatic tumours in transgenic mice expressing Pa x 6.* Diabetologia, 2000. **43**(3): p. 332-9.
265. Shahi, M.H., M. Afzal, S. Sinha, C.G. Eberhart, J.A. Rey, X. Fan, and J.S. Castresana, *Regulation of sonic hedgehog-GLI1 downstream target genes PTCH1, Cyclin D2, Plakoglobin, PAX6 and NKX2.2 and their epigenetic status in medulloblastoma and astrocytoma.* BMC Cancer, 2010. **10**: p. 614.
266. Lee, W.K., P.K. Chakraborty, and F. Thevenod, *Pituitary homeobox 2 (PITX2) protects renal cancer cell lines against doxorubicin toxicity by transcriptional activation of the multidrug transporter ABCB1.* Int J Cancer, 2013. **133**(3): p. 556-67.
267. Izrailit, J. and M. Reedijk, *Developmental pathways in breast cancer and breast tumor-initiating cells: therapeutic implications.* Cancer Lett, 2012. **317**(2): p. 115-26.
268. He, J., T. Sheng, A.A. Stelter, C. Li, X. Zhang, M. Sinha, B.A. Luxon, and J. Xie, *Suppressing Wnt signaling by the hedgehog pathway through sFRP-1.* J Biol Chem, 2006. **281**(47): p. 35598-602.
269. Guo, X. and X.F. Wang, *Signaling cross-talk between TGF-beta/BMP and other pathways.* Cell Res, 2009. **19**(1): p. 71-88.
270. Kim, J.H., H.S. Shin, S.H. Lee, I. Lee, Y.S. Lee, J.C. Park, Y.J. Kim, J.B. Chung, and Y.C. Lee, *Contrasting activity of Hedgehog and Wnt pathways according to gastric cancer cell differentiation: relevance of crosstalk mechanisms.* Cancer Sci, 2010. **101**(2): p. 328-35.
271. Schreck, K.C., P. Taylor, L. Marchionni, V. Gopalakrishnan, E.E. Bar, N. Gaiano, and C.G. Eberhart, *The Notch target Hes1 directly modulates Gli1 expression and Hedgehog signaling: a potential mechanism of therapeutic resistance.* Clin Cancer Res, 2010. **16**(24): p. 6060-70.
272. van den Brink, G.R., S.A. Bleuming, J.C. Hardwick, B.L. Schepman, G.J. Offerhaus, J.J. Keller, C. Nielsen, W. Gaffield, S.J. van Deventer, D.J. Roberts, and M.P. Peppelenbosch, *Indian Hedgehog is an antagonist of Wnt signaling in colonic epithelial cell differentiation.* Nat Genet, 2004. **36**(3): p. 277-82.
273. Raimondi, L., R. Ciarapica, M. De Salvo, F. Verginelli, M. Gueguen, C. Martini, L. De Sio, G. Cortese, M. Locatelli, T.P. Dang, N. Carlesso, L. Miele, S. Stifani, I. Limon, F. Locatelli, and R. Rota, *Inhibition of Notch3 signalling induces rhabdomyosarcoma cell differentiation promoting p38 phosphorylation and p21(Cip1) expression and hampers tumour cell growth in vitro and in vivo.* Cell Death Differ, 2012. **19**(5): p. 871-81.
274. Keller, C. and D.C. Guttridge, *Mechanisms of impaired differentiation in rhabdomyosarcoma.* FEBS J, 2013. **280**(17): p. 4323-34.
275. Lang, K.C., I.H. Lin, H.F. Teng, Y.C. Huang, C.L. Li, K.T. Tang, and S.L. Chen, *Simultaneous overexpression of Oct4 and Nanog abrogates terminal myogenesis.* Am J Physiol Cell Physiol, 2009. **297**(1): p. C43-54.
276. Boyer, L.A., T.I. Lee, M.F. Cole, S.E. Johnstone, S.S. Levine, J.P. Zucker, M.G. Guenther, R.M. Kumar, H.L. Murray, R.G. Jenner, D.K. Gifford, D.A. Melton, R. Jaenisch, and R.A. Young, *Core transcriptional regulatory circuitry in human embryonic stem cells.* Cell, 2005. **122**(6): p. 947-56.
277. Dahlqvist, C., A. Blokzijl, G. Chapman, A. Falk, K. Dannaeus, C.F. Ibanez, and U. Lendahl, *Functional Notch signaling is required for BMP4-induced inhibition of myogenic differentiation.* Development, 2003. **130**(24): p. 6089-99.
278. Fukada, S., Y. Ma, T. Ohtani, Y. Watanabe, S. Murakami, and M. Yamaguchi, *Isolation, characterization, and molecular regulation of muscle stem cells.* Front Physiol, 2013. **4**: p. 317.

279. Ge, X., C. McFarlane, A. Vajjala, S. Lokireddy, Z.H. Ng, C.K. Tan, N.S. Tan, W. Wahli, M. Sharma, and R. Kambadur, *Smad3 signaling is required for satellite cell function and myogenic differentiation of myoblasts.* Cell Res, 2011. **21**(11): p. 1591-604.
280. Wang, H., F. Noulet, F. Edom-Vovard, S. Tozer, F. Le Grand, and D. Duprez, *Bmp signaling at the tips of skeletal muscles regulates the number of fetal muscle progenitors and satellite cells during development.* Dev Cell, 2010. **18**(4): p. 643-54.
281. Kuang, S., M.A. Gillespie, and M.A. Rudnicki, *Niche regulation of muscle satellite cell self-renewal and differentiation.* Cell Stem Cell, 2008. **2**(1): p. 22-31.
282. Fukada, S., A. Uezumi, M. Ikemoto, S. Masuda, M. Segawa, N. Tanimura, H. Yamamoto, Y. Miyagoe-Suzuki, and S. Takeda, *Molecular signature of quiescent satellite cells in adult skeletal muscle.* Stem Cells, 2007. **25**(10): p. 2448-59.
283. Javelaud, D., M.J. Pierrat, and A. Mauviel, *Crosstalk between TGF-beta and hedgehog signaling in cancer.* FEBS Lett, 2012. **586**(14): p. 2016-25.
284. von Maltzahn, J., N.C. Chang, C.F. Bentzinger, and M.A. Rudnicki, *Wnt signaling in myogenesis.* Trends Cell Biol, 2012. **22**(11): p. 602-9.
285. Brack, A.S., I.M. Conboy, M.J. Conboy, J. Shen, and T.A. Rando, *A temporal switch from notch to Wnt signaling in muscle stem cells is necessary for normal adult myogenesis.* Cell Stem Cell, 2008. **2**(1): p. 50-9.
286. de Lau, W., W.C. Peng, P. Gros, and H. Clevers, *The R-spondin/Lgr5/Rnf43 module: regulator of Wnt signal strength.* Genes Dev, 2014. **28**(4): p. 305-16.
287. Federico, S., R. Brennan, and M.A. Dyer, *Childhood cancer and developmental biology a crucial partnership.* Curr Top Dev Biol, 2011. **94**: p. 1-13.
288. Curtis, S.J., K.W. Sinkevicius, D. Li, A.N. Lau, R.R. Roach, R. Zamponi, A.E. Woolfenden, D.G. Kirsch, K.K. Wong, and C.F. Kim, *Primary tumor genotype is an important determinant in identification of lung cancer propagating cells.* Cell Stem Cell, 2010. **7**(1): p. 127-33.
289. Kim, J., A.J. Woo, J. Chu, J.W. Snow, Y. Fujiwara, C.G. Kim, A.B. Cantor, and S.H. Orkin, *A Myc network accounts for similarities between embryonic stem and cancer cell transcription programs.* Cell, 2010. **143**(2): p. 313-24.
290. Li, Q., N. Bohin, T. Wen, V. Ng, J. Magee, S.C. Chen, K. Shannon, and S.J. Morrison, *Oncogenic Nras has bimodal effects on stem cells that sustainably increase competitiveness.* Nature, 2013. **504**(7478): p. 143-7.
291. Yilmaz, O.H., R. Valdez, B.K. Theisen, W. Guo, D.O. Ferguson, H. Wu, and S.J. Morrison, *Pten dependence distinguishes haematopoietic stem cells from leukaemia-initiating cells.* Nature, 2006. **441**(7092): p. 475-82.
292. Molchadsky, A., I. Shats, N. Goldfinger, M. Pevsner-Fischer, M. Olson, A. Rinon, E. Tzahor, G. Lozano, D. Zipori, R. Sarig, and V. Rotter, *p53 plays a role in mesenchymal differentiation programs, in a cell fate dependent manner.* PLoS One, 2008. **3**(11): p. e3707.
293. Stecca, B., C. Mas, V. Clement, M. Zbinden, R. Correa, V. Piguet, F. Beermann, and I.A.A. Ruiz, *Melanomas require HEDGEHOG-GLI signaling regulated by interactions between GLI1 and the RAS-MEK/AKT pathways.* Proc Natl Acad Sci U S A, 2007. **104**(14): p. 5895-900.
294. Ng, T.L., A.M. Gown, T.S. Barry, M.C. Cheang, A.K. Chan, D.A. Turbin, F.D. Hsu, R.B. West, and T.O. Nielsen, *Nuclear beta-catenin in mesenchymal tumors.* Mod Pathol, 2005. **18**(1): p. 68-74.
295. Garraway, L.A. and E.S. Lander, *Lessons from the cancer genome.* Cell, 2013. **153**(1): p. 17-37.
296. Kreso, A., C.A. O'Brien, P. van Galen, O.I. Gan, F. Notta, A.M. Brown, K. Ng, J. Ma, E. Wienholds, C. Dunant, A. Pollett, S. Gallinger, J. McPherson, C.G. Mullighan, D. Shibata, and J.E. Dick, *Variable clonal repopulation dynamics influence chemotherapy response in colorectal cancer.* Science, 2013. **339**(6119): p. 543-8.
297. Klco, J.M., D.H. Spencer, C.A. Miller, M. Griffith, T.L. Lamprecht, M. O'Laughlin, C. Fronick, V. Magrini, R.T. Demeter, R.S. Fulton, W.C. Eades, D.C. Link, T.A. Graubert, M.J. Walter, E.R. Mardis, J.F. Dipersio, R.K. Wilson, and T.J. Ley, *Functional heterogeneity of genetically defined subclones in acute myeloid leukemia.* Cancer Cell, 2014. **25**(3): p. 379-92.
298. Schafer, B.W. and F. Niggli, *Multidisciplinary management of childhood sarcoma: time to expand.* Expert Rev Anticancer Ther, 2010. **10**(8): p. 1163-6.
299. Eichenmuller, M., B. Hemmerlein, D. von Schweinitz, and R. Kappler, *Betulinic acid induces apoptosis and inhibits hedgehog signalling in rhabdomyosarcoma.* Br J Cancer, 2010. **103**(1): p. 43-51.
300. Yamanaka, H., T. Oue, S. Uehara, and M. Fukuzawa, *Hedgehog signal inhibitor forskolin suppresses cell proliferation and tumor growth of human rhabdomyosarcoma xenograft.* J Pediatr Surg, 2011. **46**(2): p. 320-5.
301. Ecke, I., A. Rosenberger, S. Obenauer, C. Dullin, F. Aberger, S. Kimmina, S. Schweyer, and H. Hahn, *Cyclopamine treatment of full-blown Hh/Ptch-associated RMS partially inhibits Hh/Ptch signaling, but not tumor growth.* Mol Carcinog, 2008. **47**(5): p. 361-72.

302. Heretsch, P., L. Tzagkaroulaki, and A. Giannis, *Cyclopamine and hedgehog signaling: chemistry, biology, medical perspectives.* Angew Chem Int Ed Engl, 2010. **49**(20): p. 3418-27.
303. Brechbiel, J., K. Miller-Moslin, and A.A. Adjei, *Crosstalk between hedgehog and other signaling pathways as a basis for combination therapies in cancer.* Cancer Treat Rev, 2014.
304. Stecca, B. and I.A.A. Ruiz, *Context-dependent regulation of the GLI code in cancer by HEDGEHOG and non-HEDGEHOG signals.* J Mol Cell Biol, 2010. **2**(2): p. 84-95.
305. Pambid, M.R., R. Berns, H.H. Adomat, K. Hu, J. Triscott, N. Maurer, N. Zisman, V. Ramaswamy, C.E. Hawkins, M.D. Taylor, C. Dunham, E. Guns, and S.E. Dunn, *Overcoming resistance to Sonic Hedgehog inhibition by targeting p90 ribosomal S6 kinase in pediatric medulloblastoma.* Pediatr Blood Cancer, 2014. **61**(1): p. 107-15.
306. Riobo, N.A., K. Lu, and C.P. Emerson, Jr., *Hedgehog signal transduction: signal integration and cross talk in development and cancer.* Cell Cycle, 2006. **5**(15): p. 1612-5.
307. Singh, R.R., J.H. Cho-Vega, Y. Davuluri, S. Ma, F. Kasbidi, C. Milito, P.A. Lennon, E. Drakos, L.J. Medeiros, R. Luthra, and F. Vega, *Sonic hedgehog signaling pathway is activated in ALK-positive anaplastic large cell lymphoma.* Cancer Res, 2009. **69**(6): p. 2550-8.
308. Wang, Y., Q. Ding, C.J. Yen, W. Xia, J.G. Izzo, J.Y. Lang, C.W. Li, J.L. Hsu, S.A. Miller, X. Wang, D.F. Lee, J.M. Hsu, L. Huo, A.M. Labaff, D. Liu, T.H. Huang, C.C. Lai, F.J. Tsai, W.C. Chang, C.H. Chen, T.T. Wu, N.S. Buttar, K.K. Wang, Y. Wu, H. Wang, J. Ajani, and M.C. Hung, *The crosstalk of mTOR/S6K1 and Hedgehog pathways.* Cancer Cell, 2012. **21**(3): p. 374-87.
309. Campos, B. and C.C. Herold-Mende, *Insight into the complex regulation of CD133 in glioma.* Int J Cancer, 2011. **128**(3): p. 501-10.
310. Ailles, L. and L.L. Siu, *Targeting the Hedgehog pathway in cancer: can the spines be smoothened?* Clin Cancer Res, 2011. **17**(8): p. 2071-3.
311. Ng, J.M. and T. Curran, *The Hedgehog's tale: developing strategies for targeting cancer.* Nat Rev Cancer, 2011. **11**(7): p. 493-501.
312. Olson, J.M., *Therapeutic opportunities for medulloblastoma come of age.* Cancer Cell, 2014. **25**(3): p. 267-9.
313. Gore, L., J. DeGregori, and C.C. Porter, *Targeting developmental pathways in children with cancer: what price success?* Lancet Oncol, 2013. **14**(2): p. e70-8.

9. Acknowledgments

I would first of all like to thank Prof. Dr. **Beat Schäfer** for giving me the opportunity to pursue my Ph.D. thesis in his laboratory, encouraging my need to develop and follow many ideas, his advice, foresight and interesting discussions both about science and otherwise, and having enough faith in me and my abilities to direct the project. The atmosphere was always open, friendly, informative and collaborative and I am indebted to him for training me to be a confident researcher.

I would also like to thank the members of my thesis committee, Prof. Dr. **Michael Hengartner** and Prof. Dr. **Lukas Sommer**, for their insightful and encouraging comments that helped shape the thesis.

I deeply appreciate the **Cancer Network Zurich** for organization highly informative and interesting courses as part of the Cancer Biology Ph.D. program. It was really beneficial to meet and network with other Ph.D. students in and around Zurich; not to mention a lot of fun.

I have truly enjoyed my Ph.D. due to the unconditional support, help and love from the former and current members of all the labs at August Forel Strasse. Thank you Dr. **Marco Wachtel** for all the discussions and answering my questions with infinite patience. Thank you **Valentina**, **Jeannette**, **Rahel**, **Giulio "Yoda" Fiaschetti**, **Alex Boro**, **David Herrero**, **Maria**, **Florian**, **Jürgen**, **Anna**, **Laura**, **Verena** and **Trish** for your friendship, laughs, 'shoulder to cry on' and making me feel wonderful every morning with your smiles and warm hugs. **Giulio** and **Florian** – this would not have been possible with you; thank you for being my 'brothers-in-arms'.

A special thank you to **Dagmar** for making me feel so welcomed when I started and teaching me the ropes. I was lucky to have you. I am grateful to **Nurhak** for allowing me to supervise her Masters' dissertation and **Réka** for her contribution to the manuscript. I am forever indebted to **Amandine** and **Gabriele** for helping me tie up many lose ends in the project, their unhinged commitment and high level of skill.

Many thanks to Dr. med. **Peter Bode** - our highly knowledgeable senior pathologist - who patiently surveyed hundreds of tumor cores over many hours and days with me looking for extremely rare entities. Thank you for answering all my questions and for all the lovely discussions. I have learnt a lot from you.

James Watson was right when he wrote ‘An intelligent teammate can shorten your flirtation with a bad idea’. That teammate for me was Dr. **Elisa Zimmermann**. Thank you for being my cheerleader, for discussing my project in its minutiae, for sharing my ups and downs and for becoming a life-long friend.

I would also like to thank the **SBB CFF FFS** rail system for being my third ‘home’; having travelled almost 300 kms everyday for three and a half years to and from work. Their efficiency, dependability and quiet ambience allowed me to focus on my literature reviews which eventually led to many new ideas.

My time here in Switzerland has been made wonderful and extremely comfortable thanks to my new family – **Marie Joseé Rappaz**, **Jean Maurice Rappaz** and **Fanny Rappaz**. Thank you for your understanding and the immeasurable amount of love and support. I would not be here if it were not for the constant faith and love from my **family and friends** back home in India and scattered around the globe. I wish to convey my deepest gratitude to my mother, **Savitri**, and father, **Satheesha**, for allowing me to venture out into the world to achieve my dreams and for being such wonderful parents. I stand on the shoulders of giants. Thank you also to my brother, **Santosh**, for always making me laugh and feel young. I love you all very dearly.

Finally, I would like to thank my husband, **Alexandre Rappaz**, for always putting things in perspective to help me enjoy my life wholly. I now owe you two theses. Thank you for loving me for who I am and letting me be me: crazy book-worm scientist lady.

11. Manuscripts

Personal contributions to manuscripts

1. *CD133 Positive Embryonal Rhabdomyosarcoma Stem-Like Cell Population Is Enriched in Rhabdospheres* (Second authorship)
   Collection and assembly of data, data analysis and interpretation
   Figures 1A; 2, A and B; 3C; 4, A-C and 5
2. *Targeting hedgehog signaling reduces self-renewal in Embryonal Rhabdomyosarcoma* (First authorship)
   Conception and design, collection and assembly of data, data analysis and interpretation, manuscript writing and final approval of manuscript
   All figures and tables (main text and supplemental)
3. *PAX3-FOXO1 increases fibroblast reprogramming efficiency and drives self-renewal in alveolar rhabdomyosarcoma* (Third authorship)
   Collection of data and data analysis
   Figures 1, A-D; 2F; 3A; Supplemental Figure S1, A and B and Supplemental Figure S5, B and C

OPEN ACCESS Freely available online

PLoS one

CD133 Positive Embryonal Rhabdomyosarcoma Stem-Like Cell Population Is Enriched in Rhabdospheres

Dagmar Walter[1], Sampoorna Satheesha[1], Patrick Albrecht[1], Beat C. Bornhauser[1], Valentina D'Alessandro[1], Susanne M. Oesch[1,2], Hubert Rehrauer[3], Ivo Leuschner[4], Ewa Koscielniak[5], Carole Gengler[6], Holger Moch[6], Michele Bernasconi[1], Felix K. Niggli[1], Beat W. Schäfer[1]*, Part of this study was conducted in cooperation with the CWS Study Group

1 Department of Oncology and Children's Research Center, University Children's Hospital, Zurich, Switzerland, **2** Roche Pharma Schweiz, Basel, Switzerland, **3** Functional Genomics Center, University of Zurich, Zurich, Switzerland, **4** Department of Pathology, University of Kiel, Kiel, Germany, **5** Pediatrics 5 (Oncology, Hematology, Immunology), Olgahospital, Klinikum Stuttgart, Stuttgart, Germany, **6** Department of Pathology, University Hospital, Zurich, Switzerland

Abstract

Cancer stem cells (CSCs) have been identified in a number of solid tumors, but not yet in rhabdomyosarcoma (RMS), the most frequently occurring soft tissue tumor in childhood. Hence, the aim of this study was to identify and characterize a CSC population in RMS using a functional approach. We found that embryonal rhabdomyosarcoma (eRMS) cell lines can form rhabdomyosarcoma spheres (short rhabdospheres) in stem cell medium containing defined growth factors over several passages. Using an orthotopic xenograft model, we demonstrate that a 100 fold less sphere cells result in faster tumor growth compared to the adherent population suggesting that CSCs were enriched in the sphere population. Furthermore, stem cell genes such as *oct4*, *nanog*, *c-myc*, *pax3* and *sox2* are significantly upregulated in rhabdospheres which can be differentiated into multiple lineages such as adipocytes, myocytes and neuronal cells. Surprisingly, gene expression profiles indicate that rhabdospheres show more similarities with neuronal than with hematopoietic or mesenchymal stem cells. Analysis of these profiles identified the known CSC marker CD133 as one of the genes upregulated in rhabdospheres, both on RNA and protein levels. $CD133^+$ sorted cells were subsequently shown to be more tumorigenic and more resistant to commonly used chemotherapeutics. Using a tissue microarray (TMA) of eRMS patients, we found that high expression of CD133 correlates with poor overall survival. Hence, CD133 could be a prognostic marker for eRMS. These experiments indicate that a $CD133^+$ CSC population can be enriched from eRMS which might help to develop novel targeted therapies against this pediatric tumor.

Citation: Walter D, Satheesha S, Albrecht P, Bornhauser BC, D'Alessandro V, et al. (2011) CD133 Positive Embryonal Rhabdomyosarcoma Stem-Like Cell Population Is Enriched in Rhabdospheres. PLoS ONE 6(5): e19506. doi:10.1371/journal.pone.0019506

Editor: Louis Chesler, Institute of Cancer Research: Royal Cancer Hospital, United Kingdom

Received January 31, 2011; **Accepted** March 30, 2011; **Published** May 13, 2011

Funding: This study was supported by grants (3100-122562) from the Swiss National Science Foundation and the Swiss Research Foundation Child and Cancer. The funders had no role in study design, data collection and analysis, decision to publish, or preparation of the manuscript.

Competing Interests: The authors have declared that no competing interests exist.

* E-mail: beat.schaefer@kispi.uzh.ch

Introduction

The cancer stem cell hypothesis suggests that a small subpopulation of cells sharing common characteristics with normal stem cells (SCs) - such as capacity to self renew, potential to differentiate, extensive proliferation *in vivo*, and resistance to chemotherapeutics - is responsible for tumor development [1] and that tumors are organized hierarchically. This concept was first established in acute myeloid leukemia (AML) [2] and subsequently also in a number of solid tumors such as breast cancer where a $CD44^+/CD24^{-/low}$ CSC population was identified [3], in brain tumors [4], colon cancer [5], and melanomas [6]. Additionally, CSCs are postulated to be more resistant to standard chemotherapy [7,8,9,10,11] and might be responsible for tumor recurrence usually observed in the clinics. However, the concept is still controversial and the frequency of CSCs might vary between tumor entities. Some tumors might not be hierarchically organized at all. Therefore, the existence of such a cellular subpopulation most likely has to be established for each tumor type [12].

Rhabdomyosarcoma (RMS) is the most common soft tissue tumor in childhood representing 5 to 8% of all pediatric malignancies [13]. RMS is a member of the small blue round cell tumors additionally comprised of neuroblastoma, non-Hodgkin's lymphoma, Ewing's sarcoma and Wilm's tumor [14]. It occurs in most parts of the body, but more frequent sites are spaces surrounding the brain, the trunk and genitourinary tract [15]. It has been suggested that mesenchymal stem cells (MSCs) might be the origin of rhabdomyosarcomas and accordingly the origin of a potential rhabomyosarcoma stem cell might also be a mesenchymal one [16,17]. However, some reports indicate that also neuronal cells can transform into malignant myogenic cells after activation and a large number of neuronal genes are expressed in RMS. Hence the origin of potential RMS stem cells remains to be determined [18,19].

CD133, also known as Prominin1, is a five transmembrane protein with eight potential N-glycosylation sites. It was first described in murine neuroepithelial cells and was recognized as a human hematopoietic SC marker, because hematopoietic $CD34^+$ progenitor cells express CD133 [20]. CD133 has been suggested

as CSC marker in brain tumors [21], breast [3], colon [22], pancreatic [23], liver [24], skin [25], prostate cancers [26] and Ewing's sarcoma [27]. Furthermore, $CD133^+$ glioma stem cells are more resistant to chemotherapy and radiation than bulk and the CD133 negative population [8]. Moreover, CD133 downregulation induced differentiation in neuroblastoma cell lines and thus increased sensitivity to drug treatment [28]. Therefore, CD133 could by itself also represent a potential marker for targeted therapy. Nevertheless, CD133 positive CSC populations in melanoma and prostate cancer are still controversially discussed [29,30].

Here, we enriched for a CSC population in rhabdosphere cultures which are 100 fold more tumorigenic than adherent cells in xenograft experiments. This subpopulation expressed the stem cell genes *sox2*, *oct4*, *nanog*, *c-myc* and *pax3* to significantly higher levels and retains the capability to differentiate into adipocytes, myocytes and neuronal cells. Furthermore, the known stem cell marker CD133 was upregulated in rhabdospheres. $CD133^+$ cells characterize a subpopulation which is more tumorigenic and resistant to chemotherapy than the negative population. In addition, high CD133 expression in human eRMS samples correlated with a poor overall survival.

Thus, our study demonstrates for the first time that rhabdospheres can be formed from eRMS cells which are enriched in a $CD133^+$ CSC population.

Materials and Methods

Cell culture methods

Rh36 (kindly provided by Peter Houghton (St Jude Children's Hospital, Memphis, TN, USA)), RD, U87MG and MRC5 (purchased from the American Type Culture collection (LGC Promochem, Molsheim Cedex, France)) and Ruch2 (established in house) were cultured in Dulbecco's modified Eagle medium containing 10% fetal calf serum (FCS).

Sphere cultures were derived from and enriched over several passages by seeding the cell lines in a defined serum free medium (SC medium) consisting of Neurobasal medium (Invitrogen) supplemented with 10ng/ml EGF (R&D Systems), 20ng/ml b-FGF (R&D Systems) and 2× B27 (10ml; Invitrogen) [31]. Adipogenesis was induced as described [32,33]. Briefly, after preparing spheroids, cells were seeded into chamber slides and treated with or without 0.1% DMSO for 3 days. After 8 days in differentiation medium, containing 85nM insulin, 2nM triiodthyronine (T_3) and 10% FCS, cells were stained with OilRedO (ThermoScientific) [34]. Neurogenesis and Myogenesis were assayed as described [35]. Briefly, cells were seeded into 6 well plates and treated with different concentrations of retinoic acid (RA; 1nM, 10nM, 300nM). After 24 days in differentiation medium containing RA and 0.5% FCS, cells were fixed in 4% paraformaldehyde (PFA) and stained for differentiation markers. Resistance to chemotherapeutics was tested by seeding 2000 cells in a 6-well plate 48 hours before treatment. The cells were treated twice a week with different concentrations of cisPlatin (Sigma; 10 μM and 50 μM) and Chlorambucil (Sigma; 6.45 μM). Twice a week, colonies were counted and documented. For visualizing the colonies, we stained them with crystal violet according to Franken, et al. [36].

Immunofluorescence, immunohistochemistry and flow cytometry/sorting

For immunofluorescence staining, cells were fixed in 4% PFA and blocked in medium containing 10% FCS and 0.5% Triton. Cells were stained over night at 4°C for CD133 (1/100) (polyclonal antibody, Abcam), GFAP (1/300) (monoclonal antibody, R&D Systems), myogenin (1/2) (F5D; monoclonal antibody, Developmental Studies Hybridoma bank) and N-CAM (1/2) (5.1H11; Developmental Studies Hybridoma bank)). Alexa Fluor 488 or 594 (1/200) (Invitrogen) antibodies were used as secondary antibodies. All stainings were analyzed with an Axioskop2 mot plus fluorescence microscope (Zeiss). Xenograft tumors were embedded in paraffin, fixed and analyzed for H&E, Myogenin (1/20) (Myf4, monoclonal antibody, Novocastra Laboratories Ltd) and desmin (1/20) (monoclonal antibody; Dako) by immunohistochemistry. As secondary antibody a horseradish peroxidase (HRP) labeled rabbit anti-mouse antibody (Epitomics) was used. Stainings were visualized with the Refine DAB-Kit (Leica).

For flow cytometry, cells were trypsinized, washed and stained (1/10) with a fluorochrome labeled antibody (CD133/2-APC, Miltenyi). All samples were measured with a BDFACSCanto II flow cytometer (BD Bioscience) or MoFlo high speed cell sorter (DakoCytomation) and analyzed with the software FlowJo.

Molecular methods

RNA was extracted using RNeasy Plus Mini Kits (Qiagen). Reverse transcription was carried out using the high-capacity cDNA reverse transcription kit (Applied Biosystems) according to the manufacturer's instructions. RNA and cDNA concentrations were measured with a Nanodrop ND1000 spectrometer. Quantitative Real-Time PCR was performed using validated TaqMan Gene Expression Assays (Applied Biosystems) for POU5F1/OCT3-4 (Hs02397400_g1), NANOG (Hs02387400_g1), SOX2 (Hs01053049_s1), CMYC (Hs00153408_m1), PAX3 (Hs00992437_m1), NMYC (Hs00232074_m1), PROM1/CD133 (Hs01009261_m1) and GAPDH (Hs99999905_m1) as an endogenous housekeeping gene for normalization. Reactions were run using the standard conditions on an ABI 7900HT Fast Real-Time PCR machine. Relative fold difference was calculated using the $-\Delta\Delta$Ct method. Gene expression profiling of different RNA samples from different sphere passages (early = passage 3; intermediate = passage 5 to 7; late = passage 10) and their corresponding adherent control was performed by an Affymetrix Exonmicroarray (HuEx-1_0-st-v2). The samples were analyzed with the Genespring10 and Ingenuity IPA software and compared with published data sets (hematopoietic (GSE2666), FM95 (GSE10435), embryonic skeletal myoblast (GSE3230), mesenchymal stem cells (GSE2248), embryonic stem cells (GSE9440), neuronal cells (GSE10691), glioblastoma cells and patient samples (GSE7181), neurospheres (GSE8049) and prostate cancer samples (GSE10832)). The correlation of the samples was analyzed with a script programmed in R (Functional Genomic Center Zurich).

Xenograft experiments

Xenograft experiments were approved by the veterinary office of the Canton of Zurich.

Different amounts of adherent cells and their corresponding sphere cultures were injected intra muscularly into the right leg of NOD.CB17-*Prkdc*^{scid}/J (NOD/Scid) and NOD.Cg-*Prkdc*^{scid} *Il2rg*^{tm1Wjl}/SzJ (NSG) mice (The Jackson Laboratory) and tumor size was determined every 2 to 3 days by measuring two diameters (d_1 and d_2) in right angles of both legs with a calliper. Tumor volumes were calculated using the following formula $V = [4/3\ \pi\ ½(d_1+d_2)]_{\text{right leg}} - [4/3\ \pi\ ½(d_1+d_2)]_{\text{left leg}}$.

Patient characteristics

76 eRMS patients, 43 male and 33 female patients, were included from the CWS95 study. The age of the patients at diagnosis varied from a few months to 22 years.

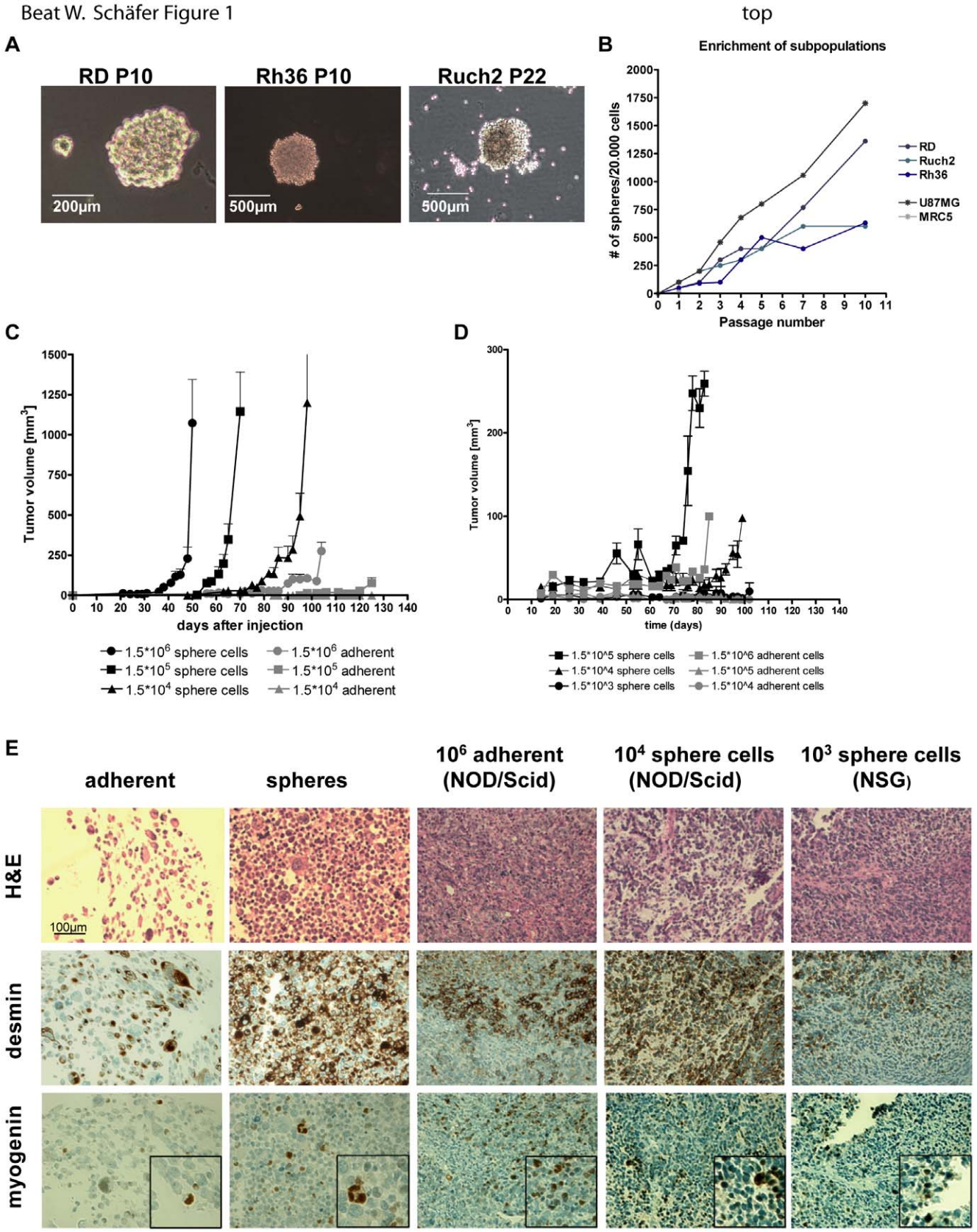

Figure 1. Cancer stem-like cells are enriched in Rhabdospheres. A), B) Embryonal rhabdomyosarcoma (eRMS) cell lines (RD, Rh36 and Ruch2) were cultured in stem cell medium (SC-medium) over several passages. A glioblastoma (U87MG) and a fibroblast (MRC5) cell line were used as controls. A) Representative phase contrast pictures of cultured RD, Ruch2 and Rh36 sphere cultures (400× magnification). B) Subpopulation

enrichment over several passages (x-axis) was estimated by counting the obtained spheres per cell (y-axis). C), D) Limited dilution (10^6, 10^5 and 10^4) of adherent versus sphere cells *in vivo*. Cells were intramuscularly (i.m.) injected into NOD/Scid (n = 6) (C) and NSG mice (n = 3) (D) at the indicated numbers and tumor growth (y-axis; tumor volume in mm^3) was measured over time (x-axis). E) Immunohistochemical (IHC) stainings of xenograft tumor sections on a xenograft tissue microarray (TMA). Adherent and sphere cells were used as controls on the TMA. The TMA was stained for H&E and RMS markers (desmin and myogenin). Representative IHC stainings are shown (400× magnification). The small inserts represent magnifications of positively stained cells.
doi:10.1371/journal.pone.0019506.g001

Statistical analysis

For in vitro experiments, Student's t test was used on triplicates. P values of less than 0.05 were considered significant.

Results

Rhabdospheres are enriched with cancer stem-like cells

To determine whether RMS cells might contain a subpopulation of CSC cells, we attempted to grow embryonal rhabdomyosarcoma (eRMS) cell lines (RD, Rh36 and Ruch2) as rhabdomyosarcoma spheres (short rhabdospheres) in stem cell medium (SC-medium). A glioblastoma cell line (U87MG) and fibroblast cells (MRC5) were used as positive and negative controls, respectively. Three eRMS cell lines (RD, Rh36 and Ruch2) formed rhabdospheres under these conditions over several passages (Figure 1A). To test, whether sphere cells could be serially enriched, we seeded 20000 sphere cells over several passages into the SC-medium and determined the number of spheres at each passage (Figure 1B). Compared to the positive control U87MG sphere cultures which showed the highest enrichment over 10 passages (up to 1750 spheres per 20000 cells), 1300 spheres were counted for RD cultures after 10 passages, while Ruch2 and Rh36 sphere cultures could also be enriched albeit to a lesser extent (600 counted spheres) indicating that a subpopulation of cells with self renewal property can be enriched from three different eRMS cell lines. To investigate whether this self renewing subpopulation is more tumorigenic than the adherent population, we injected different numbers of RD cells and their corresponding sphere cultures (10^6, 10^5 and 10^4) intramuscularly (i.m.) into the right leg of NOD/Scid mice (n = 6) and measured tumor growth over several weeks (Figure 1C). Xenograft tumors from sphere cultures started to grow around day 40 after injection, compared to adherent cells where we detected the earliest tumor growth around day 80 post injection. Moreover, tumor growth was observed when we injected 100 fold less sphere cells (10^4), whereas no tumor growth was seen using the same number of adherent cells. 125 days after injection, in two out of six NOD/Scid mice injected with 10^5 adherent cells, a small tumor was seen, while we detected tumors in every mouse injected with 10^5 sphere cells already after 60 days. These results were subsequently confirmed in a second mouse strain, namely NSG mice, where tumor growth was observed with 10^5, 10^4 and 10^3 (one out of three mice) injected sphere cells, but only with 10^6 adherent cells (Figure 1D). Therefore, in both mouse models cells from sphere cultures are more tumorigenic and fewer cells are needed for tumor growth compared to adherent cells. To demonstrate that all xenograft tumors were indeed RMS tumors, we collected tumor samples and constructed a xenograft tissue microarray (TMA) with adherent RD cells and corresponding sphere cultures as controls. Stainings of the TMA with RMS markers, myogenin and desmin, was positive in both adherent cells and spheres (Figure 1E) which were negative for markers of other small blue round cell tumors (CD45, CD99, cytokeratin (CK), S100b, Synaptosin, smooth muscle actin (SMA) and WT1; data not shown). Furthermore, all xenograft tumors displayed typical RMS hallmarks such as multinucleated cells and positive stainings for desmin and myogenin, irrespective of the mouse strain they were grown in. These results confirmed that all xenograft tumors represented RMS tumors with similar features. We conclude from these experiments that a subpopulation of RMS cells can be enriched in sphere cultures over several passages which is more tumorigenic *in vivo* and therefore could represent a potential CSC population.

Sphere cultures have stem cell characteristics

To further substantiate the notion that rhabdospheres are enriched for CSC, we quantified the expression levels of several known SC genes like *oct4*, *nanog*, *c-myc*, *sox2* and *pax3* with real-time PCR in different passages of sphere cultures (passages 3, 7, 10) compared to adherent cells. While *oct4* and *pax3* showed the highest upregulation in RD sphere cultures ($P<0.0001$), also *c-myc* ($P = 0.0016$), *sox2* ($P = 0.0068$) and *nanog* ($P = 0.0028$) were significantly upregulated (Figure 2A). Similar results were obtained with Rh36 cells with the exception of *pax3* and *c-myc* which did not change significantly (Figure 2B). This could be due to already high endogenous expression levels in the adherent Rh36 cell line when compared to RD adherent cells (data not shown). Therefore, we selected RD cells for all subsequent experiments.

It has been shown that cells with multilineage differentiation potential can differentiate into neuronal cells, myocytes and adipocytes after treatment with dimethylsulfoxid (DMSO) or retinoic acid (RA) [32,35,37,38]. On that basis, we next assessed to which extent RD cells can be differentiated towards these lineages. First, we treated adherent and sphere cultures with different concentrations of RA (1nM, 10nM and 300nM). After 24 days, cells were stained with myogenic (myogenin, N-CAM) and neuronal markers (GFAP, N-CAM) (Figure 2C, D). Although adherent cells expressed low levels of myogenin (3,6% and 11,5%) after treatment (Figure 2C), sphere cultures showed much stronger upregulation of myogenin positivity (~50%) (Figure 2D). The highest expression of N-CAM (52%) was detectable after treatment with 10nM RA. While both spheres and adherent cells were negative for myogenin when treated with 300nM RA, we observed positive stainings for N-CAM and GFAP (9,4%), indicative of neuronal differentiation, only in sphere cultures (Figure 2D) and not in adherent cells (Figure 2C). In contrast, no GFAP positive cell was found after 1 and 10nM RA treatment (data not shown). Untreated controls were negative for all markers analyzed (data not shown).

To differentiate cells towards adipocytes, we treated spheroids from both adherent and sphere cells for 3 days with DMSO. After subsequent cultivation in appropriate differentiation medium for 8 days, around 5% of DMSO treated adherent cells were positive for fatty vacuoles (Figure 2E). However, sphere cultures had positively stained fatty vacuoles in up to 90% (mean 73.75%) of the cells when treated with DMSO (Figure 2E).

In conclusion, sphere cultures had a significantly increased expression level of stem cell genes and regained the capability to differentiate towards neurogenic, myogenic and adipogenic lineages with appropriate stimulants. These results indicate that stem-like cells are enriched in rhabdospheres.

Beat W. Schäfer Figure2

top

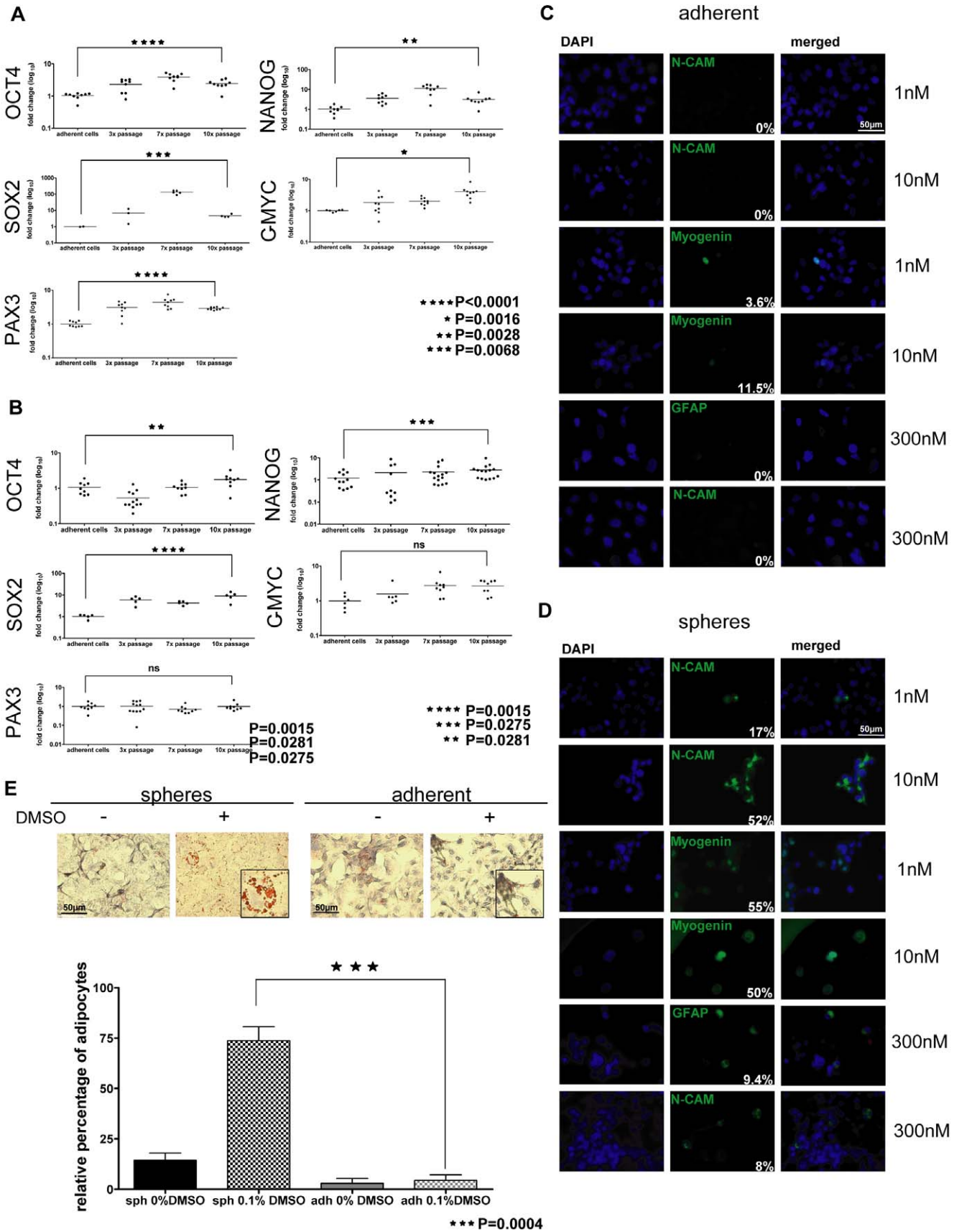

Figure 2. Sphere cultures have stem cell characteristics. A), B) Expression analysis of stem cell genes (*oct4*, *nanog*, *sox2*, *c-myc* and *pax3*) by Real-time PCR. RD (A) and Rh36 (B) adherent cells and 3 different sphere culture passages (3×, 7×, 10×) were compared. C), D) RD cells (C) and their corresponding sphere cultures (D) were treated with retinoic acid (1nM, 10nM, 300nM) for 24 days and stained for differentiation markers (N-CAM, myogenin and GFAP). Percentage of positivity was calculated by counting 3 different random microscopic fields with at least 30 cells. E) RD cells and spheres were treated with 0.1% DMSO for 3 days. After additional 8 days, cells were stained for OilRedO. Percentage of cells with fatty vacuoles was calculated by counting 4 independent slides. Representative pictures and magnifications (small box) of OilRedO stainings are shown. For A) ★★★★ $P<0.0001$; ★★ $P=0.0028$; ★ $P=0.0016$; ★★★ $P=0.0068$. For B) ★★★★ $P=0.0015$; ★★ $P=0.0281$; ★★★ $P=0.0275$. For E) ★★★ $P=0.0004$. Abbreviations: ns, not significant; GFAP, glial fibrillary acidic protein; N-CAM, neural cell adhesion molecule; sph, spheres; adh, adherent; DMSO, dimethylsulfoxid.
doi:10.1371/journal.pone.0019506.g002

CD133 is upregulated in sphere cultures

To characterize sphere cultures in further detail and to identify marker proteins specifically up- or downregulated, a gene expression profiling was performed with a human exonmicroarray (HuEx-1_0-st-v2) for both RD and Rh36 cells and three different passages (early, intermediate and late) of their corresponding spheres.

In Figure 3A, a heat map of all samples is shown which revealed that RD and Rh36 cells cluster with their corresponding sphere cells indicating that both cell lines are more different from each other than their different passages. Nevertheless, in total 2217 genes (upregulated 1568 genes, downregulated 649 genes) are differentially expressed in RD spheres compared to adherent cells with a fold change of at least two. To restrict the number of genes and to find potential markers characterizing the rhabdospheres, a metaanalysis with different microarray samples publicly available (hematopoietic, FM95, embryonic skeletal myoblast, mesenchymal stem cells, embryonic stem cells, neuronal cells, glioblastoma cells and patient samples, neurospheres and prostate cancer samples) was implemented. All RMS samples, both adherent and rhabdospheres (red (RD) and pink (Rh36)), clustered together with neuronal and glioblastoma cells and their spheres, and patient samples (depicted in green) (Figure 3B). Due to this observation, we searched for genes commonly up- or downregulated in RD and glioblastoma sphere cultures compared to their corresponding adherent cells with a fold change of at least two (Table 1). 31 genes were identified and further subgrouped according to their subcellular localization; membrane (8 genes), secreted (1 gene), endoplasmatic reticulum ER membrane (1 gene), golgi apparatus (1 gene), cytoplasm (12 genes) and nucleus (8 genes). In addition, 12 genes are commonly downregulated (membrane (6), secreted (2), cytoplasm (4)). To be able to identify and isolate a putative CSC population, we were interested mainly in membrane proteins of which we identified 14 genes. One obvious candidate gene in this list was CD133 or Prominin1 which is a well described SC and CSC marker. Therefore, we validated CD133 as a potential marker of rhabdospheres at the expression level by performing real-time PCR (Figure 3C). In sphere cultures of both RD and Rh36, CD133 expression was indeed significantly upregulated. To verify these results on protein level, RD cells and spheres were stained for CD133 and analyzed by flow cytometry (Figure 3D), fluorescence microscopy (Figure 3E) and western blotting (Figure 3F). In all experiments, CD133 is upregulated in rhabdospheres compared to adherent cells also on protein level.

These experiments suggest that $CD133^+$ cells , a known CSC marker, are enriched in rhabdospheres and CD133 might be a potential CSC marker in RMS.

$CD133^+$ RMS cells are more chemoresistant and tumorigenic

To verify whether a $CD133^+$ subpopulation is more tumorigenic and resistant to commonly used chemotherapeutics in RMS, we sorted RD cells for CD133 positive and negative ($CD133^+$, $CD133^-$) populations (Figure 4A) and performed limiting dilutions by orthotopical injections into NOD/Scid mice using adherent RD cells and unsorted bulk RD cells as controls. In contrast to the control where the highest number of cells injected (10^6 cells) developed a tumor, mice injected with $CD133^-$ cells ($10^5 - 10^2$) did not develop any tumor after 140 days. In contrast, we could detect at least one tumor in the $CD133^+$ injected mice in three out of four dilutions (Figure 4B). To demonstrate that these tumors are indeed RMS tumors, we analyzed them by immunohistochemistry using known RMS markers as described before. All tumors were positive for desmin and myogenin and histologically identical with RMS tumors (Figure 4C). To investigate potential resistance to commonly used chemotherapeutics, we seeded sorted cells at low density 48 hours before starting treatment with cisPlatin and Chlorambucil. Cells were treated twice a week and colonies obtained were counted after staining with crystal violet (Figure 4D). $CD133^+$ sorted RD cells were more resistant to treatment and formed viable colonies which developed significantly less in the $CD133^-$ population.

Therefore, rhabdospheres are enriched for a $CD133^+$ population being more tumorigenic and resistant to cisPlatin and Chlorambucil.

High expression of CD133 correlates with poor overall survival

Finally, we investigated whether a $CD133^+$ subpopulation is also present in human patient material. To this end, we stained a human RMS TMA, first described by Wachtel [19], for CD133. For quantification, we scored for two variables, namely intensity of staining and number of positive cells. The added scores were used to classify the tumors as having negative, low, middle or high expression. ERMS patients showing no or low to intermediate CD133 expression showed an overall survival around 75% which is comparable with the survival rate of translocation negative RMS patients [39]. In contrast, patients with high expression of CD133 had a clearly worse survival (less than 50%, $p=0.0272$, Figure 5A). Representative tumor sections of high, intermediate and low CD133 stainings are shown in Figure 5B.

These results therefore indicate that CD133 is a potential CSC marker in eRMS that might identify eRMS patients with a poor outcome.

Discussion

Due to a better understanding of tumor organization, new treatment approaches that target directly a CSC population now seem possible [22]. It has been reported that not only leukemia [2] and carcinomas [3] have a subpopulation of cells with self renewal properties [27], but also some sarcomas such as Ewing's sarcoma might follow the cancer stem cell model [1]. For the most common sarcoma in childhood, RMS, no clear subpopulation has been identified until now [16,17]. Therefore, we used a functional approach to investigate whether rhabdomyosarcoma tumors might

Beat W. Schäfer Figure 3

top

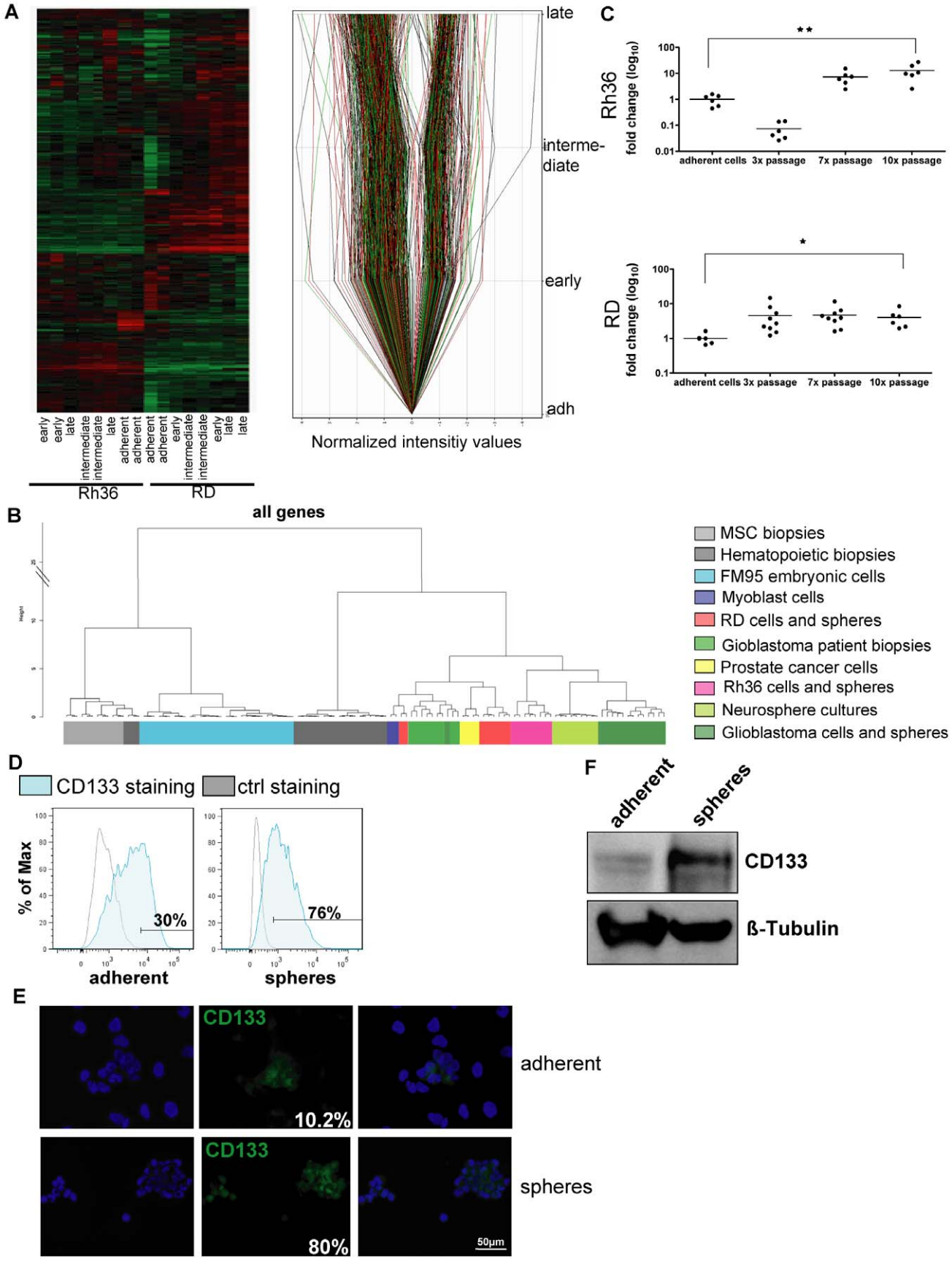

Figure 3. CD133 is upregulated in sphere cultures. Gene expression profiling (HuEx-1_0-st-v2) of two eRMS cells (RD and Rh36) and spheres (early, middle and late). A) left side: Cluster plot of RD and Rh36 cells and spheres. Right side: Analysis of RD samples. Genes, being up- or downregulated in RD spheres with a fold change of at least 2, are shown. B) Correlation plot of a metaanalysis performed with different publicly available expression data (hematopoietic and mesenchymal stem cells biopsies, FM95 cells, embryonic skeletal myoblast cells, embryonic stem cells, neuronal cells, glioblastoma spheres, cells and patient samples, neurospheres and prostate cancer samples) as indicated C) Expression of CD133 mRNA quantified by real-time PCR after correction with GAPDH levels as house-keeping gene. D) Flow cytometry analysis of CD133 (blue) expression. As controls unstained adherent and sphere cells were used, respectively (grey). E) Immunofluorescence staining of CD133 (green) of adherent and sphere cells. The nuclei were counterstained with DAPI (blue). Fields of two independent slides with at least 50 cells each were counted and the percentage of positive stained cells calculated. F) Western blot analysis of CD133 protein expression in adherent and sphere cells. ß-Tubulin was used as a loading control. A representative blot is shown. For C) ★ P = 0.0284; ★★ P = 0.0079. Abbreviations: ctrl, control; MSC, mesenchymal stem cells.
doi:10.1371/journal.pone.0019506.g003

have a subpopulation enriched in CSCs and are hierarchically organized.

We first adopted a sphere forming assay to enrich a subpopulation with stem cell properties *in vitro*. Testing different conditions of growth factor concentrations and media, sphere formation over several passages could be observed only in one condition which was described previously as a neuronal stem cell medium [31]. Several lines of evidence then indicate that these rhabdospheres are enriched for stem-like cells. First, limiting dilution in two different immunosuppressed mouse strains indicate

Table 1. List of genes up- or downregulated at least two fold in RD rhabdospheres.

upregulated			downregulated	
Localization	**Chosen Gene IDs**	**Gene Symbol**	**Chosen Gene IDs**	**Gene Symbol**
Membrane	2535	FZD2	2674	GFRA1
	7976	FZD3	3778	KCNMA1
	8842	PROM1	4907	NT5E
	23554	TSPAN12	7010	TEK
	51678	MPP6	7057	THBS1
	55704	CCDC88A	23768	FLRT2
	57633	LRRN1		
	84216	TMEM117		
Secreted	255743	NPNT	4015	LOX
			7424	VEGFC
Golgi apparatus	22836	RHOBTB3		
ER membrane	80055	PGAP1		
Cytoplasm	2037	EPB41L2	3433	IFIT2
	3157	HMGCS1	3437	IFIT3
	4133	MAP2	9060	PAPSS2
	6860	SYT4	10231	RCAN2
	9315	C5orf13		
	9456	HOMER1		
	9735	KNTC1		
	54874	FNBP1L		
	55792	PCID2		
	56992	KIF15		
	91057	CCDC34		
	113263	GLCCI1		
Nucleus	7552	ZNF711		
	9735	KNTC1		
	10926	DBF4		
	55769	ZNF83		
	64105	CENPK		
	81931	ZNF93		
	84250	ANKRD32		
	90317	ZNF616		
	151648	SGOL1		

doi:10.1371/journal.pone.0019506.t001

Beat W. Schäfer Figure 4

top

A

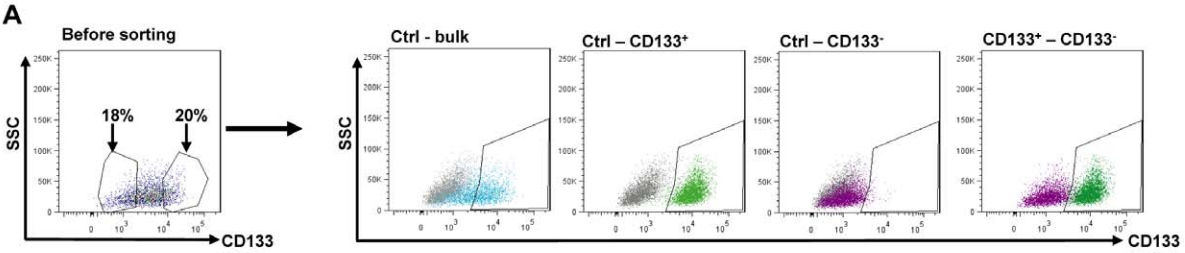

B

RD cells (10^6)	bulk cells (10^6)			
3 (4)	4 (4)			
CD133+ (10^6)	CD133+ (10^5)	CD133+ (10^4)	CD133+ (10^3)	CD133+ (10^2)
1 (1)	2 (4)	0 (4)	1 (4)	1 (4)
CD133- (10^6)	CD133- (10^5)	CD133- (10^4)	CD133- (10^3)	CD133- (10^2)
1 (1)	0 (4)	0 (4)	0 (4)	0 (4)

C

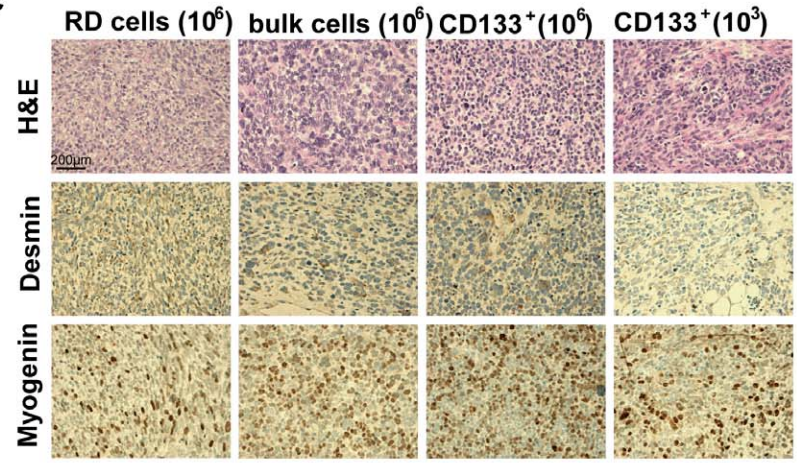

D

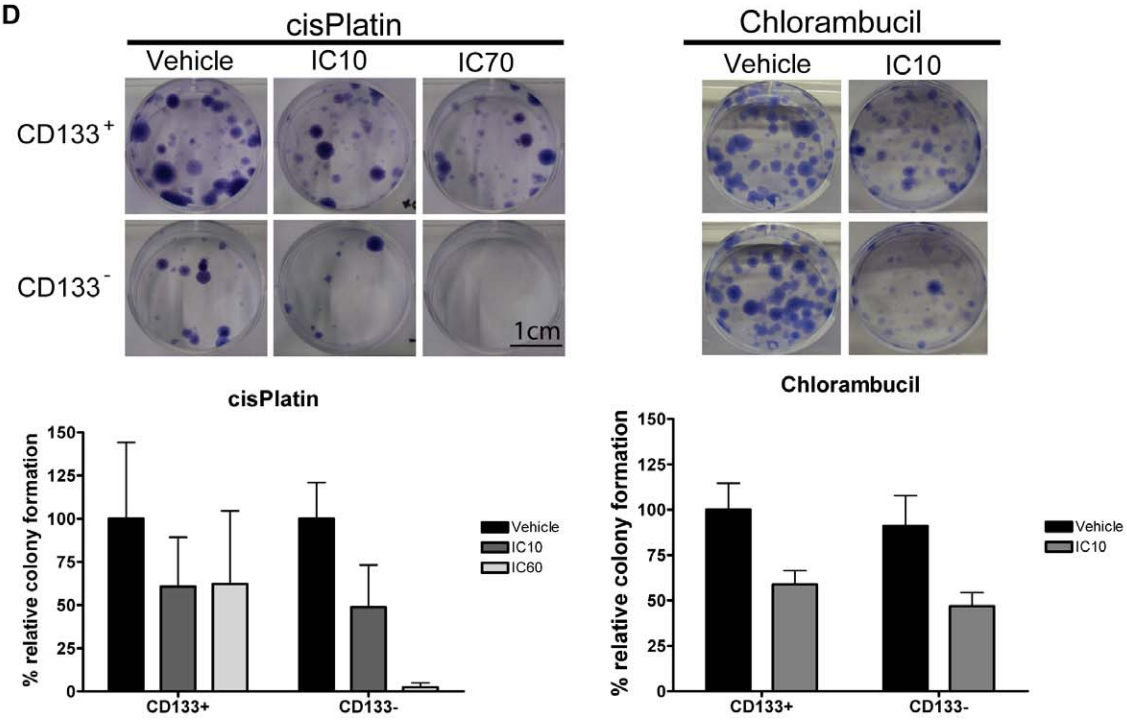

Figure 4. CD133$^+$ RMS cells are more chemoresistant and tumorigenic. A) RD cells were stained for CD133 (blue) and sorted into CD133$^+$ (green) and CD133$^-$ (violet) populations with a MoFlo high speed cell sorter (DakoCytomation). Unstained RD cells were used as control (grey). After sorting the different fractions were reanalyzed by flow cytometry. B) Limited dilutions *in vivo* of different subpopulations (10^6, 10^5, 10^4, $10^3$and 10^2). Bulk stained (10^6) and unstained cells without sorting (10^6) were used as controls. Cells were injected i.m. into NOD/Scid mice (n = 4) and tumor growth measured. Numbers indicate mice with growing tumors. C) Immunohistochemical (IHC) analysis of all xenograft tumors (H&E, Myogenin and Desmin). Representative stainings are shown. D) Clonogenic assay with sorted subpopulations (CD133$^+$ and CD133$^-$). Cells were treated with cisPlatin (IC10 = 10 μM and IC60 = 50 μM) and Chlorambucil (IC10 = 6.45 μM). Colonies were visualized by crystal violet. cisPlatin: mean of 3 independent sortings ± SEM; Chlorambucil: mean of 2 independent sortings ± SEM. For D) ★★ P = 0.0377; ★ P = 0.0241. Abbreviations: IC, inhibitory concentration; ctrl, control.
doi:10.1371/journal.pone.0019506.g004

that the rhabdosphere population is at least 100 fold more tumorigenic than adherent cells. In contrast, culturing cell lines representing the alveolar subtype of RMS in the same stem cell medium leads to formation of spheres which surprisingly were not tumorigenic after injection into immunosuppressed mice (data not shown). Hence, it seems unlikely that media conditions themselves were responsible for induction of the observed phenotypes and rather selection of a preexisting subpopulation was occurring specifically in eRMS. Second, our data analyzing expression levels of stem cell genes in rhabdospheres compared to adherent cells demonstrate that the stem cell genes *oct4*, *nanog*, *sox2*, *c-myc* as well as *pax3*, are significantly upregulated. While *sox2*, *nanog*, and *oct4* are required for induction of the pluripotent stem cell phenotype, *c-myc* expression also correlates with tumor formation and upregulation of this oncogene could trigger the higher tumor initiating potential [40]. *Pax3* is a known developmental marker expressed during muscle and brain development, repressed in adult tissue and connected to tumor formation and a poor overall survival [41,42,43].

As an additional hallmark of cancer stem cells [1], we investigated whether rhabdospheres have the potential to differentiate into multiple lineages. Indeed, rhabdospheres treated with DMSO and RA, respectively, differentiate towards adipogenic, myogenic and neurogenic lineages similar to what has been observed in cells with multilineage differentiation potential such as embryonal carcinoma cells [32,33,35]. These data support the concept that rhabdospheres contain cells with stem-like features and that RMS tumors are hierarchical organized [1].

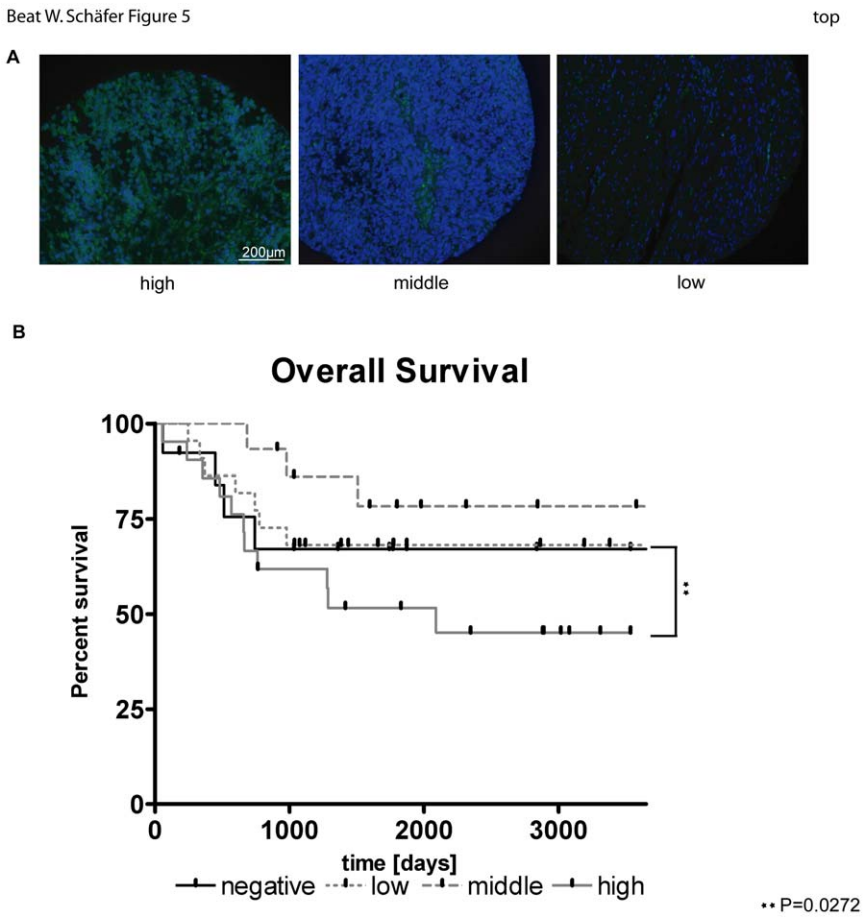

Figure 5. High expression of CD133 correlates with a poor survival rate. Immunofluorescence staining of a human RMS TMA with CD133 (green). Nuclei were counterstained with DAPI (blue). Two values were chosen for scoring: Staining intensity (1 = low, 2 = middle and 3 = bright) and number of positive cells (0 = 0; 1 = 1–10; 2 = 11–20; 3≥21). Both values were added up to the scorings negative (0 and 1), low (2 and 3), middle (4) and high (5 and 6). A) Stainings of representative tumor sections are shown for high, middle and low scorings. B) Overall survival of eRMS patients as shown by a Kaplan-Meier curve. For A) ★★ P = 0.0272.
doi:10.1371/journal.pone.0019506.g005

Previous studies have suggested that mesenchymal stem cells could be the origin of RMS [17,44,45]. In contrast, our metaanalysis of exon microarray data with published data sets revealed that RMS samples had an expression profile more similar to neuronal cells and patients than mesenchymal stem cells. Furthermore, expression profiles also detected a large number of neuronal genes being expressed in RMS biopsies [19,46,47,48] such as *pax3* which is crucial for the development of both the myogenic and neuronal lineage [42]. Interestingly, it has been demonstrated earlier that a population of myogenic, myf-5 positive cells can be derived from neural tube during mouse development [49]. These myf-5 positive cells co-express both neuronal and muscle markers, raising the intriguing possibility that the cell of origin of our CSC population could also be a multipotential stem cell derived from cells in the neuronal compartment. In support of this, it has also been described that neuronal stem cells can differentiate into malignant muscle cells after activation [18]. However, this issue needs to be addressed further in the future.

Previous studies have shown that CD133 marks hematopoietic stem cells [20] and cancer stem cells [29], in particular neuronal and mesenchymal CSCs [21]. Moreover, a $CD133^+$ population was identified as a CSC population in sarcomas such as Ewing's sarcoma [27] and osteosarcoma [50] which was more resistant to chemotherapy and radiation [7,8,9,10,11]. It was therefore not surprising that CD133 emerged as a marker for RMS CSC in our study as well. Interestingly, also the fraction of $CD133^+$ cells in both Ewing's sarcoma and RMS seem to be similar. It has been reported that expression of FGFR3 might mark a tumorigenic subpopulation in RMS. However, we did not find an increase in mRNA expression of this receptor in rhabdospheres (Figure S1). The same report also found that CD133 positive cells were not more tumorigenic than the negative population. However, the discrepancy with our study might be explained by the different CD133 epitopes that were used in the two studies. Here, using CD133 as a marker to sort cells which were then injected orthotopically into mice without prior cultivation in stem cell media, we readily detected tumor growth at lower cell numbers in CD133 positive versus CD133 negative cells. Indeed, in the $CD133^+$ injected group one mouse at every dilution developed a RMS tumor which was not observed in the $CD133^-$ population. The relatively low tumorigenicity detected in the sorted population in general is likely due to impaired viability of the cells by the sorting procedure. Interestingly, $CD133^+$ sorted cells were also more resistant to cisPlatin and Chlorambucil treatment suggesting that anti-apoptotic or mismatch repair proteins are active. Indeed, we observed upregulation of several transcripts encoding mismatch repair proteins in rhabdospheres (data not shown).

Finally, we stained a human RMS tissue microarray (TMA) [19] for CD133 to demonstrate that a $CD133^+$ population is also present in human tumor biopsies. Patients with high positivity for CD133 were found to have the worst overall survival, which could be explained by a higher recurrence. However, in a multivariate analysis using a cox regression model, we were not able to demonstrate that CD133 is an independent prognostic marker for eRMS since the number of patients in this group was too low. More patients will have to be included therefore in a future study. Nevertheless, CD133 might represent the first candidate marker to identify eRMS patients with poor survival and might be used to stratify patients in the future.

Conclusion

Overall, our results demonstrate that cells with self renewal property that can drive tumorigenicity and have the potential to differentiate into multiple lineages are enriched in rhabdospheres. With CD133, we identified an already known CSC marker in an additional sarcoma [27,50] whose expression also correlated with a poor prognosis in eRMS patients. Further characterization of this CD133 positive CSC population might lead to a better understanding of the development of RMS. It now seems possible to screen directly for therapeutically active substances targeting the CSC subpopulation in eRMS to further advance treatment of this childhood sarcoma.

Supporting Information

Figure S1 Prominin and fibroblast growth factor receptor (FGFR) expression in adherent and sphere cells. A) Prominin1 and Prominin2 gene expression profiles in adherent and sphere cells analyzed by Genespring10 software. Intensity values were normalized to adherent cells. B) FGFR1, FGFR2, FGFR3 and FGFR4 gene expression profiles in adherent and sphere cells. Intensity values were normalized to adherent cells. C) Quantitative Real-time PCR with primers for FGFR3 (Hs00997400_g1) and for GAPDH was done with cDNA of adherent cells and three different passages of sphere cells. Quantitative results are indicated in arbitrary units (AU). FGFR3 was not differentially expressed in sphere cells compared to adherent cells.
(TIF)

Acknowledgments

We thank Martina Storz and Silvia Behnke for generating a mouse tissue microarray and performing immunohistochemical stainings.

Author Contributions

Conceived and designed the experiments: DW BWS. Performed the experiments: DW SS PA BCB VD SMO. Analyzed the data: DW SS PA HR CG BWS. Contributed reagents/materials/analysis tools: IL EK. Wrote the paper: DW BWS. Financial support: HM FKN MB. Designed software: HR.

References

1. Lobo NA, Shimono Y, Qian D, Clarke MF (2007) The biology of cancer stem cells. Annu Rev Cell Dev Biol 23: 675–699.
2. Bonnet D, Dick JE (1997) Human acute myeloid leukemia is organized as a hierarchy that originates from a primitive hematopoietic cell. Nat Med 3: 730–737.
3. Al-Hajj M, Wicha MS, Benito-Hernandez A, Morrison SJ, Clarke MF (2003) Prospective identification of tumorigenic breast cancer cells. Proc Natl Acad Sci U S A 100: 3983–3988.
4. Singh S, Dirks PB (2007) Brain tumor stem cells: identification and concepts. Neurosurg Clin N Am 18: 31–38, viii.
5. Todaro M, Francipane MG, Medema JP, Stassi G (2010) Colon cancer stem cells: promise of targeted therapy. Gastroenterology 138: 2151–2162.
6. Boiko AD, Razorenova OV, van de Rijn M, Swetter SM, Johnson DL, et al. (2010) Human melanoma-initiating cells express neural crest nerve growth factor receptor CD271. Nature 466: 133–137.
7. Bertolini G, Roz L, Perego P, Tortoreto M, Fontanella E, et al. (2009) Highly tumorigenic lung cancer CD133+ cells display stem-like features and are spared by cisplatin treatment. Proc Natl Acad Sci U S A 106: 16281–16286.
8. Dean M, Fojo T, Bates S (2005) Tumour stem cells and drug resistance. Nat Rev Cancer 5: 275–284.
9. Jiang X, Gwye Y, Russell D, Cao C, Douglas D, et al. (2010) CD133 expression in chemo-resistant Ewing sarcoma cells. BMC Cancer 10: 116.
10. Todaro M, Perez Alea M, Scopelliti A, Medema JP, Stassi G (2008) IL-4-mediated drug resistance in colon cancer stem cells. Cell Cycle 7: 309–313.
11. Wang J, Wakeman TP, Lathia JD, Hjelmeland AB, Wang XF, et al. (2010) Notch promotes radioresistance of glioma stem cells. Stem Cells 28: 17–28.
12. Morrison SJ, Spradling AC (2008) Stem cells and niches: mechanisms that promote stem cell maintenance throughout life. Cell 132: 598–611.

13. De Giovanni C, Landuzzi L, Nicoletti G, Lollini PL, Nanni P (2009) Molecular and cellular biology of rhabdomyosarcoma. Future Oncol 5: 1449–1475.
14. Gregorio A, Corrias MV, Castriconi R, Dondero A, Mosconi M, et al. (2008) Small round blue cell tumours: diagnostic and prognostic usefulness of the expression of B7-H3 surface molecule. Histopathology 53: 73–80.
15. McDowell HP (2003) Update on childhood rhabdomyosarcoma. Arch Dis Child 88: 354–357.
16. Hirotsu M, Setoguchi T, Matsunoshita Y, Sasaki H, Nagao H, et al. (2009) Tumour formation by single fibroblast growth factor receptor 3-positive rhabdomyosarcoma-initiating cells. Br J Cancer 101: 2030–2037.
17. Merlino G, Khanna C (2007) Fishing for the origins of cancer. Genes Dev 21: 1275–1279.
18. Galli R, Borello U, Gritti A, Minasi MG, Bjornson C, et al. (2000) Skeletal myogenic potential of human and mouse neural stem cells. Nat Neurosci 3: 986–991.
19. Wachtel M, Runge T, Leuschner I, Stegmaier S, Koscielniak E, et al. (2006) Subtype and prognostic classification of rhabdomyosarcoma by immunohistochemistry. J Clin Oncol 24: 816–822.
20. Yin AH, Miraglia S, Zanjani ED, Almeida-Porada G, Ogawa M, et al. (1997) AC133, a novel marker for human hematopoietic stem and progenitor cells. Blood 90: 5002–5012.
21. Shu Q, Wong KK, Su JM, Adesina AM, Yu LT, et al. (2008) Direct orthotopic transplantation of fresh surgical specimen preserves CD133+ tumor cells in clinically relevant mouse models of medulloblastoma and glioma. Stem Cells 26: 1414–1424.
22. Todaro M, Alea MP, Di Stefano AB, Cammareri P, Vermeulen L, et al. (2007) Colon cancer stem cells dictate tumor growth and resist cell death by production of interleukin-4. Cell Stem Cell 1: 389–402.
23. Hermann PC, Huber SL, Herrler T, Aicher A, Ellwart JW, et al. (2007) Distinct populations of cancer stem cells determine tumor growth and metastatic activity in human pancreatic cancer. Cell Stem Cell 1: 313–323.
24. Ding W, Mouzaki M, You H, Laird JC, Mato J, et al. (2009) CD133+ liver cancer stem cells from methionine adenosyl transferase 1A-deficient mice demonstrate resistance to transforming growth factor (TGF)-beta-induced apoptosis. Hepatology 49: 1277–1286.
25. Monzani E, Facchetti F, Galmozzi E, Corsini E, Benetti A, et al. (2007) Melanoma contains CD133 and ABCG2 positive cells with enhanced tumourigenic potential. Eur J Cancer 43: 935–946.
26. Miki J, Furusato B, Li H, Gu Y, Takahashi H, et al. (2007) Identification of putative stem cell markers, CD133 and CXCR4, in hTERT-immortalized primary nonmalignant and malignant tumor-derived human prostate epithelial cell lines and in prostate cancer specimens. Cancer Res 67: 3153–3161.
27. Suva ML, Riggi N, Stehle JC, Baumer K, Tercier S, et al. (2009) Identification of cancer stem cells in Ewing's sarcoma. Cancer Res 69: 1776–1781.
28. Takenobu H, Shimozato O, Nakamura T, Ochiai H, Yamaguchi Y, et al. (2011) CD133 suppresses neuroblastoma cell differentiation via signal pathway modification. Oncogene 30: 97–105.
29. Bidlingmaier S, Zhu X, Liu B (2008) The utility and limitations of glycosylated human CD133 epitopes in defining cancer stem cells. J Mol Med 86: 1025–1032.
30. Quintana E, Shackleton M, Sabel MS, Fullen DR, Johnson TM, et al. (2008) Efficient tumour formation by single human melanoma cells. Nature 456: 593–598.
31. Babu H, Cheung G, Kettenmann H, Palmer TD, Kempermann G (2007) Enriched monolayer precursor cell cultures from micro-dissected adult mouse dentate gyrus yield functional granule cell-like neurons. PLoS ONE 2: e388.
32. Bouchard F, Paquin J (2009) Skeletal and cardiac myogenesis accompany adipogenesis in P19 embryonal stem cells. Stem Cells Dev 18: 1023–1032.
33. Pittenger MF, Mackay AM, Beck SC, Jaiswal RK, Douglas R, et al. (1999) Multilineage potential of adult human mesenchymal stem cells. Science 284: 143–147.
34. Scientific T (2009) Human Mesenchymal Stem Cell Protocol: Oil Red O Staining of Adipogenic Cultures. Thermo Scientific. https://www.thermo.com/eThermo/CMA/PDFs/Various/File_4336.pdf (13.01.2011).
35. Angello JC, Stern HM, Hauschka SD (1997) P19 embryonal carcinoma cells: a model system for studying neural tube induction of skeletal myogenesis. Dev Biol 192: 93–98.
36. Franken NA, Rodermond HM, Stap J, Haveman J, van Bree C (2006) Clonogenic assay of cells in vitro. Nat Protoc 1: 2315–2319.
37. McBurney MW (1993) P19 embryonal carcinoma cells. Int J Dev Biol 37: 135–140.
38. Skerjanc IS (1999) Cardiac and skeletal muscle development in P19 embryonal carcinoma cells. Trends Cardiovasc Med 9: 139–143.
39. Dantonello TM, Int-Veen C, Winkler P, Leuschner I, Schuck A, et al. (2008) Initial patient characteristics can predict pattern and risk of relapse in localized rhabdomyosarcoma. J Clin Oncol 26: 406–413.
40. Larsson LG, Henriksson MA (2010) The Yin and Yang functions of the Myc oncoprotein in cancer development and as targets for therapy. Exp Cell Res 316: 1429–1437.
41. Muratovska A, Zhou C, He S, Goodyer P, Eccles MR (2003) Paired-Box genes are frequently expressed in cancer and often required for cancer cell survival. Oncogene 22: 7989–7997.
42. Robson EJ, He SJ, Eccles MR (2006) A PANorama of PAX genes in cancer and development. Nat Rev Cancer 6: 52–62.
43. Young AP, Wagers AJ (2010) Pax3 induces differentiation of juvenile skeletal muscle stem cells without transcriptional upregulation of canonical myogenic regulatory factors. J Cell Sci 123: 2632–2639.
44. Astolfi A, De Giovanni C, Landuzzi L, Nicoletti G, Ricci C, et al. (2001) Identification of new genes related to the myogenic differentiation arrest of human rhabdomyosarcoma cells. Gene 274: 139–149.
45. Charytonowicz E, Cordon-Cardo C, Matushansky I, Ziman M (2009) Alveolar rhabdomyosarcoma: is the cell of origin a mesenchymal stem cell? Cancer Lett 279: 126–136.
46. Davicioni E, Finckenstein FG, Shahbazian V, Buckley JD, Triche TJ, et al. (2006) Identification of a PAX-FKHR gene expression signature that defines molecular classes and determines the prognosis of alveolar rhabdomyosarcomas. Cancer Res 66: 6936–6946.
47. Lae M, Ahn EH, Mercado GE, Chuai S, Edgar M, et al. (2007) Global gene expression profiling of PAX-FKHR fusion-positive alveolar and PAX-FKHR fusion-negative embryonal rhabdomyosarcomas. J Pathol 212: 143–151.
48. Wachtel M, Dettling M, Koscielniak E, Stegmaier S, Treuner J, et al. (2004) Gene expression signatures identify rhabdomyosarcoma subtypes and detect a novel t(2;2)(q35;p23) translocation fusing PAX3 to NCOA1. Cancer Res 64: 5539–5545.
49. Tajbakhsh S, Vivarelli E, Cusella-De Angelis G, Rocancourt D, Buckingham M, et al. (1994) A population of myogenic cells derived from the mouse neural tube. Neuron 13: 813–821.
50. Wilson H, Huelsmeyer M, Chun R, Young KM, Friedrichs K, et al. (2008) Isolation and characterisation of cancer stem cells from canine osteosarcoma. Vet J 175: 69–75.

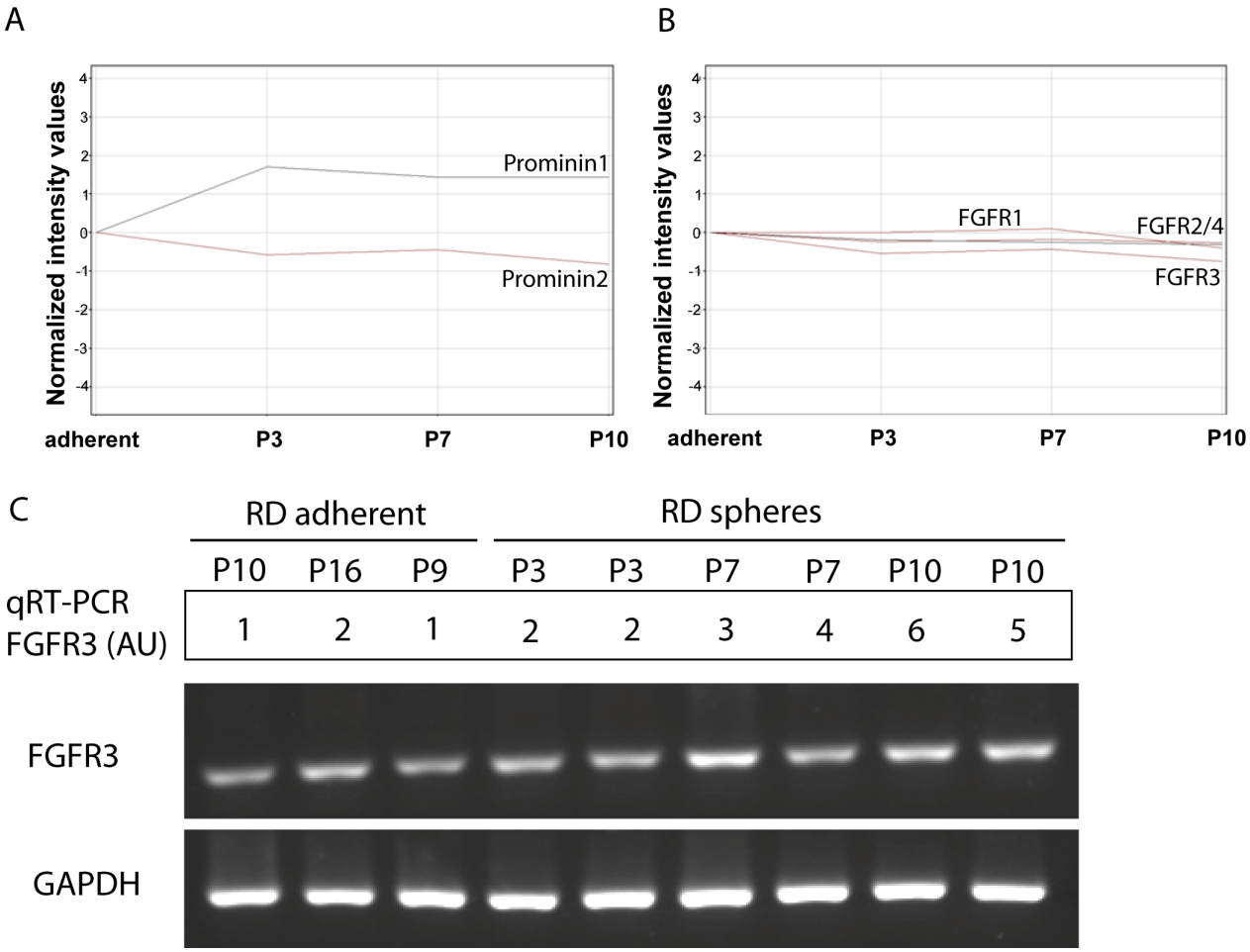

Figure S1. Prominin and fibroblast growth factor receptor (FGFR) expression in adherent and sphere cells. A) Prominin1 and Prominin2 gene expression profiles in adherent and sphere cells analyzed by Genespring10 software. Intensity values were normalized to adherent cells. B) FGFR1, FGFR2, FGFR3 and FGFR4 gene expression profiles in adherent and sphere cells. Intensity values were normalized to adherent cells. C) Quantitative Real-time PCR with primers for FGFR3 (Hs00997400_g1) and for GAPDH was done with cDNA of adherent cells and three different passages of sphere cells. Quantitative results are indicated in arbitrary units (AU). FGFR3 was not differentially expressed in sphere cells compared to adherent cells.

Targeting hedgehog signaling reduces self-renewal in Embryonal Rhabdomyosarcoma

Sampoorna Satheesha,[1] Amandine Bovay,[1,4] Gabriele Manzella,[1,4] Elisa A. Casanova,[1] Peter Bode,[1,2] Réka Belle,[1] Simone Feuchtgruber,[3] Patricia Jaaks,[1] Nurhak Dogan,[1] Ewa Koscielniak,[3] and Beat W. Schäfer[1,5]

[1]Department of Oncology and Children's Research Center, University Children's Hospital, Zurich, Switzerland
[2]Institute of Surgical Pathology, University Hospital Zurich, Zurich, Switzerland
[3]Department of Oncology/Hematology/Immunology, Olgahospital, Klinikum Stuttgart, Stuttgart, Germany
[4]These authors contributed equally to the work
[5]**Corresponding author**
Department of Oncology, University Children's Hospital, Steinwiessstrasse-75, 8032, Zurich, Switzerland
Email: Beat.Schaefer@kispi.uzh.ch
Tel: +41 (44) 266 7553
Fax: +41 (44) 634 8859

The authors declare that no conflict of interest exists.

Short title: Hedgehog-driven ERMS cancer stem cells

Keywords:

Hedgehog signaling, cancer stem cells, embryonal rhabdomyosarcoma, Nanog, pediatric cancer, sarcoma, tumor heterogeneity

Abstract

Current treatment regimens for Rhabdomyosarcoma (RMS), the most common pediatric soft tissue cancer, rely on conventional chemotherapy and although they show clinical benefit there is a significant risk of adverse side effects and secondary tumors later in life. Therefore, identifying and targeting sub-populations with higher tumorigenic potential and self-renewal capacity would offer improved patient management strategies. The self-renewing cellular compartments enriched from embryonal RMS (ERMS) cell lines using sphere assay showed upregulation of several components of the Hedgehog pathway. Genetic loss- and gain-of-function experiments and the use of clinically relevant small molecule modulators revealed that hedgehog signaling is important for determining self-renewal in vitro and tumor initiation in vivo. In addition, the hedgehog pathway altered the chemoresistance, motility and differentiation status of ERMS cells. Furthermore, NANOG was determined as an important downstream effector of active hedgehog signaling. Importantly, evaluating the presence of self-renewing cells identified by GLI1 and NANOG expression could predict patient survival. This work presents novel functional aspects of hedgehog signaling in ERMS, redefining the rationale for its targeting as means to control ERMS self-renewal and also underscores the importance of studying tumor heterogeneity in pediatric cancer in general.

Introduction

Rhabdomyosarcoma (RMS) comprises a heterogeneous set of neoplasms that possess features of halted skeletal muscle differentiation. It is the most common soft tissue cancer in the pediatric population with an incidence of 4.3 per million per year. There are two major histological subtypes: embryonal (ERMS) and alveolar (ARMS). The two variants differ in their molecular cytogenetic profiles, clinical presentations and prognosis. In 80% of ARMS cases presence of the chromosomal translocation t(2;13)(q35;q14) or t(1;13)(p36;q14) has been observed which leads to the expression of a fusion transcription factor PAX3-FOXO1 or PAX7-FOXO1 respectively. The fusion-positive status has been shown to predict poor survival (Hawkins et al. 2014). ERMS accounts for about 70% of all diagnosed RMS cases. These tumors are fusion-negative but possess a relatively more complex genomic landscape with a loss of heterozygosity at 11p15 locus and a frequent alteration of the RAS pathway (Shern et al. 2014). A multi-modal approach is routinely used in the clinics for RMS treatment which includes intensive multi-agent chemotherapy with conventional cytotoxic drugs, surgical resection and radiotherapy. After an initial improvement in overall survival the progress in clinical care has reached a plateau in recent years (Malempati and Hawkins 2012; Hawkins et al. 2013; Hawkins et al. 2014). Currently, pre-treatment histology and initial clinical presentation guide risk stratification for relapse which is used to determine therapy intensity (Hawkins et al. 2013). While a majority of ERMS patients have good prognosis with event-free survival of over 75%, the situation is dismal for high risk metastatic ERMS patients and patients with progressive or recurrent disease, with a five year survival estimate at 35% and 17%, respectively (Hawkins et al. 2014). Furthermore, current treatment regimens cause severe morbidity and lead to late sequelae (Stevens 2005). Therefore there is an urgent need to implement rationally selected targeted treatment options to reduce rate of relapse, therapy burden and improve clinical outcome (Schafer and Niggli 2010; Norris and Adamson 2012).

To this end, it will be important to delineate the molecular mechanisms which initiate and maintain ERMS tumors. Recent data suggest that ERMS is a hierarchically organized tumor. We

have previously shown that de-differentiated highly tumorigenic cells could be enriched by propagating human ERMS cancer cell lines as clonal spheres (Walter et al. 2011). Additionally, cells with activated satellite cell phenotype have been shown to possess long-term tumor propagating potential in the transgenic RAS-activated zebrafish model of ERMS (Langenau et al. 2007; Ignatius et al. 2012). Therefore the tenets of the cancer stem cell model could be used to highlight pathways that are important for ERMS cancer initiating cells (CICs) and thereby provide novel therapeutic interventions. At present little is known about the pathways employed to maintain self-renewal and initiate tumor formation in ERMS.

The master developmental pathways in ontogenesis such as Wnt, Notch, and Hedgehog signaling networks are prime candidates for cancer stem cell-based therapies since they have been recently shown to also play key roles in oncogenesis (Takebe et al. 2011). Amongst these, activation of the hedgehog pathway is the most commonly documented in ERMS. Canonical hedgehog pathway is a ligand-activated signaling system with three mammalian ligand variants – sonic (SHH), indian (IHH) and desert hedgehog (DHH) (Stecca and Ruiz 2010; Ruiz i Altaba 2011). The secreted ligands bind to the extracellular domain of the patched (PTCH) receptor leading to the release of the receptor smoothened (SMO). SMO is then free to translocate to the primary cilium to activate the downstream signaling cascade which primarily involves relieving the inhibition of suppressor of fused (SUFU) upon the activity of the GLI transcription factors. There are three GLI transcription factors, of which GLI1 is the most potent transactivator. In general ERMS tumors have higher hedgehog pathway activity than ARMS (Zibat et al. 2010; Pressey et al. 2011; Chen et al. 2013). In a recent study over 50% of ERMS cases showed increased hedgehog pathway activation (Paulson et al. 2011) and PTCH1 mRNA expression has been reported to predict poor prognosis in ERMS patients (Zibat et al. 2010). Additionally, patients with germline activation of hedgehog pathway (Gorlin syndrome) are predisposed to ERMS development. Interestingly, also all mouse models of activated hedgehog signaling develop ERMS with varying penetrance. Although there is evidence suggesting an important role for hedgehog signaling in ERMS, its role

in maintaining ERMS CIC features has not been directly investigated. This distinction would be critical in determining many aspects of treatment strategy in the clinics.

In the present study, using small molecules and various genetic approaches we show that hedgehog signaling modulates ERMS self-renewal and tumor initiation. We describe additional novel roles played by this pathway in determining ERMS chemoresistance, invasion and differentiation status. We also identify NANOG as the functionally important target gene downstream of the pathway, previously unknown in any soft tissue sarcoma. Importantly, for the first time, we show that functional intra-tumoral heterogeneity measured by the presence of hedgehog-active CIC markers in ERMS patients is clinically relevant. Therefore, targeting hedgehog signaling mediated self-renewal could be a viable therapeutic approach for ERMS management.

Results

Hedgehog signaling is necessary for ERMS self-renewal and efficient tumorigenesis

First, we analyzed the expression of hedgehog pathway components in ERMS sphere cultures which have been previously shown to be enriched in de-differentiated, self-renewing and highly tumorigenic cells (Walter et al. 2011). Real-time gene expression analysis revealed that the mRNA level of the key hedgehog target gene and effector transcription factor GLI1 was increased in both RD (+2185%) and RH36 (+191%) spheres compared to their respective adherent counterparts (Fig. 1A and Supplemental Fig. 1A). Similar changes were observed for other target genes such as GLI2, PTCH1 and HHIP. The increased expression levels of GLI1 and HHIP were also noted in ERMS xenografts (Fig. 1B). To evaluate whether hedgehog pathway might play a causative role in ERMS self-renewal the small molecule hedgehog agonist SAG1.3 was added to the sphere media during the formation of primary spheres, which were then plated at clonal density to form secondary spheres without drug. Primary sphere formation increased slightly but significantly for RD cells (+25%) and a larger relative increase in secondary sphere formation was observed for both cell lines (RD: +50% and RH36: +170%), indicating that SAG1.3 treatment increased the sphere initiating compartment (Fig. 1C). Next, we used siRNA to reduce the expression of SUFU in RD sphere cells to ensure the specificity for hedgehog pathway activation (Supplemental Fig. 1B) and indeed this led to a doubling in the RD sphere initiating ability (Fig. 1D). Additionally, to exclude any extraneous effects of the sphere media components on hedgehog pathway activation, ERMS adherent cells were treated with SAG1.3 prior to plating in normal sphere media. This treatment did not affect the cell cycle profile or viability of ERMS cells but led to increased sphere initiating capacity in a dose-dependent manner for both the cell lines studied (Fig. 1E and Supplemental Fig. 1, C-E). Taken together the data indicates that ERMS cells enriched for higher self-renewal capacity and tumorigenicity possess higher hedgehog pathway activity. Furthermore, transient activation of hedgehog pathway leads to higher self-renewal.

To study the role of hedgehog pathway activation in ERMS in more detail, we generated stable cell lines that either over-expressed GLI1 (pCMV-GLI1) or 'empty' control plasmid (pCMV-Empty). GLI1 over-expression led to upregulation in HHIP mRNA expression by 180 fold in RD cells and 2 fold in RH36 cells (Fig. 1F and Supplemental Fig. 1, F and G). HHIP was consistently found to be a more responsive target gene than PTCH1 *in vitro*. The RD pCMV-GLI1 cells showed a 30% increase in primary sphere formation while the RH36 pCMV-GLI1 cells formed twice as many spheres as control cells (Fig. 1, G and H). When plated for secondary sphere formation the relative increase in sphere initiation capacity became more apparent in both the cell lines (RD: +87% and RH36: +230%). The RD pCMV-GLI1 cells also had 50% higher adherent colony forming ability (Supplemental Fig. 1H). To investigate the consequences of increasing hedgehog pathway activity on tumor initiation and growth *in vivo* we injected the stable cell lines orthotopically in NOD/SCID mice. Both RD and RH36 pCMV-GLI1 cells displayed significantly faster tumor growth rate (Fig. 1, I and J). In the case of RH36 the number of cells injected per mouse was found to be limiting since only 2 out of the 6 mice injected with pCMV-Empty cells formed tumors, whereas the RH36 pCMV-GLI1 cells showed greater tumor initiating capacity (4 out of 6 mice). The xenografts retained GLI1 over-expression (Supplemental Fig. 1I) and were confirmed to be of ERMS histotype, as judged from the positive myogenin and desmin immunostaining (Supplemental Fig. 2). Overall, ERMS cells displaying an active hedgehog pathway possess higher self-renewal and increased tumor initiating capacity.

Next, we inhibited the hedgehog pathway both pharmacologically and genetically to evaluate its necessity for ERMS pathogenesis. ERMS cells were treated first with SMO inhibitor GDC-0449 or GLI inhibitor GANT61 during the primary sphere formation stage. This led to a decrease in the number of spheres formed in RD cells by 33% and 70%, respectively (Fig. 2A). Similar results were obtained for RH36 cells (Supplemental Fig. 3A). The GDC-0449 treatment led to a decrease of 88% in the secondary sphere initiating capacity of RD cells and there were no spheres formed in the case of RH36 cells. GANT61 treatment was more potent since no viable cells were available for

secondary sphere formation from either cell line. Using siRNA we specifically reduced GLI1 expression in RD sphere cells to corroborate the results obtained with hedgehog inhibitors. Consequently, the sphere initiation decreased by about 30% (Fig. 2B). Next, ERMS cells were treated with GDC-0449, LDE-225 (also a SMO inhibitor) or GANT61 in adherent conditions and then plated for sphere formation. Dose-dependent decrease in sphere initiation was observed with all drugs (Fig. 2C and Supplemental Fig. 3B). The pre-treatment of RD cells with GANT61 *in vitro* led to slower tumor initiation *in vivo* (Fig. 2D). The treatments did not alter the cell cycle profile or viability status of the cells (Supplemental Fig. 3, C-F). All xenografts were collected for analysis once the control arm reached the maximum allowed volume of 1 cm^3. The xenografts from the GANT61 treated cells weighed 50% lower than the control xenografts, corroborating the tumor volume difference observed from caliper measurements (Fig. 2E and Supplemental Fig. 3G). The GANT61 xenograft displayed lower desmin positivity and fewer strongly GLI1 positive cells (Supplemental Fig. 3H). Hence, the transient inhibition of hedgehog pathway with small-molecules seems to not only reduce self-renewal of ERMS cells *in vitro* but also tumor growth kinetics *in vivo*.

To study the long-term effect of inhibiting the hedgehog pathway we generated stable cell lines. ERMS cells were transfected with SUFU over-expressing vector (pCMV-SUFU) to inhibit GLI activity directly. Ligand-based hedgehog signaling was inhibited by transducing ERMS cells with shRNA against SMO (shSMO) and the 'empty' backbone vector (pLKO.1) was used as control. Both cell lines showed a decrease in GLI1 and HHIP expression as expected (Fig. 2, F and G and Supplemental Fig. 4, A-D). The adherent colony forming ability of RD cells was decreased upon SUFU over-expression and SMO knockdown by 80% and 40% respectively (Supplemental Fig. 4, E and F). Sphere initiation was decreased by 50% upon SUFU over-expression and by 30-40% upon SMO knockdown in RD. Similar results were noted for RH36 cells (Fig. 2, H and I). There were no significant changes observed in cellular proliferation or cell cycle profiles (Supplemental Fig. 4, G-M and data not shown). When injected orthotopically in immunocompromised mice both pCMV-SUFU and shSMO cells showed decreased tumor growth kinetics (Fig. 2, J to M).

Impressively, for RD cells there was no palpable tumor growth in the majority of hedgehog-inhibited xenograft mice at the time when the control xenografts reached the maximum allowed tumor volume. While tumor initiation rate was 100% for control cells, only 3 out of the 5 mice and 3 out of 7 mice injected with pCMV-SUFU and shSMO cells respectively, developed tumors. Taken together, the data supports the notion that active hedgehog signaling is necessary for ERMS self-renewal and efficient tumorigenicity.

Autocrine ligand-based activation of hedgehog pathway in ERMS

Pathway activation in ERMS seemed to be largely ligand-based since inhibition of either receptor-mediated or GLI-based hedgehog signaling led to similar effects on self-renewal and tumorigenesis. Since not much is known about ligand-based signaling mechanism in ERMS we analyzed the expression pattern of the hedgehog ligands - SHH, DHH and IHH, by quantitative PCR. We could not detect the expression of SHH in adherent cell lines, sphere cultures, xenografts or murine skeletal muscle. In contrast, DHH and IHH were expressed in all model systems. The expression of DHH was particularly higher for RD sphere cells and xenografts while both DHH and IHH expression was increased in RH36 sphere cultures and xenografts (Fig. 3, A-D). The expression levels of the ligands were also analyzed in ERMS patient samples using pooled human skeletal muscle RNA from three fetal and five adult donors as controls. Fetal skeletal muscle expressed all the ligands and at higher levels compared to adult skeletal muscle (Supplemental Fig. 5, A-C). Also, the expression of SHH was not detected in adult skeletal muscle. The expression level of the ligands varied between patient samples, but in general the levels were intermediary to fetal and adult skeletal muscle with the average expression level of DHH being higher than that of IHH (Fig. 3E). While DHH and IHH were found be expressed in all nine ERMS patient samples, SHH was detected in only four patients.

Also, to distinguish between autocrine and paracrine signalling mechanism in ERMS xenografts we used species specific PCR probes. The ligands expressed within ERMS xenografts were

determined to be primarily of human origin indicating an autocrine signalling mechanism (Fig. 3, F and G). We also noted a minor paracrine contribution, since the expression of murine Dhh was increased within xenografts when compared to murine muscle (Supplemental Fig. 5, D and E). Overall, hedgehog ligands are expressed in ERMS and importantly ligand-based signaling might be further increased under conditions of self-renewal and *in vivo* tumorigenesis.

Hedgehog signaling alters chemoresistance of ERMS cells

Therapy resistance is a clinically relevant property of CICs. Hence, we evaluated the self-renewal ability of RD cells after treatment with high concentrations of Irinotecan. After 48 hours of treatment with the drug or vehicle, equal numbers of viable cells were plated for sphere formation at clonal density. Irinotecan treatment led to a G2/M cell cycle arrest (data not shown) leading to a reduction in the overall sphere forming ability of the cells. However the cells that had been treated with the highest concentration of Irinotecan (IC_{50}) formed 74% more spheres than cells treated with the lowest concentration ($IC_{50}/4$) indicating that sphere initiating cells were enriched in the former case (Fig. 4A). Importantly, when Irinotecan treatment was combined with hedgehog pathway inhibition using LDE-225, a relative reduction of 57% in sphere formation was observed, compared to treatment with Irinotecan only (Fig. 4B).

Next, we investigated whether hedgehog pathway activity could impact upon the chemoresistance of ERMS cells. The previously described stable lines were treated with a serial dilution of Irinotecan or Doxorubicin. After 72 hours WST assay was performed and cell line-specific IC_{50} concentrations were calculated (Fig. 4C). We noted that IC_{50} value for Irinotecan for RD pCMV-GLI1 cells was on average 73% higher than empty vector control cells. Similar results were obtained for RH36 cells. Also, IC_{50} for Doxorubicin were 54% and 81% higher in RD and RH36 pCMV-GLI1 cells, respectively. Overall, ERMS cells with increased hedgehog pathway activity show increased resistance to chemotherapy. As corollary, we expected that decreasing hedgehog pathway activity would increase sensitivity of ERMS cells. Indeed, we observed that the

IC_{50} values for RD pCMV-SUFU cells were 32% and 25% lower for Irinotecan and Doxorubicin respectively. Similarly, SMO knockdown in RD cells led to a significant 50% reduction in Irinotecan IC_{50} with a minor reduction for Doxorubicin (10%). SMO knockdown in RH36 cells showed comparable reduction in IC_{50} values for both Irinotecan (57%) and Doxorubicin (53%). Overall hedgehog pathway activity levels could modulate chemoresistance of ERMS cells to cytotoxic drugs.

Hedgehog signaling modulates cell motility and differentiation status of ERMS cells

To evaluate the role of hedgehog pathway in cell motility we performed trans-well migration and invasion assays using ERMS stable lines. First, we observed that RD cells were more migratory and invasive than RH36 cells. Therefore, further experiments were performed with RD cell lines only. We noted that increasing the hedgehog pathway activity did not significantly impact cell motility since RD pCMV-GLI1 showed only a minor increase in migration and invasion (data not shown). Although inhibition of hedgehog activity significantly decreased migration by 53% in pCMV-SUFU and 37% in shSMO RD cells (Fig. 4, D and E, and Supplemental Fig. 6A) it led to an increase in the ECM invasive potential. The RD pCMV-SUFU cells showed a 5 fold increase in invasiveness and for shSMO cells the increase was 1.8 fold (Fig. 4, F and G, and Supplemental Fig. 6B). This effect was cell autonomous since coating the membrane filter with gelatin did not alter the results (Supplemental Fig. 6B).

Next, we wanted to evaluate the effect of hedgehog signaling on ERMS differentiation since conceptually a CIC maintenance pathway would affect tumor cell differentiation status. ERMS tumors have been known to express key myogenic transcription factors such as Pax7, Myod and Myogenin which control the differentiation status of skeletal muscle. The expression of Pax7 is highest in the quiescent muscle stem cells while Myogenin is expressed by committed muscle progenitor cells. Therefore the expression of these proteins is mutually exclusive and provides a convenient readout to assess differentiation status. We immunostained the stable cell lines

representing different hedgehog pathway activities for Pax7 and Myogenin. First, we noted that the expression of these transcription factors was mutually exclusive also in ERMS cells indicating that the differentiation programs present during normal myogenesis are also active in the pathological state (Fig. 5A and Supplemental Fig. 6D). Interestingly, RD pCMV-GLI1 cells increased $PAX7^+$ cells by 90% and RH36 pCMV-GLI1 cells by 154% (Fig. 5, A, B and D, and Supplemental Fig. 6D). Concomitantly we observed fewer $MYOGENIN^+$ cells (RD: -24.5% and RH36: -35%). Inhibition of the hedgehog pathway induced differentiation in RD cells as evidenced by a 65% and 54% reduction in the percentage of $PAX7^+$ cells in pCMV-SUFU cells and shSMO cells respectively (Fig. 5, A-C and Supplemental Fig. 6C). Correspondingly there was a gain in the percentage of $MYOGENIN^+$ cells (pCMV-SUFU: +19% and shSMO: +56%). Similar results were obtained for RH36 cells (Fig. 5E and Supplemental Fig. 6E). Importantly, treatment with small molecule modulators of hedgehog signaling also induced similar alterations in the differentiation status (Supplemental Fig. 6, F-H). These data suggest that activation of hedgehog signaling confers a more stem-like state to ERMS cells and pathway inhibition induces differentiation.

NANOG is a functionally important hedgehog pathway target gene for ERMS self-renewal

To identify genes that could be regulated by the hedgehog pathway in ERMS cells, we used a stem cell-focused quantitative PCR based screening approach to survey the expression levels of 162 individual genes previously associated with stem cell phenotype or components of important developmental pathways. Biologically duplicate sets of RNA from RD and RH36 cell lines with either activated (pCMV-GLI1) or inhibited hedgehog pathway (shSMO) and their respective controls were used. We found 147 genes to be reliably expressed (Ct value < 35), of which 142 were common to both cell lines. The relative fold changes in expression of the common genes were used for non-supervised hierarchical clustering to identify genes either positively or negatively regulated by hedgehog signaling. The changes in expression levels of these genes were verified on an individual basis to include only those with least 1.5 fold difference in both RD and RH36 (Fig.

5F). We found more genes to be negatively regulated by the hedgehog pathway than positively in both cell lines. A high representation of components of the TGF-β and Wnt signaling was noted amongst the negatively regulated genes indicating that these pathways could be associated with the more differentiated phenotype of ERMS cells. Interestingly, expression of the stem cell transcription factor NANOG was found to be positively regulated by hedgehog signaling in both the cell lines. Due to its important role in the maintenance of the embryonic stem cell phenotype and the recent delineation of its function in cancer (Wang et al. 2013) we chose to further study its role in the hedgehog pathway-mediated stemness observed in ERMS.

We first confirmed the alterations in NANOG mRNA expression in pCMV-GLI1 and shSMO ERMS cell lines using NANOG specific Taqman-based PCR probes and additional biological replicates (Supplemental Fig. 7, A and B). We also observed decrease in NANOG expression in pCMV-SUFU ERMS cells (Supplemental Fig. 7, C and D). Next, ERMS cell lines were co-immunostained for GLI1 and NANOG. We noted that the expression of both the proteins was heterogeneous, co-localized and correlative, that is, $GLI1^{high}$ cells were also $NANOG^{high}$ (Fig. 6A and Supplemental Fig. 7E). Upon GLI1 over-expression the percentage of cells expressing NANOG increased significantly (Fig. 6B). Accordingly, when ERMS cells were treated with hedgehog pathway agonist SAG1.3 the NANOG expressing cellular compartment increased by almost 2 fold in both the cell lines (Fig. 6C and Supplemental Fig. 7, F-H). We also noted increased NANOG expression in ERMS sphere cultures and xenografts (Supplemental Fig. 7, I-K). We performed gene expression analysis by quantitative PCR on 9 ERMS patient samples for 17 genes which included components of canonical hedgehog pathway, myogenesis and stem cell-associated factors. Upon non-supervised hierarchical clustering we found that NANOG expression clustered with that of GLI1 and PTCH1 (Supplemental Fig. 7L). Statistical analysis revealed that the expression of NANOG and GLI1 correlated significantly (Fig. 6D). We observed the positive correlation even after including expression data from four additional patient samples (9+4; Fig. 6D). These data indicate that NANOG expression correlates with hedgehog pathway activity levels in ERMS cell

lines and patient samples. Importantly, hedgehog pathway modulation can alter the expression of NANOG implying that it could be a target gene of the pathway in ERMS.

To show that NANOG is necessary for ERMS self-renewal, stable RD cell lines were generated using a lentiviral vector containing shRNA against NANOG (shNANOG). The sphere forming ability of these cells *in vitro* was 21% lower than the control pLKO.1 cells (Fig. 6E). When NANOG was over-expressed transiently in pCMV RD cells the sphere formation increased by 40-50% relative to control pCMV+pE1F cells (Fig. 6F). Importantly, NANOG expression in hedgehog inhibited cells rescued the lowered self-renewal ability of the cells (Fig. 6, F and G). We noted that the alteration in NANOG expression led to a concordant change in the expression of GLI1 (Fig. 6E and Supplemental Fig. 8A). To estimate the role of NANOG on self-renewal and tumor growth independently of this effect we generated stable rescue lines where NANOG expression was decreased in GLI1 over-expressing cells (GLI1+shNANOG). As controls we used stable lines with dual empty vector (pCMV+pLKO.1) or GLI1 over-expression and empty lentiviral backbone (GLI1+pLKO.1) (Supplemental Fig. 8, B and C). When both RD and RH36 rescue systems were allowed to form spheres, secondary sphere formation was increased significantly in the GLI1+pLKO.1 cells for both cell lines (RD: +108% and RH36: +59%) and impressively, NANOG knockdown rescued it back to almost control levels (Fig. 6, H and I). To study the effect on tumor growth *in vivo* RH36 pCMV+pLKO.1 and GLI1+shNANOG cell lines were injected in immunocompromised mice. The tumor growth rate of GLI1+shNANOG cells was significantly lower than control cells (Fig. 6J). Furthermore, GLI1+shNANOG xenografts displayed increased myogenin and desmin staining compared to control xenografts indicating that the tumor was in general more differentiated (Supplemental Fig. 8D). Taken together, NANOG seems to be a functionally important component of the hedgehog signaling in ERMS.

GLI1 and NANOG expression has prognostic value for ERMS patients

Next, we evaluated if the expression of GLI1 and NANOG is clinically relevant. To this end we performed a double-blind analysis of GLI1 and NANOG expression separately in a previously described set of tissue microarrays (TMA) with multiple tumor cores from 116 ERMS patient samples using immunohistochemistry (Wachtel et al. 2006). Reliable protein expression status was obtained for 91 ERMS patients. The distrubution of patient and tumor related parameters were similar among patient subgroups. Chi-square tests revealed no significant differences between the groups (data not shown). Most patients were negative for both proteins. However patients positive for one were in 80% of the cases also positive for the other. We found that only tumor cells expressed GLI1 and NANOG and importantly the expression was heterogeneous (Fig. 7A and Supplemental Fig. 8E). The clinical data analysis revealed that the expression of GLI1 alone could predict statistically significant worse overall survival and a similar trend was observed for NANOG expression status (Fig. 7, B and C). These patients also tended to have worse event-free survival, although the data did not reach statistical significance (Supplemental Fig. 8, F and G). However, statistically significant worse event-free and overall survival was estimated for patients who possessed $GLI1^{+}$ and $NANOG^{+}$ cellular sub-populations within their tumors (Fig. 7, D and E). Our analysis reveals that ERMS intra-tumoral heterogeneity represented by expression of both GLI1 and NANOG has significant impact on clinical outcome.

Discussion

Our study provides novel mechanistic insights into hedgehog signaling in ERMS and establishes a role specifically in the self-renewal of ERMS CIC compartment. Additionally we show that hedgehog pathway plays an important role in ERMS cell motility, differentiation, and chemoresistance. We identify NANOG as a key downstream effector and importantly, the evaluation of GLI1 and NANOG expression status within ERMS patient samples shows significant prognostic value.

Hedgehog signaling has been previously shown to modulate self-renewal of CICs in various adult malignancies such as chronic myelogenous leukaemia (CML), multiple myeloma, melanoma, glioblastoma and cancers of the pancreas, prostate and breast (Peacock et al. 2007; Stecca et al. 2007; Merchant and Matsui 2010; Zbinden et al. 2010). The role of hedgehog signaling in pediatric CICs has been largely investigated in medulloblastoma (Read et al. 2009; Po et al. 2010; Wang et al. 2012a). Although genetic evidence suggests a general role for hedgehog signaling in ERMS tumor initiation, its contribution to the functional tumor heterogeneity seen in ERMS had not been explored. Here we describe an important role of this pathway in maintaining CIC properties in ERMS by using three model systems: sphere cultures, adherent monolayer cultures and *in vivo* mouse xenografts. We have previously reported that sphere cultures could be used to enrich for ERMS CICs (Walter et al. 2011). We now show that ERMS CIC cultures and xenografts have increased hedgehog pathway activity. Importantly, modulating the pathway using either small molecules or genetic means had a significant impact on sphere initiation, adherent colony formation, sphere renewal capacity and tumor growth *in vivo*. Therefore hedgehog pathway activity is an important determinant of ERMS self-renewal and tumor initiating capacity.

It is critical to understand the mechanisms of hedgehog pathway activation in ERMS for translational applicability. Our data shows the canonical SMO-based signaling to be important for maintaining ERMS CICs since inhibiting the pathway at the level of SMO and GLI activity provided equivalent outcomes. Additionally ligand/SMO-based hedgehog signaling seems to be

occurring in sporadic ERMS primarily by autocrine secretion of IHH and DHH. Pressey et al already ruled out SHH autocrine signaling mechanism in ERMS patients, however expression of the other ligands was not evaluated (Pressey et al. 2011). Similar to previous reports we find that hedgehog pathway activity is reduced *in vitro* (Gerber et al. 2007) which could be partly explained by the reduction in ligand expression upon culturing ERMS cells as adherent monolayers. It is likely that components of the growth serum present in regular cell culture media are inhibitory to hedgehog activity since ERMS sphere cultures maintained in serum-deprived conditions show increased pathway activity. Therefore the *in vitro* culturing of ERMS cells in serum-supplemented media may obscure tumor hierarchy and associated developmental pathways which are relevant *in vivo* as described previously in medulloblastoma and glioblastoma (Lee et al. 2006; Ward et al. 2009).

CICs are also known to be responsible for tumor recurrence by being more resistant to chemotherapeutic strategies (Vidal et al. 2013). Accordingly, we show that increasing CIC properties by activating hedgehog signaling could render ERMS cells more resistant to anti-proliferative drugs, such as Irinotecan (Topoisomerase-I inhibitor) and Doxorubicin (DNA intercalating agent), which are currently used in the clinics for ERMS management. Importantly the use of high-dose Irinotecan led to enrichment in self-renewing cells which could be rescued upon combination treatment with SMO inhibitor LDE225. This is similar to previous reports on imatinib-resistant CML where SMO inhibition reduced CICs and improved survival (Zhao et al. 2009; Katagiri et al. 2013).

Previous study evaluating *in vivo* tumor heterogeneity in a zebrafish model of ERMS reported that the myogenin-expressing (differentiated) ERMS tumor cell compartment had higher invasiveness but lacked tumor-initiating capacity (Ignatius et al. 2012). Concordantly we observed that the hedgehog-inhibited ERMS cells with lowered tumorigenicity were more differentiated ($Pax7^{low}Myogenin^{high}$) and possessed increased ECM invasion capacity. Surprisingly in the absence of a basement membrane matrix the differentiated cells had much lower migratory ability indicating

that matrix adhesion probably plays an important role in determining cell motility in ERMS. Hedgehog pathway activation induced ERMS cell de-differentiation ($Pax7^{high}Myogenin^{low}$). However we could not find significant co-localization of PAX7 and GLI1 expression within ERMS cell lines indicating that PAX7 may not be a direct target of hedgehog pathway (data not shown). Therefore the hedgehog pathway probably inhibits differentiation further down the myogenic lineage (Gerber et al. 2007; Voronova et al. 2013). Interestingly, our qRT-PCR analyses revealed that hedgehog signaling modulation could impact key muscle differentiation nodes such as TGFβ, Wnt and Notch (Kuang et al. 2008). Previously, inhibition of TGFβ and Notch pathways has been shown to differentiate ERMS cells (Wang et al. 2010; Rossi et al. 2011; Raimondi et al. 2012). In contrast, we observed increased expression of pathway components in the more differentiated, hedgehog inhibited cells (Notch: data not shown). Activation of canonical Wnt signaling promotes muscle differentiation (Kuang et al. 2008) and hedgehog signaling has been reported to be antagonistic to the Wnt pathway (Roma et al. 2012). Accordingly, we observed increased expression of Wnt pathway components in hedgehog-inhibited ERMS cells. ERMS pro-differentiation therapies are being actively investigated for clinical benefit (Saab et al. 2011). Our data indicates the presence of novel negative feedback mechanisms between key developmental pathways that could control ERMS differentiation and consequently invasiveness.

A stem cell-focused qRT-PCR screen to identify downstream mediators of the hedgehog pathway led to identification of NANOG. NANOG is a homeodomain-containing transcription factor essential for derivation of ES cells, formation of primordial germ cells, establishing pluripotency (Theunissen and Silva 2011) and its increased expression has been noted in many cancer entities (Wang et al. 2013). NANOG has been characterized as a GLI target gene using chromatin immunoprecipitation assays and loss-of-function promoter reporter analyses in neural stem cells and medulloblastoma neurospheres (Po et al. 2010). Our data shows that NANOG behaves as a GLI1 target gene also in ERMS. We observed increased expression of NANOG in ERMS hedgehog activated model systems (sphere cultures and xenografts). Additionally we

detected significant positive correlation in mRNA expression of NANOG and GLI1 in ERMS patient samples, similar to previous observations in medulloblastoma (Po et al. 2010). Crucially, expression of GLI1 and NANOG proteins was observed only in a subpopulation of ERMS cells, highlighting the heterogeneous nature of hedgehog pathway activity in ERMS.

The role of NANOG in self-renewal and tumor initiation has been largely elucidated in adult solid tumors such as glioblastoma, prostate and colorectal cancer (Wang et al. 2013). The present study is the first to confirm that NANOG is functionally important in mediating "stemness" in a sarcoma. Alterations in NANOG expression led to changes in ERMS sphere initiation and importantly NANOG over-expression could completely rescue the decreased sphere forming ability observed in hedgehog-inhibited cells, indicating that it can also be epistatic to hedgehog pathway. Interestingly, although it was possible to generate stable NANOG-knockdown cells with partial protein reduction, stable over-expression was not tolerated by adherent ERMS cells. This indicates that NANOG expression is tightly controlled and maintained at a certain threshold. We noted that NANOG could provide positive feedback into the hedgehog pathway by modulating GLI1 expression as previously reported in glioblastoma-initiating cells (Zbinden et al. 2010). To evaluate the function of NANOG independent of hedgehog pathway activity we generated phenotypic rescue lines where NANOG expression was downregulated in the presence of GLI1 over-expression. We observed a complete rescue of sphere renewal capacity *in vitro* and a significant reduction in tumor growth rate *in vivo* implying that NANOG is a key mediator of hedgehog-driven CIC properties in ERMS. Furthermore it has been reported that NANOG is capable of inhibiting skeletal muscle differentiation by reducing MyoD transcriptional activity (Lang et al. 2009) and therefore its expression could have an impact also on ERMS differentiation status.

We also investigated the impact of hedgehog pathway modulation on other previously reported ERMS CIC markers, such as CD133, FGFR3 and MYF5 (Hirotsu et al. 2009; Walter et al. 2011; Ignatius et al. 2012). Although CD133 expressing cells are enriched in ERMS sphere cultures (Walter et al. 2011) we could not find evidence for positive regulation of CD133 expression by the

hedgehog pathway (data not shown). On the contrary, the expression of CD133 was highest in the SMO inhibited ERMS cells (data not shown). Also it has been reported that CD133 expression in ERMS cells increased upon *in vitro* culturing (Sana et al. 2011), unlike the effect observed on hedgehog pathway activity status *ex vivo* (this study and (Gerber et al. 2007)). $FGFR3^{+}$ cells from ERMS cell lines were shown to have increased tumorigenic potential (Hirotsu et al. 2009). In this study we noted FGFR3 expression to be positively regulated by hedgehog pathway in RD cells and negatively regulated in RH36 cells (data not shown). Therefore FGFR3 could mark active hedgehog phenotype depending on ERMS cell context. MYF5 has been identified as a component of the ERMS signature from transgenic mouse models and also marks the CIC compartment in the RAS-activated zebrafish model of ERMS (Langenau et al. 2007; Rubin et al. 2011; Ignatius et al. 2012). It has been shown to be a hedgehog target gene during myogenesis (Anderson et al. 2012). Although MYF5 mRNA expression level was reported to be higher in ERMS patient samples with high GLI1 mRNA expression (Pressey et al. 2011), we did not find a correlation in our cohort of patients which could be due to the small sample size. Importantly however, we could not detect MYF5 expression in ERMS cells lines used in this study implying that it may not be the factor responsible for hedgehog-mediated stemness in our human ERMS cancer models. Therefore, at present, the expression of GLI1 and NANOG alone could be used as a reliable indicator of hedgehog-driven CIC phenotype.

Additionally the GLI1-$NANOG^{high}$ phenotype is, as of yet, the most developmentally primitive to be described in ERMS. The expressions of transcription factors important for the development of neural crest-derived mesenchymal and neural tissues, namely PAX6, PITX2 and LMX1B (Hsieh et al. 2002; Gage et al. 2005; Liu and Johnson 2010), were positively regulated by the hedgehog pathway in both ERMS cell lines studied; while pathways that maintain a more myogenic (early or late) phenotype were downregulated. Therefore GLI1-$NANOG^{high}$ ERMS cells could possess a pre-myogenic multipotent phenotype which could be reminiscent of neural crest or non-myogenic origin for ERMS. This is concordant with recent observations in hedgehog-activated mouse models

wherein ERMS 'cell of origin' was determined to be from either pre-somitic or non-muscle mesenchyme (Nitzki et al. 2011; Hatley et al. 2012; Rajurkar et al. 2013). The phenotype of ERMS cells expressing the other CIC markers is possibly restricted to the skeletal muscle lineage. $FGFR3^{+}$ ERMS cells were reported to show increased expression of quiescent muscle stem cell markers CD34 and PAX3 (Hirotsu et al. 2009). MYF5 is a marker for activated muscle stem cells and MYF^{high} ERMS CIC compartment consequently showed increased expression of some muscle stem cell genes (Ignatius et al. 2012). CD133 could be a marker for pro-myogenic precursors since $CD133^{+}$ cells have been used to regenerate muscle in dystrophic muscle mouse models (Kuang et al. 2008), $CD133^{+}$ ERMS cells are reported to be myogenically primitive (Pressey et al. 2013) and CD133 expression was found to be highest in ERMS cells with a more myogenic rather than neural crest background (this study; data not shown). It is possible that different ERMS CIC phenotypes with varying differentiation potentials are concomitantly present within tumors. The hierarchical relationship between these compartments and their relative importance in ERMS tumorigenicity is yet to be determined and warrants further research.

In the present study we provide evidence that the functionally important GLI1-NANOG axis is also a clinically relevant ERMS CIC phenotype. Previously PTCH1 mRNA expression in ERMS patients was shown to predict poor outcome (Zibat et al. 2010), which could not be substantiated by an independent study (Pressey et al. 2011). Although PTCH1 mRNA expression correlates significantly with that of GLI1 mRNA (this study and (Zibat et al. 2010; Pressey et al. 2011)), mechanistically PTCH1 provides negative feedback cues into the hedgehog pathway obscuring the final outcome on cellular self-renewal. Hence PTCH1 expression status may not be a reliable predictor of prognosis. Therefore we propose evaluating expression of NANOG protein, a functionally important downstream target, along with GLI1 to refine the identification of hedgehog-active self renewing compartments within ERMS tumors. A previous study could not find prognostic significance for GLI1 mRNA expression in ERMS patients (Pressey et al. 2011). This discrepancy could be due to the lack of concordance between mRNA and protein expression.

Additionally the quantitative estimation of mRNA levels in bulk tumor samples precludes evaluation of tumor heterogeneity and also leads to patient stratification based on arbitrary gradient expression levels that are prone to sampling bias. In this study patients were distinguished based on presence or absence of protein expressing tumor cells irrespective of expression levels and analysis performed in a blinded manner to avoid any form of subjective bias. It is however important to note that we could not confirm the co-localization of the proteins in patient samples since serial sections were not available from the TMA. Interestingly we observed heterogeneous expression of GLI1 and NANOG also within ARMS patient tumors but it did not have prognostic significance (data not shown). Therefore the GLI1-NANOG axis could be important specifically for ERMS patient stratification and further highlights the biological disparity between the two RMS variants. Previously we reported that ERMS patients with $CD133^{high}$ expression have poor overall survival (Walter et al. 2011), but the regulation and functional role of CD133 protein is unclear: hence hindering its use as a biomarker. At present the impact of FGFR3 or MYF5 expression on ERMS patient prognosis is unknown. To our knowledge this is the first report in sarcoma showing that evaluation of intra-tumoral heterogeneity defined by a CIC pathway could help identify high-risk patients.

Although strategies to evaluate and target self renewing compartments are being actively explored in many adult tumor entities (Takebe et al. 2011; Kreso et al. 2014), research on the signaling mechanisms that modulate CICs in pediatric cancers is still in its early stages. Using various ERMS cancer models, our study is the first to evaluate the addiction to a ‘targetable’ developmental pathway - the hedgehog pathway - in the maintenance of the CIC compartment in a major pediatric sarcoma. It is possible that the hedgehog-active CIC phenotype may be a common feature in ERMS cancer since the oncogenic signaling pathways and mutational backgrounds documented in ERMS have been shown to have a positive influence on hedgehog signaling. For example key ERMS therapeutic targets, growth factor receptor tyrosine kinase signaling and PI3K-AKT;mTOR-S6K signaling positively interact with the hedgehog pathway (Stecca and Ruiz 2010;

Wang et al. 2012b; Sokolowski et al. 2013). RAS signaling, which is the most commonly mutated pathway in ERMS (Chen et al. 2013; Shern et al. 2014), is known to increase GLI activity (Stecca et al. 2007). Disruption of the p53 pathway has been documented in sporadic ERMS tumors (Chen et al. 2013; Shern et al. 2014) and in one study cohort 59% of ERMS patients had a mutant p53 signature (Rubin et al. 2011). Interestingly, active p53 has been known to repress NANOG expression and specifically loss of p53 has been shown to increase GLI-NANOG axis signaling strength in stem cells and CICs of neural origin (Po et al. 2010; Zbinden et al. 2010; Wang et al. 2013). The cell lines used in this study for functional analyses also contain the aforementioned common genetic backgrounds (RD: $NRAS^{Q61H}$; $p53^{R248V}$ and RH36: $HRAS^{Q61K}$). Therefore hedgehog pathway targeting could be of broad interest in sporadic ERMS.

Our data presents hedgehog inhibition specifically as an anti-CIC strategy. CIC-targeting requires updating the current clinical trial management protocols since the biomarkers and end points used to estimate treatment efficacy would be conceptually altered (Vermeulen et al. 2012; Schott et al. 2013; Satheesha and Schäfer 2014). Accordingly we noted that the effect of hedgehog pathway modulation on ERMS pathology was not due to changes in cell cycle, cell viability or proliferation implying that tumor regression may be an inappropriate end point to estimate treatment efficacy. Although our data suggests SMO as a viable targeting option the downstream inhibition of the pathway could avoid emergence of cross talks converging on the GLI-code and resistance mechanisms (Takebe et al. 2011; Amakye et al. 2013). A combinatorial approach using hedgehog-targeted therapy along with bulk-reducing or other pro-terminal differentiation strategies may be more promising in reducing relapse and metastatic progression since the non-CIC compartments that make up the heterogeneous ERMS cellular milieu probably also have important roles to play in tumor progression (this study and (Ignatius et al. 2012)). Our report is particularly relevant since a SMO inhibitor is already in clinical trial for progressive RMS however as a single agent (clinicaltrials.gov; NCT01125800). Severe toxicities are noticed with current generic treatment modalities for ERMS and reducing therapy burden leads to increase in relapse rates

(Stevens 2005; Jenney et al. 2014). Our data shows that combination therapy could allow use of lowered drug doses since inhibiting the hedgehog pathway in ERMS can increase sensitivity to generic drugs; therefore possibly maintaining treatment efficacy but with reduced morbidity.

Patients with progressive, recurrent or metastatic ERMS have very low survival rate. Therefore there is a clear need to select treatment strategies that are specifically based on principles of ERMS etiology. To this end it is important to consider the hierarchical ERMS tumor organization along with the mutational background since evaluating hedgehog-driven CIC markers had a significant impact on ERMS patient risk stratification, which has not yet been possible with mutational status or signature (Rubin et al. 2011; Chen et al. 2013). Our study highlights that phenotypic and functional tumor heterogeneity could have significance for clinical management of ERMS patients and suggests hedgehog inhibition as a treatment strategy aimed at reducing the rate of relapse for a long term cure.

Materials and Methods

Cell culture and treatments

Human ERMS cell lines RD (purchased from ATCC) and RH36 (kindly provided by Peter Houghton, St. Jude's Children's Hospital, USA) were maintained at 37°C in a humid atmosphere with 5% CO_2 and routinely cultured in DMEM media supplemented with 10% fetal bovine serum (FBS), 2mM L-glutamine and 100U/ml penicillin-streptomycin. Sphere cultures were maintained as previously described (Walter et al. 2011). Sphere dissociation was carried out using Accutase (Sigma-Aldrich). Trypan-Blue staining (0.4%; Sigma-Aldrich) was used to estimate live cell numbers in all experiments. For sphere initiation and renewal studies, equal numbers of cells were plated at clonal density in Ultra-Low attachment plates (Corning) or in non-treated polystyrene petri plates (BD Biosciences). SMO inhibitors GDC-0449 and LDE-225 (both purchased from Selleck Chemicals), GLI inhibitor GANT61 (Tocris Biosciences), and GLI activator SAG1.3 (Calbiochem) were used at indicated concentrations to modulate the hedgehog pathway. For IC_{50} measurements of generic chemotherapeutic drugs Irinotecan (SN-38; Sigma-Aldrich) and Doxorubicin (Sandoz), cells were plated in quadruplicate in standard 96-well plates and treated with five-step serial dilutions of the drugs for 72 hours in 10% FBS media. In all experiments DMSO (Sigma-Aldrich) was used as vehicle control except SAG1.3 which was diluted in water.

Transfection, Transduction and generation of stable cell lines

Sphere cells were transfected with Silencer® select siRNAs (Ambion, Life technologies) against GLI1 (s5816), SUFU (s28520) or scrambled control (Silencer® Negative Control# 2) using Lipofectamine® RNAiMAX (Invitrogen) following manufacturer's instructions at a final concentration of 10nM. Cells were used for sphere initiation 24 hours post transfection. The plasmids pCMV6-Entry (C-terminal Myc and DDK Tagged) referred to as pCMV-Empty, GLI1-transcript variant 1- Myc-DDK (referred to as pCMV-GLI1), SUFU-Myc-DDK tagged (referred to as pCMV-SUFU) were purchased from Origene. The plasmids pEGIP (26777; referred to as pE1F),

and pSin-EF-Nanog-Pur (16578; over-expressing NANOG) were purchased from Addgene. All plasmid transfections were carried out using Lipofectamine® 2000 (Invitrogen) on 80-90% confluent culture following manufacturer's instructions. Transduction of MISSION® TRC1.5 shRNA lentiviral particles (Sigma-Aldrich) - control (pLKO.1; SHC001V), TRCN0000014364 (shSMO) and TRCN0000004885 (shNANOG) - was carried out at a 'multiplicity of infection' of 1.5 on 70% confluent culture in 1µg/ml Polybrene (Sigma-Aldrich) supplemented media. For stable cell line generation, plasmid transfected cells were continuously cultured in media supplemented 500 µg/ml G-418 antibiotic for 3-4 weeks and thereafter 100 µg/ml antibiotic media was routinely used; viral transduced cells were continuously cultured in media supplemented with 1µg/ml Puromycin (Invivogen) for 10 days and thereafter 0.3 µg/ml antibiotic media was routinely used. Stable pCMV-Empty and pCMV-GLI1 cells were transduced with pLKO.1 and shNANOG viral particles and selected with Puromycin as described above to generate stable phenotype rescue system.

Trans-well migration and invasion assays

Migration assays were carried out using BD Falcon™ cell culture inserts (BD Biosciences; 8µm pore size) for 24-well format. For invasion assays, BioCoat™ matrigel-coated inserts (BD Biosciences) or the inserts coated manually with gelatin were used. Cells were maintained in 1% FBS media for 4 hours prior to plating. The cells were allowed to migrate over 24 hours or invade over 48 hours towards 10% FBS medium. Membrane with migrated or invaded cells was fixed with 4% paraformaldehyde (PFA; Carl Roth) and stained with 0.05% Crystal Violet. Cells were visualized using Olympus CX41microscope and images were captured from 5 viewing fields across the membrane using INFINITY software (version 6, Lumenera). Cells were counted manually using ImageJ software (version 1.47).

Orthotopic xenograft generation

RD ($3x10^5$cells/mouse) or RH36 ($2.5x10^5$cells/mouse) were injected into the femoral muscles of one leg of NOD.CB17-*Prkdc*^{scid} mice (NOD/SCID; The Jackson Laboratory). Once tumor was palpable size was determined every 4 days by measuring two diameters (d_1 and d_2) in right angles of both legs with a Vernier caliper .Tumor volumes were calculated using the following formula: $V=[4/3 \times \pi \times 1/2(d_1+d_2)]_{\text{injected leg}} -[4/3 \times \pi \times 1/2(d_1+d_2)]_{\text{control leg}}$

Freshly isolated xenografts were stored in RNAlater solution (Ambion) for RNA extraction, snap frozen in liquid N_2 for protein extraction or fixed in 4% PFA for imunohistochemistry. The experiments were performed following institutional guidelines and were approved by the veterinary office of the Canton Zurich.

Quantitative Real-Time PCR

Normal human skeletal muscle pooled RNA lysate, referred to as AdSkM_P, from five adults (R1234171_P) and individual RNA lysates from three fetal donors (R1244171; Lot # A503105, B505186, A508111) were purchased from Amsbio. The expression data from the fetal samples was pooled for analysis (referred to as FeSkM_P). Total RNA was extracted using RNeasy Mini Kit (Qiagen) following manufacturer's recommendations. Normal murine muscle RNA was extracted from femoral muscle of NOD/SCID mice.

Genomic DNA contamination was removed using RNase-free DNase (Qiagen). RNA concentration and purity was evaluated using NanoDrop ND-1000. cDNA synthesis was carried out using High-Capacity cDNA Reverse Transcription kit (Life Technologies) according to the manufacturer's instructions. Quantitative Real-Time PCR (qRT-PCR) was performed using commercially available mastermix and TaqMan® Gene Expression Assays (Life Technologies; assay IDs are listed in the Supplemental Table 1) at standard conditions on an ABI 7900 HT Real-Time PCR machine and the data was analyzed with SDS software (Version 2.2; Applied Biosystems, Life Technologies). Absolute and relative expression levels of the target genes were calculated using the □□C_t method. C_t values were normalized to mean expression of housekeeping genes: HMBS (unless otherwise

specified) and Gapdh for murine gene expression. For screening, RT^2 Profiler PCR Arrays [Stem Cell Signaling (PAHS-047ZE) and Stem Cell Transcription Factors (PAHS-501ZE)], all associated reagents for cDNA synthesis and qRT-PCR reactions were purchased from Qiagen. The reactions were set up according to manufacturer's instruction. Each plate contained biological duplicates of cDNA samples from hedgehog-modulated and the respective control cells to avoid cross plate analysis. Data analysis was performed using the RT^2 Profiler PCR Array Analysis web-based software (version 3.5; http://pcrdataanalysis.sabiosciences.com/pcr/arrayanalysis.php).

Absolute RNA expression ($2^{-\Delta Ct}$; patient samples) and relative fold change (PCR array) were used for non-supervised hierarchical clustering; analyzed by dChip (Build: 2010; http://www.hsph.harvard.edu/cli/complab/dchip/)

Western Blotting, Immunofluorescence and Immunohistochemistry

Total protein was extracted using RIPA buffer (50 mM Tris-Cl, pH 6.8, 100 mM NaCl, 1% Triton X-100, 0.1% SDS) supplemented with Complete Mini Protease Inhibitor Cocktail (Roche). Protein concentration was measured with Pierce® BCA protein Assay Kit (Thermo Scientific). Proteins were separated using NuPAGE gradient SDS-PAGE pre-cast gels (Life Technologies) and transferred for Western Blotting (XCell II™ Blot Module; Life Technologies). Specific proteins were labelled and identified by chemiluminescence using Amersham ECL Detection reagent (GE Healthcare) or SuperSignal West Femto Maximum Sensitivity Substrate (Thermo Scientific). For immunofluorescence, cells were grown in BD Falcon™ culture slides, fixed with 4% PFA and incubated over night at 4°C with primary antibodies. Coverslips were positioned using VECTASHIELD® mounting media containing DAPI (Vector Labs). Cells were visualized using Leica 6000 DM epifluorescence microscope and images were captured using OpenLab software (version 3, Improvision). Cells stained only with conjugated-secondary antibodies were used as controls. Cell count estimation and image analysis was performed using ImageJ. Immunohistochemistry was performed on 3 µm thick sections from blocks of formalin-fixed,

paraffin-embedded tissue at the Department of Pathology (University of Zurich) as previously described (Wachtel et al. 2006). The procedure for detecting GLI1 and NANOG expression was optimized by Sophistolab AG (Eglisau, Switzerland) using an array containing a series of normal tissue and cancer tissues as controls. In brief, immunohistochemistry was performed according to manufacturer's guidelines on Leica BondMax instruments using Refine HRP-Kits (Leica DS9800) and buffer-solutions from Leica Microsystems Newcastle, Ltd. Slides were visualized using Zeiss Axioskop microscope. Images were captured and analyzed using Cell^{B} software (version 3.4; Olympus Soft Imaging Solutions GmbH). All the antibodies for the abovementioned procedures are listed in Supplemental Table 2.

Patient tissue samples

All patient tissue specimens used for RNA extraction in the study were obtained from the Swiss Pediatric Oncology Group (SPOG) Tumor Bank except ZH_ERMS which was obtained from Department of Pathology (University Hospital Zurich). The use of SPOG Tumor Bank tissue samples for cancer research purposes was approved by the Ethical Review Board of Zurich (Ref. No. StV-18/02). Written informed consent was obtained from each patient by the hospital that provided the tissue samples. The Tissue Microarray (TMA) used in this study included multiple tumor cores from 149 RMS patients (116 ERMS and 33 ARMS) enrolled in the German soft-tissue sarcoma group (CWS) studies -81, -86, -91 and -96 has been previously described (Wachtel et al. 2006).

TMA scoring and data analysis

TMA was evaluated in collaboration with a senior pathologist (P.B.). A minimum of two desmin positive intact cores were required for the patient to be included in the analysis. At least three stained cells were required to label a patient as positive. Tumors from 91 ERMS and 23 ARMS patients provided reliable GLI1 and NANOG expression status. Clinical data was maintained and

analysed independently by CWS study member (S.F.). Statistical analysis was performed using SPSS software (version 21, IBM) based on all data available up to the cut-off date, 05.04.2013.The Kaplan-Meier method was used for the estimation of overall survival (OS) and event-free survival (EFS). OS was defined as the time between date of diagnosis and death from any cause. EFS was defined as the time from diagnosis to first event (disease recurrence, progression or death). Differences in survival rates were analyzed using the log-rank test.

Statistical analysis

Data was analyzed using GraphPad Prism (version 4.03). Significance was calculated using Student's t-test (unpaired, two-tailed). $P<0.05$ was considered significant.

Acknowledgements

We deeply appreciate the Swiss Pediatric Oncology Group (SPOG) for providing ERMS patient tumor samples. We would like to thank the German Soft tissue sarcoma study group (CWS) for providing the TMA sections and performing the clinical data analysis. We are also indebted to Silvia Behnke (Sophistolab AG) and the technicians at the Institute of Surgical Pathology (University Hospital Zurich) for their excellent service. The work was supported by grants from Swiss National Science Fund (31003A-138460), Sciex (F-80016-02-01) and Cancer League Canton Zurich.

References

Amakye D, Jagani Z, Dorsch M. 2013. Unraveling the therapeutic potential of the Hedgehog pathway in cancer. *Nat Med* **19**: 1410-1422.

Anderson C, Williams VC, Moyon B, Daubas P, Tajbakhsh S, Buckingham ME, Shiroishi T, Hughes SM, Borycki AG. 2012. Sonic hedgehog acts cell-autonomously on muscle precursor cells to generate limb muscle diversity. *Genes Dev* **26**: 2103-2117.

Chen X, Stewart E, Shelat AA, Qu C, Bahrami A, Hatley M, Wu G, Bradley C, McEvoy J, Pappo A et al. 2013. Targeting oxidative stress in embryonal rhabdomyosarcoma. *Cancer Cell* **24**: 710-724.

Gage PJ, Rhoades W, Prucka SK, Hjalt T. 2005. Fate maps of neural crest and mesoderm in the mammalian eye. *Invest Ophthalmol Vis Sci* **46**: 4200-4208.

Gerber AN, Wilson CW, Li YJ, Chuang PT. 2007. The hedgehog regulated oncogenes Gli1 and Gli2 block myoblast differentiation by inhibiting MyoD-mediated transcriptional activation. *Oncogene* **26**: 1122-1136.

Hatley ME, Tang W, Garcia MR, Finkelstein D, Millay DP, Liu N, Graff J, Galindo RL, Olson EN. 2012. A mouse model of rhabdomyosarcoma originating from the adipocyte lineage. *Cancer Cell* **22**: 536-546.

Hawkins DS, Gupta AA, Rudzinski ER. 2014. What is new in the biology and treatment of pediatric rhabdomyosarcoma? *Curr Opin Pediatr* **26**: 50-56.

Hawkins DS, Spunt SL, Skapek SX. 2013. Children's Oncology Group's 2013 blueprint for research: Soft tissue sarcomas. *Pediatr Blood Cancer* **60**: 1001-1008.

Hirotsu M, Setoguchi T, Matsunoshita Y, Sasaki H, Nagao H, Gao H, Sugimura K, Komiya S. 2009. Tumour formation by single fibroblast growth factor receptor 3-positive rhabdomyosarcoma-initiating cells. *Br J Cancer* **101**: 2030-2037.

Hsieh YW, Zhang XM, Lin E, Oliver G, Yang XJ. 2002. The homeobox gene Six3 is a potential regulator of anterior segment formation in the chick eye. *Dev Biol* **248**: 265-280.

Ignatius MS, Chen E, Elpek NM, Fuller AZ, Tenente IM, Clagg R, Liu S, Blackburn JS, Linardic CM, Rosenberg AE et al. 2012. In vivo imaging of tumor-propagating cells, regional tumor heterogeneity, and dynamic cell movements in embryonal rhabdomyosarcoma. *Cancer Cell* **21**: 680-693.

Jenney M, Oberlin O, Audry G, Stevens MC, Rey A, Merks JH, Kelsey A, Gallego S, Haie-Meder C, Martelli H. 2014. Conservative approach in localised rhabdomyosarcoma of the bladder and prostate: Results from International Society of Paediatric Oncology (SIOP) studies: Malignant mesenchymal tumour (MMT) 84, 89 and 95. *Pediatr Blood Cancer* **61**: 217-222.

Katagiri S, Tauchi T, Okabe S, Minami Y, Kimura S, Maekawa T, Naoe T, Ohyashiki K. 2013. Combination of ponatinib with Hedgehog antagonist vismodegib for therapy-resistant BCR-ABL1-positive leukemia. *Clin Cancer Res* **19**: 1422-1432.

Kreso A, van Galen P, Pedley NM, Lima-Fernandes E, Frelin C, Davis T, Cao L, Baiazitov R, Du W, Sydorenko N et al. 2014. Self-renewal as a therapeutic target in human colorectal cancer. *Nat Med* **20**: 29-36.

Kuang S, Gillespie MA, Rudnicki MA. 2008. Niche regulation of muscle satellite cell self-renewal and differentiation. *Cell Stem Cell* **2**: 22-31.

Lang KC, Lin IH, Teng HF, Huang YC, Li CL, Tang KT, Chen SL. 2009. Simultaneous overexpression of Oct4 and Nanog abrogates terminal myogenesis. *Am J Physiol Cell Physiol* **297**: C43-54.

Langenau DM, Keefe MD, Storer NY, Guyon JR, Kutok JL, Le X, Goessling W, Neuberg DS, Kunkel LM, Zon LI. 2007. Effects of RAS on the genesis of embryonal rhabdomyosarcoma. *Genes Dev* **21**: 1382-1395.

Lee J, Kotliarova S, Kotliarov Y, Li A, Su Q, Donin NM, Pastorino S, Purow BW, Christopher N, Zhang W et al. 2006. Tumor stem cells derived from glioblastomas cultured in bFGF and EGF more closely mirror the phenotype and genotype of primary tumors than do serum-cultured cell lines. *Cancer Cell* **9**: 391-403.

Liu P, Johnson RL. 2010. Lmx1b is required for murine trabecular meshwork formation and for maintenance of corneal transparency. *Dev Dyn* **239**: 2161-2171.

Malempati S, Hawkins DS. 2012. Rhabdomyosarcoma: review of the Children's Oncology Group (COG) Soft-Tissue Sarcoma Committee experience and rationale for current COG studies. *Pediatr Blood Cancer* **59**: 5-10.

Merchant AA, Matsui W. 2010. Targeting Hedgehog--a cancer stem cell pathway. *Clin Cancer Res* **16**: 3130-3140.

Nitzki F, Zibat A, Frommhold A, Schneider A, Schulz-Schaeffer W, Braun T, Hahn H. 2011. Uncommitted precursor cells might contribute to increased incidence of embryonal rhabdomyosarcoma in heterozygous Patched1-mutant mice. *Oncogene* **30**: 4428-4436.

Norris RE, Adamson PC. 2012. Challenges and opportunities in childhood cancer drug development. *Nat Rev Cancer* **12**: 776-782.

Paulson V, Chandler G, Rakheja D, Galindo RL, Wilson K, Amatruda JF, Cameron S. 2011. High-resolution array CGH identifies common mechanisms that drive embryonal rhabdomyosarcoma pathogenesis. *Genes Chromosomes Cancer* **50**: 397-408.

Peacock CD, Wang Q, Gesell GS, Corcoran-Schwartz IM, Jones E, Kim J, Devereux WL, Rhodes JT, Huff CA, Beachy PA et al. 2007. Hedgehog signaling maintains a tumor stem cell compartment in multiple myeloma. *Proc Natl Acad Sci U S A* **104**: 4048-4053.

Po A, Ferretti E, Miele E, De Smaele E, Paganelli A, Canettieri G, Coni S, Di Marcotullio L, Biffoni M, Massimi L et al. 2010. Hedgehog controls neural stem cells through p53-independent regulation of Nanog. *EMBO J* **29**: 2646-2658.

Pressey JG, Anderson JR, Crossman DK, Lynch JC, Barr FG. 2011. Hedgehog pathway activity in pediatric embryonal rhabdomyosarcoma and undifferentiated sarcoma: a report from the Children's Oncology Group. *Pediatr Blood Cancer* **57**: 930-938.

Pressey JG, Haas MC, Pressey CS, Kelly VM, Parker JN, Gillespie GY, Friedman GK. 2013. CD133 marks a myogenically primitive subpopulation in rhabdomyosarcoma cell lines that are relatively chemoresistant but sensitive to mutant HSV. *Pediatr Blood Cancer* **60**: 45-52.

Raimondi L, Ciarapica R, De Salvo M, Verginelli F, Gueguen M, Martini C, De Sio L, Cortese G, Locatelli M, Dang TP et al. 2012. Inhibition of Notch3 signalling induces rhabdomyosarcoma cell differentiation promoting p38 phosphorylation and p21(Cip1) expression and hampers tumour cell growth in vitro and in vivo. *Cell Death Differ* **19**: 871-881.

Rajurkar M, Huang H, Cotton JL, Brooks JK, Sicklick J, McMahon AP, Mao J. 2013. Distinct cellular origin and genetic requirement of Hedgehog-Gli in postnatal rhabdomyosarcoma genesis. *Oncogene*.

Read TA, Fogarty MP, Markant SL, McLendon RE, Wei Z, Ellison DW, Febbo PG, Wechsler-Reya RJ. 2009. Identification of CD15 as a marker for tumor-propagating cells in a mouse model of medulloblastoma. *Cancer Cell* **15**: 135-147.

Roma J, Almazan-Moga A, Sanchez de Toledo J, Gallego S. 2012. Notch, wnt, and hedgehog pathways in rhabdomyosarcoma: from single pathways to an integrated network. *Sarcoma* **2012**: 695603.

Rossi S, Stoppani E, Puri PL, Fanzani A. 2011. Differentiation of human rhabdomyosarcoma RD cells is regulated by reciprocal, functional interactions between myostatin, p38 and extracellular regulated kinase signalling pathways. *Eur J Cancer* **47**: 1095-1105.

Rubin BP, Nishijo K, Chen HI, Yi X, Schuetze DP, Pal R, Prajapati SI, Abraham J, Arenkiel BR, Chen QR et al. 2011. Evidence for an unanticipated relationship between undifferentiated pleomorphic sarcoma and embryonal rhabdomyosarcoma. *Cancer Cell* **19**: 177-191.

Ruiz i Altaba A. 2011. Hedgehog signaling and the Gli code in stem cells, cancer, and metastases. *Sci Signal* **4**: pt9.

Saab R, Spunt SL, Skapek SX. 2011. Myogenesis and rhabdomyosarcoma the Jekyll and Hyde of skeletal muscle. *Curr Top Dev Biol* **94**: 197-234.

Sana J, Zambo I, Skoda J, Neradil J, Chlapek P, Hermanova M, Mudry P, Vasikova A, Zitterbart K, Hampl A et al. 2011. CD133 expression and identification of CD133/nestin positive cells in rhabdomyosarcomas and rhabdomyosarcoma cell lines. *Anal Cell Pathol (Amst)* **34**: 303-318.

Satheesha S, Schäfer BW. 2014. Cancer Stem Cells in Pediatric Sarcomas. in *Stem Cells and Cancer Stem Cells: Therapeutic Applications in Disease and Injury* (ed. MA Hayat), pp. 111-126. Springer, Dordrecht.

Schafer BW, Niggli F. 2010. Multidisciplinary management of childhood sarcoma: time to expand. *Expert Rev Anticancer Ther* **10**: 1163-1166.

Schott AF, Landis MD, Dontu G, Griffith KA, Layman RM, Krop I, Paskett LA, Wong H, Dobrolecki LE, Lewis MT et al. 2013. Preclinical and clinical studies of gamma secretase inhibitors with docetaxel on human breast tumors. *Clin Cancer Res* **19**: 1512-1524.

Shern JF, Chen L, Chmielecki J, Wei JS, Patidar R, Rosenberg M, Ambrogio L, Auclair D, Wang J, Song YK et al. 2014. Comprehensive Genomic Analysis of Rhabdomyosarcoma Reveals a Landscape of Alterations Affecting a Common Genetic Axis in Fusion-Positive and Fusion-Negative Tumors. *Cancer Discov*.

Sokolowski E, Turina CB, Kikuchi K, Langenau DM, Keller C. 2013. Proof-of-concept rare cancers in drug development: the case for rhabdomyosarcoma. *Oncogene*.

Stecca B, Mas C, Clement V, Zbinden M, Correa R, Piguet V, Beermann F, Ruiz IAA. 2007. Melanomas require HEDGEHOG-GLI signaling regulated by interactions between GLI1 and the RAS-MEK/AKT pathways. *Proc Natl Acad Sci U S A* **104**: 5895-5900.

Stecca B, Ruiz IAA. 2010. Context-dependent regulation of the GLI code in cancer by HEDGEHOG and non-HEDGEHOG signals. *J Mol Cell Biol* **2**: 84-95.

Stevens MC. 2005. Treatment for childhood rhabdomyosarcoma: the cost of cure. *Lancet Oncol* **6**: 77-84.

Takebe N, Harris PJ, Warren RQ, Ivy SP. 2011. Targeting cancer stem cells by inhibiting Wnt, Notch, and Hedgehog pathways. *Nat Rev Clin Oncol* **8**: 97-106.

Theunissen TW, Silva JC. 2011. Switching on pluripotency: a perspective on the biological requirement of Nanog. *Philos Trans R Soc Lond B Biol Sci* **366**: 2222-2229.

Vermeulen L, de Sousa e Melo F, Richel DJ, Medema JP. 2012. The developing cancer stem-cell model: clinical challenges and opportunities. *Lancet Oncol* **13**: e83-89.

Vidal SJ, Rodriguez-Bravo V, Galsky M, Cordon-Cardo C, Domingo-Domenech J. 2013. Targeting cancer stem cells to suppress acquired chemotherapy resistance. *Oncogene*.

Voronova A, Coyne E, Al Madhoun A, Fair JV, Bosiljcic N, St-Louis C, Li G, Thurig S, Wallace VA, Wiper-Bergeron N et al. 2013. Hedgehog signaling regulates MyoD expression and activity. *J Biol Chem* **288**: 4389-4404.

Wachtel M, Runge T, Leuschner I, Stegmaier S, Koscielniak E, Treuner J, Odermatt B, Behnke S, Niggli FK, Schafer BW. 2006. Subtype and prognostic classification of rhabdomyosarcoma by immunohistochemistry. *J Clin Oncol* **24**: 816-822.

Walter D, Satheesha S, Albrecht P, Bornhauser BC, D'Alessandro V, Oesch SM, Rehrauer H, Leuschner I, Koscielniak E, Gengler C et al. 2011. CD133 positive embryonal rhabdomyosarcoma stem-like cell population is enriched in rhabdospheres. *PLoS One* **6**: e19506.

Wang ML, Chiou SH, Wu CW. 2013. Targeting cancer stem cells: emerging role of Nanog transcription factor. *Onco Targets Ther* **6**: 1207-1220.

Wang S, Guo L, Dong L, Li S, Zhang J, Sun M. 2010. TGF-beta1 signal pathway may contribute to rhabdomyosarcoma development by inhibiting differentiation. *Cancer Sci* **101**: 1108-1116.

Wang X, Venugopal C, Manoranjan B, McFarlane N, O'Farrell E, Nolte S, Gunnarsson T, Hollenberg R, Kwiecien J, Northcott P et al. 2012a. Sonic hedgehog regulates Bmi1 in human medulloblastoma brain tumor-initiating cells. *Oncogene* **31**: 187-199.

Wang Y, Ding Q, Yen CJ, Xia W, Izzo JG, Lang JY, Li CW, Hsu JL, Miller SA, Wang X et al. 2012b. The crosstalk of mTOR/S6K1 and Hedgehog pathways. *Cancer Cell* **21**: 374-387.

Ward RJ, Lee L, Graham K, Satkunendran T, Yoshikawa K, Ling E, Harper L, Austin R, Nieuwenhuis E, Clarke ID et al. 2009. Multipotent CD15+ cancer stem cells in patched-1-deficient mouse medulloblastoma. *Cancer Res* **69**: 4682-4690.

Zbinden M, Duquet A, Lorente-Trigos A, Ngwabyt SN, Borges I, Ruiz i Altaba A. 2010. NANOG regulates glioma stem cells and is essential in vivo acting in a cross-functional network with GLI1 and p53. *EMBO J* **29**: 2659-2674.

Zhao C, Chen A, Jamieson CH, Fereshteh M, Abrahamsson A, Blum J, Kwon HY, Kim J, Chute JP, Rizzieri D et al. 2009. Hedgehog signalling is essential for maintenance of cancer stem cells in myeloid leukaemia. *Nature* **458**: 776-779.

Zibat A, Missiaglia E, Rosenberger A, Pritchard-Jones K, Shipley J, Hahn H, Fulda S. 2010. Activation of the hedgehog pathway confers a poor prognosis in embryonal and fusion gene-negative alveolar rhabdomyosarcoma. *Oncogene* **29**: 6323-6330.

Figure legends

Figure 1. Activation of hedgehog signaling increases self renewal and tumorigenicity of ERMS cells. (**A**) Left panel: Expression levels of hedgehog signaling components in RD spheres compared to adherent monolayer cultures by quantitative PCR (Log_2 scale; N=2-3). Right panel: Western Blot anaysis showing GLI1 protein expression in RD sphere and adherent cells. (**B**) Western Blot analysis of GLI1 and HHIP protein expression in ERMS xenografts. (**C**) Sphere initiation capacity of ERMS cells treated with hedgehog agonist SAG1.3 (500nM) every 48h (3 rounds) during primary sphere formation and thereafter plated for secondary sphere formation in normal sphere

media (N=2-3). (**D**) Sphere formation after siRNA mediated knockdown of SUFU (10nM) in RD sphere cells compared to scrambled control siRNA (N=2). (**E**) Sphere formation following 48 hours treatment of ERMS adherent cultures with SAG1.3 (N=4-5). (**F**) Western Blot analysis of indicated proteins in ERMS stable cell lines. Primary (1°) and secondary (2°) sphere formation measured in ERMS stable lines (**G**: RD; N=3 and **H**: RH36; N=2-3). (**I**) Tumor growth rate followed by caliper measurements of RD-based stable lines pCMV-Empty (N=6) and pCMV-GLI1 (N=5) injected orthotopically in NOD/SCID mice. (**J**) Tumor growth rate followed by caliper measurements of RH36-based stable lines pCMV-Empty (N=6) and pCMV-GLI1 (N=6) injected orthotopically in NOD/SCID mice. **P*<0.05; ***P*<0.01; ****P*<0.001. Data represent mean ± S.D. Each data point in the Scatter plots represents a technical replicate with the line drawn at the mean.

Figure 2. Inhibition of hedgehog signaling decreases self renewal and tumorigenicity of ERMS cells. (**A**) Sphere initiation capacity of RD cells treated with small-molecule inhibitors GDC-0449 or GANT61 every 48h (3 rounds) during primary sphere formation and further plated for secondary sphere formation in normal sphere media (N=2-3). **§** No viable cells were recovered for secondary sphere formation (**B**) Sphere formation measured following siRNA (10nM) mediated GLI1 knockdown in RD sphere cells (N=2). (**C**) Sphere formation ability of RD adherent cells after 48 hour treatment with hedgehog inhibitors (N=2-6). Tumor growth rate (**D**) and tumor weight (**E**) of RD cells pre-treated *in vitro* with GANT61 (3µM) (N=5 per condition). Western Blot analysis of indicated proteins in stable ERMS lines over-expressing tagged SUFU (**F**; Myc-DDK) and knockdown of SMO (**G**). Primary (1°) and secondary (2°) sphere formation measured in ERMS stable lines (**H**: N=2 per cell line; **I**: N=2-4 per cell line). Tumor growth kinetics of hedgehog inhibited pCMV-SUFU (**J**: RD; N=5 and **K**: RH36; N=6) and control pCMV-Empty (**J**: RD;N=5 and **K**: RH36; N=6) cells in NOD/SCID mice. Tumor growth kinetics of hedgehog inhibited shSMO (**L**: RD; N=3/7 and **M**: RH36; N=6/7) and control pLKO.1 (**L**: RD; N=7/7 and **M**: RH36; N=7/7) cells in NOD/SCID mice. **P*<0.05; ***P*<0.01; ****P*<0.001. Data represent mean ± S.D.

Figure 3. Cell autonomous ligand-based hedgehog pathway activation in ERMS. Relative RNA expression level of hedgehog ligands in ERMS sphere cells compared to adherent cells (**A**: RD, N=2; **B**: RH36, N=3). Absolute RNA expression level of hedgehog ligands in ERMS xenografts (**C**: RD; **D**: RH36; N=4 per cell line) and their respective *in vitro* cultured cells (N=3 per cell line) normalized to housekeeping gene *HMBS*. (**E**) Absolute RNA expression of hedgehog ligands normalized to geometric mean of *HMBS* and *GAPDH* in ERMS patients samples (N=8). Each data point represents a single patient and the line represents median expression level in the cohort. Species specific ligand RNA expression estimated in ERMS xenografts (**F**: RD; **G**: RH36; N=4-16). h - human; m - mouse. Data represent mean ± S.D.

Figure 4. Hedgehog signaling alters ERMS chemoresistance and cell motility. (**A**) Sphere initiation ability of RD cells treated for 48 hours with Irinotecan (N=3). (**B**) Sphere initiation ability of RD cells treated for 48 hours with Irinotecan alone or in combination with SMO inhibitor LDE-225 (N=2). (**C**) IC_{50} values of indicated conventional cytotoxic drugs estimated from WST-based cell viability assays for ERMS cells treated with 5-step drug dilutions (N=4-5 per cell line per drug). (**D** and **E**) Relative migration of RD cells across porous membrane filter towards a growth serum gradient over 48 hours (N=3; 5 fields counted per experiment). (**F** and **G**) Total number of RD cells that could invade through matrigel-coated porous membrane filter towards a growth serum gradient over 48 hours (N=3). *P<0.05, **P<0.01, ***P<0.001. Data represent mean ± S.D.

Figure 5. Hedgehog signaling alters the differentiation status of ERMS cells. (**A**) Representative images of RD cells stained for PAX7 and MYOGENIN expression. All images were taken at 400x magnification. Scale bar represents 20µm (**B** and **C**) Quantification of percentage of PAX7 or MYOGENIN positive RD cells normalized to DAPI stained nuclei counted per viewing field, using ImageJ (N=4). (**D** and **E**) Quantification of PAX7 or MYOGENIN positive RH36 cells (N=5). (**F**)

Non-supervised hierarchical clustering of common positively and negatively regulated genes by hedgehog pathway in ERMS cells. *P<0.05, **P<0.01, ***P<0.001. Data represent mean ± S.D.

Figure 6. Nanog is a functionally important target gene of hedgehog pathway in ERMS. (**A**) Representative images of RD cells co-stained for GLI1 and NANOG expression. All images were taken at 400x magnification. Scale bar represents 20μm. Quantification, using ImageJ, of NANOG expressing cellular compartments normalized to DAPI stained nuclei per viewing field in ERMS stable lines (**B**; N=6-9) and RD cells treated with SAG1.3 (500nM) for 48 hours (**C**; N=5-7). (**D**) Correlation analysis of normalized mRNA expression levels of indicated genes in ERMS patient tumor samples. The geometric mean of *GAPDH* and *HMBS* was used for normalization. (**E**) Left panel: Sphere formation in RD cells with stable knockdown of NANOG (shNANOG; N=3). Right panel: Western blot analysis of RD stable lines. (**F** and **G**) Primary sphere formation upon transient over-expression of NANOG in RD cells (N=2). Secondary sphere formation in RD (**H**) and RH36 (**I**) rescue systems (N=3). (**J**) Tumor growth rate of RH36 cells in NOD/SCID mice (N=6 per cell line). *P<0.05, **P<0.01, ***P<0.001. ns – not significant. Data represent mean ± S.D.

Figure 7. Presence of $GLI1^+$ and $NANOG^+$ compartment predicts adverse patient survival. (**A**) Representative images of immunohistochemical staining for GLI1 and NANOG within an ERMS patient tumor core. All images were taken at 400x magnification. Scale bar represents 20μm. Kaplan-Meier curve representing overall survival of 91 ERMS patients determined to be either negative (black line) or positive (grey line) for GLI1 (**B**) or NANOG (**C**) alone. Kaplan-Meier curve representing event-free survival (**D**) and overall survival (**E**) of 91 ERMS patients determined to be either negative (black line) or positive (grey line) for GLI1-NANOG co-expression. The *P*-value was generated using log rank test.

Satheesha_Fig 1

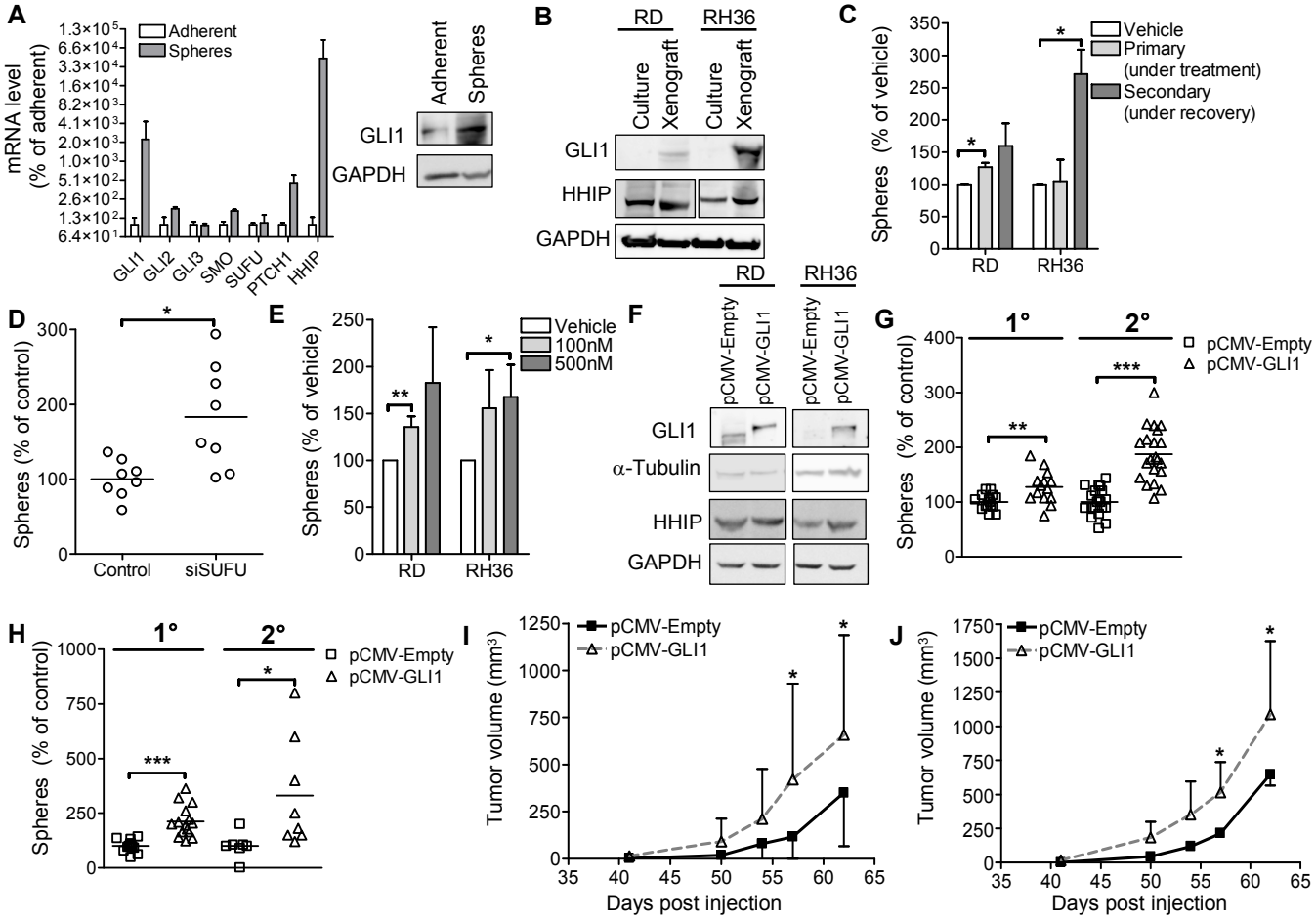

Satheesha_Fig 2

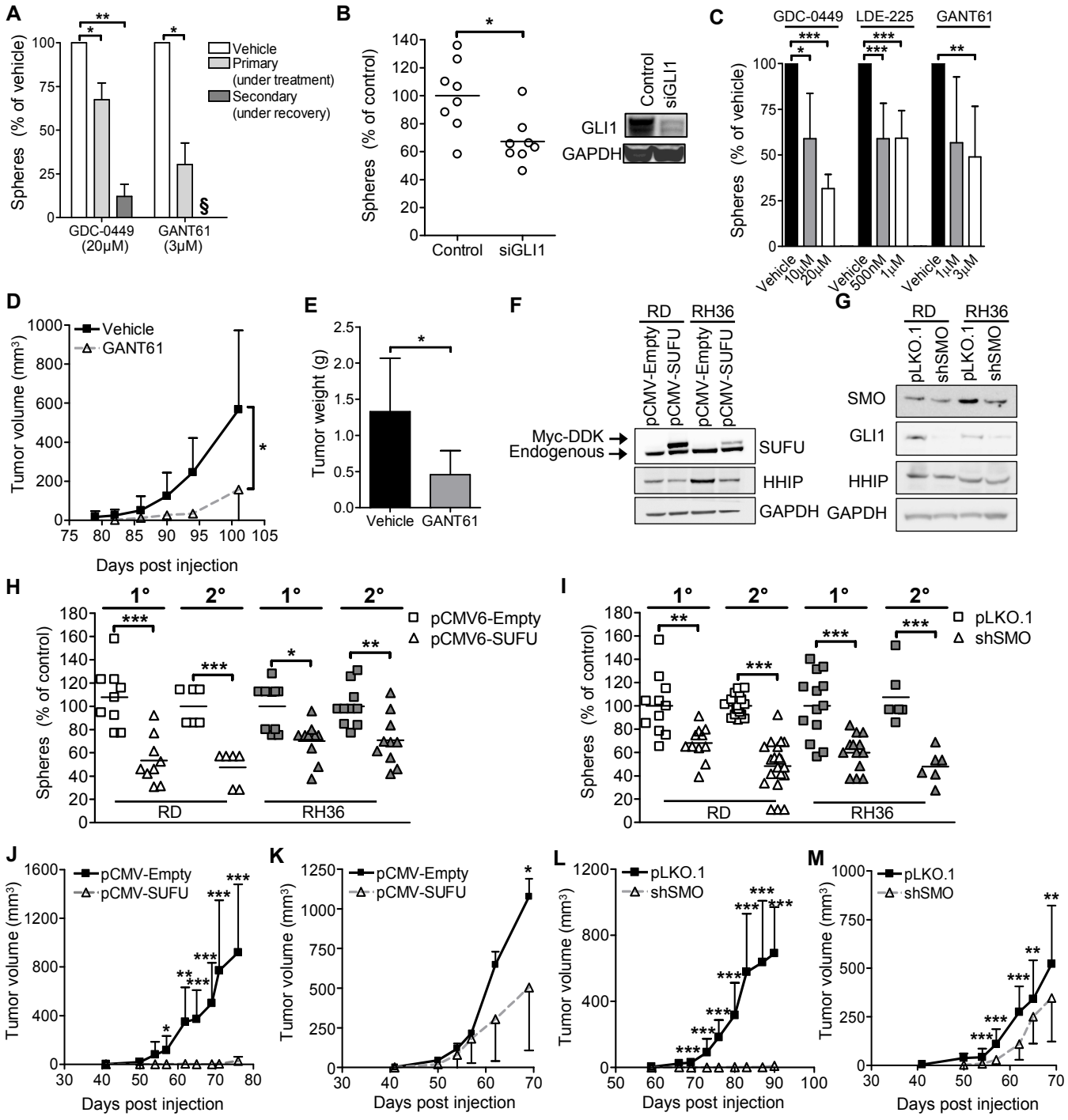

Satheesha_Fig 3

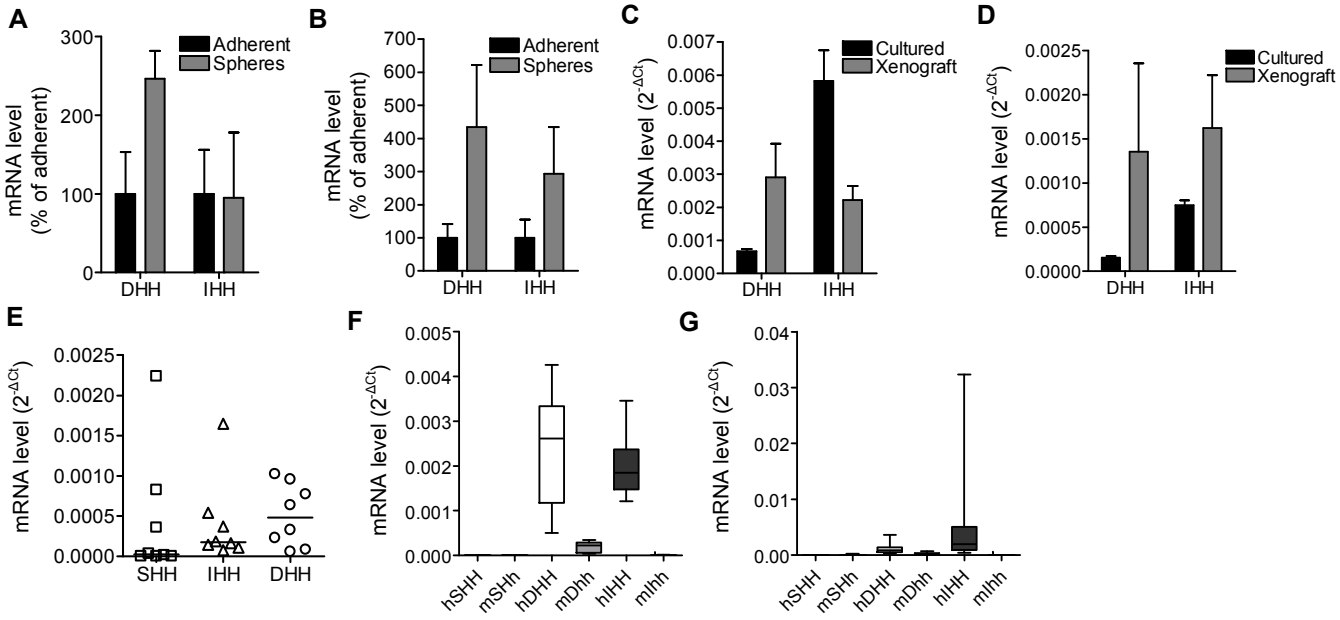

Satheesha_Fig 4

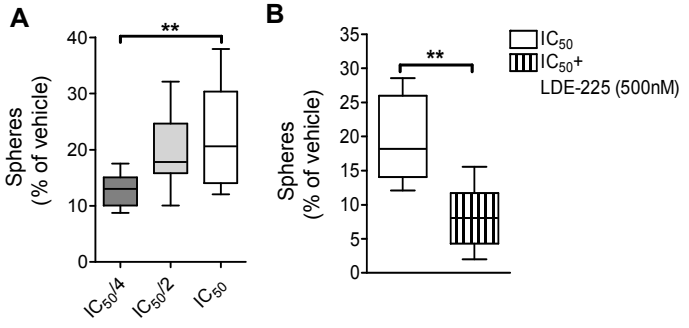

C

Cell lines		Mean IC_{50} at 72 hours (nM±S.D.)		Phenotype	
Parental	Transgenic	Irinotecan	Doxorubicin	Hedgehog pathway activity	Relative Resistance
RH36	pCMV-Empty	11 ± 6	157 ± 84	Control	
	pCMV-GLI1	19 ± 15	284 ± 205	Increased	Increased
RD	pCMV-Empty	54 ± 30	186 ± 124	Control	
	pCMV-GLI1	94 ± 55	286 ± 249	Increased	Increased
	pCMV-SUFU	37 ± 15	139 ± 135	Decreased	Decreased
RH36	pLKO.1	23 ± 15	221 ± 130	Control	
	shSMO	10 ± 5	105 ± 28	Decreased	Decreased
RD	pLKO.1	78 ± 36	198 ± 135	Control	
	shSMO	39 ± 16	177 ± 121	Decreased	Decreased

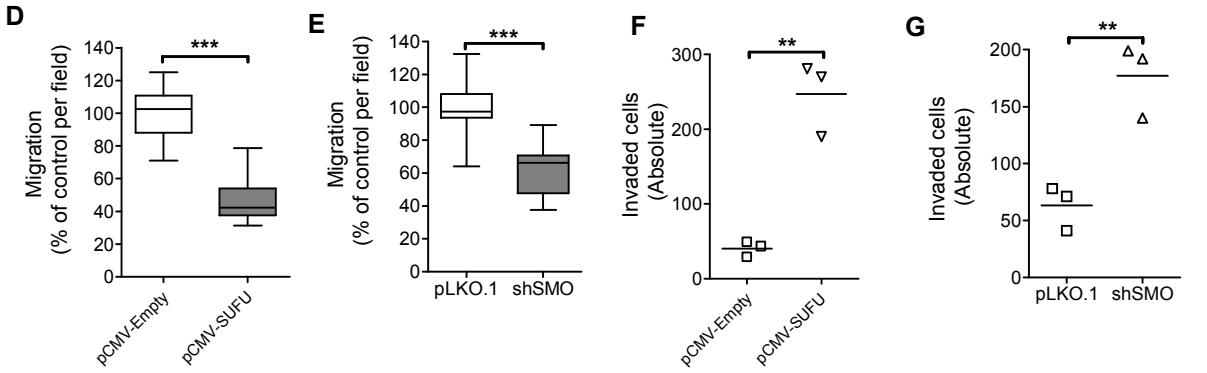

Satheesha_Fig 5

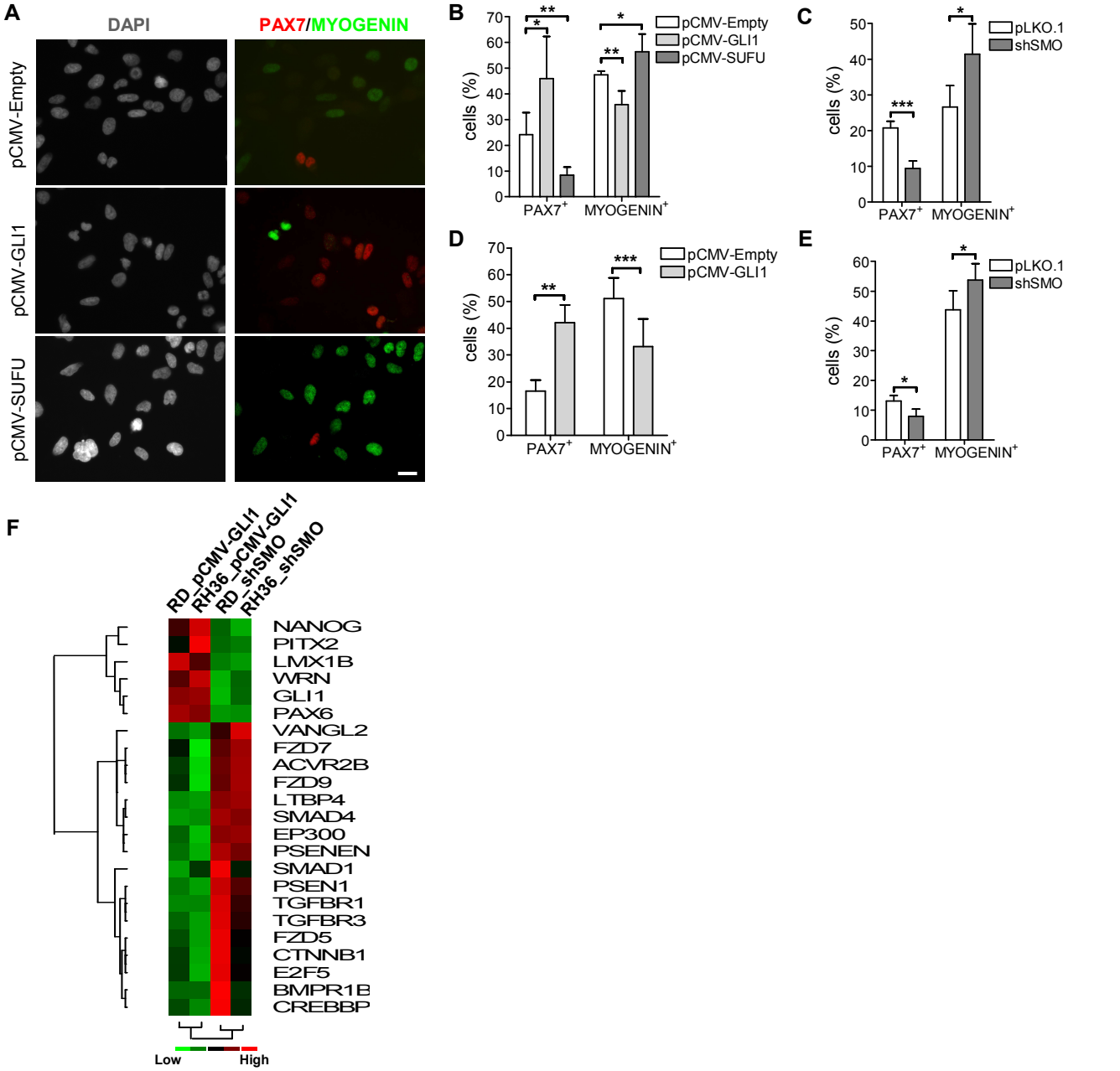

Satheesha_Fig 6

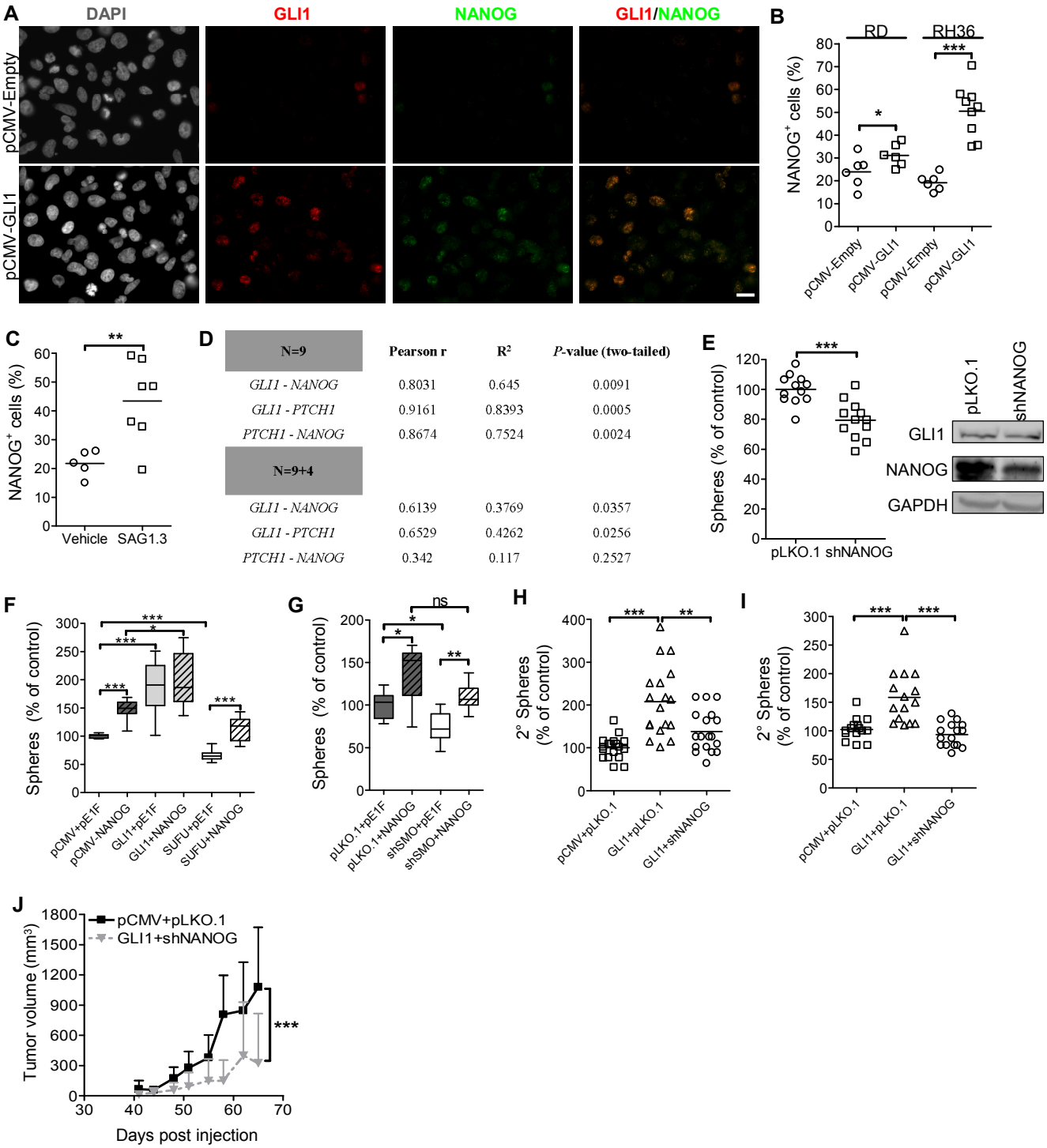

Satheesha_Fig 7

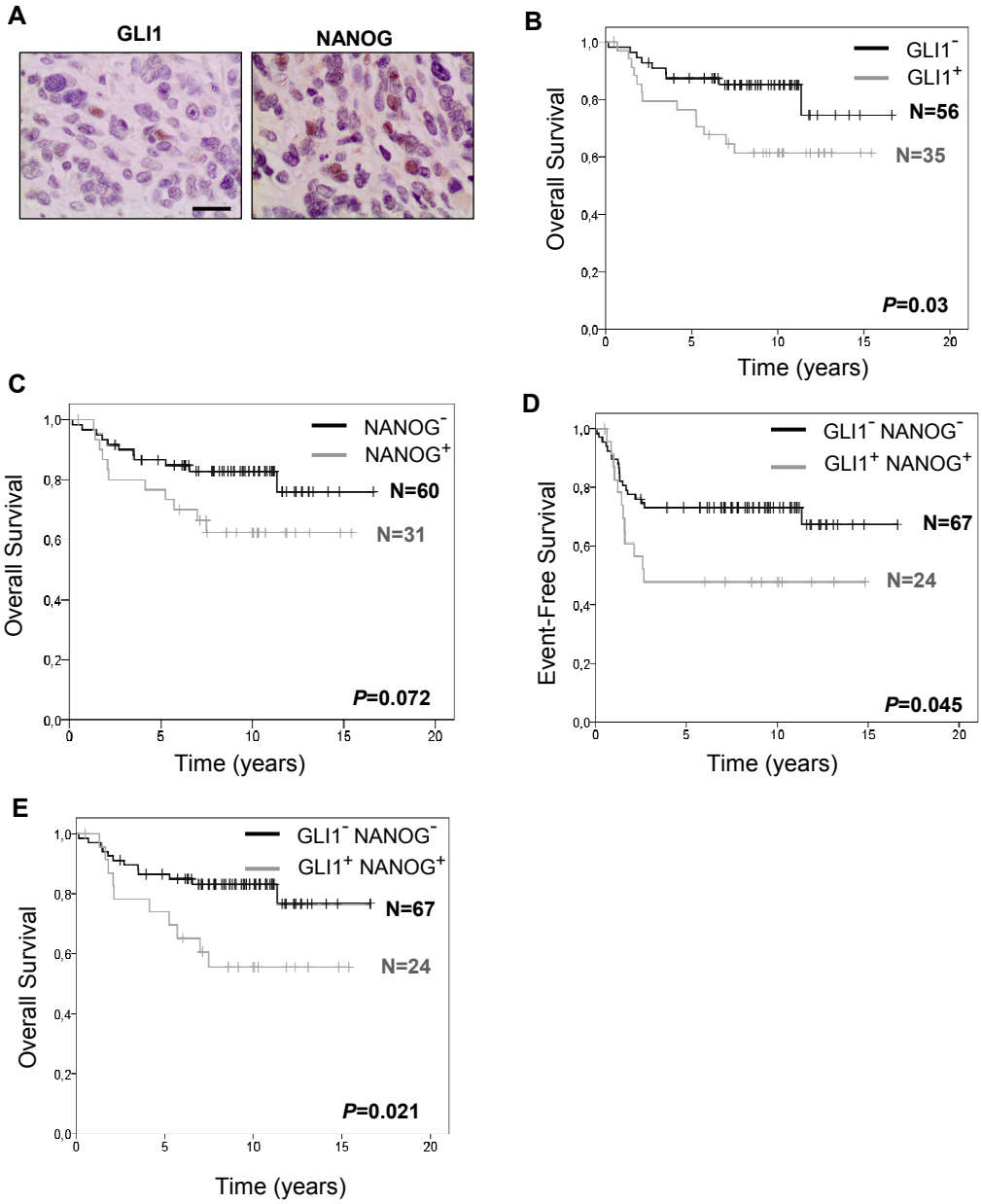

Supplementary Materials

Additional Materials and Methods

Cell viability, proliferation and clonogenic assays

To assess cell viability and proliferation, cells were plated in quadruplicate per condition in 96-well plates. After the indicated treatment viability was measured using Cell Proliferation Reagent WST-1 (Roche) following manufacturer's instruction. Cell proliferation was measure 24 hours post plating using Cell Proliferation ELISA, BrdU (chemiluminescent) assay (Roche) following manufacturer's instruction. Clonogenic assay was performed as described in (Franken et al. 2006). In brief, cells were plated at clonal density in 6-well plates in triplicates in normal media. Media was changed every 3 days until colonies (>50 cells) were visible. Colonies were fixed and stained using with Crystal Violet staining solution (0.5% Crystal Violet and 6% gluteraldehye in water. Colonies were quantified using ImageJ software (version 1.47).

Flow Cytometry

For cell cycle analysis, cells were fixed with ice-cold 70% ethanol, stored overnight at -20° and re-suspended in propidium iodide solution (PBS, 1% Triton X-100, 100mg/ml RNaseA, 1mg/ml Propidium Iodide solution) just before analysis. Cells were analyzed in the 488nm channel. For intra-cellular staining cells were fixed with cold 4% PFA and permeabilized with 0.2% Triton X-100. Cells were indirectly stained using indicated antibodies (Supplementary table 2). Unstained cells were used to set the gate for data collection. Cells stained only with conjugated secondary were used to set the positivity gate in the 488nm channel. Flow cytometry analysis was performed on a BD FACS Canto II instrument (BD Biosciences) using BD FACSDiva software. Data was analyzed with FlowJo software (version 7.6.1, TreeStar Inc.).

Franken NA, Rodermond HM, Stap J, Haveman J, van Bree C. 2006. Clonogenic assay of cells in vitro. *Nat Protoc* **1**: 2315-2319.

Supplemental Table 1. List of TaqMan®-probe based gene expression assays used in the study.

Gene	Species	TaqMan® Gene Expression Assay ID
HMBS	Human	Hs00609297_m1
GAPDH	Human	Hs02758991_g1
GLI1	Human	Hs01110766_m1
GLI2	Human	Hs01119974_m1
GLI3	Human	Hs00609233_m1
PTCH1	Human	Hs00181117_m1
HHIP	Human	Hs01011008_m1
SMO	Human	Hs01090242_m1
SUFU	Human	Hs00171981_m1
SHH	Human	Hs00179843_m1
IHH	Human	Hs00745531_s1
DHH	Human	Hs00368306_m1
NANOG	Human	Hs02387400_g1
PAX7	Human	Hs00242962_m1
MYF5	Human	Hs00929416_g1
MYOD1	Human	Hs02330075_g1
MYOG	Human	Hs01072232_m1
PROM1	Human	Hs01009261_m1
Shh	Mouse	Mm00436528_m1
Dhh	Mouse	Mm01310203_m1
Ihh	Mouse	Mm00439613_m1
Gapdh	Mouse	Mm99999915_g1

Supplemental Table 2. Details of antibodies used in the study

Primary antibodies (Anti-human)[A]						
Detected protien (clone)	**Catalogue #**	**Company**	**Species**	**Clonality**	**Application**	**Dilution**
GLI1 (V812)	2534	Cell Signaling Technology	Rabbit	poly	WB	1/1000
HHIP (R-20)	sc-9408	Santa Cruz	Goat	poly	WB	1/100
SUFU (C81H7)	2522	Cell Signaling Technology	Rabbit	mono	WB	1/1000
SMO (N-19)	sc-6366	Santa Cruz	Goat	poly	WB	1/500
NANOG	ab21624	Abcam	Rabbit	poly	WB	1/500
NANOG (D73G4)	4903	Cell Signaling Technology	Rabbit	mono	WB	1/1000
GAPDH (D16H11)	5174	Cell Signaling Technology	Rabbit	mono	WB	1/10000
□-TUBULIN (DM1A)	T9026	Sigma-Aldrich	Mouse	mono	WB	1/40000
PAX7	PAX7	Developemtal Studies Hybridoma Bank	Mouse	mono	IF and IC-FC	1/50
MYOGENIN (M-225)	sc-576	Santa Cruz	Rabbit	poly	IF and IC-FC	1/1000
GLI1 (H-300)	sc-20687	Santa Cruz	Rabbit	poly	IF	1/100
NANOG (hNanog.2)	14-5768-82	eBioscience	Mouse	mono	IF	1/50
MYOGENIN (L026)	PA0226	Novocastra, Leica	Mouse	mono	IHC	1/20
DESMIN (D33)	M076029	Dako	Mouse	mono	IHC	1/20
MIB-1 (30-9)	-	Ventana, Roche	Rabbit	mono	IHC	Prediluted (Ventana, Roche)
GLI1 (H-300)	sc-20687	Santa Cruz	Rabbit	poly	IHC	1/75
NANOG (NNG-811)	ab62734	Abcam	Mouse	mono	IHC	1/2000
Secondary Antibodies[B]						
Detected species	**Catalogue no.**	**Company**	**Species**	**Conjugation**	**Application**	**Dilution**
Anti-Mouse IgG	7076	Cell Signaling Technology	Horse	HRP	WB	1/2000
Anti-Rabbit IgG	7074	Cell Signaling Technology	Goat	HRP	WB	1/2000
Anti-Goat IgG	A50-201P	Bethyl	Donkey	HRP	WB	1/2000
Anti-Mouse IgG	A21202	Life technologies	Donkey	Alexa Fluor-488	IF and IC-FC	1/500
Anti-Rabbit IgG	A21206	Life technologies	Donkey	Alexa Fluor-488	IF and IC-FC	1/500
Anti-Mouse IgG	A21203	Life technologies	Donkey	Alexa Fluor-594	IF	1/500
Anti-Rabbit IgG	A21207	Life technologies	Donkey	Alexa Fluor-594	IF	1/500

[A] Abbreviations: WB – Western Blotting, IF – Immunofluorescence, IC-FC – Intra-cellular Flow Cytometry, IHC – Immunohistochemistry, HRP – Horseradish peroxidise

[B] HRP-conjugated secondary antibodies for IHC were purchased pre-diluted in the reagents associated with the automated systems used for processing (see text).

Supplemental Figure Legends

Supplemental Figure 1. Analysis of RH36 spheres and effect of GLI1 over-expression on ERMS cells. (**A**) Left panel: Increased expression of multiple hedgehog signaling components was seen in RH36 spheres compared to adherent monolayer cultures by quantitative PCR (Log2 scale; N=2-3). (**B**) SUFU protein expression is decreased upon siRNA mediated knockdown in RD sphere cells, which led to an increase in GLI1 expression. Flow cytometry-based cell cycle profile estimation from Propidium Iodide staining of RD (**C**) and RH36 (**D**) cells treated with SAG1.3 for 48 hours (N=2 per cell line per condition). (**E**) Viability of ERMS cells, evaluated by WST assay, was not greatly affected by the 48 hours treatment with SAG1.3 (N=3-4). Upon stable over-expression of GLI1 in RD (**F**; N=5) and RH36 (**G**; N=4) cells the expression of target genes of hedgehog pathway was increased. (**H**) Right panel: Colony forming ability of RD cells stably over-expressing GLI1 was higher than empty vector transfected cells (N=4). Left panel: Representative images of the colonies stained with Crystal Violet in one well of a standard 6-well plate. (**I**) GLI1 over-expression is maintained in the xenografts from the stable cell lines. ***$P<0.001$. Data represent mean ± S.D.

Supplemental Figure 2. Immunohistochemical analysis of ERMS xenografts. Representative images of immunohistochemistry performed on formalin-fixed paraffin-embedded (FFPE) sections of ERMS xenografts grown in NOD/SCID mice. The images for H&E (Hematoxylin and Eosin), Myogenin and Desmin were taken at 200x magnification. Scale bar represents 50µm. The images for GLI1 staining were taken at 400x magnification. Scale bar represents 20µm. GLI1 staining was found to be heterogeneous within xenografts and the over-expression was more readily detected in case of RD. The RH36 pCMV-GLI1 xenograft contained more number of strongly positive GLI1 cells and in general the tumor appeared to be composed of more primitive looking cells.

Supplemental Figure 3. Effect of hedgehog inhibition by synthetic small molecules on ERMS cells. (**A**) RH36 cells plated in sphere media and treated with small-molecule inhibitors GDC-0449 or GANT61 every 48h (3 rounds) showed decreased primary sphere formation and a further decrease in secondary sphere formation in recovery conditions (N=2). # No spheres formed. **§** No viable cells were recovered for secondary sphere formation. (**B**) RH36 adherent cells treated with hedgehog inhibitors for 48 hours had decreased sphere initiation capacity (N=2-3). Cell cycle profiles generated by flow cytometry-based measurement of Propidium Iodide staining of RD (**C**) and RH36 (**D**) cells treated with hedgehog inhibitors for 48 hours were not different from vehicle treated cells (N=2 per cell line per condition). Viability evaluated by WST assay, of RD (**E**) and RH36 (**F**) cells was not greatly affected by the 48 hours treatment with hedgehog inhibitor (N=2-4).

(**G**) Representative whole mounts of xenograft tumors formed by injecting RD cells either pre-treated with vehicle or GANT61 (3μM) for 48 hours *in vitro*. (**H**) Representative images of immunohistochemistry performed on FFPE sections of xenograft tumors formed by injecting RD cells either pre-treated with vehicle or GANT61 (3μM). The images for H&E, Myogenin, Desmin and Ki-67 were taken at 200x magnification. Scale bar represents 50μm. The images for GLI1 staining were taken at 400x magnification. Scale bar represents 20μm. **P*<0.05, ***P*<0.01. Data represent mean ± S.D.

Supplemental Figure 4. Effect of stable genetic hedgehog inhibition on ERMS cells.Upon stable over-expression of SUFU in RD (**A**; N=2) and RH36 (**B**; N=1) cells the expression of target genes of hedgehog pathway were decreased. Stable knockdown of SMO in RD (**C**; N=3) and RH36 (**D**; N=3) cells led to decrease in expression of target genes of hedgehog pathway. (**E**) Right panel: Colony forming ability of pCMV-SUFU RD cells was lower than pCMV-Empty cells (N=2). Left panel: Representative images of the Crystal Violet stained colonies in one well of a standard 6-well plate. (**F**) Right panel: Colony forming ability of shSMO RD cells was lower than empty vector transfected cells (N=2). Left panel: Representative images of the Crystal Violet stained colonies formed in one well of a standard 6-well plate. (**G** and **H**) Cell proliferation measured by BrdU incorporation in RD cells (N=2). (**I**) Histogram plots of cell cycle profiles generated from Propidium Iodide (PI) staining of RD stable lines by flow cytometry. (**J** and **K**) Quantification of cell cycle stage distributions observed in RD cell lines with different hedgehog pathway status. (**L** and **M**) Quantification of cell cycle stage distributions observed in RH36 cell lines with different hedgehog pathway status. ****P*<0.001. Data represent mean ± S.D.

Supplemental Figure 5. Real-time gene expression analysis of hedgehog ligands in ERMS patient samples and xenografts.(**A**, **B** and **C**) Quantitative PCR for hedgehog ligands performed on nine ERMS patient tumor samples. Data normalized to geometric mean of *HMBS* and *GAPDH*. Expression of *Dhh* is particularly higher within ERMS tumors (**D**: RD; **E**: RH36; N=4-10) compared to normal murine skeletal muscle (N=2). Expression levels are normalized to *Gapdh*. FeSkM_P - Pool of Fetal Skeletal Muscle RNA (N=3); AdSkM_P - Pool of Adult Skeletal Muscle RNA (N=5); m - mouse. Data represent mean ± S.D.

Supplemental Figure 6. Effect of hedgehog pathway modulation on ERMS cell motility and differentiation. Representative images of RD cells stained with Crystal Violet post-migration (**A**) and post-invasion (**B**) in trans-well assay. All images were taken at 200x magnification. Scale bar represent 50μm. (**C**) Representative images of RD cells stained for PAX7 and MYOGENIN

expression. (**D** and **E**) Representative images of RH36 cells stained for PAX7 and MYOGENIN expression. All images were taken at 400x magnification. Scale bar represents 20µm. Intra-cellular flow cytomtery performed on RH36 cells treated with hedgehog inhibitors GDC-0449 (**F**) and GANT61 (**G**) for 48 hours showed relative decrease in PAX7 positivity and increase in MYOGENIN positive cellular compartment indicating differentiation of cells, while treatment with hedgehog agonist SAG1.3 (**H**) for 48 hours induced de-differentiation of cells since PAX7 positivity increased and MYOGENIN positivity decreased (N=2). Data represent mean ± S.D.

Supplemental Figure 7. Modulation of Nanog expression by hedgehog signaling. (**A**) GLI1 over-expression increases *NANOG* RNA expression (N=4-5) while the expression decreases in shSMO (**B**; N=3) and pCMV-SUFU (**C**; N=1-2) ERMS cells. (**D**) NANOG protein expression (arrow) decreases upon inhibition of hedgehog pathway activity in ERMS cells. (**E**) Representative images of RH36 stable cells co-immunostained for GLI1 and NANOG expression. All images were taken at 400x magnification. Scale bar represents 20µm. (**F**) RH36 NANOG expressing cells increased upon 48 hours treatment with SAG1.3 (N=3). Representative images for RD (**G**) and RH36 (**H**) cells treated with SAG1.3 and stained for NANOG. All images were taken at 400x magnification. Scale bar represents 20µm. *NANOG* RNA expression, normalized to *HMBS*, is higher in RD (**I**) and RH36 (**J**) xenografts (N=2 per condition). (**K**) NANOG protein expression level (arrow) is higher in ERMS sphere and xenografts compared to adherent cultures. (**L**) Non-supervised hierarchical clustering of normalized expression levels of indicated genes in nine ERMS patient samples and pooled samples of normal human muscle (FeSkM_P and AdSkM_P). $^{**}P<0.01$. Data represent mean ± S.D.

Supplemental Figure 8. Characterization of phenotype rescue cell lines and additional clinical data analysis. (**A**) Western Blot analysis of RD stable lines indicates that expression of GLI1 increases upon NANOG over-expression. Expression analysis to verify the stable cell lines generated from RD (**B**) and RH36 (**C**) cells with knockdown of NANOG in the presence of GLI1 over-expression. Error bars represent S.D. (**D**) Representative images of immunohistochemistry performed on FFPE sections of RH36 stable line xenografts grown in NOD/SCID mice. The images were taken at 200x magnification. Scale bar represents 50µm. (**E**) Representative images of immunohistochemistry staining for GLI1 and NANOG within an ERMS patient tumor core. All images were taken at 400x magnification. Scale bar represents 20µm. Kaplan-Meier curve for event-free survival of 91 ERMS patients determined to be either negative (black line) or positive (grey line) for expression of GLI1 (**F**) or NANOG (**G**) alone. The *P*-values were generated using log rank test.

Satheesha_Supplemental Fig. 1

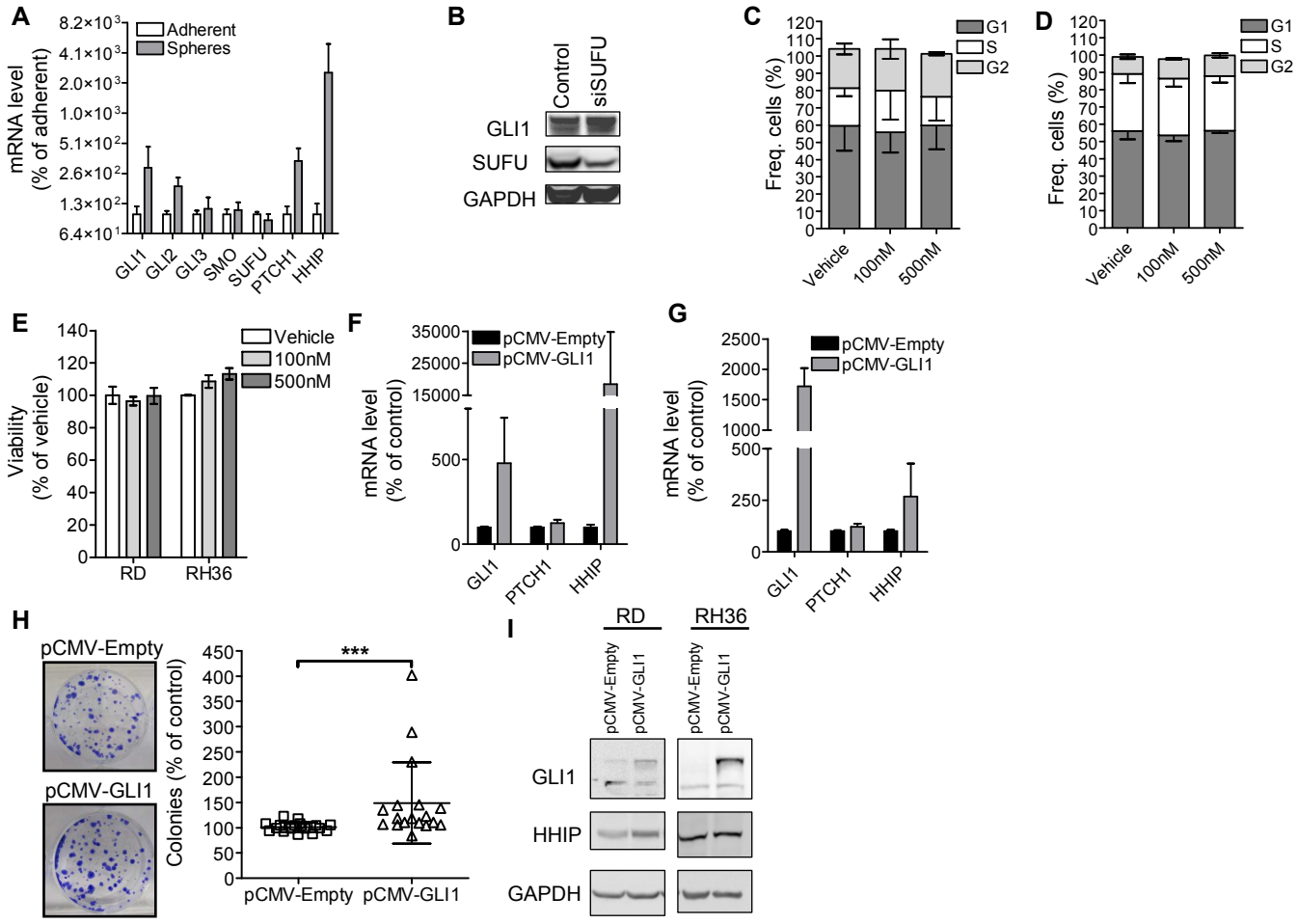

Satheesha_Supplemental Fig. 2

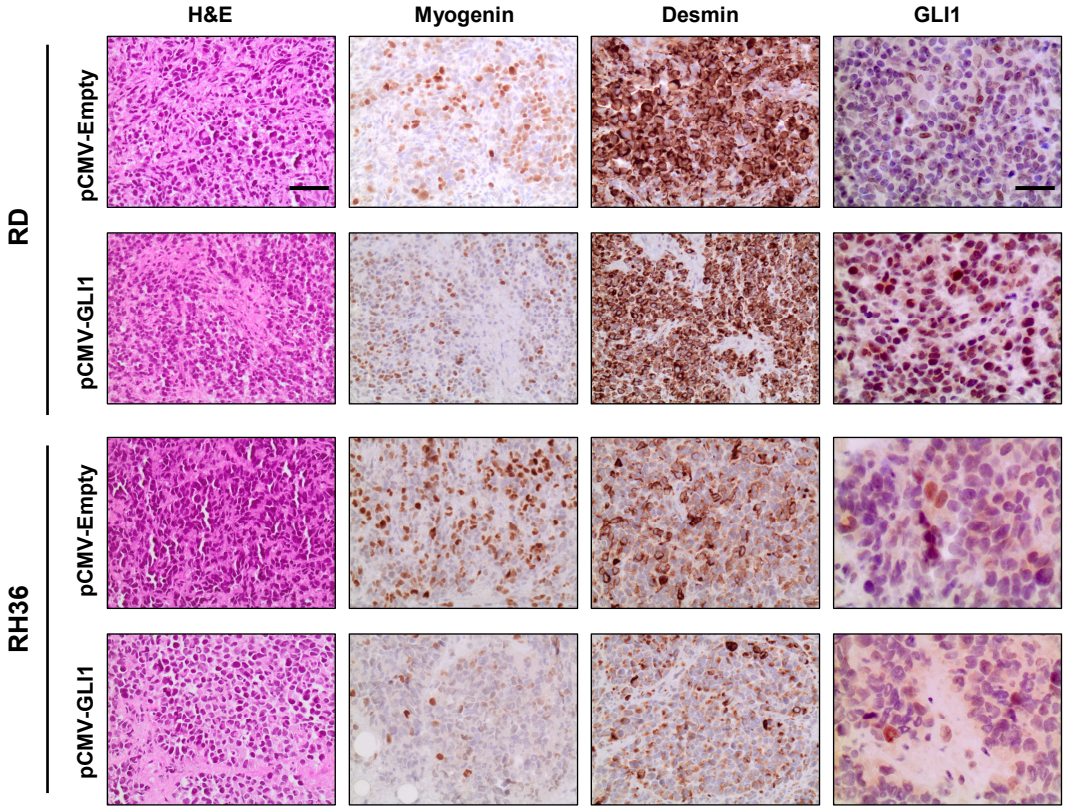

Satheesha_Supplemental Fig. 3

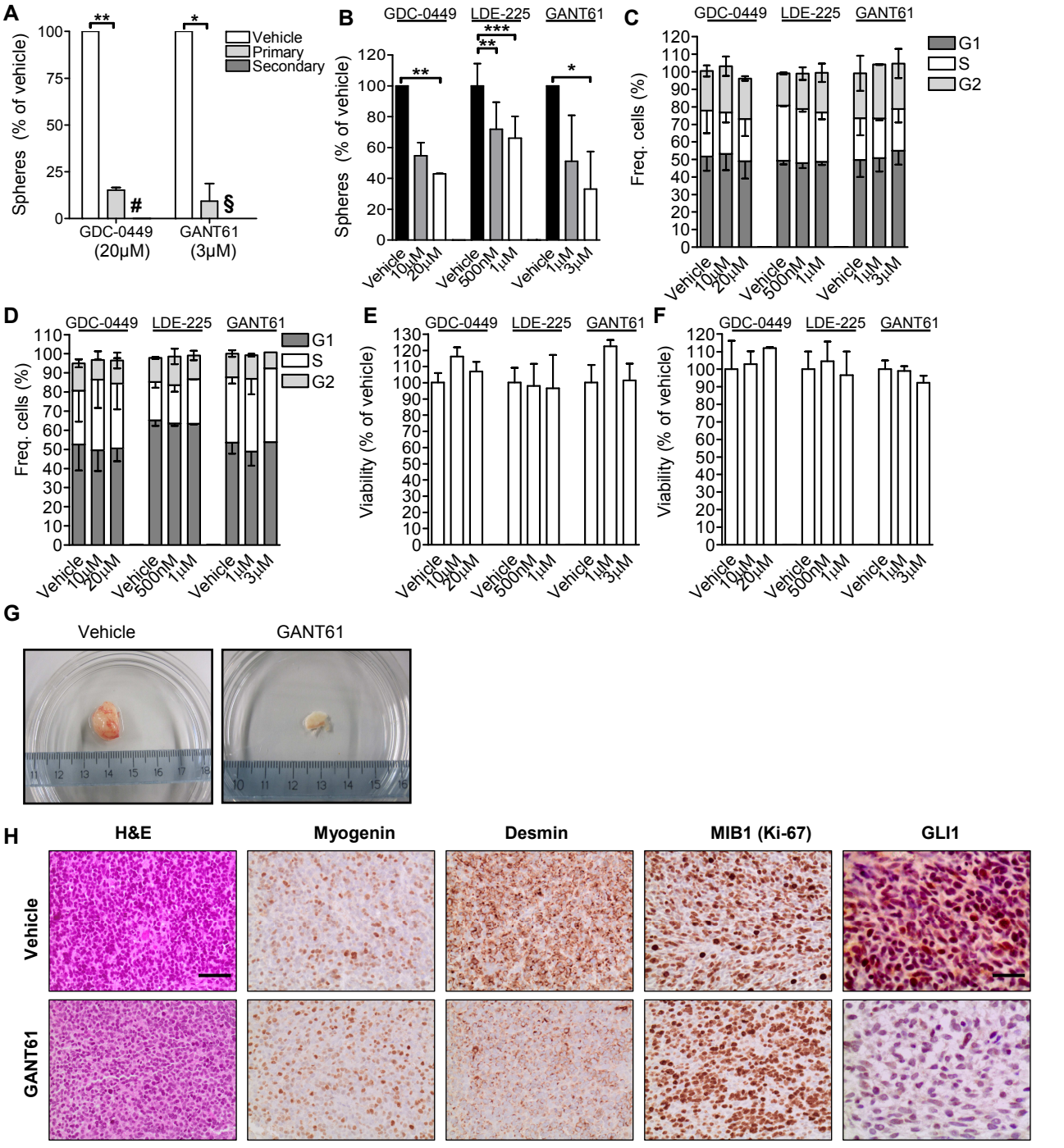

Satheesha_Supplemental Fig. 4

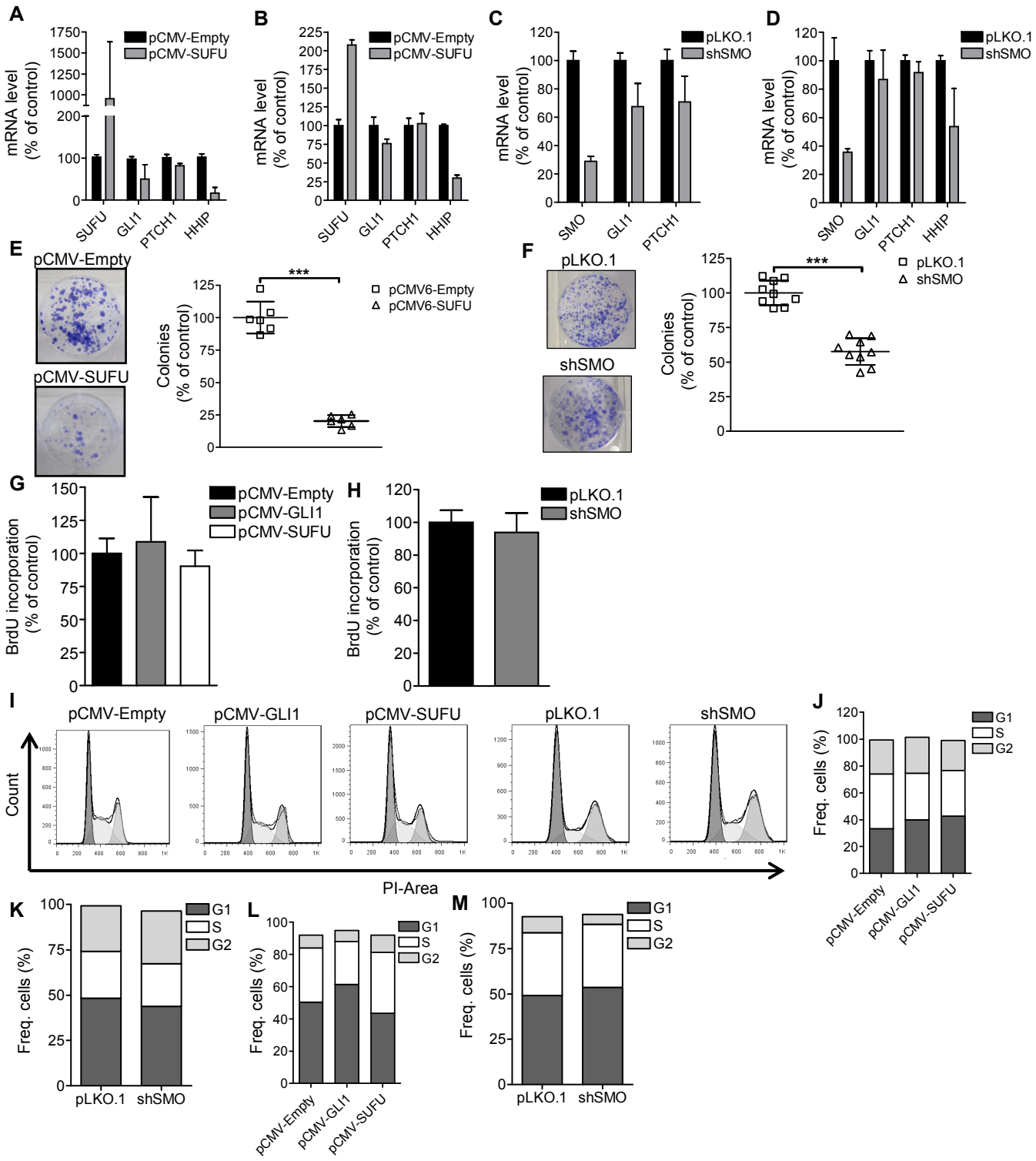

Satheesha_Supplemental Fig. 5

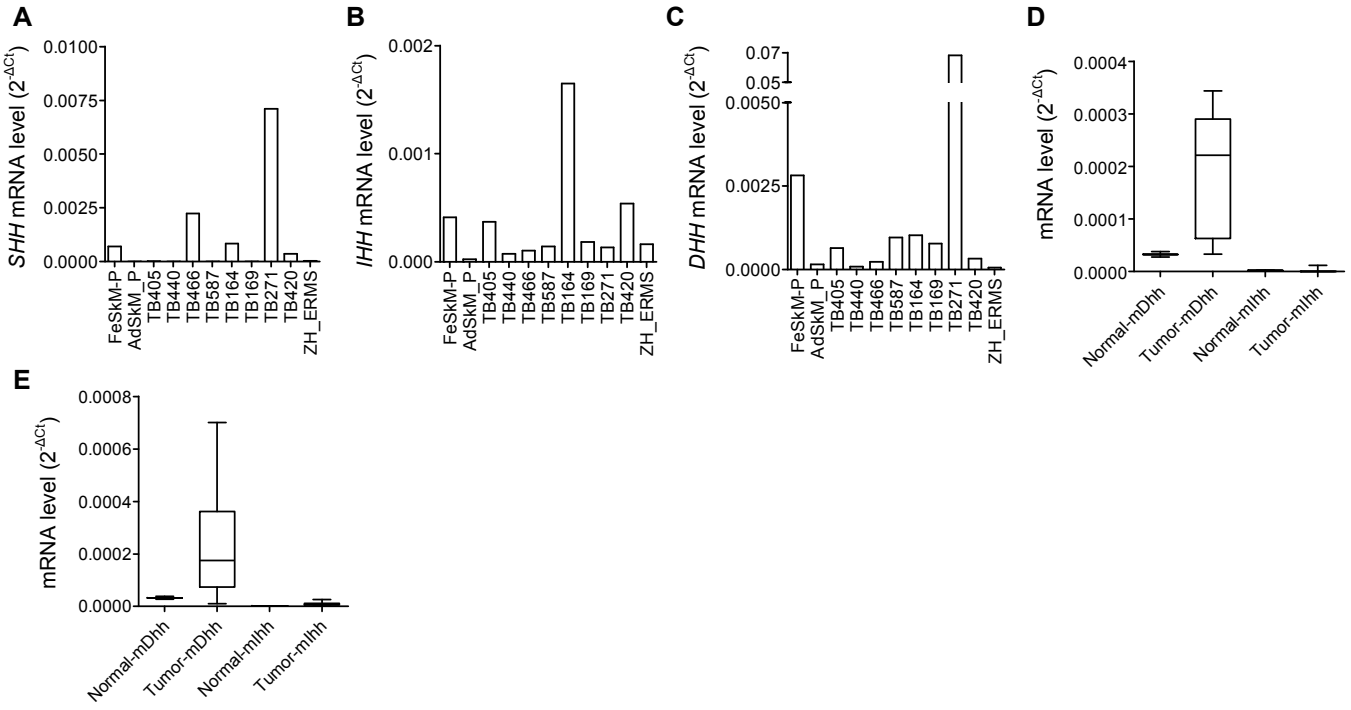

Satheesha_Supplemental Fig. 6

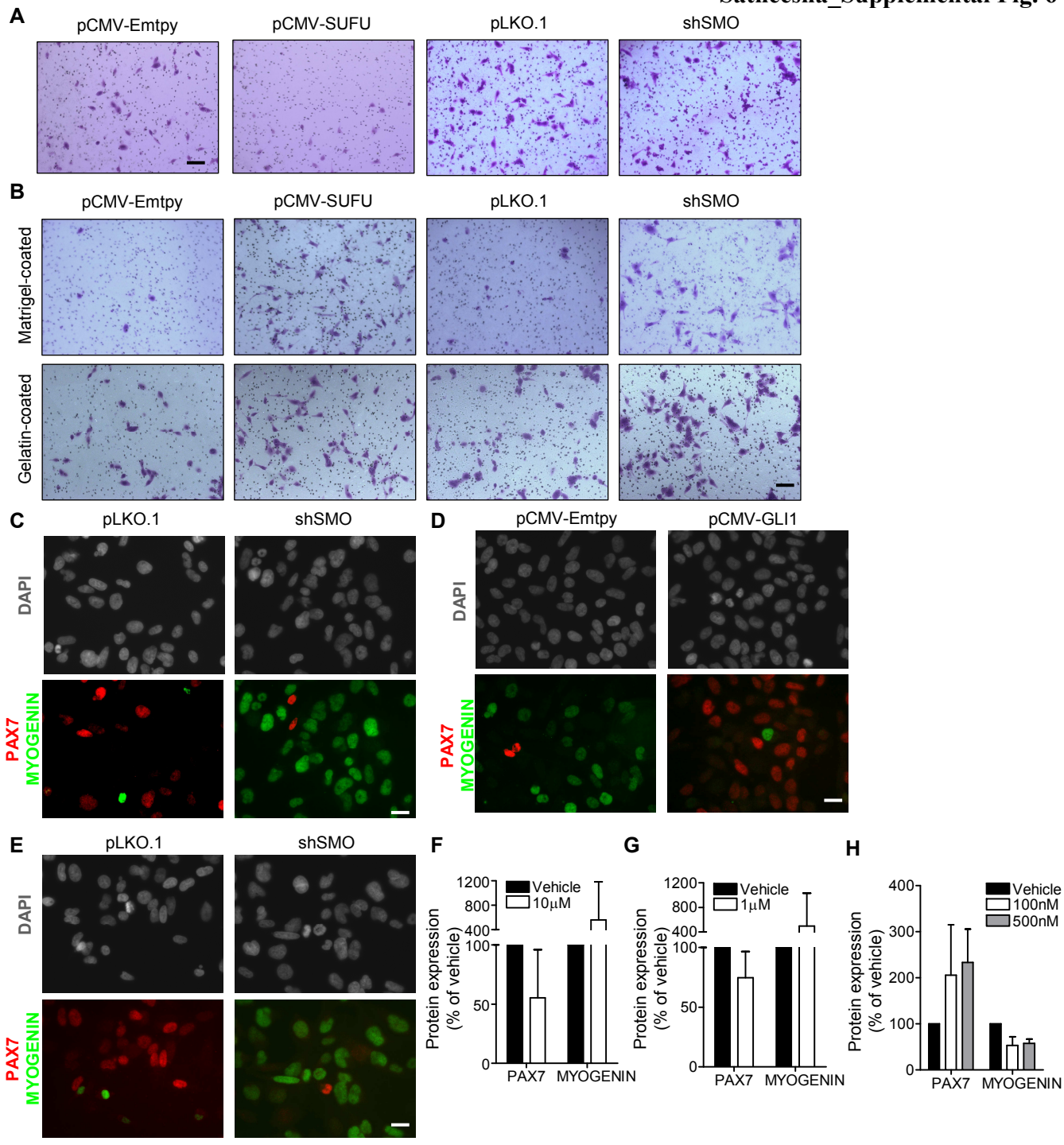

Satheesha_Supplemental Fig. 7

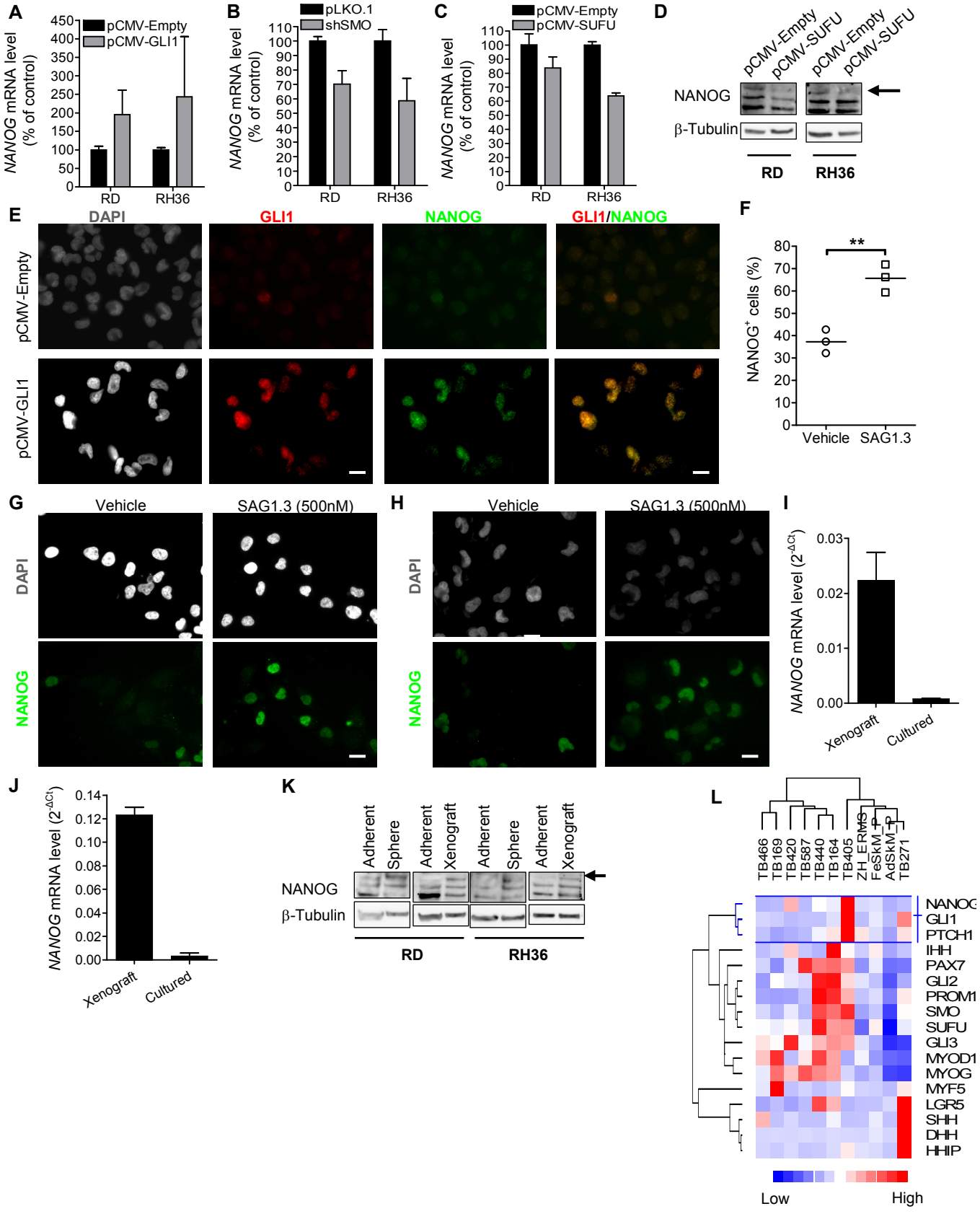

Satheesha_Supplemental Fig. 8

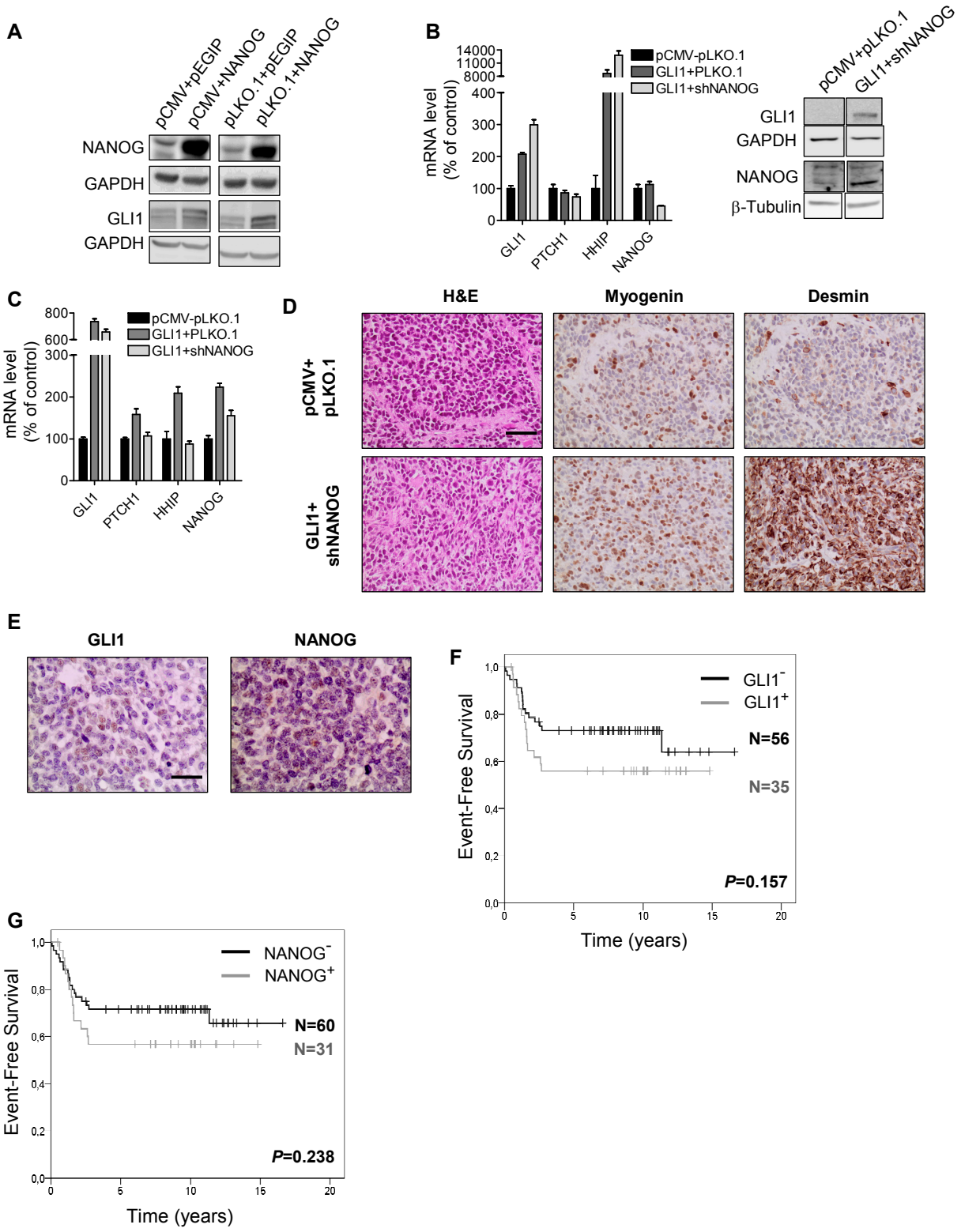

PAX3-FOXO1 increases fibroblast reprogramming efficiency and drives self-renewal in alveolar rhabdomyosarcoma

Elisa A. Casanova[1], Melanie Generali[1], Sampoorna Satheesha[1], Peter K. Bode[2], Paolo Cinelli[3] and Beat W Schäfer[1]*

Author affiliations

1. Department of Oncology and Children's Research Center, University Children's Hospital, Zurich, Switzerland
2. Institute of Surgical Pathology, University Hospital Zurich, Zurich, Switzerland
3. Division of Trauma Surgery, University Hospital Zurich, Zurich, Switzerland

*** Corresponding author**

Department of Oncology, University Children's Hospital, Steinwiessstrasse-75, 8032, Zurich, Switzerland
Email: Beat.Schaefer@kispi.uzh.ch
Tel: +41 (44) 266 7553
Fax: +41 (44) 634 8859

The authors declare that no conflict of interest exists.

Abstract

Rhabdomyosarcoma (RMS) is the most common soft tissue sarcoma in children. Most alveolar (aRMS) cases bear the chimeric transcription factor PAX3/7-FOXO1 and have a poor prognosis compared to the more common embryonal (eRMS) subtype. Previous studies have characterized eRMS as being a hierarchically organized tumor with rare cancer-initiating populations but there have been no reports on the cellular organization in aRMS. This knowledge would be important to guide future treatment strategies. In this study we show that no cancer stem cells (CSC) subpopulation could be detected in aRMS by a range of common methods whereas 100 aRMS cells were sufficient to generate tumors in NOD/SCID mice. The stem cell factors Nanog, Oct4, and Sox2 were homogeneously expressed in aRMS cell lines and their genetic loss- or gain-of-function did not change cellular physiology unlike silencing of PAX3-FOXO1, which caused cell cycle arrest and apoptosis. Importantly, the addition of PAX3-FOXO1 to standard human fibroblast reprogramming protocol led to significant increase in generation of induced pluripotent stem cells (iPSC). Strikingly, PAX3-FOXO1 iPSC showed reduced ability to differentiate in vitro into all three germ layers and initiated undifferentiated tumors in vivo unlike control iPSC that could generate bona fide teratomas. In conclusion, PAX3-FOXO1 is a general inhibitor of differentiation in iPSC and it could act as ‘stemness’ mediator in aRMS. Moreover, contrary to eRMS, fusion-positive aRMS tumors are comprised of a majority of cancer-initiating cells which are dependent on PAX3-FOXO1 activity, and therefore could follow the stochastic clonal evolution model.

Introduction

For the development of more effective cancer therapies, it is of fundamental importance to determine which cancer cells have the potential to contribute to disease progression. Since tumors consist of populations with heterogeneous proliferation and differentiation capacities, in the past years at least two models of tumor propagation have been postulated: the clonal evolution model and the cancer stem cell (CSC) model. The clonal evolution model postulates that tumor cells are under selective pressure. This process leads to the generation of genetically heterogeneous and highly aggressive clones with equipotent tumorigenic potential. On the other side numerous studies, first in leukemia and later in solid tumors, have demonstrated that often only a subset of cancer cells has the capability to extensively proliferate and generate new tumors [1, 4, 32]. These CSCs after transplantation give rise to new CSCs as wells as a heterogeneous, more differentiated population of non-tumorigenic cells. The origin of CSCs is not yet clear; nevertheless they share many features with embryonic (ESC) and adult stem cells. Two common characteristics define normal and CSCs: their ability to undergo indefinite mitotic self-renewal and to differentiate into a range of specialized cell types. Based on phenotypic traits such as cell surface markers and on functional properties such as quiescence and drug resistance, CSC can nowadays be isolated from a number of primary tumors or cell lines and, after establishing the optimal conditions, can be maintained and enriched *in vitro*.

Rhabdomyosarcoma (RMS) is the most frequent soft tissue sarcoma in children (reviewed in [12]). RMS share features with skeletal muscle and based on histologic criteria they are divided into two groups: embryonal RMS (eRMS) and alveolar RMS (aRMS). eRMS have higher incidence, are less aggressive, and mainly affect children in the age of 0-5 years [34]. On the other hand aRMS occur in adolescents and young adults, and are more aggressive tumors with poor response to therapy and in general worse prognosis than eRMS [7, 36, 37]. The pathogenic marker of aRMS is the result of specific chromosomal translocations [33, 43]. The most common translocations are t(2;13)(q35;q14) or t(1;13)(p36;q14), which generate the chimeric transcription factor PAX3-FOXO1 (also known as PAX3-FKHR) or PAX7-FOXO1 respectively. The resulting fusion protein contains the DNA-binding domain of PAX3 or PAX7 and the transactivation domain of FOXO1 [11]. Several studies have proven the oncogenic role of the fusion protein and have demonstrated its fundamental importance in maintaining aRMS cells [2, 3, 14, 25, 40]. Importantly, it was demonstrated that PAX3-FOXO1 actively contributes to the undifferentiated myogenic phenotype typical of RMS cells, in which it suppresses the transcriptional activity of *MyoD*-target genes [8]. Moreover, recently JARID2, a protein involved in

recruiting various complexes with histone-methylating activity, was identified as a novel PAX3-FOXO1 target gene [51]. Thus, the chimeric protein controls cellular differentiation programs and interacts with epigenetic regulators, maintaining aRMS cells in a pre-differentiated state. Similar features are possessed by transcription factors, which regulated stemness in ESC and induced pluripotent stem cells (iPSC). Recently, it was demonstrated that the core stem cell factors NANOG, OCT4, and SOX2 together with KLF4, c-MYC, and LIN28 are sufficient for de-differentiate or reprogram terminally differentiated cells into iPSC [45, 46, 54]. Not surprisingly, most of these reprogramming factors are found expressed and upregulated in cancer (stem) cells where they are involved in maintaining the tumorigenic state and sustaining cell self-renewal [17, 22, 28].

Although CSC have been already identified in many sarcomas [16, 29, 44] and among them recently also in eRMS [50], it is still unclear as to whether the most aggressive aRMS subtype possesses a subpopulation of CSC. In this study we present evidence that aRMS contrary to eRMS does not possess an exclusive subpopulation of cells with tumor potential but rather more each aRMS cell exhibits similar tumorigenic potential. Survival and maintenance of aRMS cells is strictly PAX3-FOXO1 dependent. Here we demonstrate that the chimeric protein confers also stemness properties and is able to enhance the efficiency of reprogramming human fibroblasts. Importantly, we prove for the first time that PAX3-FOXO1 inhibits not only mesodermal, and specifically skeletal muscle differentiation, but also ectodermal and endodermal differentiation. In sum, this iPSC system offers new possibilities for understanding the biology of PAX3(or 7)-FOXO1, which is an essential step for developing novel therapies for aRMS.

Materials and Methods

Cell lines

Alveolar Rhabdomyosarcoma (aRMS) cell lines RH4, RH41 (both kindly provided by Peter Houghton, The Research Institute at Nationwide Children's Hospital, Columbus, OH, USA), RH3, RH5 (kindly provided by Susan Ragsdale, St.Jude Children`s Research Hospital, Memphis TN, USA), CW9019 (kindly provided by Soledad Gallego, Hospital Universitari Vall d'Hebron, Barcelona, Spain), RMS13 (kindly provided by Roland Kappler, Ludwig-Maximilians-Universität München, Munich, Germany), RH30 (purchased from the American Type Cell Culture Collection, LGC Promochem, Molsheim Cedex, France), the human testicular embryonal carcinoma cell line NTERA-2 clone D1 (purchased from Biological Bank and Cell factory, IRCCS university hospital San Martino, Genoa, Italy), 293-GPG

cells, neonatal human foreskin fibroblast (PC501A-HFF-SBI, purchased from System Biosciences, CA, US) were routinely maintained in complete medium: DMEM supplemented with 10% fetal bovine serum (FBS), 2mM L-glutamine, and 100 U/ml penicillin/streptomycin.

Sphere assay, transgenic aRMS cell lines, and siRNA

For sphere assay, cells were seeded at clonal dilution in petri dishes and cultured in sphere medium consisting of DMEM/HAM's F12, 20% knockout Serum Replacement (GIBCO), 2mM L-glutamine, 100 U/ml penicillin/streptomycin either supplemented with 10ng/ml bFGF or with 10ng/ml bFGF, 10ng/ml EGF, and 10ng/ml PDGF (all from R&D Systems). At each passage spheres were quantified and passaged at clonal density. All experiments were performed in triplicates. Transgenic cell lines stably overexpressing NANOG, OCT4, and SOX2 were generated using jetPRIME Transfection Reagent (Polyplus) according to manufacturer's instructions. The following plasmids have been used: control EGFP pEGIP (Addgene no. 26777, [56]), pSin-EF-Sox2-Pur, pSin-EF-Nanog-Pur, pSin-EF-Oct4-Pur (all from Addgene no. 16577-16579, [54]). Overexpression of the genes was proven at RNA and protein levels. For knockdown experiments cells were transfected using INTERFERin^{TM} siRNA Transfection Reagent (Polyplus) as described in the manufacturer's instructions. Silencer® Select siRNAs (Ambion, Life technologies) against SOX2 (1-siSOX2: Silencer® Select ID s13296, 2-siSOX2: s13295, 3-siSOX2: s13294), against PAX3-FOXO1 (siP2F [26]), and scrambled control (Silencer® Negative Control No. 2 siRNA) were used at a final concentration of 5nM. Cells were harvested after 48h and 72h for further functional assays. Gene silencing was controlled on RNA and protein levels.

Cancer stem cell markers, Aldefluor assay, and separation of ALDH1 high cells

For CSC marker analysis, single cell suspensions were incubated at room temperature for 30 min with 1:10 diluted fluorochrome labeled antibody for: CD133/2-APC, CD133/1-APC (both Miltenyi), CD44-FITC, CXCR4-APC (both BD Bioscience). Flow cytometry analysis was performed on a BD FACS Canto II instrument (BD Biosciences). Data were collected with DIVA software (BD Biosciences) and analyzed with FlowJo software (TreeStar Inc., Ashland, OR, USA). To monitor ALDH1 enzymatic activity Aldefluor® assay system (Stem Cell Technologies) was used according to manufacturer's instructions. In brief, 10^6 cells/ml were incubated with activated ALDH1 substrate for 40 min at 37°C. Using identical conditions as a negative control for each experiment a set of cells was stained with ALDH1 inhibitor DEAB. ALDH1 high cells were detected with FACS as described before. For ALDH1 activity after drug selection, aRMS cells were incubated for 72h with the chemotherapeutics Vincristine

(5nM and 5μM, Teva Pharma AG, Switzerland), Actinomycin D (5nM and 5μM, Sigma Aldrich, Switzerland), and Mafosfamide (5μM and 30μM, Santa Cruz, CA, USA). Thereafter, cells were stained with Aldefluor® assay and processed for flow cytometry analysis. Only viable, 7AAD (BD Bioscience) negative cells were investigated for ALDH1 activity as described above. Aldefluor® labeled RH30 aRMS cells were sorted with FACS Aria III and fractioned into ALDH1 high, ALDH1 low, and a mixed population. The three populations were cultured either in monolayer conditions and analysed for ALDH1 activity after 3, 6, and 10 days or sphere assay was performed as previously described.

Clonogenic, Proliferation, viability, and cell cycle analysis

For clonogenic assay 2000 cells were seeded on 6 well plates in triplicates. Cells were cultured with complete medium and allowed to grow till clones were visible. Cells were stained with crystal violet and clones were quantified. For proliferation assay Cell Proliferation ELISA, BrdU assay (Roche Applied Science) was used following manufacturer's instruction. For knockdown experiments the data were normalized with the scrambled control, whereas for transgenic overexpressing cell lines the data were normalized with EGFP control line. For cell viability assay Cell Proliferation Reagent WST-1 (Roche Applied Science) was used following manufacturer's instruction. All experiments were performed in triplicates. For cell cycle analysis siRNA treated cells were harvested after 24h, 48h, and 72h and they were fixed in ice-cold 70% ethanol. Cells were resuspended in propidium iodide solution (PBS, 1% Triton X-100, 100mg/ml RNaseA, 1mg/ml PI), and processed for FACS analysis as previously described.

Real-time PCR

Total RNA was extracted using RNeasy Mini Kits (Qiagen) and reverse transcription was carried out using high-capacity cDNA reverse transcription kit (Life Technologies) according to the manufacturer's instructions. Quantitative Real-Time PCR (qRT-PCR) was performed using commercially available mastermix and TaqMan Gene Expression Assays (Life Technologies, Supplemental Table 1). Reactions were run using standard conditions on an ABI 7900 HT Real-Time PCR machine and the data were analyzed with SDS2.2 software. C_T values were normalized to GAPDH or HMBS housekeeping genes. Relative expression levels of the genes were calculated using the □□C_T method. All experiments were performed in triplicate and repeated at least three times. Data analysis was done with the GraphPad prism software and statistical analysis using the Student's t-test. Heat map for aRMS clone analysis was generated with dChip software.

Western blotting, immunofluorescence, and immunohistochemical analysis

For western blot, total protein extracts were obtained from cells lysed with RIPA buffer (50 mM Tris-Cl, pH 6.8, 100 mM NaCl, 1% Triton X-100, 0.1% SDS) supplemented with Complete Mini Protease Inhibitor Cocktail (Roche Applied Sciences). Protein concentration was measured with Pierce® BCA protein Assay Kit (Thermo Scientific). Proteins were identified by SDS-PAGE and western blotting using antibodies reported in Supplemental Table 2. Signal was detected by chemiluminescence using SuperSignal West Femto Maximum Sensitivity Substrate (Thermo Scientific). For immunofluorescence analysis, aRMS cells were grown on chamber slides whereas iPSC were cultured on 3.5 cm cell culture dishes, fixed with 4% paraformaldehyde (Carl Roth, Arlesheim), and incubated over night at 4°C with primary antibodies. aRMS staining were analyzed with an Axioskop2 mot plus fluorescence microscope (Zeiss, Jena, Germany). iPSC staining were analyzed with Axiovert 40 CFL (Zeiss, Jena, Germany) and AxioVision Rel. 4.6 software. For immunohistochemical analysis of xenografts and teratomas, three-micron thick sections of blocks of formalin-fixed, paraffin-embedded tissue were mounted on glass slides (SuperFrost Plus), deparaffinized, rehydrated and stained with hematoxylin and eosin (H&E) using standard histological techniques. Immunohistochemical staining were performed with Ventana Benchmark automated staining system (Ventana Medical Systems) using Ventana UltraView DAB reagents. All primary antibodies were diluted in Ventana diluent. Slides were counterstained with hematoxylin, dehydrated and mounted.

Generation of human induced pluripotent stem cells (iPSC)

iPSC were generated as described in [56]. In brief, 293-GPG cells were cultured with complete medium and were transfected using jetPRIME Transfection Reagent (Polyplus) with the following retroviral plasmids: pMXs-hOCT3/4, pMXs-hSOX2, pMXs-hKLF4, pMXs-hc-MYC (all from Addgene no. 17217-17220 [46]). PAX3-FOXO1 full sequence was cloned into pMSCV-pBabeMCS-IRES-GFP (Addgene no. 33336) and the same plasmid without PAX3-FOXO1 was used as a control. 72h post-transfection the virus-containing medium was collected. A solution containing equal amount of the four reprogramming factors plus either PAX3-FOXO1 or the control plasmid was prepared and immediately used for fibroblast transduction. Equal amount of human fibroblasts were plated onto gelatinized 6 well plates and the cells were incubated over night with virus-containing medium. Thereafter, viruses were removed and the cells were cultured for additionally 5 days with complete medium. At day 5 same amounts of infected fibroblasts were transferred on plates coated with mitotically inactivated mouse

embryonic fibroblasts (MEFs). From day 6 on cells were cultured with iPSC medium consisting of DMEM/HAM's F12, 20% knockout Serum Replacement (GIBCO), 10ng/ml of bFGF (R&D Systems), 100□M nonessential amino acids (Life Technologies), 100□M 2-mercaptoethanol (Sigma), 1mM L-glutamine, 50 U/ml penicillin/streptomycin. Two weeks later single iPSC colonies were picked and expanded as clones on MEF coated plates. Total DNA (DNeasy Blood & Tissue Kit, Qiagen) form iPSC clones was isolated and PAX3-FOXO1 was detected with PCR (fwd: GCACTGTACACCAAAGCACG, rev: AACTGTGATCCAGGGCTGTC). qRT-PCR analyses of the iPSC clones were performed as described above.

***In vitro* differentiation of iPSC clones**

iPSC were separated from MEF and cultured in suspension for 7 days in iPSC-medium without bFGF to form embryoid bodies (EB), which were then analyzed for gene expression as described above or were plated onto 0.1% gelatin-coated dishes for further differentiation. For mesodermal (muscle) differentiation, attached EB were culture in high-glucose DMEM, 10% FBS , 5% horse serum (Sigma), 100μM nonessential amino acids, 100μM 2-mercaptoethanol, 1mM L-glutamine, 50 U/ml penicillin/streptomycin. After 14 days the amount of serum was reduced to 1% and cells were additionally cultured for 3 weeks. For ectodermal (neural) differentiation, attached EB were cultured for 10 days in DMEM/HAM's F12, 50x B27 Supplement (GIBCO), 100x N2 Supplement (GIBCO), 2% FBS, 10ng/ml bFGF, 1mM L-glutamine, 50 U/ml penicillin/streptomycin. For endodermal (pancreatic) differentiation, iPSC were separated from MEF and plated on gelatin-coated dishes in medium consisting of RPMI 1640, 1% FBS, 50x B27 Supplement, 1mM L-glutamine, 50 U/ml penicillin/streptomycin supplemented with Activin A (100ng/ml, GIBCO). Cells were cultured for 6 days under these conditions, and thereafter the medium was changed into: DMEM/HAM's F12, 50x B27 Supplement, 100x N2 Supplement, 1% FBS, 100□M nonessential amino acids, 100μM 2-mercaptoethanol, 1mM L-glutamine, 50 U/ml penicillin/streptomycin. Cells were additionally cultured for 8 days. All differentiated cells were then either fixed for immunofluorescence or lysed for total RNA extraction.

Generation of xenografts and teratomas

The veterinary office of the Canton Zurich approved all xenograft and teratoma experiments. For the generation of xenograft, different amount of aRMS cells were injected intra muscularly (i.m) into the left leg of NOD/Scid mice. Tumor size was determined every 4 days by measuring two diameters (d_1

and d_2) in right angles of both legs with a caliper. Tumor volumes were calculated using the following formula:

$V=[4/3x\ \pi/2(d_1+d_2)]_{left\ leg} - [4/3x\ \pi/2(d_1+d_2)]_{right\ leg}$

For secondary tumor formation, primary xenografts were isolated and tumor dissociation was performed as described in [35] for 30 min at 37°C in a rotator oven. An aliquot of each cell suspension was analyzed by flow cytometry for determining the percentage of viable (7-AAD negative), EGFP positive cells. Based on these data cell dilutions with 10^4 cells were prepared and injected as described before into NOD/Scid mice. Approximately $1cm^3$ tumors were dissected and analyzed. For teratoma generation, $1\text{-}3x10^6$ undifferentiated, MEF free iPSC were injected either subcutaneously into one dorsal flank or i.m into the left leg of NOD/Scid mice. Tumors were measured once a week and allowed to grow till $1cm^3$. Subcutaneous tumor volumes were calculated using the following formula:

$V= ½(length\ x\ width^2)$.

Results

Identification of putative cancer stem cell subpopulation in aRMS cell lines

Recently, we demonstrated that CSCs can be enriched in eRMS by using the sphere assay [50]. In order to understand whether also the more aggressive aRMS possess a subpopulation of CSC we performed sphere assays with aRMS cells. Sphere medium was either supplemented with bFGF (referred as FGF-medium) or with bFGF, EGF, and PDGF (ALL-medium). Seven human aRMS cell lines were tested for their ability to generate spherical clones and to self-renew in anchorage-independent, serum-starved culture, using either FGF- or ALL-medium. While all aRMS cell lines were able to grow and to form spheres in both media (data not shown), only three cell lines (RH4, RMS13, and RH30) showed enhanced self-renewal at clonal density and could be passaged for more than 5 weeks (Fig. 1A and Supplemental Fig. 1A-B). Although the increase of cells forming spheres was very moderate over the passages, no upregulation of the core stem cell genes NANOG and OCT4 was observed in RH4 and RH30 spheres when compared to the same cells cultivated under standard, adherent conditions. Only a slight increase was monitored in RMS13 spheres for NANOG and in RH30 spheres for SOX2 (Fig. 1A and Supplemental Fig. 1A-B). Thus, in contrast to eRMS cells with the sphere assay no clear enrichment of CSC was observed in aRMS spheres.

We further analyzed the expression of three cell surface markers known to characterize different CSC types. The glycoprotein CD133 (PROMININ 1) is upregulated in CSC of different tumors [15, 31, 39] and importantly also in eRMS [50]. Most of the aRMS cell lines were negative for CD133 expression, with the exception of RMS13, which was composed of an almost 100% positive population and RH3, which had a subpopulation of about 30% positive cells (Fig. 1B). CD44 is a major hyaluronan receptor used as a marker for mesenchymal stem cells and CSC [38, 49]. CD44 was shown to play a crucial role in the activation of tumor-promoting signaling pathways [5, 6]. Four out of seven aRMS cell lines possessed a population of CD44 positive cells, which was varying from 15% in RH3 to almost 100% in RH30 and CW9019 lines (Fig. 1C). In contrast, RH4, RMS13, and RH5 were negative for CD44. The expression of the chemokine receptor CXCR4 has been associated with metastasis, poor prognosis in primary tumors, and CSC [10, 13]. No subpopulation was identified in the analyzed aRMS cell lines but almost all the lines showed high expression of CXCR4 (Fig. 1D). CXCR4 gene was identified as target of PAX3-FOXO1 [30, 47] hence explaining the high expression observed in almost all aRMS cell lines with the exception of RH4 and RH41 (Fig. 1D). Thus, none of the analyzed markers characterize a small subpopulation in all seven aRMS cell lines, which could be further studied for stemness properties.

aRMS cell lines possess a dynamic subpopulation of ALDH1 high cells which do not have stem cell properties

The cytosolic enzyme aldehyde dehydrogenases (ALDHs) are involved in oxidizing intracellular aldehydes into carboxylic acids. Recently, ALDH1 was identified as a marker for CSC in many different tumors such as breast [18], ovary [27], lung [23], and sarcomas [21]. Based on these data, we analyzed seven aRMS cell lines for their ALDH1 activity using Aldefluor® assay system and flow cytometry [24]. All aRMS cell lines possessed a subpopulation of ALDH1 high cells, which varied from 3% in RH41 to about 40% in RH3 (Fig. 1E). RH30 was selected for further investigation and ALDH1 high and ALDH1 low fractions were separated. As a control a mixed population of positive and negative cells was used for all the experiments (Supplemental Fig. 2A). We next assessed the capability of the three cell populations to maintain or modulate ALDH1 activity over the time. Sorted and control cells were cultivated and ALDH1 activity was measured after 3, 6, and 10 days (Fig. 1F). The ALDH1 high fraction generated ALDH1 positive and negative cells, as it would be expected from stem cells. Nevertheless, ALDH1 low fraction already after 3 days of culture showed a small population of ALDH1 positive cells, which increased after 10 days (Fig. 1F). Thus, ALDH1 high cells are not a fixed population but rather more a dynamic population. Gene expression analysis of the

sorted populations showed no upregulation of the core stem cell genes in the ALDH1 high fraction (Fig. 1G). Interestingly, NANOG expression was strongly reduced in the ALDH1 high cells and no differential expression of aRMS specific genes was observed (Fig. 1G). The three fractions were analyzed also under sphere conditions: ALDH1 high cells generated slightly more primary spheres; nevertheless the difference was not significant (Fig. 1H). Over the passages no enhanced self-renewal was observed in any of the fractions (Fig. 1I). These data confirm the fact that ALDH1 positive cells are dynamic and can therefore not be maintained in culture as exclusively negative or positive population. All these results were confirmed with the aRMS cell line RH4 (data not shown).

The ALDH enzymes are an important component of cellular defenses against toxic aldehydes [42] and are therefore supposed to be involved in CSC drug resistance. Therefore we investigated whether drug selection could enrich for ALDH1 high cells in aRMS cells cultivated as a monolayer under standard culture conditions. Since aRMS tumors are usually treated with the VAC-protocol (Vincristine, Actinomycin D, and Cyclophosphamide), RH30 cells were incubated for 72 hours with either high or low concentrations of the chemotherapeutics Vincristine, Actinomycin D, or the metabolic active form of Cyclophosphamide, called Mafosfamide. Thereafter, viable cells were analyzed for ALDH1 activity by flow cytometry. Treatment with Vincristine and Actinomycin D reduced the population of ALDH1 high cells with both drug concentrations (Fig. 1J). ALDH1 population was not affected when the cells were treated with the lower concentration of the alkylating agent Mafosfamide but decreased with the highest concentration (Fig. 1J). Thus, treatment with the VAC-protocol is sufficient for eliminating ALDH1 high cells in aRMS cell lines.

In sum, aRMS cell lines possess a subpopulation of cells with high ALDH1 activity; nevertheless these cells do not have stem cell properties and are sensitive to chemotherapeutics treatment.

Silencing of PAX3-FOXO1 but not of the stem cell regulators NANOG, OCT4, and SOX2 affects aRMS cellular physiology

The transcription factors NANOG, OCT4, and SOX2 are key regulators of pluripotency in mammalian ESC and iPSC but they also play crucial roles in the maintenance of CSC in many different tumors [9, 17, 19, 29]. Expression analysis of the core stem cell genes in seven aRMS cell lines revealed that all cells expressed NANOG, OCT4, and SOX2 although at very low levels (Fig. 2A and Supplemental Fig. 3A-C). To understand the function of the stem cell regulators in aRMS, siRNA mediated silencing of the three factors was performed in RH4 and RH3 and thereafter gene expression, cell cycle distribution, cell proliferation and viability was investigated. Surprisingly, knockdown of the pluripotency factors

never affected aRMS cells on molecular or functional levels. For instance, silencing of SOX2 using three specific siRNA sequences did not induce upregulation of differentiation markers like MYL1 or alter gene expression of PAX3-FOXO1 and its target genes AP2β and OLIG2 (Fig. 2B). Similar results were obtained after silencing of NANOG and OCT4 with several specific siRNA sequences (data not shown). Contrary to the stem cell factors, silencing of PAX3-FOXO1 induced downregulation of its target genes and strong upregulation of muscle differentiation factors (Fig. 2C). Cell viability was significantly altered upon downregulation of the oncogene but not upon reduction of NANOG, OCT4, and SOX2 expression (Fig. 2D). Moreover, reduction in cell proliferation (Fig. 2E) and cell cycle arrest at G1 phase (Fig. 2F) occurred only upon silencing of PAX3-FOXO1 whereas no detectable changes could be observed upon downregulation of the stem cell genes. Taken together our data confirm that PAX3-FOXO1 expression is essential for aRMS cell maintenance whereas in contrast to other types of cancer, the expression of the core stem cell genes in aRMS is dispensable.

Forced expression of NANOG, OCT4, and SOX2 negatively correlates with stemness properties in aRMS cell lines

All analyzed aRMS cell lines expressed NANOG, OCT4, and SOX2, although not at levels comparable to pluripotent stem cells. For better understanding of their role in aRMS, we generated RH30 and RH4 cells transgenic lines (Supplemental Fig. 4A) overexpressing NANOG, OCT4 or SOX2, or the three genes simultaneously (referred as 'NOS'). These cell lines were tested for enhanced stemness properties. Gene expression analysis of the transgenic lines displayed different behaviors between RH4 and RH30 cells. Briefly, all RH4 transgenic lines never showed differential expression of PAX3-FOXO1 or its target gene AP2β (Fig. 2G). Nevertheless, the muscle specific differentiation marker MYL1 was reduced in the cell lines overexpressing SOX2 and NOS (Fig. 2G) highlighting a less differentiated state compared to the control cells. In RH30 cell system, OCT4 overexpression induced a slight upregulation of PAX3-FOXO1 and a strong increase of AP2β (Supplemental Fig. 4B). Similarly AP2β was upregulated in the SOX2 and NOS transgenic cells. Nevertheless, no downregulation of MYL1 was observed in any of these transgenic cells (Supplemental Fig. 4B). Analysis of cell proliferation demonstrated that RH4 transgenic cells proliferated faster (Fig. 2H) whereas RH30 cells proliferated slower than the control cells (Supplemental Fig. 4C). Interestingly, also the ability of generating clones was affected by the overexpression of the stem cell genes: in RH4 cells NANOG, OCT4, and SOX2 forced expression reduced the number of clones, whereas no difference was

observed upon overexpression of NOS (Fig. 2I). Also RH30 transgenic cells formed fewer clones after forced expression of OCT4, SOX2, and NOS (Supplemental Fig. 4D). Since in the adherent culture system none of the transgenic cell lines gained stemness properties, we performed sphere assay. Both RH4 and RH30 cells overexpressing NANOG, OCT4, and SOX2 showed reduced ability to form primary spheres (Fig. 2J and Supplemental Fig. 4E) and reduced self-renew over a period of 5 weeks (Fig. 2K and Supplemental Fig. 4F).

In sum, overexpression of the core pluripotency stem cell genes in aRMS cells does not increase stem cell properties, confirming a minor role of these genes in aRMS.

High frequency of tumor initiating cells in aRMS

Since our data did not support the presence of CSC subpopulations in aRMS we hypothesized that aRMS does not follow the CSC model but rather the clonal evolution model, which postulates that each cell is equally able to propagate the tumor. We therefore performed *in vivo* limiting dilutions with RH30 cell line. Three dilutions of cells (10^5, 10^4, and 100 cells) were injected i.m. into the left leg of NOD/Scid mice. All mice injected with 10^5 (n = 3) and 10^4 (n = 4) cells developed tumors (Fig. 3A) and after about 80 days post-injections also 3 out of 5 mice injected with only 100 cells formed tumors (Fig. 3A). Immunohistochemical analysis of the xenografts confirmed aRMS diagnosis, with the typical small blue round cell morphology and the expression if the skeletal muscle markers MYOGENIN and DESMIN (Supplemental Fig. 5A). In order to clarify whether each aRMS cell possesses tumorigenic potential we performed clonal analysis. RH30 cells expressing EGFP were plated with a dilution of 0.5 cells/100µl into several 96 well plates and the following day each well was analyzed for the presence of one single cell expressing EGFP. Sixteen clones were expanded and analyzed for their heterogeneous gene expression by qRT-PCR. PAX3-FOXO1 and several target genes as well as the stem cell factors and differentiation markers were differentially expressed between the clones (Fig. 3B), confirming their heterogeneous clonal origins. Based on these data we selected 8 clones for testing their tumorigenic potential in immunocompromised mice, which were also highly divergent in their gene expression profiles. $5x10^4$ cells for each clone were injected i.m. into the left leg of NOD/Scid mice (n = 4). After a period of time varying between 40 and 140 days post-injection all mice developed tumors (Fig. 3C and Supplemental Fig. 5B). To prove that each clone had the capability to self-renew and to propagate the tumors, we selected six primary tumors for generating secondary xenografts. Dilutions with $1x10^4$ primary xenograft cells were prepared and injected i.m. in NOD/Scid mice. Once more after a period varying between 50 and 100 days post-injection all clones generated

secondary tumors (Fig. 3C and Supplemental Fig. 5C). Immunohistochemical analysis of primary and secondary xenografts confirmed aRMS histology (Fig. 3D). Interestingly, xenografts originating from different clones showed variable expression of the aRMS markers MYOGENIN and DESMIN (Fig. 3D), highlighting dissimilar levels of differentiation and confirming their heterogeneous origin.

In conclusion, we demonstrated that 100 cells are sufficient for generating aRMS tumors in immunocompromised mice. Moreover, all clones had equal tumor potential, implying that aRMS arise from stochastic rather than hierarchical differentiation processes.

In the presence of c-MYC PAX3-FOXO1 enhances reprogramming efficiency of human fibroblasts

The fact that each aRMS cells possess equal tumorigenic potential together with the observations that PAX3-FOXO1 is the key regulator of aRMS cell maintenance, we hypothesized that PAX3-FOXO1 itself might confer stem cell properties to all aRMS cells. We therefore investigated whether PAX3-FOXO1 can contribute to reprogramming differentiated cells into iPSC. For this purpose human fetal fibroblast (HFF) were transduced with retroviruses separately encoding human OCT4, KLF4, SOX2, and c-MYC along with either EGFP (control iPSC) or PAX3-FOXO1 (PAX3-FOXO1 iPSC). Gene expression analysis five days post-infection revealed upregulation of the pluripotency factors NANOG, REXO1, and DNMT3β as well as of PAX3-FOXO1 and its target gene AP2β (Supplemental Fig. 6A). Around 14 days post-transduction iPSC colonies began to arise in the control cells as well as in the PAX3-FOXO1 cells and the total number of iPSC-like colonies was quantified. Interestingly, PAX3-FOXO1 transduced cells generated about 45% more iPSC colonies than the control cells (Fig. 4A), indicating that the fusion protein increases the reprogramming efficiency. Morphology of the iPSC colonies was similar in both cell types and showed the classical round and compact shape of undifferentiated embryonic stem-like cells (Fig. 4B). Both control and PAX3-FOXO1 iPSC were positive for the pluripotency markers NANOG, OCT4, SSEA4, and TRA60, confirming that both cell types were true iPSC (Fig. 4C and Supplemental Fig. 6B).

We next assessed whether PAX3-FOXO1 could replace one or more reprogramming factors. A known target gene of PAX3-FOXO1 is the proto-oncogene n-MYC. This gene shares cellular functions with the family member c-MYC. Since reprogramming with three factors in the absence of c-MYC is sufficient for generating iPSC, although with lower efficiency, we hypothesized that replacing c-MYC with PAX3-FOXO1 might re-establish the original efficiency obtained in the presence of c-MYC. Five days post-transduction PAX3-FOXO1 and AP2β were strongly upregulated in the transduced cells,

confirming transcriptional activity of PAX3-FOXO1 (Supplemental Fig. 7A). On the contrary no strong upregulation of the stem cell genes was observed (Supplemental Fig. 7A). Moreover, iPSC colonies appeared only 30 days post-transduction. Although the overall efficiency in the absence of c-MYC was much lower than the cells reprogrammed with c-MYC; the control cells generated slightly more colonies compared to the cells transduced with the chimeric oncogene (Supplemental Fig. 7B). Thus, we hypothesized that the simultaneous expression of PAX3-FOXO1 and c-MYC might have synergistic effects during reprogramming and that PAX3-FOXO1 alone cannot replace c-MYC.

Reprogramming with PAX3-FOXO1 and the combination of only two reprogramming factors (OCT4-SOX2, OCT4-KLF4, KLF4-SOX2) never generated iPSC-like colonies (data not shown), indicating that PAX3-FOXO1 cannot substitute OCT4, SOX2, KLF4, or c-MYC but it increases the efficiency of reprogramming in the presence of all four factors.

PAX3-FOXO1 prevents differentiation of iPSC

Single iPSC colonies obtained from the transduction with the four reprogramming factors plus PAX3-FOXO1 were clonally expanded. Clone number 1 showed genomic integration of PAX3-FOXO1 transgene and a strong expression of the oncogene as well as of AP2β (Fig. 4D), confirming transcriptional activity. Three other clones (clone 5, 6, and 25) showed neither genomic integration nor expression of PAX3-FOXO1 (Fig. 4D) and were therefore selected as control (wild type) iPSC. The expression of AP2β was varying between the wild type clones but was much lower than in clone 1 (Fig. 4D). The pluripotency markers NANOG, DNMT3β, OCT4, and SSEA4 were expressed in wild type and PAX3-FOXO1 clones at very high levels (Fig. 4E-F and Supplemental Fig. 8). Additionally, PAX3-FOXO1 cells co-expressed together with the pluripotency markers also the target gene AP2β (Fig. 4F). Thus, having confirmed the undifferentiated state of the iPSC clones we investigated their pluripotent potential *in vitro* as well as *in vivo.* PAX3-FOXO1 clone 1 and the wild type clone 6 (control) were selected for *in vitro* differentiation into the three germ layers. Embryoid bodies (EB) were generated with control and PAX3-FOXO1 iPSC (Fig. 5A) and were analyzed for their differentiation level. The endodermal markers GATA4 and AFP were strongly upregulated in control EB whereas their expression was undetectable in PAX3-FOXO1 EB (Fig. 5B). Similar results were obtained for the mesodermal markers PAX7 and MSX1, which were strongly upregulated in the control EB and barely expressed in PAX3-FOXO1 EB (Fig. 5B). Control EB also showed higher expression of the ectodermal markers PAX6, SOX1, and DCX (Fig. 5B). Nevertheless, the pluripotency markers NANOG and DNMT3β were in both control and PAX3-FOXO1 EB downregulated, whereas the

oncogene and its target gene AP2β were still highly expressed exclusively in the PAX3-FOXO1 EB (Supplemental Fig. 9A). These data indicate that PAX3-FOXO1 expression interferes with the ability of iPSC cells to differentiate towards the three germ layers.

In order to prove whether the oncogene can also block terminal differentiation, control and PAX3-FOXO1 iPSC were differentiated into muscle cells (mesoderm), pancreatic cells (endoderm), and neurons (ectoderm). Differentiation levels were thereafter assessed by qRT-PCR and by immunofluorescence. When iPSC were differentiated into muscle cells, wild type cells migrated out from the attached EB and formed single layers as well as myofiber-like clusters (Supplemental Fig. 9B). On the contrary, much less PAX3-FOXO1 cells migrated out and no myofiber-like clusters were visible after 14 days of differentiation (Supplemental Fig. 9B). Expression of the fusion protein as well as of AP2β was still high (Supplemental Fig. 9C). After 3 additional weeks of culture with reduced serum multinucleated myofibers were visible exclusively in the control cells (Fig. 5C). Analysis of mesodermal and muscle differentiation markers confirmed strong upregulation in the control cells but not in the PAX3-FOXO1 cells (Fig. 5D), whereas the oncogene and its target gene were exclusively expressed in PAX3-FOXO1 cells (Supplemental Fig. 9D). Thus, similarly like in aRMS tumor cells PAX3-FOXO1 impairs mesodermal differentiation and blocks terminal muscle differentiation in iPSC.

For endodermal differentiation, control cells showed cytosolic expression of AMYLASE (Fig. 5E) and strong upregulation of GATA4 and AFP (Fig. 5F). Interestingly, PAX3-FOXO1 differentiated cells had different morphology compared to the control cells being much smaller and round shaped (Fig. 5E). The expression of the endoderm markers GATA4 and AFP was reduced compared to the differentiated control cells but AMYLASE was similarly expressed in both clones (Fig. 5F). PAX3-FOXO1 cells still expressed high levels of the transgene and of AP2β (Supplemental Fig. 9E). Thus, these data show for the first time that PAX3-FOXO1 can block endodermal differentiation in iPSC.

During neural differentiation, wild type cells migrated out from the attached EB and generated many mature neurons and glia cells (Fig. 5G). On the contrary, much less PAX3-FOXO1 cells migrated out and formed neurons (Fig. 5G). Expression analysis of neural differentiation markers like PAX6, SOX1, and DCX confirmed higher expression in the control cells and reduced expression in the PAX3-FOXO1 cells (Fig. 5H and Supplemental Fig. 9F). These data indicate that PAX3-FOXO1 interferes also with ectodermal differentiation and blocks neural differentiation of iPSC.

In conclusion, despite the expression of all the pluripotency markers, PAX3-FOXO1 iPSC are surprisingly not able to differentiate into derivatives of all the three germ layers. In order to further prove that, undifferentiated iPSC were injected into immunocompromised mice for generating

teratomas. iPSC of the wild type clones 6, 5, and 25 and PAX3-FOXO1 positive clone 1 were injected either subcutaneously or i.m. in NOD/Scid mice. After a period of about 10 weeks post-injections teratomas were isolated and analyzed for their differentiation levels. Independent from the site of injection, teratomas generated from the three control clones presented derivatives of the three germ layers (Fig. 6A), confirming the pluripotent potential of the iPSC. For instance we observed in the control teratomas glands with intestinal type mucosa and colon crypt (both endodermal origin), squamous epithelium (ectoderm), and bones, cartilage, and smooth muscle (all mesodermal tissues) (Fig. 6A). On the contrary, PAX3-FOXO1 expressing cells generated homogeneous tumors with plump to spindle like cells and frequent mitotic figures, indicating an undifferentiated tumor type (Fig. 6B). qRT-PCR confirmed the expression of PAX3-FOXO1 in the tumor as well as the expression of AP2β (Fig. 6C). Independently from the location of the tumor (subcutaneous or intra muscular), all PAX3-FOXO1 tumors showed homogeneous high expression of AP2β whereas all controls showed only sporadic expression of the gene (Fig. 6D and Supplemental Fig 10A). Moreover, in line with a less differentiated state all PAX3-FOXO1 tumors were highly proliferative and were homogeneously positive for the proliferation marker MIB1, whereas all control tumors showed less proliferative state (Fig. 6E and Supplemental Fig 10B).

Discussion

Our study demonstrates that aRMS develop and progress via stochastic rather than hierarchical differentiation processes. It was already reported that the fusion oncogene PAX3-FOXO1 ensures aRMS cells survival [2, 3, 14] and hence its expression and transcriptional activity is crucial. Here we report for the first time that the fusion protein not only controls survival processes, but can also confers stem cell-like properties since it could contribute to reprogramming human fibroblasts. Moreover, we demonstrate that the differentiation inhibitory effect of PAX3-FOXO1 on the iPSC system is not restricted to the mesoderm lineage like in aRMS, but also to the endodermal and ectodermal lineages.

Rhabdomyosarcoma is the most common soft tissue cancer in childhood. Especially for the translocation positive aRMS the survival rates are low, and in cases of recurrence the disease is almost always fatal. Therefore, establishment of novel therapies is necessary for improving clinical outcome of aRMS patients. To this end, a fundamental and complex question in cancer research is to understand whether tumor heterogeneity arises from clonal evolution or from hierarchical evolution. We previously demonstrated that the fusion negative eRMS possess a small subpopulation of cells

with stem cell-like potential [50]. These cells were positive for the CSC marker CD133 and generated spheres, which were enriched for CSC as proved by the expression of the core stem cell factors and by the *in vivo* enhanced tumorigenic potential [50]. Three out of four CSC markers analyzed in this study were either highly abundant in the entire population or not expressed at all. Only ALDH1 distinguished a small subpopulation in all investigated cell lines. However, a conventional requirement for CSC is to be able to self-renew and generate identical and tumorigenic progeny but also to asymmetrically divide and give rise to non-tumorigenic cells. The ALDH1 high aRMS cells did not fulfill this prerequisite, thus indicating their non-CSC state. Another approach often used for identifying CSC is the sphere assay, which was employed in several cancers and among them also in eRMS [50]. We examined four different compositions of sphere media and among them also the one employed for eRMS spheres (data not shown) but only in the medium used in this study all aRMS cells formed spheres, which were able to self-renew for a prolonged period of time. Nevertheless, no enrichment of CSC and therefore no upregulation of the core stem cell genes was observed in the spheres when compared to cells cultured under standard conditions. In sum, aRMS cells highly express some CSC marker and are able to propagate under stem cell-like conditions. These observations lead to the hypothesis that aRMS possess high percentage of cells with tumor initiating potential. Limiting dilution and clonal analysis experiments performed in immunocompromised mice confirmed that 100 aRMS cells are sufficient for generating tumors and moreover all analyzed clones possess tumorigenic potential despite their heterogeneous origin. Thus, the *in vitro* and *in vivo* experiments reinforced the notion that aRMS in contrary to eRMS follow the clonal evolution model in which not only an exclusive subpopulation of cells but rather the entire population can propagate the tumor.

The core stem cell factors NANOG, OCT4, and SOX2 were reported in several tumors to be involved in promoting tumorigenesis, mainly acting on the regulation of the CSC population [22, 29]. In numerous malignancies high expression of these stem cell factors is associated with poor outcome [20, 41, 48]. On the other side, their ablation correlates with a decrease in the CSC population and a consequent reduction in the tumorigenic potential [9, 17, 55]. Interestingly, aRMS cells homogeneously express the core stem cell genes, although at very low level if compared to ESC and iPSC. Nevertheless, contrary to all other cancer types, silencing of the pluripotency factors in aRMS cells never influenced biological processes nor altered the expression of the chimeric protein or its target genes. Surprisingly, overexpression of NANOG, OCT4, and SOX2 did not induce de-differentiation of the cells like it was observed for instance for melanoma cells [28] but on the contrary it reduced the ability of aRMS cells to

form clones and spheres. Hence, forced expression of the stem cell genes did not confer enhanced stemness properties, but rather it reduced them, highlighting a gene dosage effect. In contrast to the pluripotency genes, as already reported [14, 26], downregulation of PAX3-FOXO1 immediately resulted in a strong upregulation of muscle differentiation factors, cell cycle arrest, and later apoptosis. Thus, PAX3-FOXO1 and not the stem cell factors is the key regulator in aRMS.

Due to the fact that silencing of the chimeric protein in aRMS cells results in cell death, a more permissive cell system is needed for better studying the function of PAX3-FOXO1. Ectopic expression of the chimeric protein is highly cell context-dependent. It was reported that high levels of PAX3-FOXO1 in immortalized mouse fibroblasts causes cell death [52] whereas high expression induces transformation in immortalized human myoblasts but only in combination with N-MYC [53]. Thus, finding the right context in which PAX3-FOXO1 can be studied is an urgent but challenging goal. Pluripotent iPSC possess a differentiation spectrum, which extends to all type of cells of the body, without restrictions. We therefore reasoned that the iPSC system could be used for better understanding the role of PAX3-FOXO1. Interestingly, we proved that not only is it possible to generate iPSC in the presence of the chimeric protein without inducing cell death, but its presence in collaboration with the four reprogramming factors enhances the efficiency of generating iPSC. Also, PAX3-FOXO1 could not replace one or more reprogramming factors, but showed an effect only in the presence of all four factors. These data highlight once more the context dependent influence of the chimeric protein. Further analyses during reprogramming processes are needed for determining which mechanisms and which PAX3-FOXO1 target genes contribute to the increased reprogramming efficiency. Nevertheless, these data confirm the stemness potential of PAX3-FOXO1. Additionally this system offers the opportunity to study processes which are very close to the early events of cancer progression and therefore it could facilitate the identification of early biomarkers or novel therapeutic pathways active in the initial stages of the disease.

Also confirming that iPSC represent a good model for studying the chimeric protein is the fact that PAX3-FOXO1 iPSC showed another typical aRMS feature: impaired differentiation potential. The fusion protein inhibited mesodermal differentiation and specifically skeletal muscle differentiation as already known for aRMS cells [8, 51]. We could further demonstrate for the first time that PAX3-FOXO1 can block also ectodermal and endodermal differentiation. Therefore it is possible that PAX3-FOXO1 guides processes involving complex networks of transcription factors and chromatin remodeling

proteins which finally lead to the activation or repression of tissue specific genes that are not only restricted to the mesodermal lineage. Corroborating this observation is also the fact that *in vivo*, once injected into immunocompromised mice, PAX3-FOXO1 iPSC generated highly undifferentiated and proliferating tumors. Nevertheless, these tumors were not aRMS tumors. Although, they still highly expressed the chimeric protein and its target gene AP2β, other aRMS specific markers like DESMIN and MYOGENIN were not detected. Genome wide analyses of these tumors are needed to elucidate their similarity to primary aRMS tumors and xenografts.

In conclusion, expanding the knowledge about PAX3-FOXO1 biology is an essential step for developing effective therapies for aRMS. Here for the first time we demonstrate that the iPSC system represents, in the absence of the aRMS cell of origin, an optimal strategy for studying tumor development and maintenance, which could be extended to other fusion-positive tumors.

References

1 Al-Hajj M, Wicha MS, Benito-Hernandez A, Morrison SJ, Clarke MF (2003). Prospective identification of tumorigenic breast cancer cells. *Proc Natl Acad Sci USA* **100:** 3983-3988.

2 Ayyanathan K, Fredericks WJ, Berking C, Herlyn M, Balakrishnan C, Gunther E *et al* (2000). Hormone-dependent tumor regression in vivo by an inducible transcriptional repressor directed at the PAX3-FKHR oncogene. *Cancer research* **60:** 5803-5814.

3 Bernasconi M, Remppis A, Fredericks WJ, Rauscher FJ, Schäfer BW (1996). Induction of apoptosis in rhabdomyosarcoma cells through down-regulation of PAX proteins. *Proceedings of the National Academy of Sciences of the United States of America* **93:** 13164-13169.

4 Bonnet D, Dick JE (1997). Human acute myeloid leukemia is organized as a hierarchy that originates from a primitive hematopoietic cell. *Nat Med* **3:** 730-737.

5 Bourguignon LYW (2008). Hyaluronan-mediated CD44 activation of RhoGTPase signaling and cytoskeleton function promotes tumor progression. *Semin Cancer Biol* **18:** 251-259.

6 Bourguignon LYW, Xia W, Wong G (2009). Hyaluronan-mediated CD44 interaction with p300 and SIRT1 regulates beta-catenin signaling and NFkappaB-specific transcription activity leading to MDR1 and Bcl-xL gene expression and chemoresistance in breast tumor cells. *J Biol Chem* **284:** 2657-2671.

7 Breneman JC, Lyden E, Pappo AS, Link MP, Anderson JR, Parham DM *et al* (2003). Prognostic factors and clinical outcomes in children and adolescents with metastatic rhabdomyosarcoma--a report from the Intergroup Rhabdomyosarcoma Study IV. *J Clin Oncol* **21:** 78-84.

8 Calhabeu F, Hayashi S, Morgan JE, Relaix F, Zammit PS (2012). Alveolar rhabdomyosarcoma-associated proteins PAX3/FOXO1A and PAX7/FOXO1A suppress the transcriptional activity of MyoD-target genes in muscle stem cells. *Oncogene*.

9 Chen S, Xu Y, Chen Y, Li X, Mou W, Wang L *et al* (2012). SOX2 gene regulates the transcriptional network of oncogenes and affects tumorigenesis of human lung cancer cells. *PLoS ONE* **7:** e36326.

10 D'Alterio C, Barbieri A, Portella L, Palma G, Polimeno M, Riccio A *et al* (2012). Inhibition of stromal CXCR4 impairs development of lung metastases. *Cancer Immunol Immunother* **61:** 1713-1720.

11 Davis RJ, Bennicelli JL, Macina RA, Nycum LM, Biegel JA, Barr FG (1995). Structural characterization of the FKHR gene and its rearrangement in alveolar rhabdomyosarcoma. *Hum Mol Genet* **4:** 2355-2362.

12 De Giovanni C, Landuzzi L, Nicoletti G, Lollini P-L, Nanni P (2009). Molecular and cellular biology of rhabdomyosarcoma. *Future Oncol* **5:** 1449-1475.

13 Dubrovska A, Hartung A, Bouchez LC, Walker JR, Reddy VA, Cho CY *et al* (2012). CXCR4 activation maintains a stem cell population in tamoxifen-resistant breast cancer cells through AhR signalling. *Br J Cancer* **107:** 43-52.

14 Ebauer M, Wachtel M, Niggli FK, Schäfer BW (2007). Comparative expression profiling identifies an in vivo target gene signature with TFAP2B as a mediator of the survival function of PAX3/FKHR. *Oncogene* **26:** 7267-7281.

15 Ferrandina G, Petrillo M, Bonanno G, Scambia G (2009). Targeting CD133 antigen in cancer. *Expert Opin Ther Targets* **13:** 823-837.

16 Fujii H, Honoki K, Tsujiuchi T, Kido A, Yoshitani K, Takakura Y (2009). Sphere-forming stem-like cell populations with drug resistance in human sarcoma cell lines. *Int J Oncol* **34:** 1381-1386.

17 Gangemi RMR, Griffero F, Marubbi D, Perera M, Capra MC, Malatesta P *et al* (2009). SOX2 silencing in glioblastoma tumor-initiating cells causes stop of proliferation and loss of tumorigenicity. *Stem cells (Dayton, Ohio)* **27:** 40-48.

18 Ginestier C, Hur MH, Charafe-Jauffret E, Monville F, Dutcher J, Brown M *et al* (2007). ALDH1 is a marker of normal and malignant human mammary stem cells and a predictor of poor clinical outcome. *Cell stem cell* **1:** 555-567.

19 Guo Y, Liu S, Wang P, Zhao S, Wang F, Bing L *et al* (2011). Expression profile of embryonic stem cell-associated genes Oct4, Sox2 and Nanog in human gliomas. *Histopathology* **59:** 763-775.

20 Han X, Fang X, Lou X, Hua D, Ding W, Foltz G *et al* (2012). Silencing SOX2 Induced Mesenchymal-Epithelial Transition and Its Expression Predicts Liver and Lymph Node Metastasis of CRC Patients. *PLoS ONE* **7:** e41335.

21 Honoki K, Fujii H, Kubo A, Kido A, Mori T, Tanaka Y *et al* (2010). Possible involvement of stem-like populations with elevated ALDH1 in sarcomas for chemotherapeutic drug resistance. *Oncol Rep* **24:** 501-505.

22 Jeter CR, Badeaux M, Choy G, Chandra D, Patrawala L, Liu C *et al* (2009). Functional evidence that the self-renewal gene NANOG regulates human tumor development. *Stem cells (Dayton, Ohio)* **27:** 993-1005.

23 Jiang F, Qiu Q, Khanna A, Todd NW, Deepak J, Xing L *et al* (2009). Aldehyde dehydrogenase 1 is a tumor stem cell-associated marker in lung cancer. *Mol Cancer Res* **7:** 330-338.

24 Jones RJ, Barber JP, Vala MS, Collector MI, Kaufmann SH, Ludeman SM *et al* (1995). Assessment of aldehyde dehydrogenase in viable cells. *Blood* **85:** 2742-2746.

25 Keller C, Arenkiel BR, Coffin CM, El-Bardeesy N, DePinho RA, Capecchi MR (2004). Alveolar rhabdomyosarcomas in conditional Pax3:Fkhr mice: cooperativity of Ink4a/ARF and Trp53 loss of function. *Genes & development* **18:** 2614-2626.

26 Kikuchi K, Tsuchiya K, Otabe O, Gotoh T, Tamura S, Katsumi Y *et al* (2008). Effects of PAX3-FKHR on malignant phenotypes in alveolar rhabdomyosarcoma. *Biochemical and biophysical research communications* **365:** 568-574.

27 Kryczek I, Liu S, Roh M, Vatan L, Szeliga W, Wei S *et al* (2012). Expression of aldehyde dehydrogenase and CD133 defines ovarian cancer stem cells. *Int J Cancer* **130:** 29-39.

28 Kumar SM, Liu S, Lu H, Zhang H, Zhang PJ, Gimotty PA *et al* (2012). Acquired cancer stem cell phenotypes through Oct4-mediated dedifferentiation. *Oncogene*.

29 Levings PP, McGarry SV, Currie TP, Nickerson DM, McClellan S, Ghivizzani SC *et al* (2009). Expression of an exogenous human Oct-4 promoter identifies tumor-initiating cells in osteosarcoma. *Cancer Res* **69:** 5648-5655.

30 Libura J, Drukala J, Majka M, Tomescu O, Navenot JM, Kucia M *et al* (2002). CXCR4-SDF-1 signaling is active in rhabdomyosarcoma cells and regulates locomotion, chemotaxis, and adhesion. *Blood* **100:** 2597-2606.

31 Liu G, Yuan X, Zeng Z, Tunici P, Ng H, Abdulkadir IR *et al* (2006). Analysis of gene expression and chemoresistance of CD133+ cancer stem cells in glioblastoma. *Mol Cancer* **5:** 67.

32 Magee JA, Piskounova E, Morrison SJ (2012). Cancer stem cells: impact, heterogeneity, and uncertainty. *Cancer Cell* **21:** 283-296.

33 Mercado GE, Barr FG (2007). Fusions involving PAX and FOX genes in the molecular pathogenesis of alveolar rhabdomyosarcoma: recent advances. *Curr Mol Med* **7:** 47-61.

34 Ognjanovic S, Linabery AM, Charbonneau B, Ross JA (2009). Trends in childhood rhabdomyosarcoma incidence and survival in the United States, 1975-2005. *Cancer* **115:** 4218-4226.

35 Panchision DM, Chen H-L, Pistollato F, Papini D, Ni H-T, Hawley TS (2007). Optimized flow cytometric analysis of central nervous system tissue reveals novel functional relationships among cells expressing CD133, CD15, and CD24. *Stem cells (Dayton, Ohio)* **25:** 1560-1570.

36 Parham DM, Ellison DA (2006). Rhabdomyosarcomas in adults and children: an update. *Arch Pathol Lab Med* **130:** 1454-1465.

37 Paulino AC, Okcu MF (2008). Rhabdomyosarcoma. *Curr Probl Cancer* **32:** 7-34.

38 Polyak K, Weinberg RA (2009). Transitions between epithelial and mesenchymal states: acquisition of malignant and stem cell traits. *Nat Rev Cancer* **9:** 265-273.

39 Ricci-Vitiani L, Lombardi DG, Pilozzi E, Biffoni M, Todaro M, Peschle C *et al* (2007). Identification and expansion of human colon-cancer-initiating cells. *Nature* **445:** 111-115.

40 Scheidler S, Fredericks WJ, Rauscher FJ, Barr FG, Vogt PK (1996). The hybrid PAX3-FKHR fusion protein of alveolar rhabdomyosarcoma transforms fibroblasts in culture. *Proceedings of the National Academy of Sciences of the United States of America* **93:** 9805-9809.

41 Siu MKY, Wong ESY, Kong DSH, Chan HY, Jiang L, Wong OGW *et al* (2012). Stem cell transcription factor NANOG controls cell migration and invasion via dysregulation of E-cadherin and FoxJ1 and contributes to adverse clinical outcome in ovarian cancers. *Oncogene*.

42 Sládek NE (2003). Human aldehyde dehydrogenases: potential pathological, pharmacological, and toxicological impact. *Journal of biochemical and molecular toxicology* **17:** 7-23.

43 Sorensen PHB, Lynch JC, Qualman SJ, Tirabosco R, Lim JF, Maurer HM *et al* (2002). PAX3-FKHR and PAX7-FKHR gene fusions are prognostic indicators in alveolar rhabdomyosarcoma: a report from the children's oncology group. *J Clin Oncol* **20:** 2672-2679.

44 Suvà M-L, Riggi N, Stehle J-C, Baumer K, Tercier S, Joseph J-M *et al* (2009). Identification of cancer stem cells in Ewing's sarcoma. *Cancer Res* **69:** 1776-1781.

45 Takahashi K, Yamanaka S (2006). Induction of pluripotent stem cells from mouse embryonic and adult fibroblast cultures by defined factors. *Cell* **126:** 663-676.

46 Takahashi K, Tanabe K, Ohnuki M, Narita M, Ichisaka T, Tomoda K *et al* (2007). Induction of pluripotent stem cells from adult human fibroblasts by defined factors. *Cell* **131:** 861-872.

47 Tomescu O, Xia SJ, Strezlecki D, Bennicelli JL, Ginsberg J, Pawel B *et al* (2004). Inducible short-term and stable long-term cell culture systems reveal that the PAX3-FKHR fusion oncoprotein regulates CXCR4, PAX3, and PAX7 expression. *Lab Invest* **84:** 1060-1070.

48 Tsai L-L, Yu C-C, Chang Y-C, Yu C-H, Chou M-Y (2011). Markedly increased Oct4 and Nanog expression correlates with cisplatin resistance in oral squamous cell carcinoma. *Journal of oral pathology & medicine : official publication of the International Association of Oral Pathologists and the American Academy of Oral Pathology* **40:** 621-628.

49 Visvader JE, Lindeman GJ (2008). Cancer stem cells in solid tumours: accumulating evidence and unresolved questions. *Nat Rev Cancer* **8:** 755-768.

50 Walter D, Satheesha S, Albrecht P, Bornhauser BC, D'Alessandro V, Oesch SM *et al* (2011). CD133 positive embryonal rhabdomyosarcoma stem-like cell population is enriched in rhabdospheres. *PLoS ONE* **6:** e19506.

51 Walters ZS, Villarejo-Balcells B, Olmos D, Buist TWS, Missiaglia E, Allen R *et al* (2013). JARID2 is a direct target of the PAX3-FOXO1 fusion protein and inhibits myogenic differentiation of rhabdomyosarcoma cells. *Oncogene*.

52 Xia SJ, Barr FG (2004). Analysis of the transforming and growth suppressive activities of the PAX3-FKHR oncoprotein. *Oncogene* **23:** 6864-6871.

53 Xia SJ, Holder DD, Pawel BR, Zhang C, Barr FG (2009). High expression of the PAX3-FKHR oncoprotein is required to promote tumorigenesis of human myoblasts. *The American journal of pathology* **175:** 2600-2608.

54 Yu J, Vodyanik MA, Smuga-Otto K, Antosiewicz-Bourget J, Frane JL, Tian S *et al* (2007). Induced pluripotent stem cell lines derived from human somatic cells. *Science (New York, NY)* **318:** 1917-1920.

55 Zbinden M, Duquet A, Lorente-Trigos A, Ngwabyt S-N, Borges I, Ruiz i Altaba A (2010). NANOG regulates glioma stem cells and is essential in vivo acting in a cross-functional network with GLI1 and p53. *The EMBO journal* **29:** 2659-2674.

56 Zou J, Maeder ML, Mali P, Pruett-Miller SM, Thibodeau-Beganny S, Chou B-K *et al* (2009). Gene targeting of a disease-related gene in human induced pluripotent stem and embryonic stem cells. *Cell stem cell* **5:** 97-110.

Figure legends

Figure 1:

No subpopulations of cancer stem cells in aRMS cell lines

(**A**) Sphere assay with RH4 line cultivated in sphere medium supplemented with bFGF or with bFGF, EGF, and PDGF (ALL) over several passages. Percentage of cells forming spheres was calculated at each passage (left panel). Expression of NANOG, OCT4, and SOX2 in spheres at passage 3, 4, and 5 compared to RH4 cells cultured as a monolayer (right panel). (**B-C-D**) Flow cytometry analysis of the CSC markers CD133 (antibody for epitope 1 and for epitope 2), CD44, and CXCR4 in aRMS cell lines. (**E**) Aldefluor assay and flow cytometry analysis for ALDH1 high cells in aRMS cell lines. (**F**) ALDH1 distribution of sorted ALDH1 high, low, and mixed population (control) from RH30 cell line after 10 days of culture. At day 3, 6, and 10 the percentage of ALDH1 positive cells was analyzed with Aldefluor assay and flow cytometry. (**G**) Expression analysis of sorted ALDH1 high cells compared to sorted ALDH1 low cells for the indicated genes. (**H-I**) Sphere assay with RH30 sorted ALDH1 high, low, and control fractions. Cells were cultured at clonal density in ALL-sphere medium and primary sphere formation (**H**) as well as self-renewal ability over 4 passages (**I**) was quantified. (**J**) ALDH1 analysis in RH30 cells after 72h of drug selection with Vincristine, Actinomycin D, and Mafosfamide. Viable cells were analyzed for ALDH1 activity by flow cytometry.

Figure 2:

aRMS cells express the core stem cell factors but only differential expression of PAX3-FOXO1 affects aRMS cellular physiology.

(**A**) Immunofluorescence for NANOG, OCT4, and SOX2 in RH3 cell line. (**B**) RNA expression analysis for the indicated genes upon 72h of SOX2 silencing with three specific siRNAs in RH3 and RH4 cell lines. Fold changes are calculated compared to cells treated with scrambled siRNA. Knockdown with siRNA 3-siSOX2 was confirmed at protein level (siSc = siScrambled; siS = 3-siSOX2). (**C**) RNA expression analysis for the indicated genes upon 72h of silencing of PAX3-FOXO1 in RH3 and RH4 cell lines. Fold changes are calculated compared to cells treated with scrambled siRNA. (**D**) Cell viability measurements (WST-1 assay) upon 48h and 72h of knockdown of PAX3-FOXO1 (siP3F), NANOG, OCT4, and SOX2 in RH4 cells. Percentage of viable cells was calculated compared to scrambled cells (siScr). (**E**) Cell proliferation assay (BrdU incorporation) after 48h and 72h of PAX3-FOXO1, NANOG, OCT4, and SOX2 knockdown in RH4 cells. (**F**) Flow cytometric analysis of RH4 cell cycle distributions using propidium iodide (PI) upon silencing of PAX3-FOXO1 (siP3F), NANOG,

OCT4, and SOX2 for the indicated time. (**G**) RNA expression analysis for the indicated genes in RH4 cell lines stably overexpressing EGFP (control), NANOG, OCT4, SOX2, or the three stem cell genes simultaneously (NOS). Fold changes are calculated compared to EGFP control line. (**H**) Proliferation assay (BrdU incorporation) in RH4 transgenic lines overexpressing the stem cell genes. Percentages are calculated relative to EGFP control line. (**I**) Clonogenic assay with RH4 transgenic cell lines overexpressing the stem cell genes. Clones were stained with crystal violet and quantified. (**J**) Primary sphere formation with transgenic RH4 cell lines overexpressing the stem cell genes. (**K**) Sphere assay with RH4 lines overexpressing the stem cell genes. (unpaired t-test, *** $p<0.0005$; ** $p<0.005$, *$p<0.05$)

Figure 3:

High frequency of tumor initiating cells in aRMS cell lines

(**A**) *In vivo* limiting dilution with RH30 cell line. 10^5 (n=3), 10^4 (n=4), and 100 cells (n=5) were injected intramuscularly (i.m.) into the left leg of NOD/Scid mice. Tumor growth was monitored over a period of 180 days. (**B**) Heat map of qRT-PCR of total RNA relative to GAPDH from RH30 clones generated from one cell. Sixteen clones were analyzed for the expression of the indicated genes. Scale bar $\ln(2^{-\Delta Ct})$. (**C**) Generation of primary and secondary xenografts with 8 selected RH30 clones. For primary xenograft generation $5x10^4$ cells were injected i.m into the left leg of NOD/Scid mice (n=4). Single cell suspensions (10^4 cells) of primary tumors were injected i.m into mice (n=2) for secondary tumor formation. (**D**) Immunohistochemical staining of primary (I) and secondary (II) xenograft sections of four clones. Tumors were stained with H&E and the aRMS markers MYOGENIN and DESMIN.

Figure 4:

PAX3-FOXO1 enhances generation of induced pluripotent stem cells

(**A**) Quantification of colonies of iPSC generated from human fibroblast (HFF) transduced with the four Yamanaka's factors plus either PAX3-FOXO1 or EGFP (control). (**B**) Representative image of control and PAX3-FOXO1 iPSC colony. (**C**) Immunofluorescence of control and PAX3-FOXO1 iPSC for the pluripotency markers OCT4, SSEA4 (upper panel) and NANOG, TRA60 (lower panel). Nuclei were counterstained with Hoechst (blue). Total amount of single or double positive colonies was quantified (right panel). (**D**) RNA expression of PAX3-FOXO1 and AP2β in iPSC clone 1, clone 5, 6, and 25 (upper panel) compared to HFF prior transduction. Genomic PCR (lower panel) for PAX3-FOXO1 in the same clones (+ = positive control, - = negative control). (**E**) Expression analysis compared to HFF

for pluripotency factors NANOG and DNMT3β in PAX3-FOXO1 clone 1 and in the wild type clones 5, 6, and 25. (**F**) Immunofluorescence of the pluripotency marker SSEA4 and for PAX3-FOXO1 target gene AP2β in wild type clone 6 and in PAX3-FOXO1 clone 1. Nuclei were counterstained with Hoechst. (unpaired t-test, * p< 0.05)

Figure 5:

PAX3-FOXO1 blocks *in vitro* differentiation of iPSC

(**A**) Representative image of embryoid bodies (EB) generated from wild type clone 6 iPSC (control) and from PAX3-FOXO1 expressing clone 1 (5x magnification). (**B**) Expression analysis of the indicated differentiation markers for endoderm, mesoderm, and ectoderm in EB. Fold changes are calculated compared to undifferentiated iPSC from wild type clone 6. (**C-D**) Muscle differentiation: representative picture of muscle differentiating cells (**C**). Arrows indicate multinucleated myoblasts. Cells are counterstained with Hoechst and PHALLOIDIN. qRT-PCR analysis for mesoderm and muscle differentiation markers (**F**) after 14 days of culture with 15% serum (+ FBS) and after additionally 21 days of culture with 1% serum (-FBS). (**E-F**) Endoderm differentiation: immunofluorescence staining for the pancreatic marker AMYLASE (**E**). Cells are counterstained with Hoechst and PHALLOIDIN. qRT-PCR analysis for endoderm markers (**F**) for control and PAX3-FOXO1 differentiated cells compared to undifferentiated iPSC clone 6. **G-H** Neural differentiation: immunofluorescence staining for GFAP and 3βTUBULIN for differentiated control and PAX3-FOXO1 cells (**G**). qRT-PCR analysis for ectodermal and neural differentiation markers (**H**) for control and PAX3-FOXO1 differentiated cells compared to undifferentiated iPSC clone 6.

Figure 6:

PAX3-FOXO1 iPSC generate undifferentiated and highly proliferative teratomas

(**A**) Histological analysis of teratomas generated after subcutaneously (s.c) injections of $1x10^6$ iPSC from control clones 6, 5, and 25. Sections were stained with H&E. Represented are derivatives of the three germ layers. (→ endoderm, * mesoderm, ° ectoderm). (**B**) Histological analysis of teratoma generated from s.c. injections of $1x10^6$ iPSC from PAX3-FOXO1 clone 1. Sections were stained with H&E. Represented are three magnifications of the tumor. (**C**) qRT-PCR of total RNA relative to undifferentiated clone 6 iPSC for PAX3-FOXO1 and its target gene in control and PAX3-FOXO1 teratomas. (**D**) Immunohistochemical staining for AP2β in control and PAX3-FOXO1 teratomas. (**E**) Immunohistochemical analysis of proliferation marker MIB1 in control and PAX3-FOXO1 teratoma. (**F**)

Tumor growth analysis of control clone 6 iPSC and PAX3-FOXO1 iPSC. $3x10^6$ cells were injected s.c. and tumor growth was weekly monitored.

SUPPLEMENTAL FIGURES

Supplemental figure 1:

No CSC enrichment in spheres generated from RH30 and RMS13 aRMS cell lines

(**A-B**) Sphere assay with RH30 (**A**) and RMS13 (**B**) cell lines cultivated at clonal dilution in sphere medium supplemented with bFGF or with bFGF, EGF, and PDGF (ALL) over several passages. Percentage of cells forming spheres was calculated at each passage (left panel). Expression of NANOG, OCT4, and SOX2 was analyzed by qRT-PCR from total RNA of spheres at passage 3, 4, and 5 and compared with the same cell lines cultured as a monolayer (right panel).

Supplemental figure 2:

Sorting of ALDH1 high and ALDH1 low fraction

(**A**) RH30 cells were stained with Aldefluor kit and ALDH1 high, low, and mixed population (control) were sorted by FACS. In black are depicted cells treated with DEAB, which were used for set up the gating.

Supplemental figure 3:

Expression of ESC genes in aRMS cell lines

(**A-B-C**) Immunofluorescence for the stem cell genes NANOG (**A**), OCT4 (**B**), and SOX2 (**C**) in 7 aRMS cell lines (upper panel). Basal level RNA expression relative to GAPDH for the stem cell genes in the indicated aRMS cell lines (lower panel).

Supplemental figure 4:

Characterization of aRMS cell lines overexpressing ESC genes

(**A**) Western blot analysis for RH4 and RH30 cell lines stably overexpressing NANOG, OCT4, SOX2, or the three genes simultaneously (NOS). The embryonic carcinoma line NTERA-2 was used as a positive control. (GFP = EGFP cell line, N = NANOG overexpressing cell line, O = OCT4 overexpressing cell line, S = SOX2 overexpressing cell line, NT2 = NTERA-2). (**B**) RNA expression analysis for the indicated genes in RH30 cell lines stably overexpressing EGFP (control), NANOG, OCT4, SOX2, or NOS. Fold changes are calculated compared to the EGFP control line. (**C**)

Proliferation assay (BrdU incorporation) for RH30 transgenic lines overexpressing the stem cell genes. Percentages are calculated compared to EGFP control line. (**D**) Clonogenic assay with RH30 transgenic cell lines overexpressing the stem cell genes. Clones were stained with crystal violet and quantified. (**E**) Primary sphere formation with transgenic RH30 cell lines overexpressing the stem cell genes. (**F**) Sphere assay with RH30 transgenic lines overexpressing the stem cell genes. At each passage the number of spheres was quantified. (unpaired t-test, * $p<0.01$, ** $p<0.05$, ***$p<0.0005$)

Supplemental figure 5:

Alveolar Rhabdomyosarcoma follows the clonal evolution model

A Immunohistochemical analysis of xenografts generated from RH30 cell lines after injection of 10^5, 10^4, and 100 cells. Tumors were stained with H&E and the aRMS markers MYOGENIN and DESMIN. **B-C** Tumor growth of clones generated from one RH30 cell. For primary xenograft generation (**B**) NOD/Scid mice (n=4) were injected with $5x10^4$ cells. For secondary xenograft generation (**C**) NOD/Scid mice (n=2) were injected with $1x10^4$ cells.

Supplemental figure 6:

PAX3-FOXO1 increases reprogramming efficiency of human fibroblast

(**A**) Gene expression analysis for the indicated genes 5 days post-transduction of human fibroblast (HFF) with OCT4, SOX2, KLF4, c-MYC, and either PAX3-FOXO1 or EGFP (control). Fold changes are calculated compared to HFF before transduction. (**B**) Immunofluorescence staining and quantification for the pluripotency factors NANOG, SSEA4 (upper panel) and OCT4, TRA60 (lower panel) in control and PAX3-FOXO1 iPSC. Nuclei were counterstained with Hoechst.

Supplemental figure 7:

PAX3-FOXO1 increases reprogramming efficiency of human fibroblast only in the presence of c-MYC

(**A**) Gene expression analysis for the indicated genes 5 days post-transduction of human fibroblast (HFF) with OCT4, SOX2, KLF4, and either PAX3-FOXO1 or EGFP (control). Fold changes are calculated compared to HFF before transduction. (**B**) Quantification of induced pluripotent stem cell (iPSC) colonies in fibroblast transduced with OCT4, SOX2, KLF4, and either EGFP (control) or PAX3-FOXO1. (unpaired t-test, * $p<0.05$)

Supplemental figure 8:

Wild type and PAX3-FOXO1 clones express NANOG and OCT4

(**A-B**) Immunofluorescence analysis for OCT4 (**A**) and NANOG (**B**) in wild type iPSC (clone 5, 6 and 25) and in PAX3-FOXO1 expressing clone 1. Nuclei were counterstained with Hoechst.

Supplemental figure 9:

PAX3-FOXO1 transgene is expressed in differentiating iPSC

(**A)** qRT-PCR for pluripotency markers, PAX3-FOXO1 and AP2β in embryoid bodies (EB). Fold changes are calculated compared to undifferentiated iPSC from wild type clone 6. (**B**) Representative image of attached EB cultured for 14 days in muscle differentiation medium supplemented with FBS. (**C-D**) qRT-PCR for PAX3-FOXO1 and AP2 in cells cultured either for 14 days under muscle differentiation conditions in the presence of serum (**C**) or for additional 21 days in the absence of serum (**D**). Fold changes are calculated compared to undifferentiated iPSC from wild type clone 6. (**E**) qRT-PCR for PAX3-FOXO1 and its target gene in cells differentiated towards endoderm lineages. Fold changes are calculated compared to undifferentiated iPSC from wild type clone 6. (**F**) qRT-PCR for PAX3-FOXO1 and its target gene AP2β after neural differentiation.

Supplemental figure 10:

PAX3-FOXO1 tumors express AP2β and are highly proliferating

(**A**) Immunohistochemical analysis for AP2β expression in wild type teratomas (clone 5 and 6) and PAX3-FOXO1 clone 1 tumors injected either subcutaneously (s.c.) or intramuscularly (i.m.). For PAX3-FOXO1 clone 1 i.m. two tumors are showed isolated from two mice marked as left (L) and right (R). (**B**) Immunohistochemical staining fro the proliferation marker MIB1 in control teratomas and PAX3-FOXO1 clone 1 tumors.

FIGURE 1

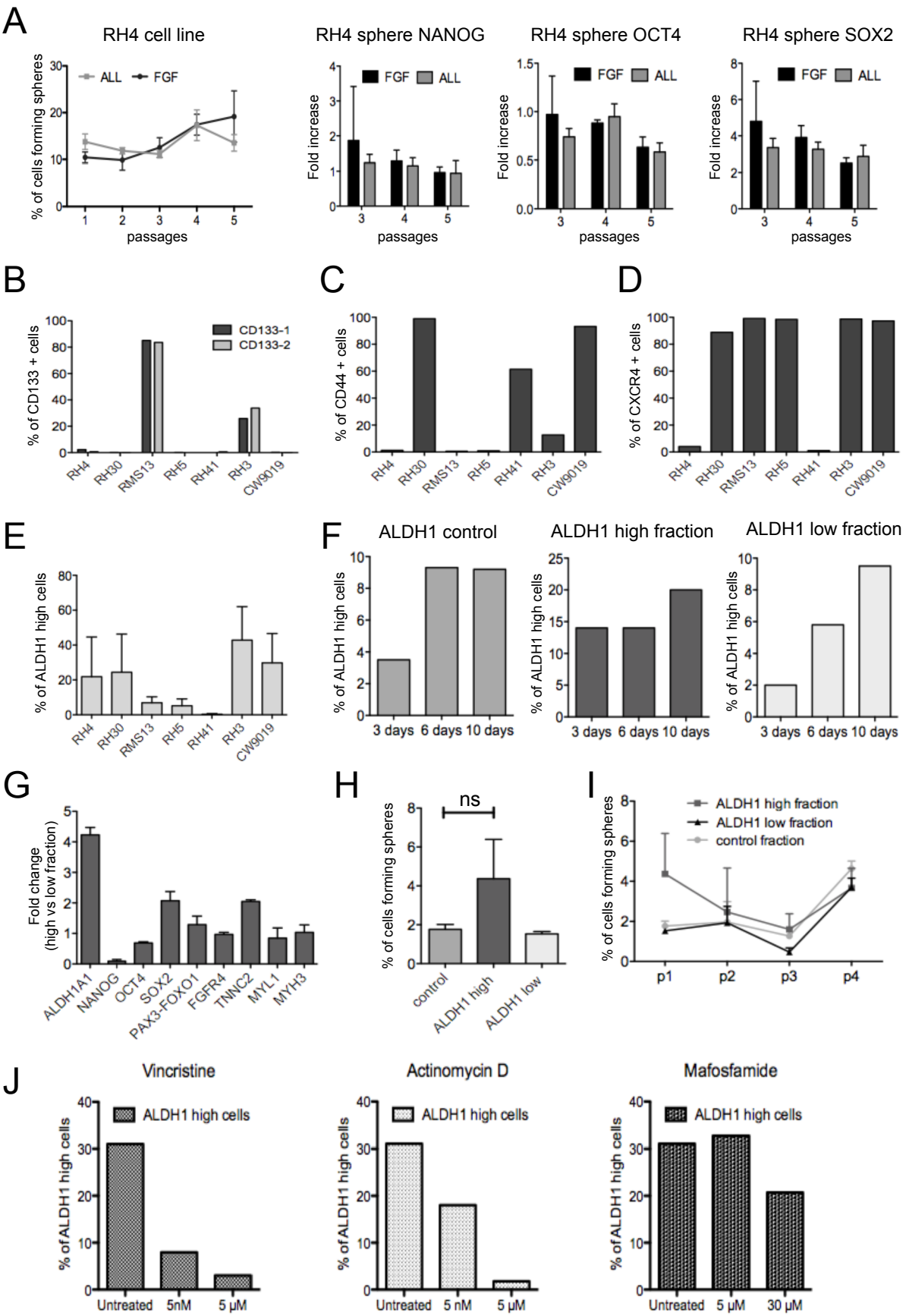
A
RH4 cell line
% of cells forming spheres
ALL
FGF
passages
RH4 sphere NANOG
RH4 sphere OCT4
RH4 sphere SOX2
Fold increase
B
% of CD133 + cells
CD133-1
CD133-2
C
% of CD44 + cells
D
% of CXCR4 + cells
RH4
RH30
RMS13
RH5
RH41
RH3
CW9019
E
% of ALDH1 high cells
F
ALDH1 control
ALDH1 high fraction
ALDH1 low fraction
3 days
6 days
10 days
G
Fold change
(high vs low fraction)
ALDH1A1
NANOG
OCT4
SOX2
PAX3-FOXO1
FGFR4
TNNC2
MYL1
MYH3
H
ns
control
ALDH1 high
ALDH1 low
I
ALDH1 high fraction
ALDH1 low fraction
control fraction
p1
p2
p3
p4
J
Vincristine
Actinomycin D
Mafosfamide
ALDH1 high cells
Untreated
5nM
5 nM
5 µM
30 µM

FIGURE 2

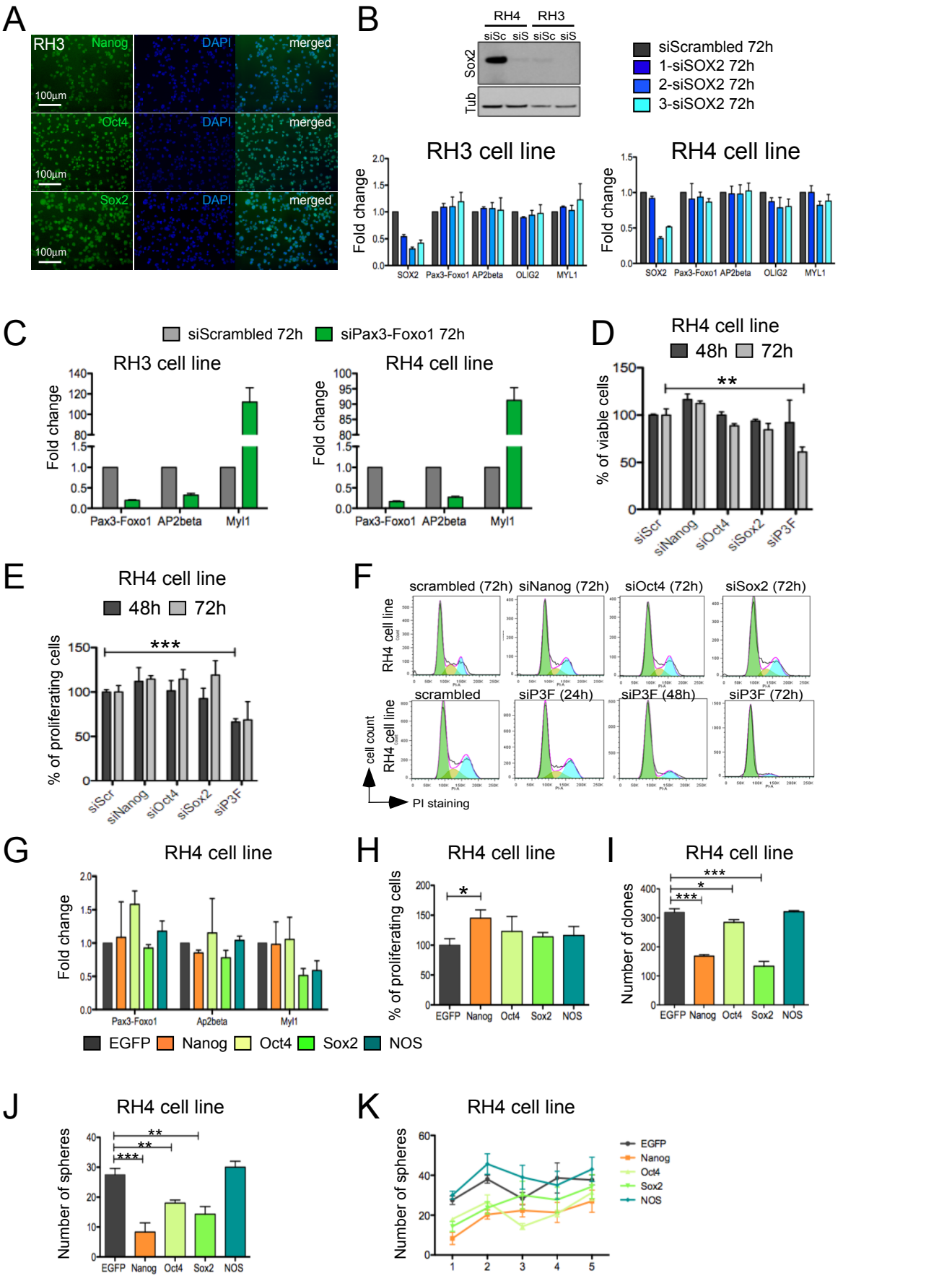
A
RH3
Nanog
DAPI
merged
100µm
Oct4
Sox2
B
RH4
RH3
siSc siS siSc siS
Sox2
Tub
siScrambled 72h
1-siSOX2 72h
2-siSOX2 72h
3-siSOX2 72h
RH3 cell line
RH4 cell line
Fold change
SOX2 Pax3-Foxo1 AP2beta OLIG2 MYL1
C
siScrambled 72h
siPax3-Foxo1 72h
RH3 cell line
RH4 cell line
Fold change
Pax3-Foxo1 AP2beta Myl1
D
RH4 cell line
48h 72h
% of viable cells
**
siScr siNanog siOct4 siSox2 siP3F
E
RH4 cell line
48h 72h
% of proliferating cells
***
siScr siNanog siOct4 siSox2 siP3F
F
scrambled (72h)
siNanog (72h)
siOct4 (72h)
siSox2 (72h)
RH4 cell line
scrambled
siP3F (24h)
siP3F (48h)
siP3F (72h)
cell count
PI staining
G
RH4 cell line
Fold change
Pax3-Foxo1 Ap2beta Myl1
EGFP Nanog Oct4 Sox2 NOS
H
RH4 cell line
% of proliferating cells
*
EGFP Nanog Oct4 Sox2 NOS
I
RH4 cell line
Number of clones
***
*
***
EGFP Nanog Oct4 Sox2 NOS
J
RH4 cell line
Number of spheres
**
**
***
EGFP Nanog Oct4 Sox2 NOS
K
RH4 cell line
Number of spheres
EGFP
Nanog
Oct4
Sox2
NOS

FIGURE 3

A

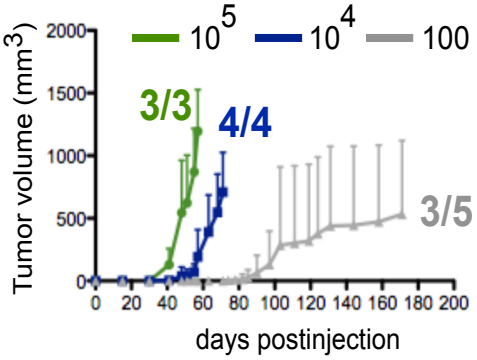

B

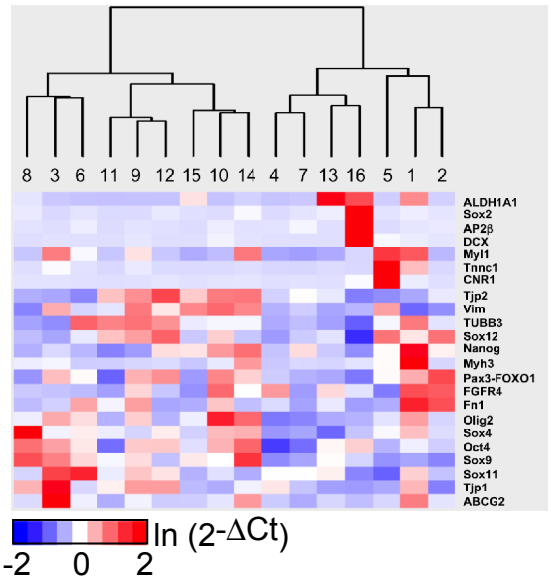

C

clone number	PRIMARY xenograft/ injection (50'000cells)	SECONDARY xenograft/ injection (10'000cells)
clone 1	4/4	1/1
clone 3	4/4	not performed
clone 5	4/4	not performed
cone 7	4/4	2/2
clone 8	4/4	2/2
clone 9	4/4	2/2
clone 14	4/4	2/2
clone 16	4/4	2/2

D

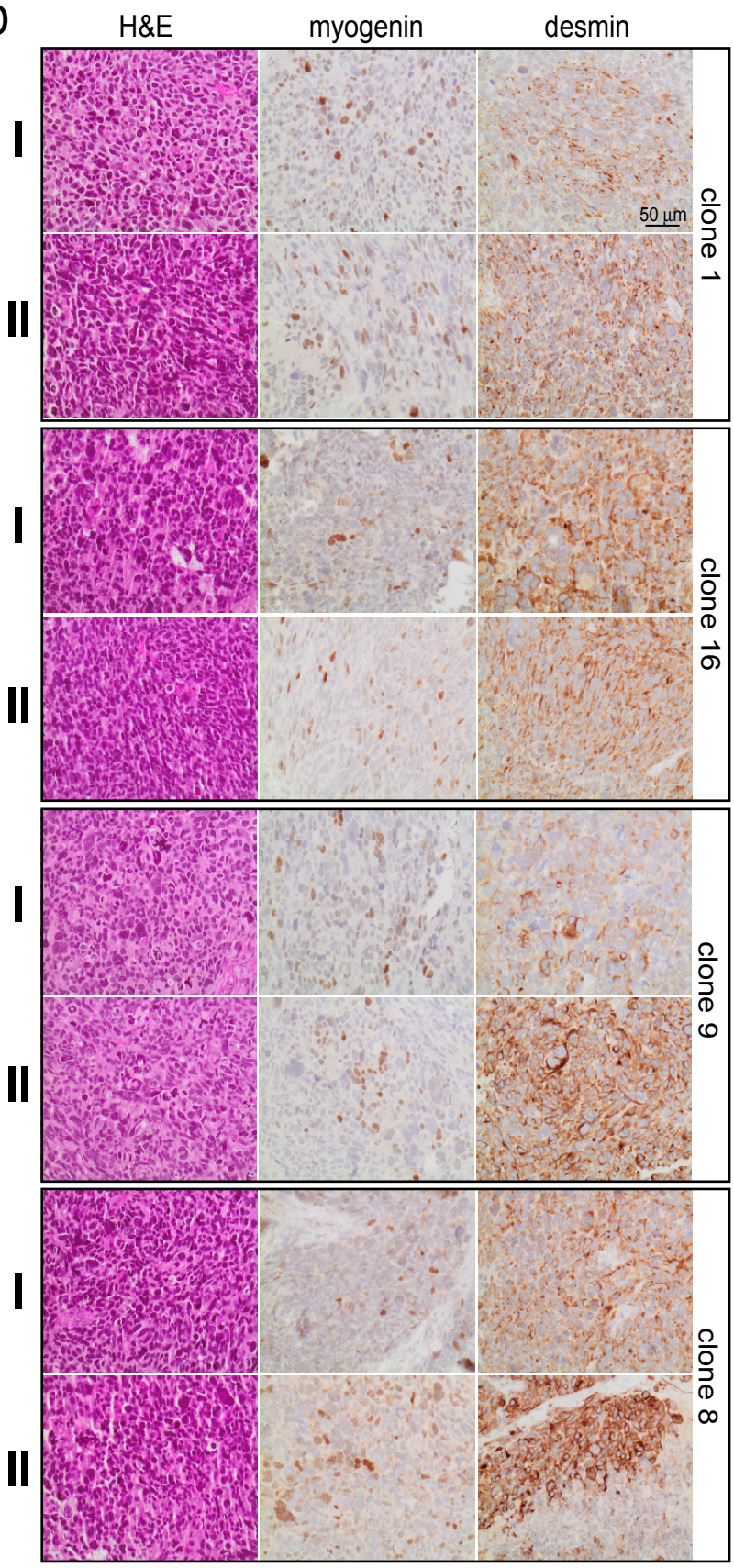

FIGURE 4

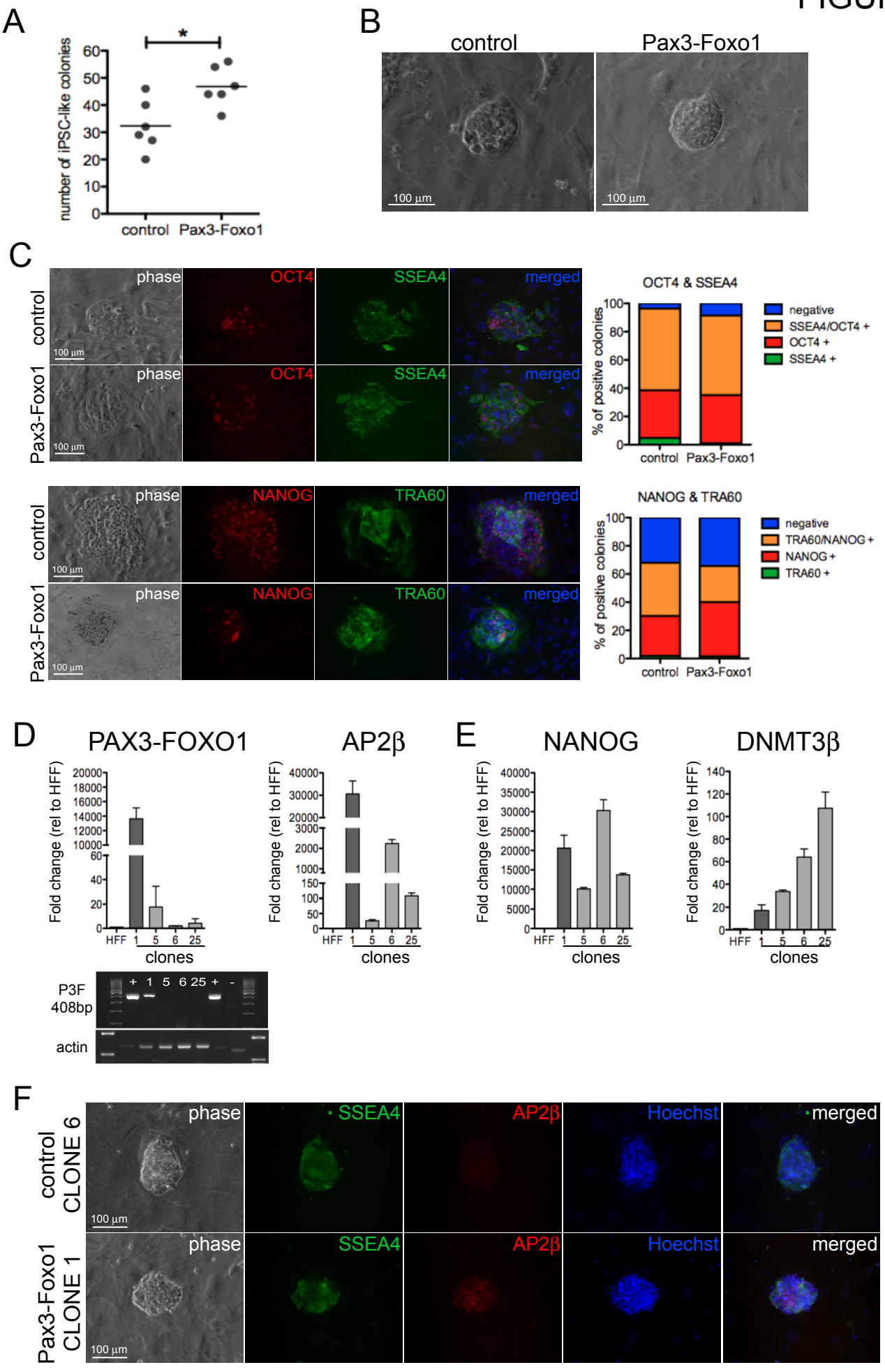
A
number of iPSC-like colonies
control
Pax3-Foxo1
B
control
Pax3-Foxo1
100 µm
C
phase
OCT4
SSEA4
merged
control
Pax3-Foxo1
OCT4 & SSEA4
% of positive colonies
negative
SSEA4/OCT4 +
OCT4 +
SSEA4 +
NANOG
TRA60
NANOG & TRA60
TRA60/NANOG +
NANOG +
TRA60 +
D
PAX3-FOXO1
AP2β
Fold change (rel to HFF)
HFF 1 5 6 25
clones
P3F 408bp
actin
E
NANOG
DNMT3β
F
control CLONE 6
Pax3-Foxo1 CLONE 1
Hoechst

FIGURE 5

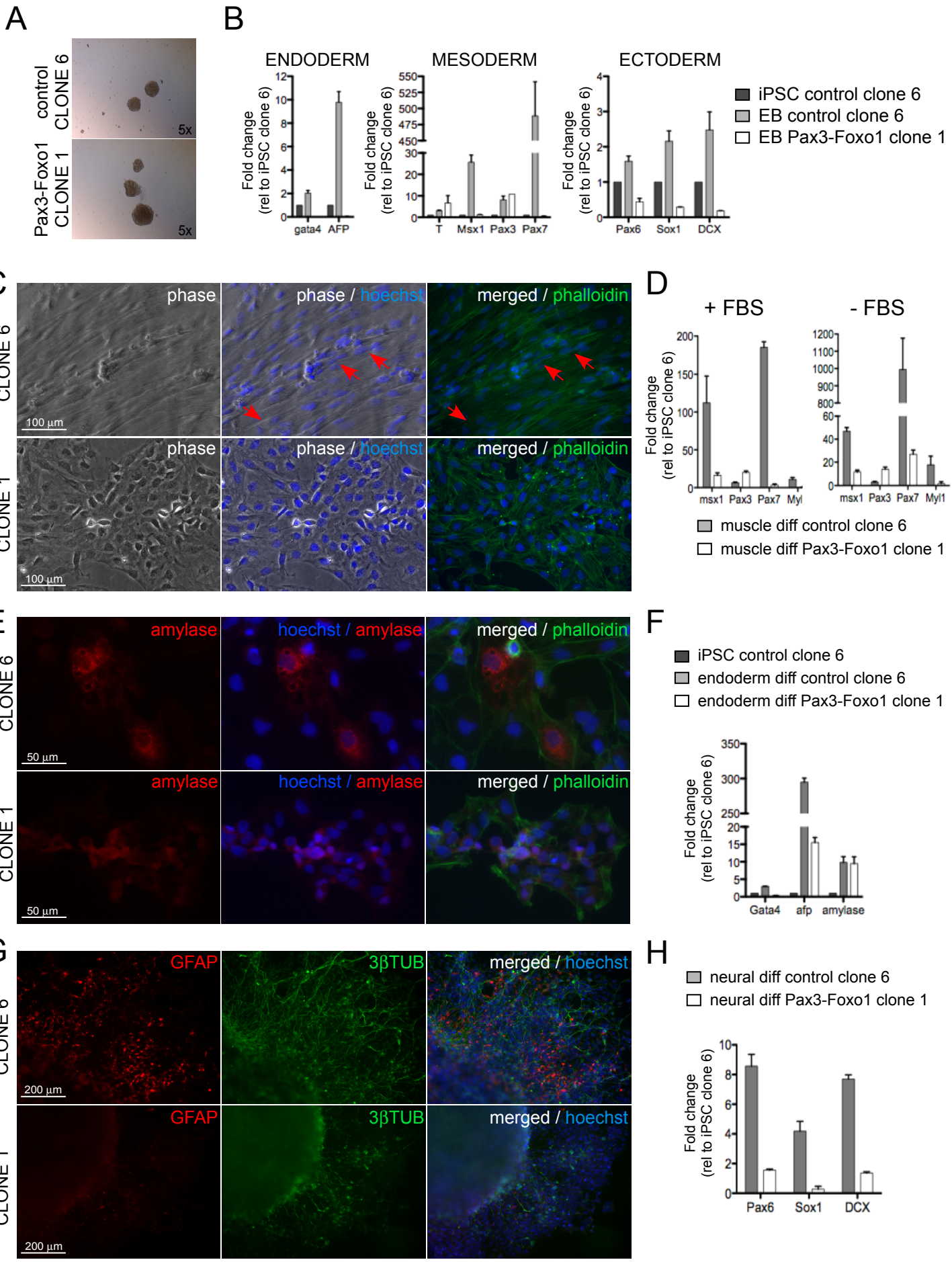
A
control CLONE 6
Pax3-Foxo1 CLONE 1
5x
5x
B
ENDODERM
MESODERM
ECTODERM
Fold change (rel to iPSC clone 6)
gata4 AFP
T Msx1 Pax3 Pax7
Pax6 Sox1 DCX
iPSC control clone 6
EB control clone 6
EB Pax3-Foxo1 clone 1
C
control CLONE 6
Pax3-Foxo1 CLONE 1
phase
phase / hoechst
merged / phalloidin
100 µm
D
+ FBS
- FBS
Fold change (rel to iPSC clone 6)
msx1 Pax3 Pax7 Myl
muscle diff control clone 6
muscle diff Pax3-Foxo1 clone 1
E
amylase
hoechst / amylase
merged / phalloidin
50 µm
F
iPSC control clone 6
endoderm diff control clone 6
endoderm diff Pax3-Foxo1 clone 1
Gata4 afp amylase
G
GFAP
3βTUB
merged / hoechst
200 µm
H
neural diff control clone 6
neural diff Pax3-Foxo1 clone 1
Pax6 Sox1 DCX

FIGURE 6

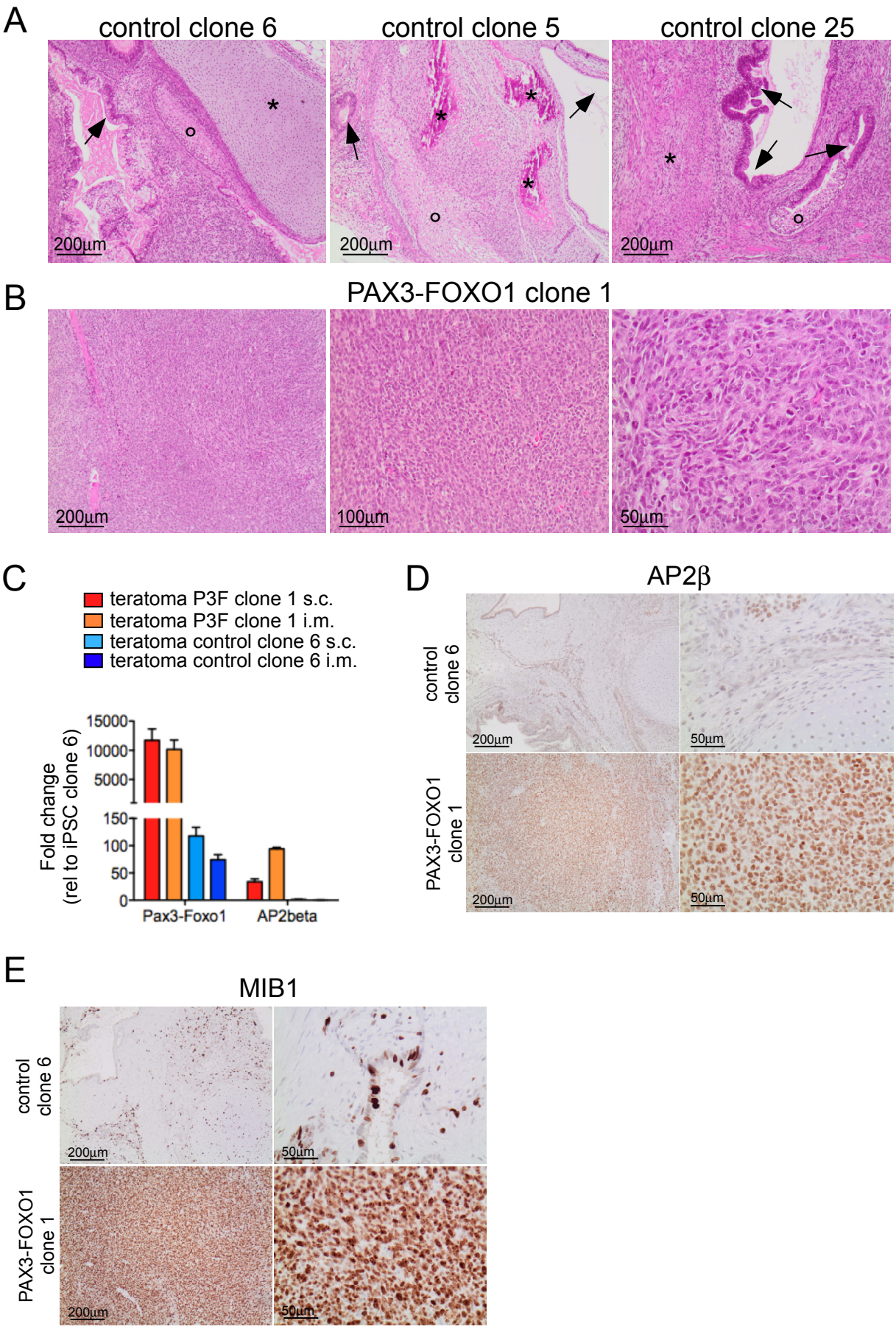
A
control clone 6
control clone 5
control clone 25
200µm
200µm
200µm
B
PAX3-FOXO1 clone 1
200µm
100µm
50µm
C
teratoma P3F clone 1 s.c.
teratoma P3F clone 1 i.m.
teratoma control clone 6 s.c.
teratoma control clone 6 i.m.
Fold change (rel to iPSC clone 6)
15000
10000
5000
150
100
50
0
Pax3-Foxo1
AP2beta
D
AP2β
control clone 6
PAX3-FOXO1 clone 1
200µm
50µm
200µm
50µm
E
MIB1
control clone 6
PAX3-FOXO1 clone 1
200µm
50µm
200µm
50µm

SUPPL FIG 1

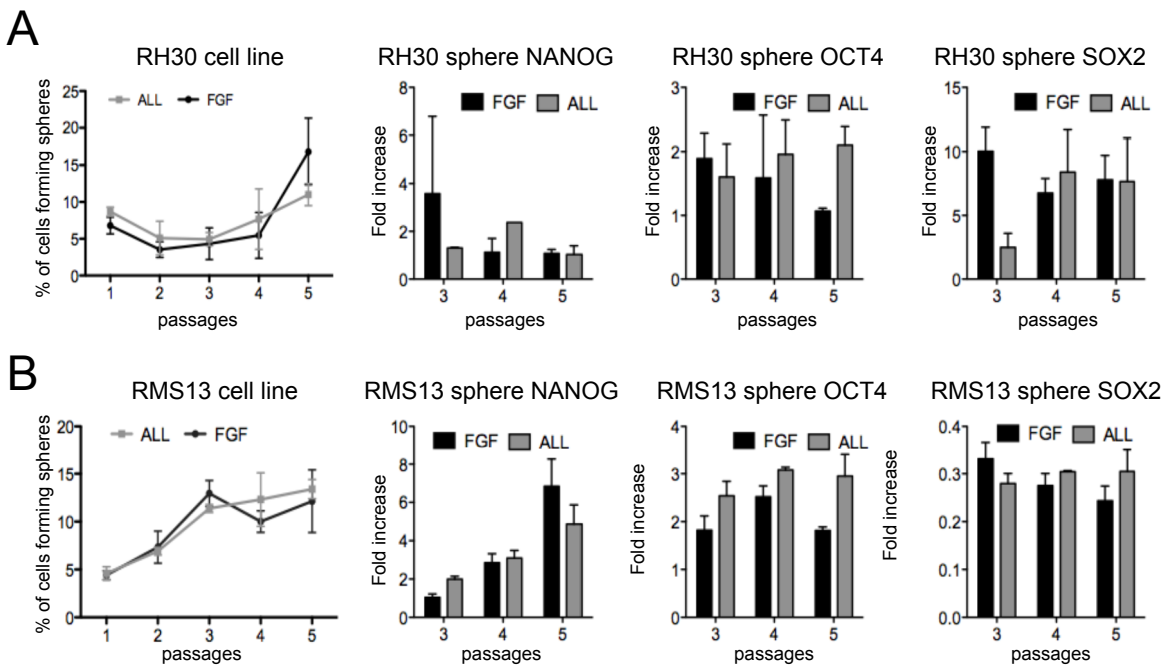
A
RH30 cell line
% of cells forming spheres
ALL
FGF
passages
RH30 sphere NANOG
Fold increase
FGF
ALL
passages
RH30 sphere OCT4
Fold increase
FGF
ALL
passages
RH30 sphere SOX2
Fold increase
FGF
ALL
passages
B
RMS13 cell line
% of cells forming spheres
ALL
FGF
passages
RMS13 sphere NANOG
Fold increase
FGF
ALL
passages
RMS13 sphere OCT4
Fold increase
FGF
ALL
passages
RMS13 sphere SOX2
Fold increase
FGF
ALL
passages

SUPPL FIG 2

A

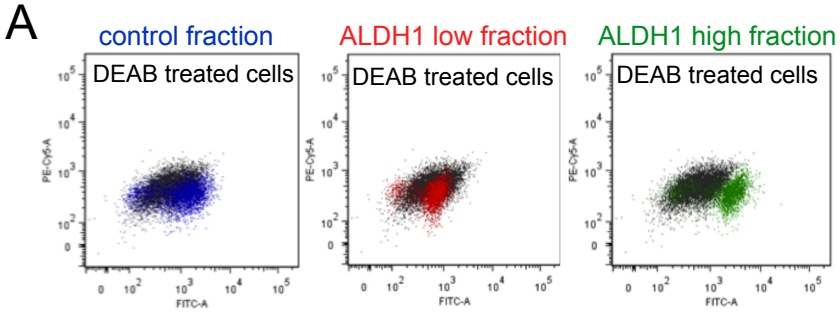
control fraction
ALDH1 low fraction
ALDH1 high fraction
DEAB treated cells
DEAB treated cells
DEAB treated cells
PE-Cy5-A
FITC-A

SUPPL FIG 3A

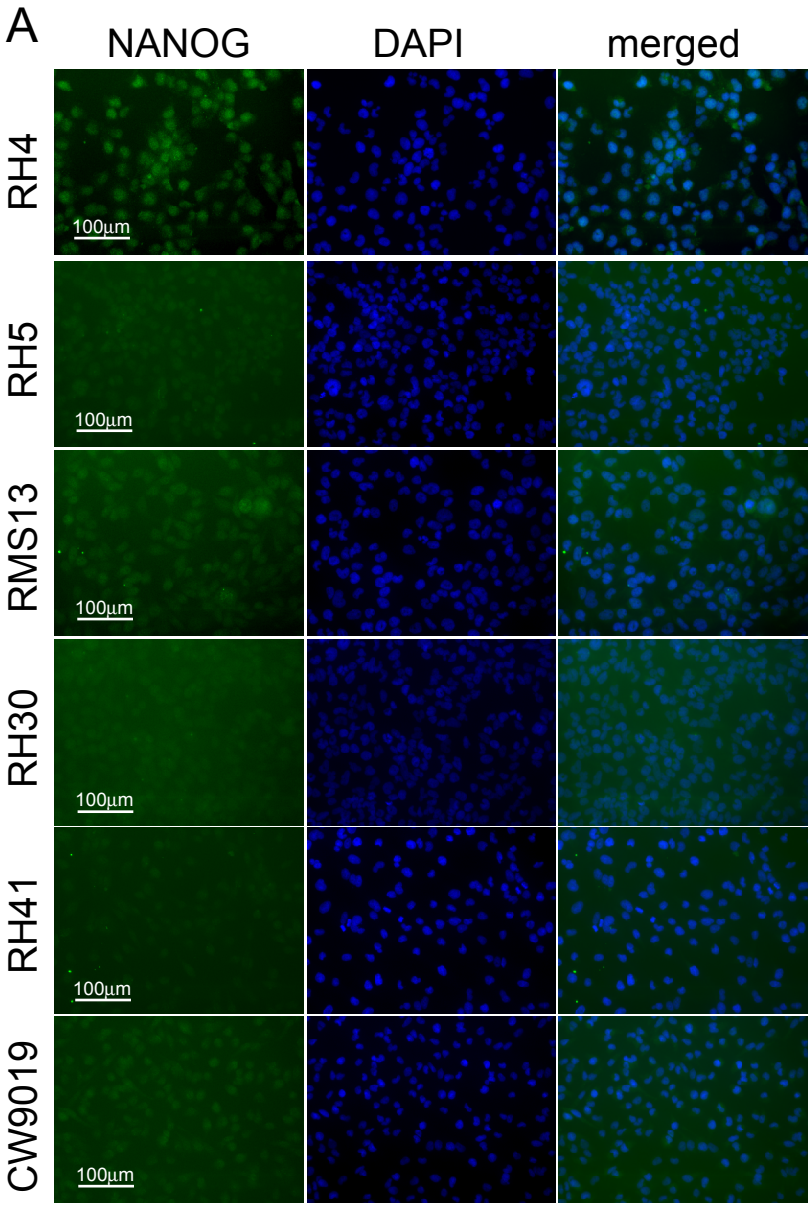
A
NANOG
DAPI
merged
RH4
RH5
RMS13
RH30
RH41
CW9019
100µm

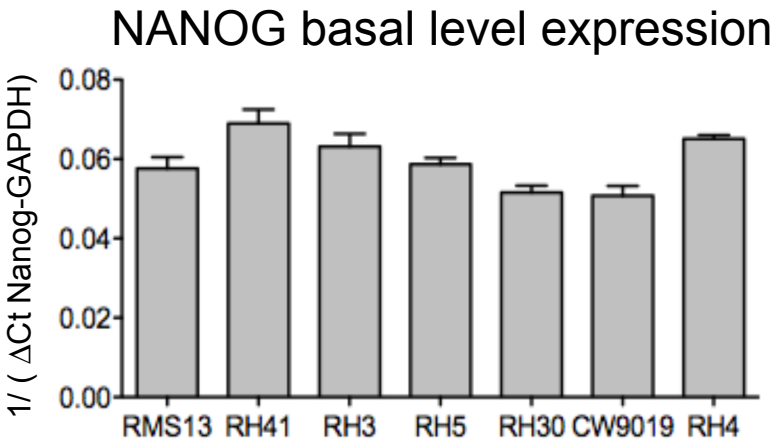
NANOG basal level expression
1/ (ΔCt Nanog-GAPDH)
0.08
0.06
0.04
0.02
0.00
RMS13
RH41
RH3
RH5
RH30
CW9019
RH4

SUPPL FIG 3B

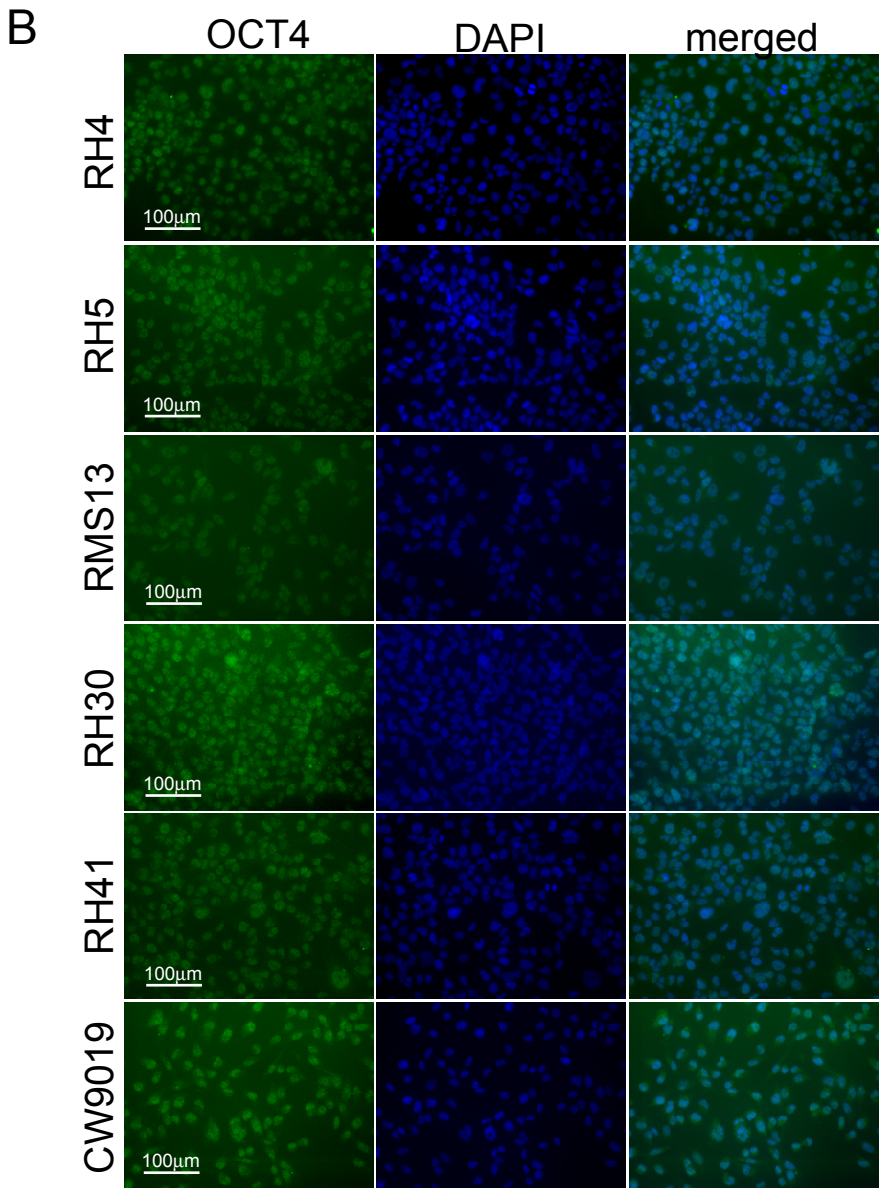
B
OCT4
DAPI
merged
RH4
RH5
RMS13
RH30
RH41
CW9019
100µm

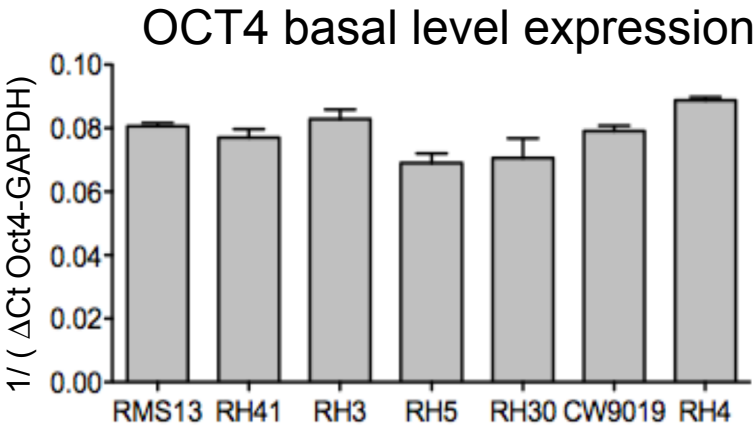
OCT4 basal level expression
1/ (ΔCt Oct4-GAPDH)
0.10
0.08
0.06
0.04
0.02
0.00
RMS13
RH41
RH3
RH5
RH30
CW9019
RH4

SUPPL FIG 3C

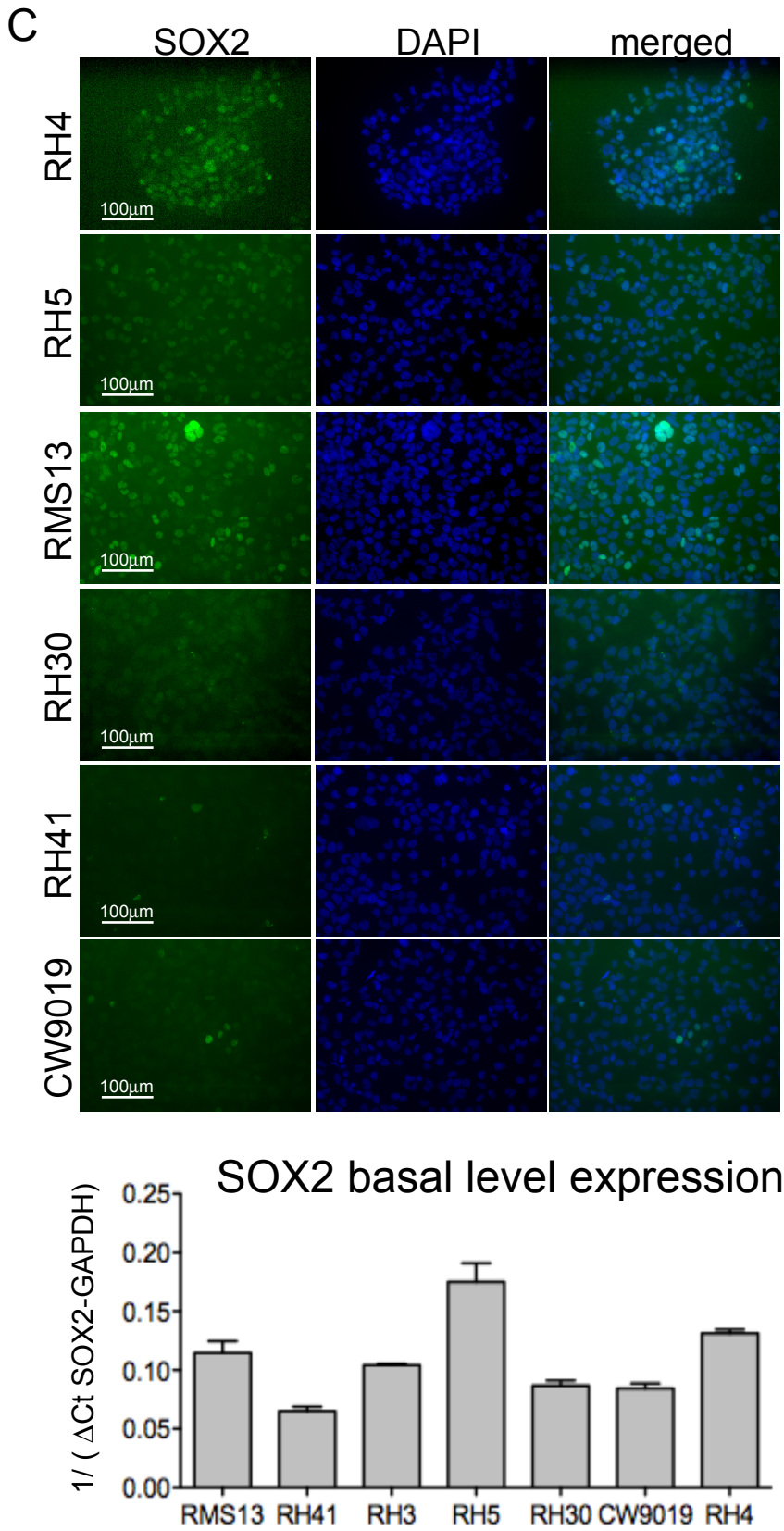
C
SOX2
DAPI
merged
RH4
RH5
RMS13
RH30
RH41
CW9019
100µm
SOX2 basal level expression
1/ (ΔCt SOX2-GAPDH)
0.25
0.20
0.15
0.10
0.05
0.00
RMS13
RH41
RH3
RH5
RH30
CW9019
RH4

SUPPL FIG 4

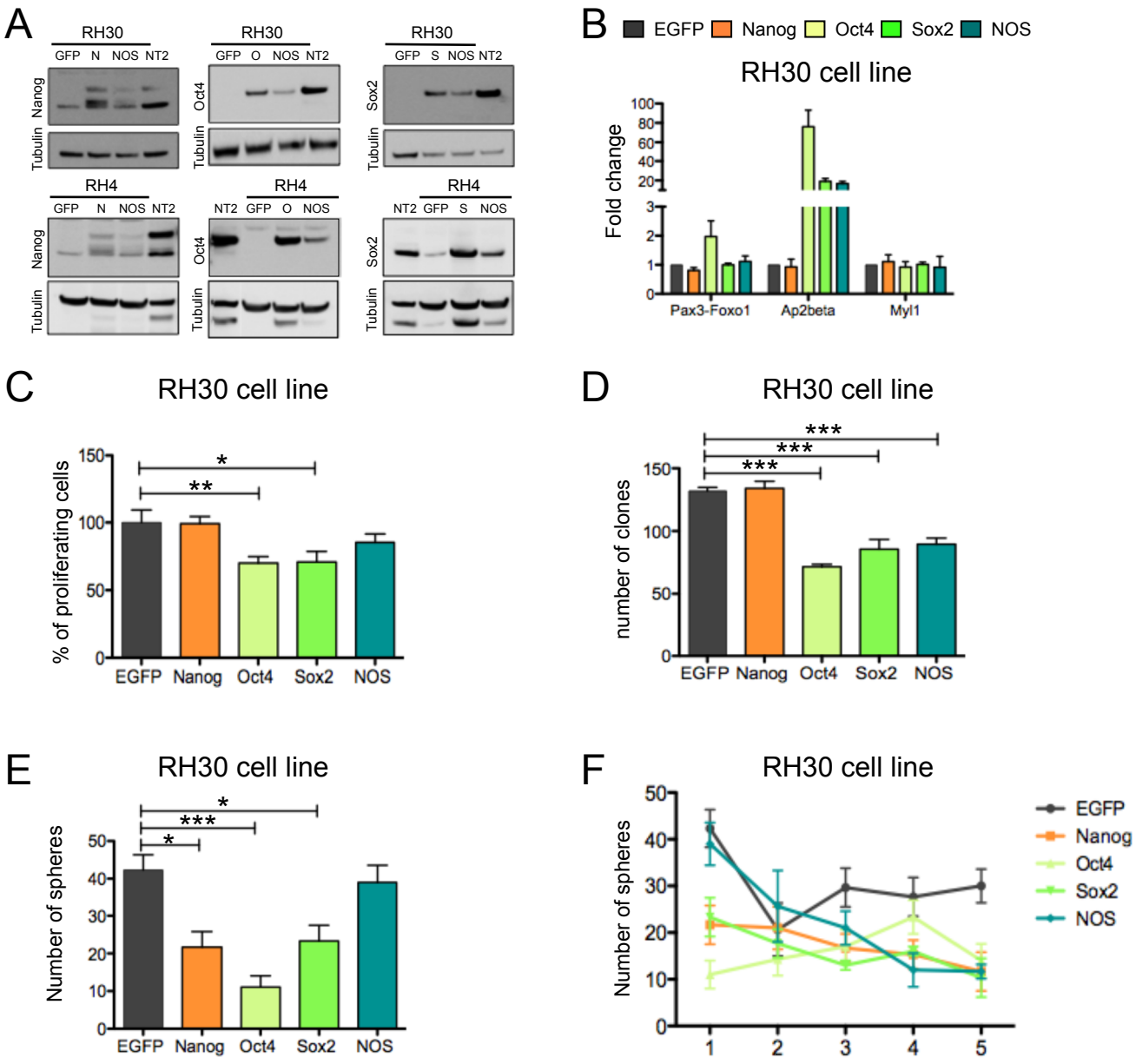
A
RH30
GFP N NOS NT2
Nanog
Tubulin
RH30
GFP O NOS NT2
Oct4
Tubulin
RH30
GFP S NOS NT2
Sox2
Tubulin
RH4
GFP N NOS NT2
Nanog
Tubulin
RH4
NT2 GFP O NOS
Oct4
Tubulin
RH4
NT2 GFP S NOS
Sox2
Tubulin
B
EGFP Nanog Oct4 Sox2 NOS
RH30 cell line
Fold change
100
80
60
40
20
3
2
1
0
Pax3-Foxo1
Ap2beta
Myl1
C
RH30 cell line
% of proliferating cells
150
100
50
0
*
**
EGFP Nanog Oct4 Sox2 NOS
D
RH30 cell line
number of clones
***
***
***
150
100
50
0
EGFP Nanog Oct4 Sox2 NOS
E
RH30 cell line
Number of spheres
*
***
*
50
40
30
20
10
0
EGFP Nanog Oct4 Sox2 NOS
F
RH30 cell line
Number of spheres
50
40
30
20
10
0
1
2
3
4
5
EGFP
Nanog
Oct4
Sox2
NOS

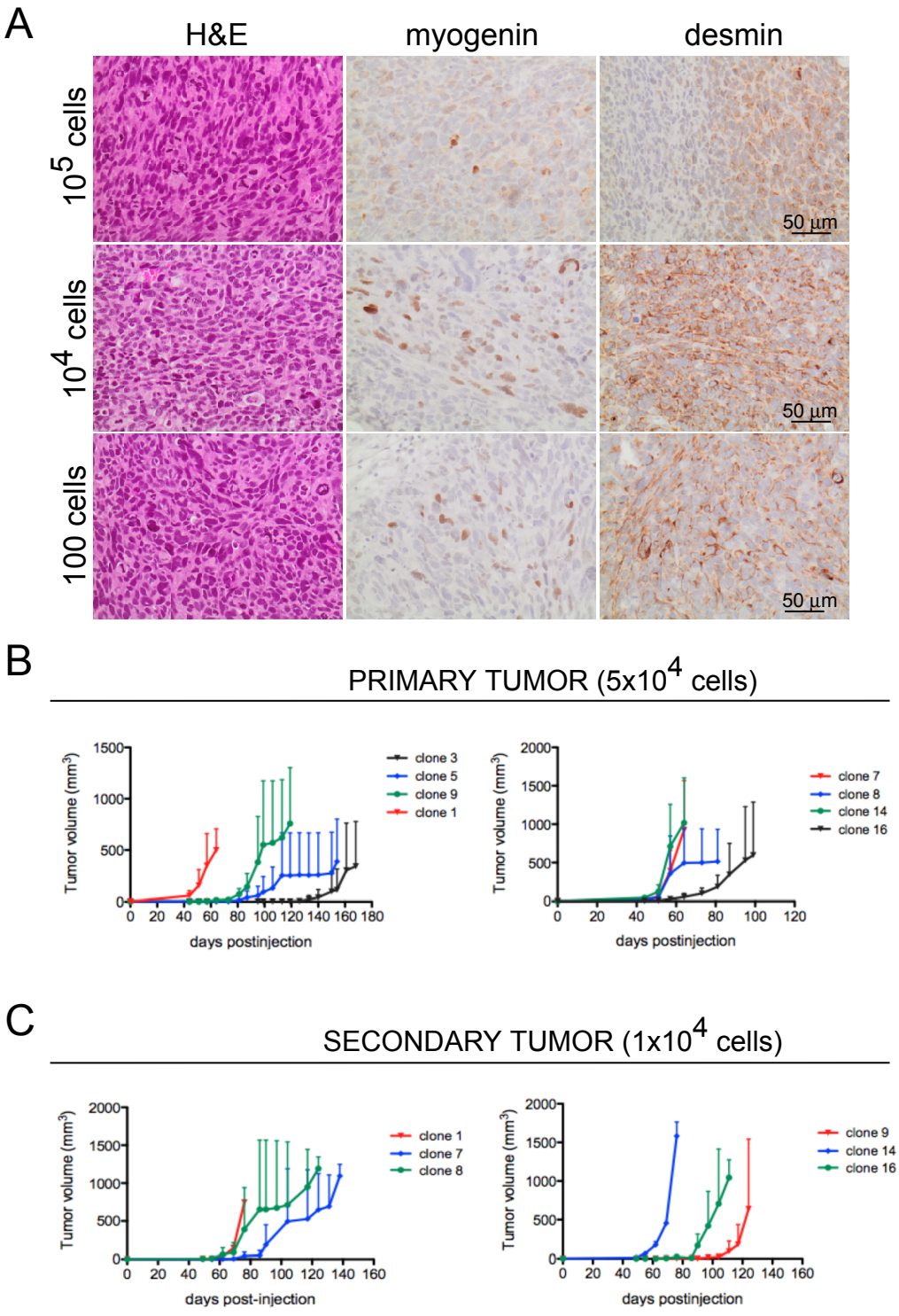
A
H&E
myogenin
desmin
10^5 cells
10^4 cells
100 cells
50 µm
50 µm
50 µm
B
PRIMARY TUMOR (5x10^4 cells)
Tumor volume (mm^3)
days postinjection
clone 3
clone 5
clone 9
clone 1
clone 7
clone 8
clone 14
clone 16
C
SECONDARY TUMOR (1x10^4 cells)
Tumor volume (mm^3)
days post-injection
days postinjection
clone 1
clone 7
clone 8
clone 9
clone 14
clone 16

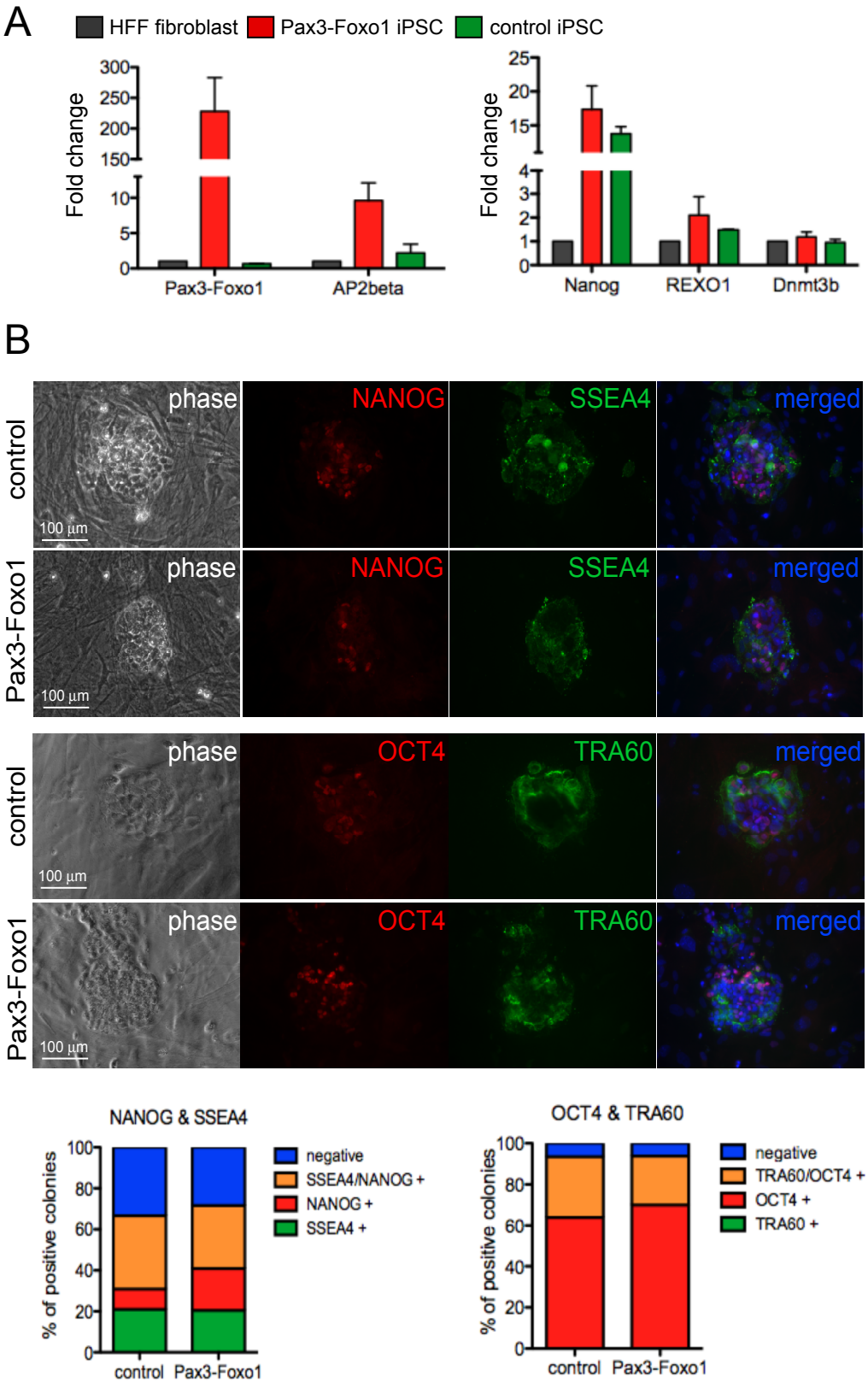
A
HFF fibroblast
Pax3-Foxo1 iPSC
control iPSC
Fold change
Pax3-Foxo1
AP2beta
Nanog
REXO1
Dnmt3b
B
control
Pax3-Foxo1
phase
NANOG
SSEA4
merged
OCT4
TRA60
100 µm
NANOG & SSEA4
% of positive colonies
negative
SSEA4/NANOG +
NANOG +
SSEA4 +
OCT4 & TRA60
TRA60/OCT4 +
OCT4 +
TRA60 +

SUPPL FIG 7

A

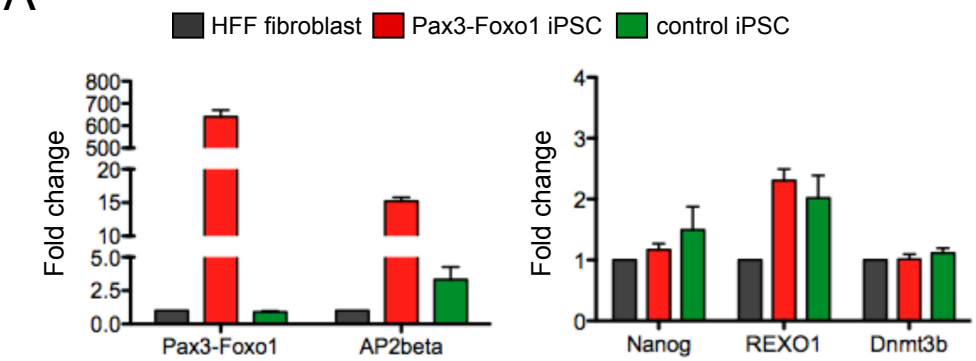

B

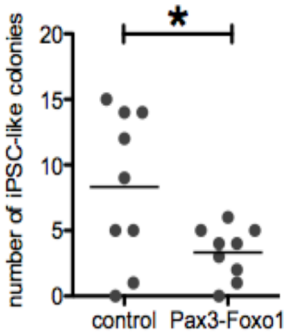

SUPPL FIG 8

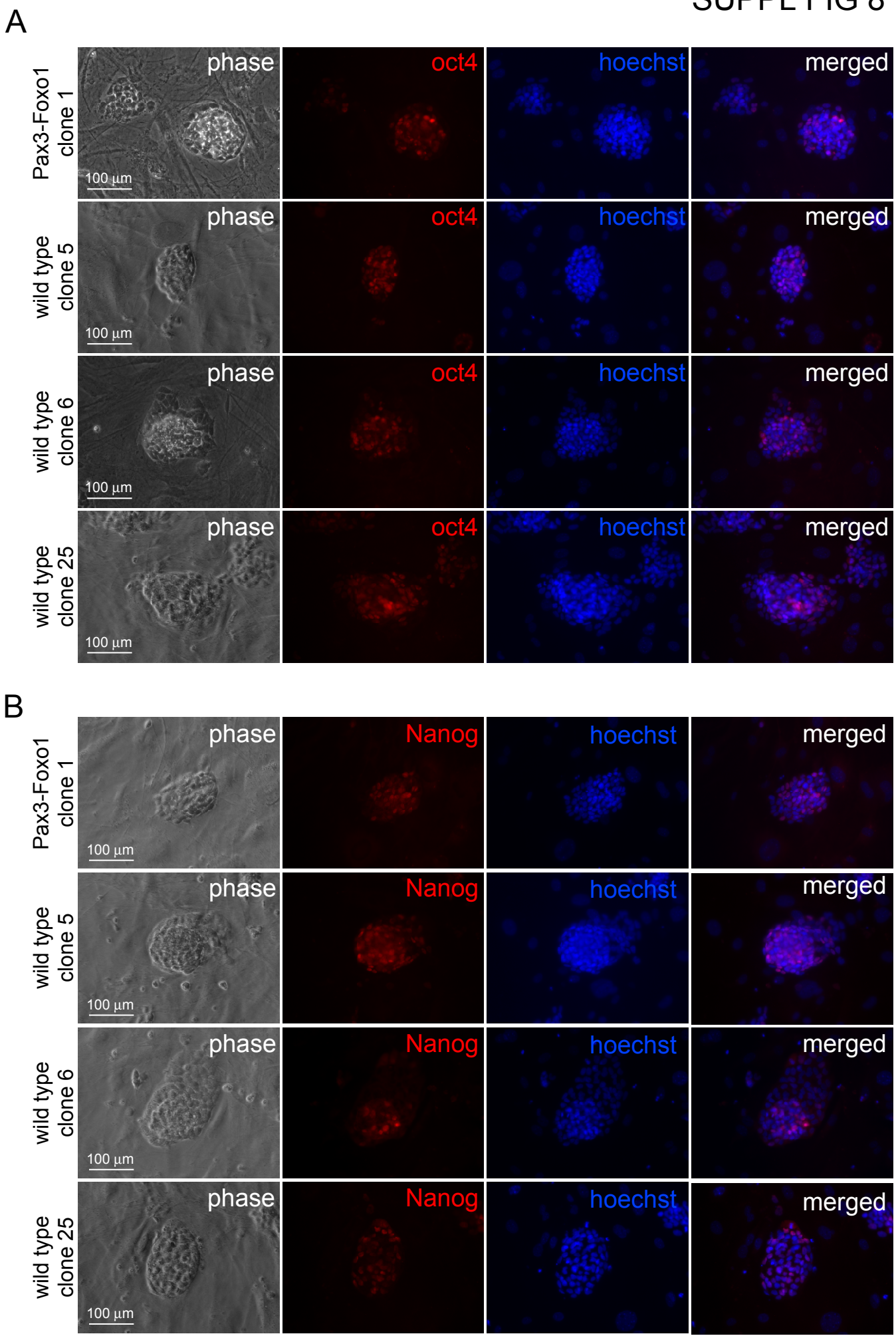
A
Pax3-Foxo1 clone 1
wild type clone 5
wild type clone 6
wild type clone 25
phase
oct4
hoechst
merged
100 µm
B
Pax3-Foxo1 clone 1
wild type clone 5
wild type clone 6
wild type clone 25
phase
Nanog
hoechst
merged
100 µm

SUPPL FIG 9

A

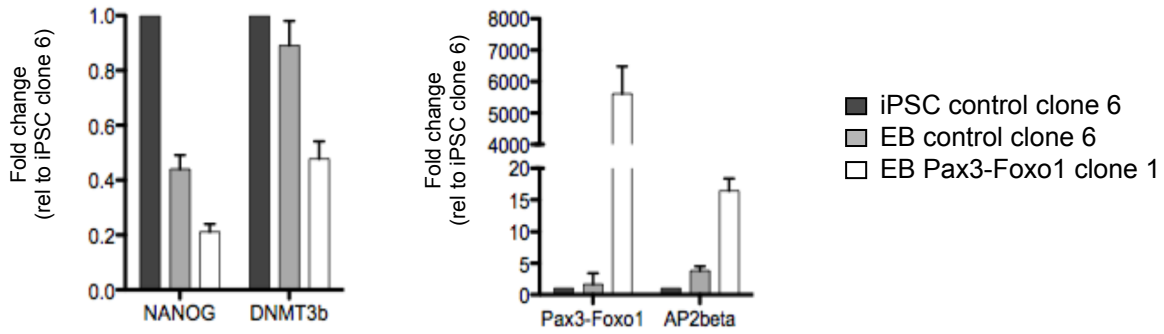

B

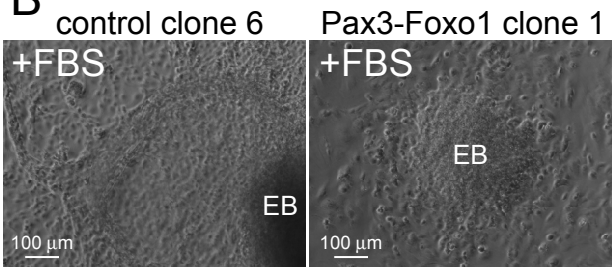

C

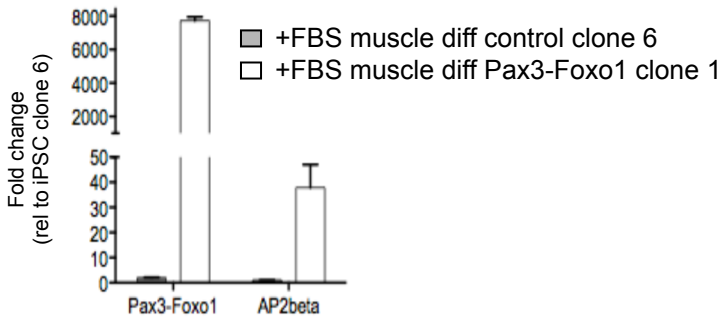

D

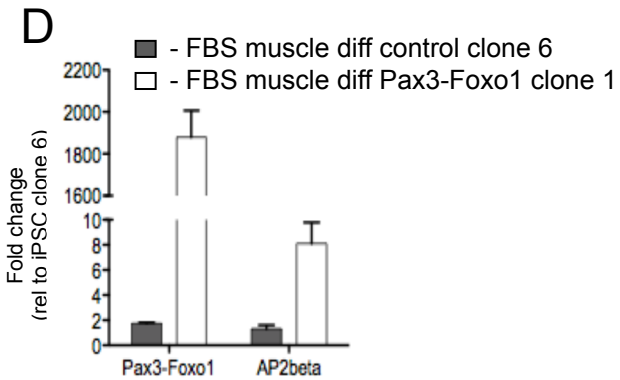

E

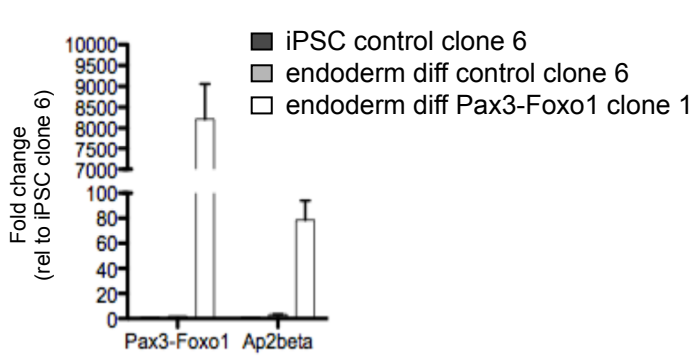

F

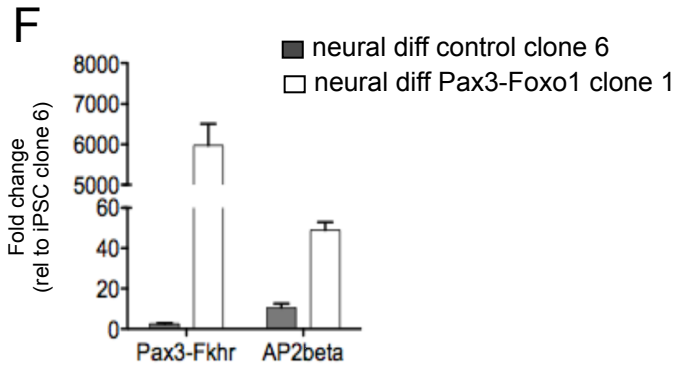

SUPPL FIG 10

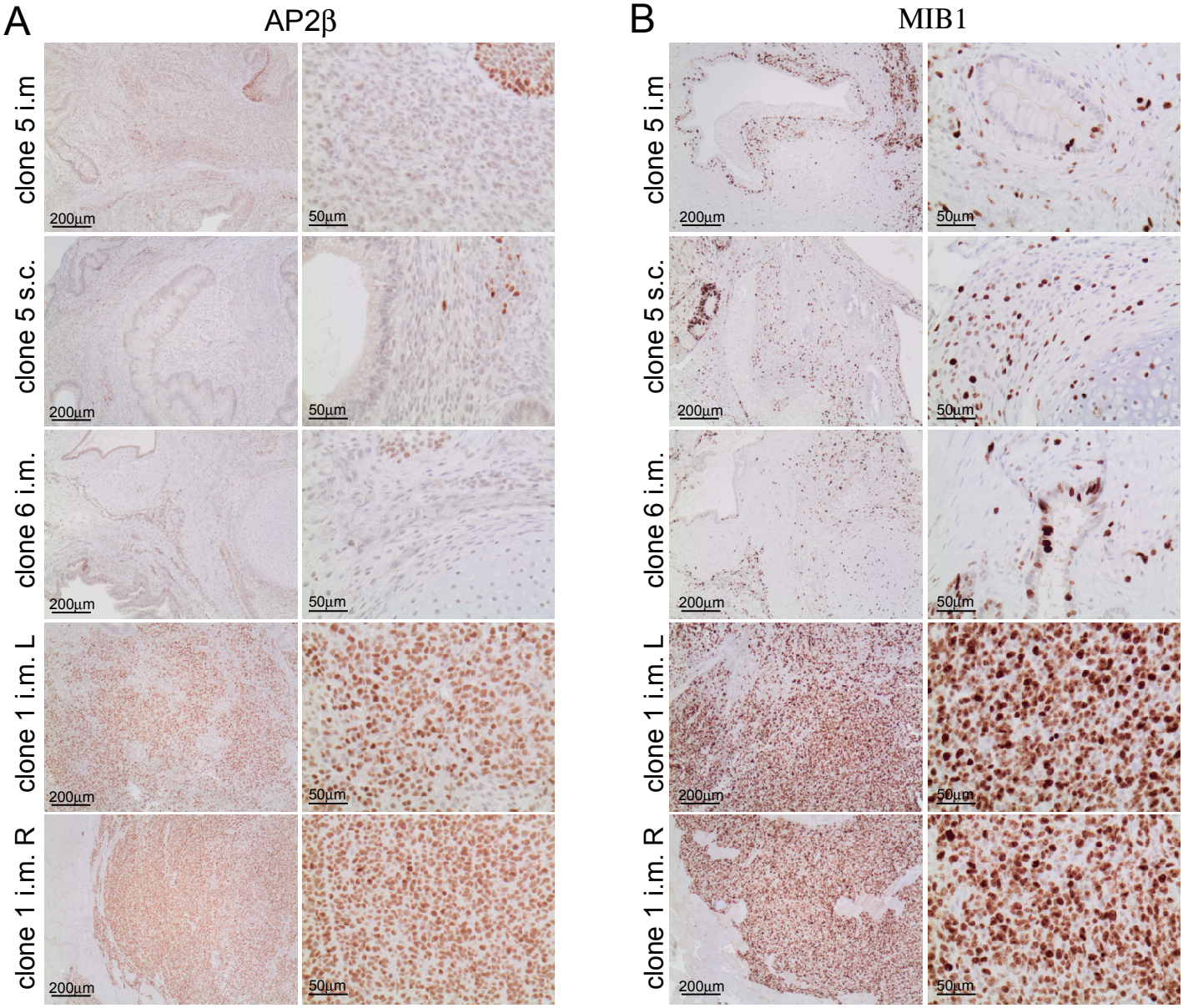
A
AP2β
B
MIB1
clone 5 i.m
clone 5 s.c.
clone 6 i.m.
clone 1 i.m. L
clone 1 i.m. R
200µm
50µm

Supplemental Table 1: TaqMan® Gene Expression Assays (Life Technologies)

Gene name	TaqMan assay number
ABCG2	Hs01053790_m1
AFP	Hs00173490_m1
ALDH1A1	Hs00946916_m1
AMY2A; AMY+	Hs00420710_g1
AP2ḅ (TFAP2b)	Hs01560931_m1
BRACHYURY T	Hs00610080_m1
CNR1	Hs01038522_s1
DCX	Hs00167057_m1
DNMT3B	Hs00171876_m1
FGFR4	Hs01106908_m1
GAPDH	Hs02758991_g1
GATA4	Hs00171403_m1
HMBS	Hs00609297_m1
MSX1	Hs00427183_m1
MYH3	Hs01074230_m1
MYL1	Hs00984899_m1
NANOG	Hs02387400_g1
OLIG2	Hs00300164_s1
PAX3	Hs00992437_m1
PAX3-FOXO1	Hs03024825_ft
PAX6	Hs00240871_m1
PAX7	Hs00242962_m1
POU5F1 (OCT4)	Hs04260367_gH
REXO1	Hs00810654_m1
SOX1	Hs01057642_s1
SOX11	Hs00846583_s1
SOX12	Hs00272869_s1
SOX2	Hs04234836_s1
SOX4	Hs00268388_s1
SOX9	Hs01001343_g1
TNNC1	Hs00896999_g1
TUBB3	Hs00801390_s1

Supplemental Table 2: Antibodies list

Primary antibody (clone)	Company	Application (dilution)
mouse anti-NANOG (hNanog.2)	eBioscience	WB (1:500), IF (1:50 aRMS & 1:200 iPSC)
rabbit anti-OCT4 (C52G3)	Cell Signaling	WB (1:500), IF (1:50 aRMS & 1:200 iPSC)
rabbit anti-SOX2 (D6D9)	Cell Signaling	WB (1:500), IF (1:50 aRMS)
mouse anti-TUBULIN (B5-1-2)	Sigma-Aldrich	WB (1:40'000)
mouse anti-SSEA4 (MC-813-70)	Developmental Studies Hybridoma Bank	IF (1:200)
anti-human TRA-1-60 biotin	eBioscience	IF (1:200)
polyclonal rabbit anti-AP2β	Thermo Scientific	IF (1:200)
polyclonal rabbit anti-AMYLASE	Sigma	IF (1:1000)
rabbit anti-GFAP (Z 0334)	Dako Cytomotion	IF (1:500)
mouse anti-3βTUBULIN (TU-20)	Cell Signaling	IF (1:500)
mouse anti-human Desmin (D33)	DAKO	IHC (1:20)
mouse anti-Myf4 (L026)	Novocastra Laboratories Ltd	IHC (1:20)
rabbit anti-mib1 (30-9)	Ventana-Roche	-
phalloidin-FITC	Enzo	IF (1:2000)
Secondary antibody	**Company**	**Application (dilution)**
anti-mouse HRP-linked 7076S	Cell Signaling	WB (1:2000)
anti-rabbit HRP-linked 7074S	Cell Signaling	WB (1:2000)
anti rabbit Alexa Fluor 594	Invitrogen	IF (1:500)
anti mouse Alexa Fluor 594	Invitrogen	IF (1:500)
anti mouse Alexa Fluor 488	Invitrogen	IF (1:500)
anti rabbit Alexa Fluor 488	Invitrogen	IF (1:500)

WB: Western Blotting; IF: Immunofluorescence; IHC: Immunohistochemistry